

## **1.1. General Principles of Cancer Chemotherapy**

The term cancer or neoplasia, is used to define a broad group of diseases where there is uncontrolled proliferation and spread of abnormal forms of the body's own cells. Neoplastic cells are distinguished from the body's normal cells by their ability to continually divide and proliferate often forming a localised tumour.<sup>1</sup> Other characteristics of neoplastic cells include invasiveness and the capacity to metastasise resulting in growth of tumours at secondary sites. The uncontrolled growth of tumours and their spread throughout the body eventually leads to nutritive starvation and death of normal tissue cells.<sup>2</sup>

The treatment of cancer using chemotherapy involves the use of drugs to selectively target rapidly proliferating neoplastic cells in preference to the body's own cells. The use of chemotherapy alone rarely cures cancer<sup>3</sup> but inhibits proliferation of neoplastic cells and can effect a cure when used in combination with surgery and/or radiation therapy.<sup>4</sup> The introduction of chemotherapy has revolutionised the treatment of several cancers including testicular cancer, leukaemias and several childhood cancers<sup>3</sup> where the survival rate for childhood cancers has more than doubled since 1963.<sup>4</sup>

Advances in new cancer treatments require an in-depth understanding of how regulation of cell division and proliferation is disrupted in neoplastic cells. The life cycle of a cell has been well studied and is known to involve several phases.<sup>1,2</sup> The process of cell division begins when a cell emerges from a resting phase known as  $G_0$  and enters the cell life cycle, which culminates in mitosis. Following mitosis the cell is then signalled to enter the  $G_0$  resting phase or begin the cell cycle again. Normal cells of the body spend most of their time in the  $G_0$  or resting phase while neoplastic cells never enter the  $G_0$  phase and are always in the

replicating cell cycle. This implies that the mechanism by which cells are signalled to enter the G<sub>0</sub> phase is somehow disrupted in neoplastic cells.

The disruption of the regulatory process in a normal cell leading to a neoplastic cell is known to occur when a particular region of the DNA mutated to give an oncogene.<sup>5</sup> Several oncogenes have been identified and implicated in the mechanism by which normal cells become neoplastic cells.

Anticancer drugs generally exert their activity by inhibiting one or more processes occurring in the normal cell cycle (Figure 1.1a)<sup>1</sup>. Interaction with any of the biomolecules whose normal function is necessary for cell division interrupts normal cellular processes resulting in cell death.<sup>1</sup> The most common target of many currently used chemotherapy drugs is DNA, which is either being replicated in the S phase or being used to make proteins and enzymes in the other phases of the cell cycle (Figure 1.1a). Although drugs are able to target any phase of the cell cycle, their effect is usually apparent during the S phase when DNA replication is blocked, subsequently leading to cell death.<sup>1</sup>

Drug-DNA interactions may be classified as either (i) covalent binding, or (ii) non-covalent binding. Covalent binding involves alkylation or coordination of the drug to DNA. For example mitomycin (Figure 1.1b) covalently binds to DNA through the guanine bases.<sup>1</sup> There are three types of non-covalent binding mechanisms relevant to DNA-drug interactions; (i) intercalation, (ii) groove binding, and (iii) electrostatic interactions. Intercalation occurs when planer, aromatic drugs stack between the base pairs of the hydrophobic interior of helical DNA. Doxorubicin is an

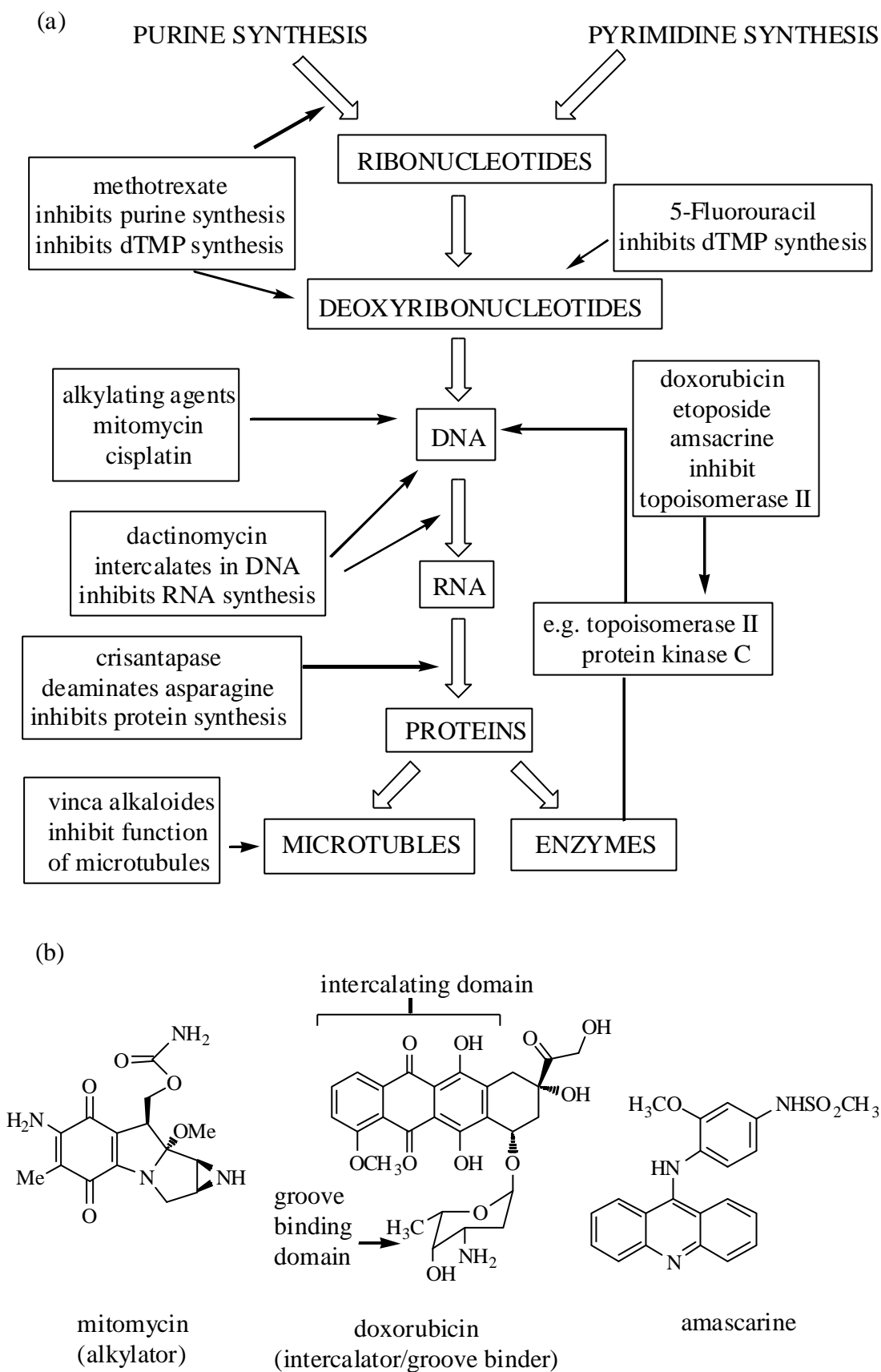


**Figure 1.1:** (a) Inhibition of processes occurring in the cell cycle by anticancer drugs  
(b) Structure of DNA-binding drugs

example of a drug with a planar, aromatic region that can intercalate between the base pairs of the DNA but also has groove binding domain (Figure 1.1b).<sup>1</sup> Groove binding occurs in either the minor or major groove of DNA. Drugs bind in the grooves through hydrogen bond donor or acceptor sites. Electrostatic interactions occur between the negatively charged phosphate backbone and positively charged groups such as is the case with the amino group in amsacrine at physiological pH (Figure 1.1b).<sup>6</sup>

The dominant type of anticancer drugs have traditionally been organic compounds (Figure 1.1). However, the use of metal complexes in cancer therapy has been a rapidly growing field of research.

## **1.2. Metal Complexes as Antitumour Drugs**

The use of metals in drug design provides new opportunities in the development of new generation antitumour drugs. The large number of metals available, combined with access to a range of coordination geometries and types of complexes, and the almost infinite number of organic ligands that may be coordinated to the metal centre, provides access to a huge number of metal complexes that could be screened for activity.

In terms of rational drug design of potential anticancer metal complexes, DNA is an obvious cellular target. The DNA bases contain a number of heterocyclic nitrogen and oxygen atoms as well as the phosphate (O) groups on the DNA backbone that may potentially form coordination complexes with metal-based drugs (Figure 1.2).

The role of metals in cancer therapy and biological chemistry has gained much interest since the discovery of the potent anticancer drug cisplatin (Figure 1.3) in 1967.<sup>7</sup> To date,

cisplatin (Figure 1.3), and its second generation analogue carboplatin

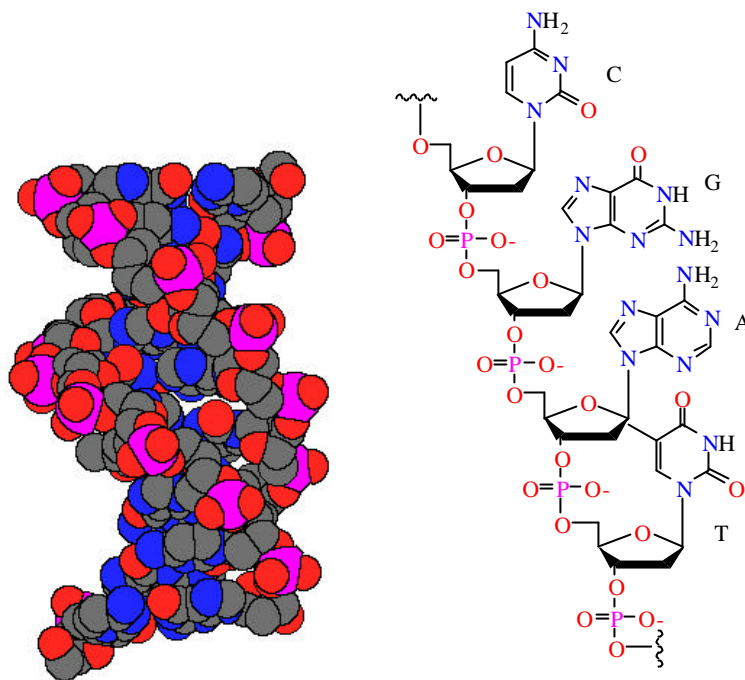


**Figure 1.2:** Structure of DNA highlighting coordination sites

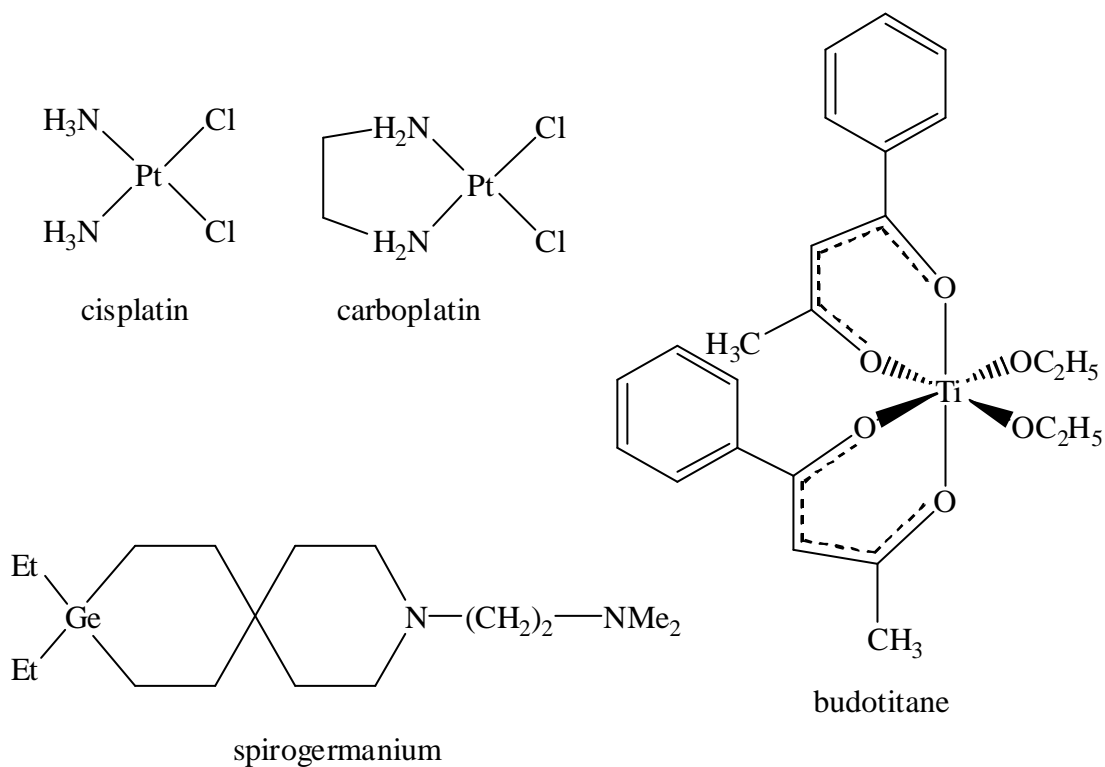


**Figure 1.3:** Metal based drugs in clinical trials

(Figure 1.3), are the most successful of the anticancer metal complexes and are currently widely used in the treatment of cancer.<sup>8</sup> Cisplatin is believed to crosslink DNA through coordination of the Pt center to the N7 guanine bases. This results in formation of an adduct, which induces a kink in the DNA and therefore disrupts the normal processes of DNA replication and transcription.

Following the discovery of cisplatin, metal complexes, derived from a range of metals, have been shown to have anticancer activity. Metal complexes of gold, iron, ruthenium, rhodium, iridium, palladium, and tin have shown some promising antitumour activity but have not yet been introduced into clinical trials.<sup>8</sup> These metal complexes, along with many others, have been screened in either *in vitro* studies or *in vivo* studies (Figure 1.4).<sup>8</sup> To date, only a few metal complexes other than the platinum based drugs (Figure 1.3) have entered clinical trials. These include gallium trinitrate which has shown potential as a chemotherapeutic agents following phase II clinical trials in combination with cisplatin<sup>9-11</sup> and also spirogermanium (Figure 1.3)<sup>12</sup> Budotitane (Figure 1.3) is a titanium complex that has also shown significant antitumour activity and has entered clinical trials<sup>13</sup> along with the organometallic complex titanocene dichloride **1** (Figure 1.5).<sup>14-16</sup>

### 1.3. Metallocenes as Antitumour Drugs

The antitumour properties of an extensive range of metallocene dihalides and diacido complexes  $Cp_2MX_2$  ( $Cp = \eta^5-C_5H_5$ ;  $M = Ti, V, Nb, Mo, Re$ ;  $X = \text{halide or diacido ligand}$ ) (Figure 1.5) have been reported against a range of tumour models in mice and several xenografted human tumours transplanted into athymic mice.<sup>17-19</sup>





### Periodic Table of Elements

1																		18
1 H	2												13	14	15	16	17	2 He
3 Li	4 Be												5 B	6 C	7 N	8 O	9 F	10 Ne
11 Na	12 Mg	3	4	5	6	7	8	9	10	11	12	13 Al	14 Si	15 P	16 S	17 Cl	18 Ar	
19 K	20 Ca	21 Sc	22 Ti	23 V	24 Cr	25 Mn	26 Fe	27 Co	28 Ni	29 Cu	30 Zn	31 Ga	32 Ge	33 As	34 Se	35 Br	36 Kr	
37 Rb	38 Sr	39 Y	40 Zr	41 Nb	42 Mo	43 Tc	44 Ru	45 Rh	46 Pd	47 Ag	48 Cd	49 In	50 Sn	51 Sb	52 Te	53 I	54 Xe	
55 Cs	56 Ba	57 La	72 Hf	73 Ta	74 W	75 Re	76 Os	77 Ir	78 Pt*	79 Au	80 Hg	81 Tl	82 Pb	83 Bi	84 Po	85 At	86 Rn	

**Magenta:** Complexes of these metals have entered clinical trials for their antitumour activity

**Red:** Complexes of these metals show antitumour activity *in vitro* or/and *in vivo*

**Green:** Metallocene complexes of these metals show sporadic antitumour activity *in vivo*

**Blue:** Metallocene complexes of these metals show no antitumour activity *in vivo*

\* Cisplatin is widely used in chemotherapy treatments

**Figure 1.4:** Periodic table of elements showing metals derived from active antitumour complexes (adapted from Fricker, S.P.<sup>8</sup>)

Titanocene dichloride **1** has been the focus of most studies, and this is the only metallocene dihalide to have entered clinical trials.<sup>14,16,20</sup> In addition to antitumour activity, titanocene dichloride **1** exhibits antiviral, anti-inflammatory and insecticidal activity in mice.<sup>17,19</sup> Formation of metallocene-DNA complexes has been implicated in the mechanism of antitumour properties of the metallocenes, as both titanocene dichloride **1** and vanadocene dichloride **2** inhibit DNA and RNA synthesis,<sup>21,22</sup> and titanium and vanadium accumulate in nucleic acid-rich regions of tumour cells<sup>23,24</sup>. However, in contrast to the well characterised platinum-based antitumour drugs,<sup>25</sup> the active species responsible for antitumour activity *in vivo* has not been identified. Furthermore, the mechanism whereby irreparable DNA damage and/or structural modification of DNA or other cellular targets occurs is poorly understood.

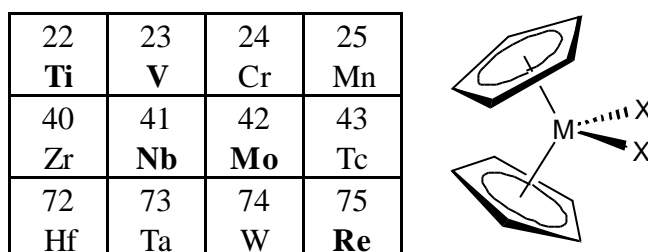


**Figure 1.5:** Structure of antitumour metallocene dihalides highlighting derivatives with maximum activity against fluid EAT (bold **M**).

Studies during the last decade of the hydrolysis chemistry, stability at different pH values and the interaction(s) with nucleic acid constituents have confirmed that each of the antitumour metallocenes has an independent mechanism of action. Most studies have focused on titanocene dichloride **1**, which is currently in phase II clinical trials.<sup>20</sup> Structure-activity studies as well as studies of the interactions with a range of potential biomolecular targets

including proteins and DNA have provided some important clues to the mechanism of action of titanocene dichloride **1**. In contrast, only limited studies have been reported on other compounds in this class.

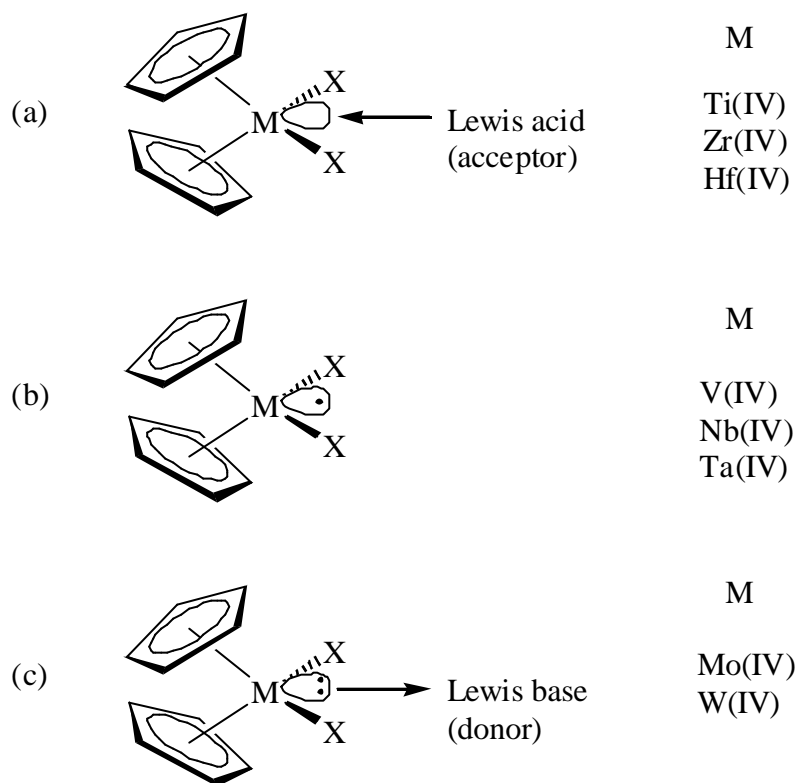
### 1.3.1. Structural Properties

The antitumour metallocenes are structurally and chemically unrelated to the well-studied platinum based antitumour drugs. These complexes are characterised by a distorted tetrahedral structure in which two cyclopentadienyl (Cp) ligands and two halide or acido ligands are coordinated to a transition metal, generally in the +IV oxidation state (Figure 1.5). The two cyclopentadienyl rings, which each have a delocalised negative charge, are coordinated to the metal centre *via* pentahapto metal-carbon coordination in a "bent sandwich" configuration where the angle between the rings is less than 180°.26

The aromatic cyclopentadienyl rings donate 6 electrons each to the Cp-metal bond. The cyclopentadienyl rings act both as  $\pi$ -donors and  $\pi$ -acceptors resulting in a highly covalent bond with little charge separation between the transition metal and the Cp rings.27 The metallocenes  $\text{Cp}_2\text{MX}_2$ , where  $\text{M} = \text{Ti}, \text{Zr}, \text{Hf}$ , all have a 16-electron configuration in their outer shell. This results since  $\text{M(IV)}$  has lost all 4 electrons in the outer  $d$  orbitals (i.e.  $d^0$ ) and each Cp and halide ligand donate 6 and 2 electrons respectively to give a total of 16 electrons (ionic counting convention).27 This configuration is electron deficient compared to the energetically favourable 18-electron configuration of the noble gases. However, the tetrahedral arrangement allows the 16-electron configuration to be comparable energetically to the 18-electron configuration.27 The 16-electron configuration provides an unfilled  $d$  orbital, which can act as a Lewis acid and accept a 2 electron donating ligand (Figure 1.6a).

However, Ti(IV) in  $\text{Cp}_2\text{Ti}^{2+}$  is normally restricted to two donor ligands (such as two halide ligands) due to its relatively small ionic radius.<sup>27</sup>

**Figure 1.6:** Structural properties of metallocene dihalides highlighting the Lewis character of



the complexes

In contrast, the  $d^2$  metallocenes where  $M = \text{Mo(IV)}$  and  $\text{W(IV)}$  in  $\text{Cp}_2\text{MX}_2$  have an 18-electron configuration. As a result all  $d$  orbitals are filled with one  $d$  orbital possessing a non-bonding pair of electrons which can act as a ligand donor or Lewis base (Figure 1.6c).<sup>27</sup> In the case of  $d^1$  complexes of  $\text{Cp}_2\text{MX}_2$  where  $M = \text{V(IV)}$ ,  $\text{Nb(IV)}$  and  $\text{Ta(IV)}$ ; the metal center has a 17-electron configuration resulting in a paramagnetic complex where 1  $d$  orbital only has 1 electron (Figure 1.6b).

### 1.3.2. Preclinical Trials with Titanocene Dichloride **1**

Extensive studies on the antitumour activity of titanocene dichloride **1** against a range of cell lines in mice including fluid and solid sarcoma 180,<sup>28</sup> leukemias P388 and L1210,<sup>29</sup> colon 38 carcinoma and B16 melanoma,<sup>30</sup> Lewis lung carcinomas,<sup>12</sup> fluid and solid EAT,<sup>31</sup> and several xenografted human tumours<sup>12,30,32</sup> of the colon, rectum, stomach, lung, breast, head and neck transplanted into athymic mice have been carried out by Köpf and Köpf-Maier. The results have been summarised in a number of reviews.<sup>12,17,18</sup> Briefly, titanocene dichloride **1** showed a range of activity against the animal tumour models. An OCR of 100 % was observed against fluid EAT tumour, as well as significant reductions (up to 80 %) in the growth of colon 38 carcinoma, B16 melanoma, and Lewis lung carcinoma in solid animal tumour systems.<sup>12,30</sup> The growth-inhibiting effects against the rather insensitive colon 38 adenocarcinoma were clearly more pronounced than that of cisplatin.

Significant growth inhibition of up to 90% was reported against a range of xenografted human gastrointestinal carcinomas which are much less sensitive to cisplatin and 5-fluorouracil (the most effective clinically used cytostatic drug for gastrointestinal carcinoma).<sup>12,32</sup> Titanocene dichloride **1** also showed significant and increased activity compared to cisplatin against some xenografted human lung carcinomas.<sup>12,30</sup>

More recent studies have reported that titanocene dichloride **1** has a significantly higher antineoplastic activity than cisplatin against human ovarian cancer xenografts in nude mice. This provides potential new therapeutic options for women with ovarian carcinoma where standard chemotherapy has not been successful.<sup>33,34</sup> These results are consistent with the earlier findings of an *in vitro* and *in vivo* study<sup>35</sup>, which reported that titanocene

dichloride **1**, had activity against a human ovarian carcinoma cell line that was resistant to doxorubicin or cisplatin.

### 1.3.3. Clinical Trials with Titanocene Dichloride **1**

As a result of the encouraging antitumour activity reported in animal systems, two separate phase I clinical trials of titanocene dichloride **1** have been reported.<sup>14-16</sup> In contrast to the preclinical studies, where hepatic or liver toxicity was the dose-limiting side effect, nephrotoxicity (i.e. kidney toxicity) was identified as the dose-limiting side effect.<sup>14,16</sup> Hypoglycaemia, nausea, reversible metallic taste immediately after administration and pain during infusion were also apparent.<sup>14,16</sup> However, proliferative activity of the bone marrow, which is a typical side-effect of most currently used antitumour drugs, was not reported at any significant level.

Due to the hydrolytic instability of titanocene dichloride **1** at  $\text{pH} < 5$  (discussed in the next section), a formulation that prevented hydrolysis and precipitation reactions, was required for clinical trials.<sup>36</sup> In first clinical study titanocene dichloride **1** was administered in a lyophilised form dissolved in malate buffer ( $\text{pH} 3.2$ ; formulation MKT 5 is supplied by Medac-Gesellschaft für klinische Spezialpräparate, Hamburg) and gave a MTD of  $140 \text{ mg m}^{-2}$  which was also the recommended dose for phase II trials.<sup>16</sup> The second study used a similar formulation (MKT 4) of lyophilised titanocene dichloride **1** in malic acid ( $\text{pH} 3.5$ ) which gave a MTD of  $315 \text{ mg m}^{-2}$  and a recommended dose of  $240 \text{ mg m}^{-2}$  for phase II clinical trials.<sup>14</sup>

The promising results of the phase I clinical trials concluded with the planning of disease-oriented phase II clinical trials.<sup>37</sup> Reports of synergistic activity of titanocene dichloride **1** with the antitumour agent 5-fluorouracil *in vitro*, lead to the suggestion of clinical

trials involving formulations containing both antitumour agents.<sup>37</sup> A recent phase II clinical trial of titanocene dichloride **1** in eleven patients with advanced renal-cell carcinoma reported no therapeutic effect following two cycles of titanocene dichloride **1** administered at a MTD of 270 mg m<sup>-2</sup> (determined following a pilot study) every 21 days.<sup>20</sup> The authors highlighted the limitations of such clinical trials noting that as with many chemotherapeutic agents, titanocene dichloride **1** does not produce responses as a single-agent and should be considered for clinical trials involving systemic therapy.

#### **1.4. Structure-Activity Studies**

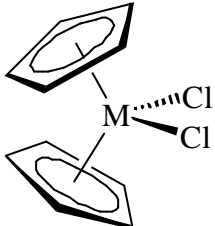
In order to determine the key structural aspects required for antitumour activity, a number of structure-activity studies of the metallocene dihalides have been carried out.<sup>17,18</sup> From a structural point of view there are three elements that may be varied (i) the transition metal ion (ii) the halide ligand and (iii) the cyclopentadienyl ligands. Key analogues that have been tested are summarised in Tables 1.1-1.5. Analogues in these three categories reported until 1988 are summarised in a number of reviews.<sup>17,18</sup>

##### **1.4.1. Influence of the Central Transition Metal Atom**

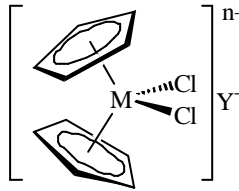
Variation of the central metal is tolerated in the series Cp<sub>2</sub>MCl<sub>2</sub> with OCRs of 100 % against EAT in mice obtained for M = Ti(IV) **1**, V(IV) **2**, Nb(IV) **3** and Mo(IV) **4** (Table 1.1).<sup>31,38-43</sup> Sporadic cure rates of < 25% were obtained for Ta(IV) **5** and W(IV) **6** and the Zr(IV) **7** and Hf(IV) **8** analogues showed no activity.<sup>31,39,43</sup> More recently, ionic Nb(V) **9-11**, Mo(VI) **15** and Re(V) **12-14** analogues have also been screened for activity, and showed an OCR of 100 % against fluid EAT tumours. The toxicity, however, was markedly broadened (LD<sub>50</sub> 65-250 mg/kg; Table 1.2) in comparison to the neutral antitumour

metallocene complexes.<sup>44,45</sup> Preliminary studies to determine the growth inhibiting properties of these ionic analogues against human carcinoma xenografts confirmed antitumour activity for both rhenocene complexes **12** and **13** against colon and breast carcinoma with growth inhibition between 50-65%.<sup>12</sup>

**Table 1.1:** Structure activity studies of the influence of the central transition metal atom against fluid EAT; samples administered in 10%DMSO/saline (pH~3.0)

Compound		OCR (%)	ODR (mg/kg)	LD <sub>50</sub> (mg/kg)	Ref.	
	No.	M				
	<b>1</b>	Ti(IV)	100	40-60	100	31
	<b>2</b>	V(IV)	100	80-90	110	40
	<b>3</b>	Nb(IV)	100	20-25	35	43
	<b>4</b>	Mo(IV)	100	75-100	175	43
	<b>5</b>	Ta(IV)	25	80-170	200	43
<b>6</b>	W(IV)	13	100-400	500		

**Table 1.2:** Structure activity studies of ionic analogues with various central transition metal atom against fluid EAT; samples administered in 10%DMSO/saline (pH~3.0)

Compound		OCR (%)	ODR (mg/kg)	LD <sub>50</sub> (mg/kg)	Ref.		
	No.	M	Y				
	<b>9</b>	Nb(V)	BF <sub>4</sub> <sup>-</sup>	63	10-20	65	44
	<b>10</b>	Nb(V)	AsF <sub>6</sub> <sup>-</sup>	100	20-40	105	44
	<b>11</b>	Nb(V)	SbF <sub>6</sub> <sup>-</sup>	100	10-40	72	44
	<b>12</b>	Re(V)	Cl <sup>-</sup>	100	60-160	240	45
	<b>13</b>	Re(V)	AsF <sub>6</sub> <sup>-</sup>	100	80-180	250	45
	<b>14</b>	Re(V)	SbF <sub>6</sub> <sup>-</sup>	50	60	170	44
	<b>15</b>	Mo(IV)	2SbF <sub>6</sub> <sup>-</sup>	100	20-80	105	

While these results imply that all metallocenes give similar activity, and the metallocenes are often referred to as a general class of drugs,<sup>12,17,18</sup> it should be noted that the results are mostly for fluid EAT and independent studies have shown that the results are clearly specific for different tumour models. For example, vanadocene dichloride **2** gives a distinct pattern of activity against numerous lung and breast carcinomas compared to titanocene dichloride **1**.<sup>18</sup> A comparison of the relative antitumour activity of the various central metal ions is currently restricted to fluid EAT tumours. Full screening of the neutral metallocenes  $\text{Cp}_2\text{MCl}_2$  ( $\text{M} = \text{Nb}$  **3**,  $\text{Mo}$  **4**,  $\text{Ta}$  **5**,  $\text{W}$  **6**,  $\text{Zr}$  **7**,  $\text{Hf}$  **8**) against different tumour types under identical conditions has not been carried out and there are currently only limited studies of the ionic analogues where  $\text{M} = \text{Mo(VI)}$  **15**,  $\text{Nb(V)}$  **9-11**,  $\text{Re(V)}$  **12-14** against colon and breast carcinomas.

#### 1.4.2. Influence of the Halide or Acido Group

Variation of the halide ligand, in the case of titanocene dichloride **1**, has been extensively studied. The nature of the halide does not appear to significantly affect the antitumour properties. Equally potent tumour inhibition against EAT tumours has been demonstrated for a variety of halide and diacido ligands within the series  $\text{Cp}_2\text{TiX}_2$  (Table 1.3).<sup>17,46-48</sup> Reduced activity in the *p*-nitrophenoxy analogue **24** (Table 1.3) and  $\text{Cp}_2\text{TiClX}$  ( $\text{X} = 2,4,6\text{-OPhCl}_3$  **31**, *o*- $\text{SC}_6\text{H}_4\text{CH}_3$  **32**, *o*- $\text{SC}_6\text{H}_4\text{NH}_2$  **33**) (Table 1.4) was attributed to the lack of lability of the Ti-X bond which is unable to dissociate in solution and generate the active species which is assumed to coordinate to DNA.<sup>17</sup> Titanocene dibromide **9** has also been tested for antitumour activity against solid sarcoma 180,<sup>28</sup> B16 melanoma,<sup>30</sup> colon 38 adenocarcinoma,<sup>30</sup> and Lewis lung carcinosarcoma.<sup>12</sup> It shows similar activity to

titanocene dichloride **1**.<sup>12,17</sup> Testing against various tumour models show similar results for  $\text{Cp}_2\text{TiX}_2$  ( $\text{X} = \text{SPhNH}_3\text{Cl}$  **21**,  $\text{OCOCCl}_3$  **22**, *cis*  $\text{OCOCH}=\text{CHCO}_2\text{H}$  **23**).<sup>28,30,32</sup> This further confirms that, provided the Ti-X bond is labile in aqueous solution, the halide or acido group can be modified without significant perturbation of antitumour properties.

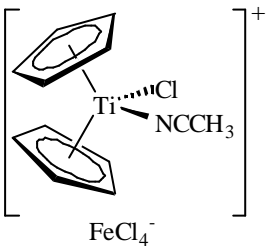
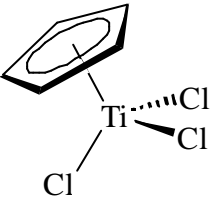
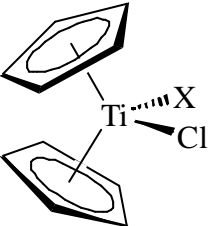
**Table 1.3:** Structure activity studies of the influence of the halide or acido group in titanocene complexes against fluid EAT; samples administered in 10% DMSO/saline (pH~3.0)

Compound		OCR (%)	ODR (mg/kg)	LD <sub>50</sub> (mg/kg)	Ref
No.	X				
<b>16</b>	F	100	40	60	46
<b>17</b>	Br	100	40-80	135	46
<b>18</b>	I	100	60-100	145	46
<b>19</b>	NCS	100	80	135	46
<b>20</b>	N <sub>3</sub>	100	50-70	95	47
<b>21</b>	SC <sub>6</sub> H <sub>4</sub> NH <sub>3</sub> Cl	100	60-140	175	47
<b>22</b>	OCOCCl <sub>3</sub>	100	100-360	440	47
<b>23</b>	<i>cis</i> OCOCH=CHCO <sub>2</sub> H	100	60-120	170	17
<b>24</b>	<i>p</i> -OC <sub>6</sub> H <sub>4</sub> NO <sub>2</sub>	10	180-240	260	48
<b>25</b>	OC <sub>6</sub> F <sub>5</sub>	100	340-360	480	49
<b>26</b>	SC <sub>6</sub> F <sub>5</sub>	100	120-180	260	49
<b>27</b>	OCOCH <sub>2</sub> NH <sub>3</sub> Cl	50	100-120	>160	
<b>28</b>	(L)-OCOCH(CH <sub>3</sub> )NH <sub>3</sub> Cl	50	160	185	

Introduction of hydrophilic and charged acido ligands (e.g. **21**, **22** and **23**; Table 1.3) has provided a mechanism whereby the aqueous solubility can be improved while maintaining maximum antitumour properties.<sup>47</sup> In the case of the trichloroacetate **22** derivative, a significant improvement in toxicity (LD<sub>50</sub> = 440 mg/kg; Table 1.3) was achieved.<sup>47</sup> The synthesis of highly water soluble amino acid derivatives **27** and **28** (Table 1.3) has recently

been reported.<sup>49-51</sup> However, in contrast to all previously studied titanocenes containing weakly coordinating halide or acido ligands **1** and **16-23**, antitumour testing of the amino acid derivatives **27** and **28** respectively gave reduced activity with an OCR of only 50 % against EAT.<sup>49</sup>

**Table 1.4:** Structure activity studies of the influence of monosubstituted titanium complexes against fluid EAT; samples administered in 10%DMSO/saline (pH~3.0)

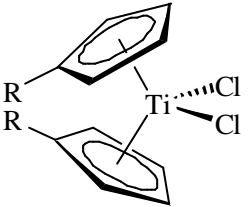
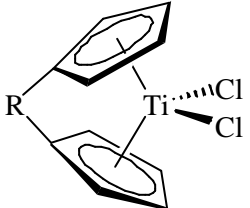
Compound		OCR (%)	ODR (mg/kg)	LD <sub>50</sub> (mg/kg)	Ref	
	No. <b>29</b>	75	80-140	180	52	
	<b>30</b>	31	50-130	130	53	
		X				
	<b>31</b>	2,4,6-OPhCl <sub>3</sub>	50	60-140	200	48
	<b>32</b>	<i>o</i> -SC <sub>6</sub> H <sub>4</sub> CH <sub>3</sub>	25	30-60	60	53
	<b>33</b>	<i>o</i> -SC <sub>6</sub> H <sub>4</sub> NH <sub>2</sub>	13	50-100	100	53

### 1.4.3. Influence of Substitution of the Cyclopentadienyl Rings

Limited studies have been carried out on substitution of the Cp ligands, with all studies to date restricted to titanocene derivatives. Titanocene dichloride **1** analogues with alkyl substituted Cp rings **34-37**, bridged Cp rings **38-40**, or only one Cp ring **30**, showed

significantly reduced antitumour activity compared to the parent compound **1** (Table 1.5).<sup>17,53,54</sup> The methyl groups introduce both potential steric and electronic effects on the Cp rings and the strength of the Cp-Ti bond. Steric effects, however, do not appear to be a significant contributor to the reduced antitumour activity, as substitution of the Cp rings with bulky phenyl groups gave significant antitumour properties compared to the methyl substituted derivative.<sup>17,55</sup> It should be noted, however, that introduction of the alkyl and/or aryl groups reduces aqueous solubility. Thus reduced activity may be related to solubility and transport processes.<sup>56</sup>

**Table 1.5:** Structure activity studies of the influence of substitution of the Cp rings in titanocene complexes against fluid EAT; samples administered in 10%DMSO/saline (pH~3.0)

Compound		OCR (%)	ODR (mg/kg)	LD <sub>50</sub> (mg/kg)	Ref	
	No.	R				
	<b>34</b>	CH <sub>3</sub>	-	-	30	54
	<b>35</b>	N(CH <sub>3</sub> ) <sub>2</sub>	10	80-160	200	54
	<b>36</b>	Si(CH <sub>3</sub> ) <sub>3</sub>	20	280-300	360	54
<b>37</b>	Ge(CH <sub>3</sub> ) <sub>2</sub>	28	240-320	400	54	
	<b>38</b>	CH <sub>2</sub>	13	220-260	360	54
	<b>39</b>	CHCH <sub>3</sub>	10	200-260	320	54
	<b>40</b>	SiHCH <sub>3</sub>	30	160-220	300	54

### 1.5. Hydrolysis Chemistry

While most metallocene dihalides exhibit good solubility and stability in organic solvents, in aqueous solutions, hydrolysis of both the halide ligands and the cyclopentadiene

rings occurs.<sup>17,57-61</sup> The rates of these two processes are highly dependent on the transition metal ion, the nature of the halide ligand, and the solution pH. Freshly prepared solutions of  $\text{Cp}_2\text{MCl}_2$  (M = Ti **1**, Mo **4**, Zr **7**, Hf **8**) in water have pH values 2-3 (depending on sample concentration). When the pH is raised to values approximating physiological values (pH > 6) insoluble precipitates form, and the soluble hydrolysis products are biologically inactive.<sup>46</sup> In the case of titanocene dichloride **1**, the precipitate is likely to include species such as  $\text{TiO}_2$ <sup>62</sup> and polymeric species eg.,  $[(\text{CpTiO})_4\text{O}_2]_n$ <sup>63</sup> or  $\text{Ti}(\text{C}_5\text{H}_5)_{0.31}\text{O}_{0.30}(\text{OH})$ ,<sup>58</sup> which clearly need to be considered in the mechanism of antitumour activity *in vivo*. Due to these problems, most metallocenes have been administered in 10% DMSO/saline solutions at low pH (~3.0). Hence studies have focused on identification of the major species present under these conditions and on the subsequent chemistry that may occur *in vivo* at higher pH values.

### 1.5.1. Halide Hydrolysis

Marks and coworkers have carried out detailed mechanistic studies to establish both the rate of Cp and chloride hydrolysis of several metallocenes in aqueous solutions.<sup>58-61</sup> In unbuffered solutions of water (pH ~3) or in 0.32 M  $\text{KNO}_3$ , reversible rapid hydrolysis of the first chloride ligand occurs in  $\text{Cp}_2\text{MCl}_2$  (M = Ti **1**, V **2**, Mo **4**, Zr **7**) to give an aquated intermediate, followed by a slower dissociation of the second chloride (50 min M = Ti **1**; 30 min M = V **2**; 24 min M = Zr **7**; 6.7 min Mo **4**; Figure 1.7). From Figure 1.7, it can be seen that both the concentration and solution pH will affect the equilibrium reactions, with the rate of chloride hydrolysis expected to be decreased at low pH and/or in high concentrations of salt since the equilibrium lies in favour of the metallocene dichloride. Detailed studies of the hydrolysis of other halide or acido ligands have not been reported, however, all studies are

consistent with a similar rapid dissociation of these ligands (e.g.  $\text{Cp}_2\text{TiX}_2$ ;  $\text{X} = \text{Br}$  **17**<sup>64</sup>,  $\text{X} = \text{OCOCH}=\text{CHCO}_2\text{H}$  **23**,<sup>62</sup>  $\text{OCOCCl}_3$  **22**<sup>62</sup>) to generate aquated species in which the Cp ligands remain coordinated to the metal at low pH.<sup>62,64</sup> It has also been noted that loss of chloride or acido ligands seems to be associated with dissolution of the complexes.<sup>58</sup>

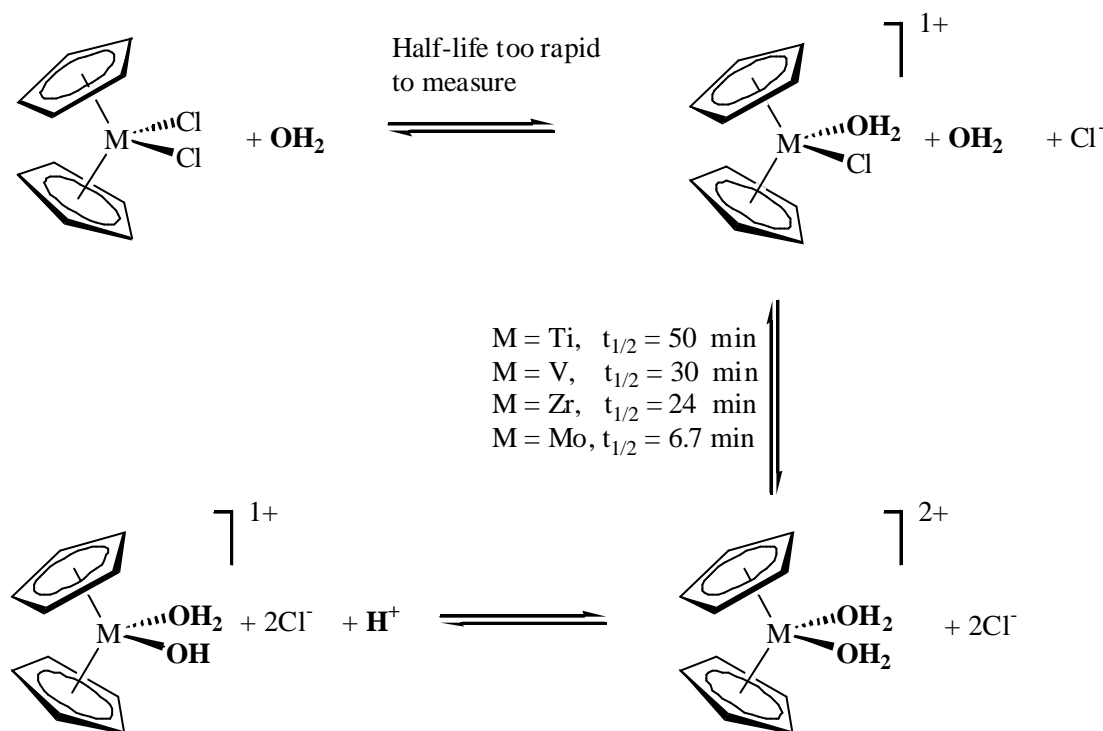


**Figure 1.7:** Hydrolysis of halide ligands in  $\text{Cp}_2\text{MCl}_2$

### 1.5.2. Cyclopentadienyl Ring Hydrolysis

The estimated half lives for loss of the Cp rings in  $\text{Cp}_2\text{MCl}_2$  ( $\text{M} = \text{Ti}$  **1**,  $\text{V}$  **2**,  $\text{Mo}$  **4**,  $\text{Zr}$  **7**) in water or in 0.32 M  $\text{KNO}_3$  at 37 °C and at low pH (pH ~ 3), are as follows:  $\text{Cp}_2\text{ZrCl}_2$  **7** ( $t_{1/2} = 14\text{h}$ )  $\ll$   $\text{Cp}_2\text{TiCl}_2$  **1** ( $t_{1/2} = 57$  h)  $<$   $\text{Cp}_2\text{VCl}_2$  **2** ( $t_{1/2} = 10$  days)  $<$   $\text{Cp}_2\text{MoCl}_2$  **4** (Figure 1.8).<sup>58,60</sup> No ring hydrolysis was reported at low pH for  $\text{Cp}_2\text{MoCl}_2$  **4** for up to 4 weeks.<sup>58</sup>  $\text{Cp}_2\text{MoCl}_2$  **4** and  $\text{Cp}_2\text{VCl}_2$  **2** are the only metallocenes in which the Cp ligands remain metal bound for significant periods of time ( $>24$  h) in aqueous solutions at pH 7.0.

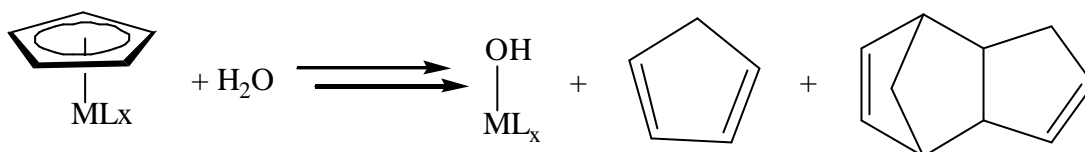


**Figure 1.8:** Hydrolysis of cyclopentadienyl ligands in  $\text{Cp}_2\text{MCl}_2$

The aqueous chemistry of  $\text{Cp}_2\text{NbCl}_2$  **3**, recently reported,<sup>65</sup> has established that the predominant species is a Nb(V) complex. The  $^1\text{H}$  NMR spectrum of  $\text{Cp}_2\text{NbCl}_2$  **3** in 10%  $\text{d}_6$ -DMSO/ $\text{D}_2\text{O}$  contains two sharp singlets consistent with hydrolysis of the halide ligands and oxidation of the paramagnetic Nb(IV) complex to a diamagnetic Nb(V) complex.  $\text{Cp}_2\text{NbCl}_2$  **3** does not dissolve in the absence of oxygen and  $\text{Cp}_2\text{NbCl}_2(\text{OH})$  and  $\text{Cp}_2\text{NbCl}_2$  **3**, when dissolved in 10% DMSO/ $\text{D}_2\text{O}$ , have identical  $^1\text{H}$  NMR spectra, consistent with formation of a Nb(V) complex as the antitumour active species in the solution. On the basis of these studies, it was suggested that the highly water soluble  $\text{Cp}_2\text{NbCl}_2(\text{OH})$  is an excellent candidate for antitumour testing.<sup>65</sup> The rate of Cp hydrolysis increases at higher pH values for niobocene dichloride **3** in aqueous solutions.<sup>65</sup> The half-lives for dissociation of the Cp rings were estimated to be 3 days (pH 1.8), 8-10 h (pH 4.0), 1-2 h (pH 4.8), and < 15 min (pH 6.6).

$\text{Cp}_2\text{ZrCl}_2$  **7** and  $\text{Cp}_2\text{HfCl}_2$  **8** are biologically inactive,<sup>31</sup> consistent with the hydrolytic instability of these metallocenes at both low and high pH values.<sup>58,66</sup> In the case of  $\text{Cp}_2\text{ZrCl}_2$  **7**, ~80-90% of the Cp rings are metal bound after 15 min (pH 2.9); while for  $\text{Cp}_2\text{HfCl}_2$  **8**, extensive hydrolysis was still observed at pH 3.1 and only 40-50% of the Cp rings were metal bound.<sup>66</sup>

### 1.5.3. Infusion Solutions for Clinical Administration

Due to the hydrolysis reactions outlined above, in biological assays, titanocene dichloride **1** has been administered as a 10% DMSO/saline solution (pH ~3).<sup>17</sup> However, reduction in toxic properties was observed when buffered solutions of titanocene dichloride **1** were administered.<sup>46</sup> Samples were prepared at low pH, buffered to pH 5.0-6.0 by addition of NaHCO<sub>3</sub>, and rapidly injected prior to formation of precipitates in the sample.<sup>46</sup>

The species present in the infusion solutions of titanocene dichloride **1** used in clinical trials have been determined.<sup>67</sup> The hydrolysis products in the infusion solutions corresponded to those previously reported in the literature (Figure 1.7 and 1.8) and were dependent on the pH of the infusion solution.<sup>67</sup> The main hydrolysis product, in which the chlorides have been aquated, was stabilised at low pH (pH 1), low concentration of malic acid, and high concentration of chloride ions. However, as infusion of pH ~1 solutions is impractical, the infusion solution used in the clinical studies was raised to pH 3.2-3.5 to reduce destruction of the biological tissue. At this pH, degradation of the main hydrolysis product was slow enough to maintain the applicability of the infusion solution for more than 4h.<sup>67</sup> Analysis of human blood plasma taken from a patient infused with a solution of titanocene dichloride **1** showed no evidence of free titanocene species indicating that significant and rapid hydrolysis of the Cp rings had occurred *in vivo*.<sup>67</sup>

### 1.6. Mechanism of Antitumour Action

While extensive biological and chemical studies have been carried out on titanocene dichloride **1**, the exact mechanism of antitumour action is still not fully understood. The main evidence for DNA as the prime cellular target for titanocene dichloride **1** is from electron

energy loss spectroscopy studies.<sup>23,24</sup> These studies showed that metals derived from  $\text{Cp}_2\text{TiCl}_2$  **1** and  $\text{Cp}_2\text{VCl}_2$  **2**, administered *in vivo*, accumulate in nucleic acid rich regions of EAT cells.<sup>23,24</sup> The same result was also found in xenografted human tumours where intracellular localisation of titanium was observed following administration of titanocene dichloride **1**.<sup>68</sup> The highest concentrations of metals were detected in the nuclear heterochromatin while lower concentrations of metal were detected in the euchromatin. In support of these studies, significant inhibition of DNA and RNA synthesis in tumour cells after *in vivo* and *in vitro* treatment with titanocene dichloride **1** and vanadocene dichloride **2** has been demonstrated.<sup>21,22</sup> DNA synthesis was most suppressed where vanadocene dichloride **2** effected irreversible inhibition of DNA synthesis by 20 % (*in vitro*) at doses as low as  $5 \times 10^{-6}$  mol/L <sup>21</sup>. No data is available on whether any of the other metallocene dihalides exhibit similar effects on nucleic acids, and hence consideration of current mechanisms of antitumour action is restricted to titanocene dichloride **1** and vanadocene dichloride **2**.

Given the hydrolytic instability of titanocene dichloride **1**, the hydrolysis products have been tested as possible active species that are released upon administration. For example, the polymer,  $[(\text{CpTiO})_4\text{O}_2]_n$ , a major hydrolysis product, has been suggested to be slowly decomposing and thus release low doses of cyclopentadiene.<sup>63</sup> Although both monocyclopentadiene and dicyclopentadiene cause non-specific, local tumour inhibition at high doses, they do not have the same systemic antitumour activity as titanocene dichloride **1**, even at ten times the dose of titanocene dichloride **1**.<sup>17</sup> Typical hydrolysis products of  $\text{Cp}_2\text{TiCl}_2$  **1**, such as the polynuclear species  $[(\text{C}_5\text{H}_5)_2\text{TiCl}]_2(\mu\text{-O})$ , which is also a precursor to the insoluble polymer  $[(\text{CpTiO})_4\text{O}_2]_n$ , have shown reduced or sporadic activity against EAT.<sup>17,53</sup> Since titanocene dichloride **1** hydrolysis is rapid at physiological pH, to form species with reduced or

sporadic antitumour activity; lipids, proteins or plasma constituents may stabilise and transport the active titanocene species in blood.<sup>17</sup> In support of this, titanocene dichloride **1** is readily soluble in an aqueous lipid emulsion to give a galenical preparation, which is stable against hydrolysis over a long period with retained antitumour activity.<sup>17</sup> For these reasons a lyophilised preparation of titanocene dichloride **1** has been administered in all human clinical trials carried out so far.<sup>14,16,20</sup>

### 1.6.1. Metallocene-DNA Interactions

*In vitro* studies to fully characterise the nature of titanocene-DNA interactions at the molecular level have been restricted due to the hydrolytic instability of titanocene dichloride **1** under physiological conditions. Hence, studies of both solution and solid-state structures of Cp<sub>2</sub>MC<sub>2</sub> (M= Ti **1**, V **2**, Nb **3**, Mo **4**, Zr **7**, Hf **8**) with nucleic acid constituents (sugars, nucleic bases, nucleosides and nucleotides) have been carried out in order to identify potential coordination complexes that may form *in vivo* with DNA or nucleotides. The key results have been reported in several reviews<sup>12,17,18,57,69</sup>. Illustrative examples of the types of coordination complexes formed are shown in Figure 1.9. Titanocene dichloride **1**<sup>66</sup> and molybdocene dichloride **4**<sup>60</sup> coordinate to both the nucleobase nitrogens and the phosphate oxygens of nucleotides forming discrete complexes (Figure 1.9). However, vanadocene dichloride **2** shows only labile outer-sphere complexation to the phosphate groups.<sup>61</sup> The biologically inactive metallocene dihalides, zirconocene dichloride **7** and hafnocene dichloride **8**, showed no interaction with nucleic acid constituents as a result of rapid hydrolysis (within minutes) of these complexes.<sup>66</sup>

In contrast, whilst niobocene dichloride **3** behaves like titanocene dichloride **1** and

molybdocene dichloride **4**, and forms aquated species with Cp ligands metal bound in solution that could potentially form complexes similar to those shown in Figure 1.9, discrete complexes with nucleotides are not formed. No evidence of binding was detected by  $^1\text{H}$  NMR spectroscopy on addition of up to 2.0 equivalents of niobocene dichloride **3**, with nucleosides, nucleotides and dipeptides.<sup>65</sup> In the case of 5'-dAMP, a minor complex (10%) was detected with 0.5 equiv  $\text{Cp}_2\text{NbCl}_2$  **3** (pH 5.2). The lack of interaction of niobocene dichloride **3** with nucleic acid constituents and amino acids is markedly different to  $\text{Cp}_2\text{MCl}_2$  (M = Ti **1**, V **2**, Mo **4**). This suggests that the mechanism of antitumour action of  $\text{Cp}_2\text{NbCl}_2$  **3** is significantly different to other metallocene dihalides.

Extension of NMR spectroscopy studies of nucleotides to short oligonucleotides has only been possible with molybdocene dichloride **4**. Formation of stable short duplexes requires pH 6-7 where molybdocene dichloride **4** is the only metallocene which shows appreciable hydrolytic stability under these conditions. Studies with oligonucleotides are important, as simultaneous coordination to phosphate (O) and nucleic base (N) sites, which can occur with nucleotides (Figure 1.9), is not possible with DNA. In addition, the steric accessibility of phosphate (O) coordination sites in a DNA duplex is significantly different to these sites in isolated nucleotides. Analysis of a metallocene-DNA complex formed between molybdocene dichloride **4** and sonicated calf thymus DNA (~200 base pairs) using  $^{31}\text{P}$  NMR spectroscopy confirmed the occurrence of phosphate-centred complexes on the backbone and/or termini of the DNA strands.<sup>70</sup> Initial studies of molybdocene dichloride **4** with 6 base-pair oligonucleotides concluded that the formation of phosphate centred complexes on the termini of the duplexes was possible.<sup>57</sup>

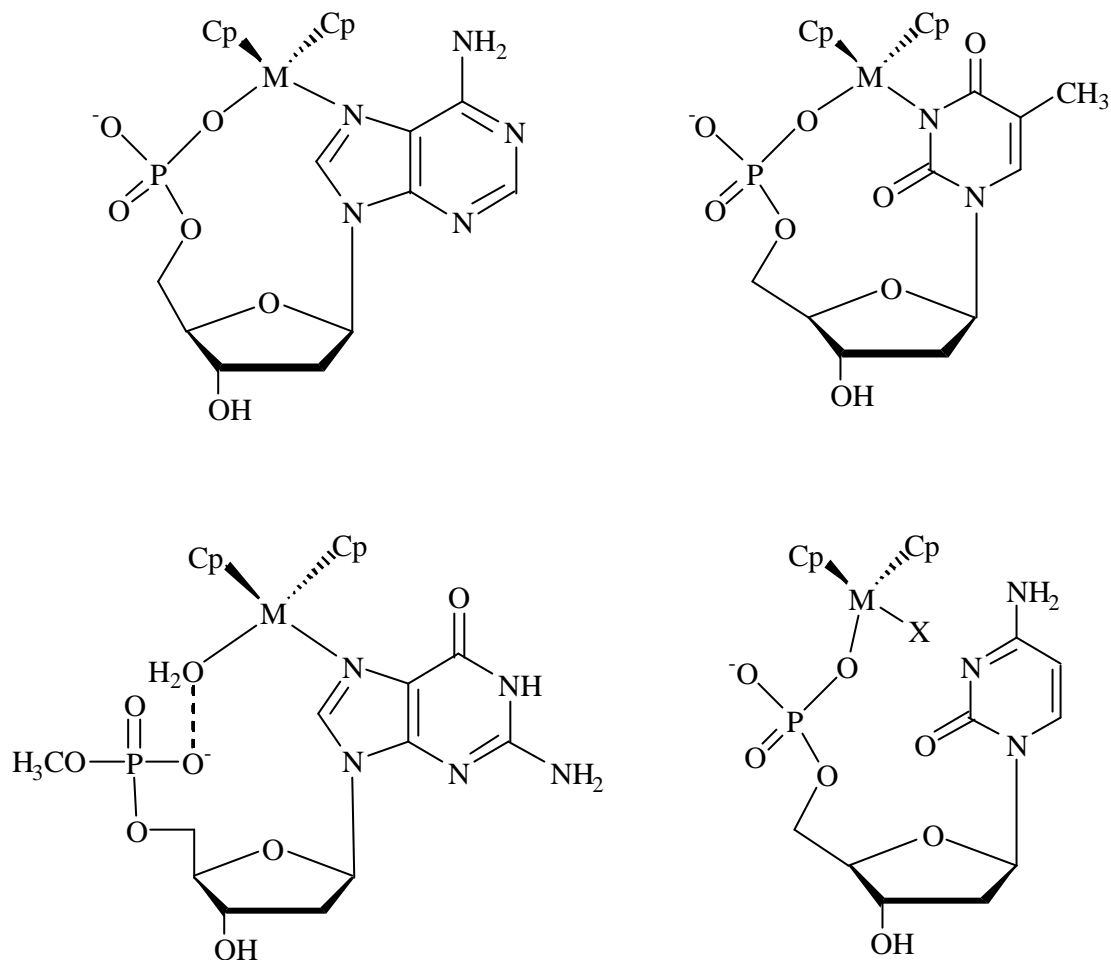


**Figure 1.9:** Representative examples of metallocene complexes with nucleotides

The first experimental data in support of the formation of metallocene-DNA adducts was provided by the characterisation of adducts formed between metallocene dihalides and DNA by inductively coupled plasma (ICP) spectroscopy.<sup>71</sup> However, while distinct adducts were observed with the antitumour active metallocene dichlorides  $\text{Cp}_2\text{TiCl}_2$  **1** and  $\text{Cp}_2\text{NbCl}_2$  **3**, they were not detected with  $\text{Cp}_2\text{VCl}_2$  **2**, which is the most active metallocene *in vitro*. The significance of these results is unclear, as DNA adducts were also detected with  $\text{Cp}_2\text{ZrCl}_2$  **7** and  $\text{Cp}_2\text{HfCl}_2$  **8**, which show no anticancer activity. In the case of  $\text{Cp}_2\text{TiCl}_2$  **1**, the use of

tritium labelled DNA showed that two distinct adducts were formed. At pH 5.3 two Cp rings are associated with the DNA adduct while at pH 7.0 only one Cp ring was associated with the DNA adduct. AAS has also been used recently to show that the Ti from Cp<sub>2</sub>TiCl<sub>2</sub> **1** binds DNA.<sup>37</sup> The amount of adduct formation increased with time and was most prominent after 15 h of treatment of the DNA with Cp<sub>2</sub>TiCl<sub>2</sub> **1**.<sup>37</sup>

UV Spectroscopy has also been used in an attempt to characterise the interaction of metallocenes with DNA.<sup>41,72,73</sup> *In vitro* incubation of DNA or RNA with metallocenes has shown that the secondary structure of the nucleic acids may be disrupted.<sup>41</sup> In a separate study, an interaction between DNA and titanocene dichloride **1** has been attributed to the decreasing UV absorbance of DNA incubated with titanocene dichloride **1** over time.<sup>72</sup>

### 1.6.2. Metallocene-Protein Interactions

The hydrolysis chemistry and lack of interaction of several metallocenes, notably Cp<sub>2</sub>MoCl<sub>2</sub> **4**, with oligonucleotides as models of DNA at pH 7.0, has resulted in consideration of amino acids and proteins as potential binding targets for metallocenes. The synthesis of the amino acid analogues of titanocene dichloride, **27** and **28** respectively, confirmed that coordination of amino acids such as glycine and L-alanine to titanium in preference to chloride can occur under certain conditions.<sup>50,51</sup>

Targeting of proteins involved in cellular proliferation can potentially lead to cell death due to a disruption in this process. Preliminary studies have shown that both protein kinase C, an enzyme involved in cellular proliferation, and bacterial topoisomerase II, are significantly inhibited by Cp<sub>2</sub>VCl<sub>2</sub> **2** and Cp<sub>2</sub>MoCl<sub>2</sub> **4**.<sup>57</sup> These studies implicate these proteins in the mechanism of action of antitumour metallocenes. However, full details of these studies have

not been published. Topoisomerase II was investigated as a target since antitumour metallocenes were observed to inhibit cellular DNA synthesis *in vitro* by arresting cells preferentially at the G2 or at the G1/G2 phases of the cell cycle.<sup>41</sup> This phenomenon has been observed for other antitumour drugs that target topoisomerase II.<sup>74</sup>

Rapid hydrolysis of titanocene dichloride **1** occurs in the absence of biomolecules to give insoluble precipitates. Titanium species, upon intravenous administration, nevertheless are transported into cells. Therefore, the stabilisation and/or transport of  $\text{Cp}_2\text{TiCl}_2(\text{aq})$  **1** *in vivo* must be considered in the mechanism of antitumour action.

Human blood plasma contains about 600 proteins. In reactions of metal complexes with plasma proteins, their concentration and size, relative affinity between the metal ion and protein and the type and amounts of the amino acids exposed on the surface of the protein need to be considered.<sup>75</sup> Analysis of human blood plasma taken from a patient infused with a solution of titanocene dichloride **1** showed no evidence of free titanocene species (see 1.5. Hydrolysis Chemistry). Furthermore, following separation of the of the plasma proteins, all the titanium was associated with a single unidentified protein.<sup>67</sup>

Pharmacokinetic studies, which accompanied the clinical trials, also confirm that Ti-protein interactions are important. Following intravenous injection into patients the titanium from titanocene dichloride **1** is > 70 % of the protein bound in plasma.<sup>14,16</sup> The concentration of titanium in a sample of plasma was compared to the amount of titanium in a sample of ultrafiltrate plasma (MWCO 30 000) using AAS. Only the titanium content could be measured since efforts to measure the amount of titanocene dichloride **1** in blood or plasma were unsuccessful.<sup>14</sup> This result supports previous results that show rapid hydrolysis of

titanocene dichloride **1** at pH 7.4 and suggests that a Ti(IV) species is protein bound and delivered to cancer cells once titanocene dichloride **1** is injected intravenously.

Despite the presence of a large number of proteins in blood plasma, which serve a number of roles, there are relatively few proteins that are involved in metal transport. The two proteins of major importance are serum albumin and transferrin.<sup>75</sup> No comprehensive studies on serum albumin binding have been reported. However, several very recent papers, published in the course of this work, have focused on titanocene-transferrin interactions and provided important new data regarding both the biologically active species generated *in vivo* and potential transport mechanisms.<sup>76,77</sup> Ti(IV) derived from titanium(IV) citrate<sup>76,77</sup> or titanocene dichloride **1**<sup>76</sup> was shown to form a strong complex with human serum transferrin by binding to each of the two specific Fe(III) binding sites in this protein.<sup>76,77</sup> The Ti<sub>2</sub>-transferrin complex is quite stable within the pH range 5.5-9.0.<sup>77</sup>

Sadler and co-workers<sup>78</sup> have also reported that upon uptake of Cp<sub>2</sub>TiCl<sub>2</sub> **1** by transferrin into the specific iron binding sites, Cp and Cl ligands are released to form Ti<sub>2</sub>-hTF. These results imply that a labile Cp-Ti bond is essential to generate a Ti(IV) species that is bound to transferrin.

The binding of Ti(IV) to hTF is favoured at pH 7.4, requiring several hours for completion, but complexation is reversible at pH ca. 5.5.<sup>78-80</sup> A model study using *N,N'*-ethylenebis(*o*-hydroxyphenylglycine) as a mimic of the transferrin binding site showed that Ti(IV) binds selectively to the chelating agent at neutral pH. However, at pH < 5.5, intermolecular Ti(IV) transfer from the complex to ATP occurs.<sup>78,80</sup>

As human serum transferrin has been implicated in the transport of Ga(III) and Ru(III)

(among other metals), to cancer cells, a mechanism whereby titanium derived from titanocene dichloride **1** is delivered to cancer cells was proposed.<sup>79</sup> At pH 5.5 Ti(IV) is released from transferrin and preferentially binds to ATP.<sup>78,80</sup> Thus, following delivery of the Ti(IV) by transferrin to the cancer cells which are known to over-express transferrin receptors and have a lower intracellular pH (ca. 5.5), the Ti(IV) could be released and become available for complexation with DNA.<sup>78,80</sup> An earlier serum fractionation study involving <sup>45</sup>Ti radiolabelling experiments provided supporting evidence for this mechanism since Ti(IV) was only found to be associated with transferrin and no other protein both *in vivo* and *in vitro*.<sup>81</sup>

The stabilisation of vanadocene dichloride **2** by blood plasma has also been investigated.<sup>82</sup> However, in contrast to titanocene dichloride **1**, EPR spectroscopy studies showed no evidence for the interaction of vanadocene dichloride **2** with any of the blood components investigated.<sup>82</sup>

### **1.7. Aims of this Work**

While titanocene dichloride **1** is in phase II clinical trials, the molecular level basis for the antitumour activity of the complex is poorly understood. The design of experiments to provide details of these interactions has been hampered by the poor solubility and stability of titanocene dichloride **1** in water at pH 7. While DNA has been implicated in the mechanism of antitumour action, there are no detailed studies of the binding sites of titanocene dichloride **1** with DNA or DNA fragments under physiological conditions. Furthermore, the interaction of titanocene dichloride **1** with other potential coordinating groups present in blood plasma proteins or cellular proteins involved in cell replication has not been considered in detail.

The major aim of this thesis was to study the aqueous chemistry and interactions with

biomolecules of metallocene dihalides, using a range of techniques, and thus contribute to the understanding of the mechanism of antitumour action. Most of the work focused on titanocene dichloride **1**, as this is the only metallocene in clinical trials, and side-effects and problems with administration have been identified. In contrast to titanocene dichloride **1**, much less is known about the fundamental coordination chemistry, or the principle cellular targets related to antitumour activity for the other antitumour metallocenes in which the central metal has been varied ( $\text{Cp}_2\text{MCl}_2$ ,  $\text{M} = \text{V}$  **2**,  $\text{Nb}$  **3**,  $\text{Mo}$  **4**). Hence studies were also carried out on these metallocene dihalides, which have vastly different coordination chemistries and stabilities to titanocene dichloride **1**. In the long term, this information is required for the rational design of new metallocene based drugs that may have improved or different biological activity to titanocene dichloride **1**.

Chapter 2 outlines a study of the interactions of molybdocene dichloride **3** with oligonucleotides under approximate physiological conditions. Chapter 3 describes the design and synthesis of hydrolytically stable derivatives of titanocene dichloride **1**, suitable for administration under physiological conditions and Chapter 4 reports the effect of DMSO on the solubility, stability and coordination chemistry of  $\text{Cp}_2\text{TiY}_2$  where  $\text{Y} = \text{Cl}$ , **1**,  $\text{OCOCCl}_3$  **22**,  $\text{OCOCH}_2\text{NH}_3\text{Cl}$  **27**. Chapters 5 and 6 report the interactions of metallocene dichlorides with topoisomerase II, calf thymus DNA, HSA and glutathione. The Experimental procedures are summarised in Chapter 7, followed by overall conclusions to the work outlined in this thesis.

While the bulk of current evidence suggests that DNA is the principal cellular target of the metallocene dihalides, no molecular level picture of the nature of metallocene-DNA interactions has emerged. As discussed in Section 1.5, studies of the hydrolysis and coordination chemistry of several metallocenes,<sup>58-61,65,66</sup> as well as their interaction with calf thymus DNA,<sup>70,71</sup> strongly suggests that each of the metallocene dihalides acts *via* an independent, and probably unrelated, mechanism. Full characterisation of metallocene-DNA adducts has been hampered by their hydrolytic instability in water at physiological pH values,<sup>58,59</sup> and therefore the basis for rational modification of the metallocene framework or the development of related complexes as antineoplastic agents is lacking.

From an experimental point of view, Cp<sub>2</sub>MoCl<sub>2</sub> **4** offers the advantage of appreciable stability to Cp hydrolysis at approximately physiological pH.<sup>59,60</sup> Therefore, Cp<sub>2</sub>MoCl<sub>2</sub> **4** is the most promising candidate for characterising the nature of metallocene-DNA interactions at the molecular level using <sup>1</sup>H and <sup>31</sup>P NMR spectroscopy. The characterisation of both solution and solid-state molybdocene adducts with a range of nucleic acid constituents has been reported previously,<sup>60</sup> confirming that formation of molybdocene-nucleic acid adducts *in vivo* is feasible. Recent preliminary studies reported that Cp<sub>2</sub>MoCl<sub>2</sub> **4** interacts primarily with the terminal phosphorylated end of short oligonucleotides.<sup>57</sup> Independent <sup>31</sup>P NMR spectroscopy studies with calf thymus DNA, supported formation of phosphate-centred complexes on the backbone and/or termini of the DNA strand.<sup>70</sup>

In this work, the first detailed analysis of the interaction of Cp<sub>2</sub>MoCl<sub>2</sub> **4** with oligonucleotides in aqueous solutions at approximately physiological pH was carried out. These studies were undertaken in order to provide a molecular level picture of molybdocene-

DNA interactions using high field NMR spectroscopy. Oligonucleotides were chosen in order to assess whether  $\text{Cp}_2\text{MoCl}_2$  **4** shows any base sequence selectivity, preferential interaction with phosphate (O) versus nucleic base (N) coordination sites and to obtain further information on the relative stabilities of molybdocene-DNA adducts under physiological conditions.

## 2.1. Hydrolysis Chemistry of Molybdocene Dichloride **4**

Prior to carrying out titration experiments, the hydrolysis of  $\text{Cp}_2\text{MoCl}_2$  **4** under the conditions required for preparation of oligonucleotide samples was studied. The hydrolysis in water of the Cp and chloride ligands in  $\text{Cp}_2\text{MoCl}_2$  **4** has been well characterised by Kuo *et al.*<sup>60</sup> Rapid hydrolysis of the two chloride ligands occurs to give an acidic solution (pH 2.0); the predominant species is believed to be the charged complex  $\text{Cp}_2\text{Mo}(\text{OH})(\text{OH}_2)^+$ .<sup>60</sup> Negligible hydrolysis of the Cp rings occurs in the range pH 2.0-7.0. In order to provide reference spectra for comparison with titration spectra obtained with d(ATGGTA) and d(CG CATATGCG)<sub>2</sub> and the dinucleotides dAT and dCG, the rate of Cp hydrolysis in  $\text{Cp}_2\text{MoCl}_2$  **4** at different pH values in 50 mM NaCl was determined. The saline concentration was chosen so that it fell in the range that is typically found *in vivo*, i.e. 4 mM inside the cell to 104 mM in the blood.

<sup>1</sup>H NMR spectra of freshly prepared samples of  $\text{Cp}_2\text{MoCl}_2$  **4** in 50 mM NaCl at pD 2.4 showed the presence of two sharp Cp signals (Figure 2.1a). The spectrum remained unchanged after 24 h, consistent with the presence of two molybdocene species in which the Cp rings are metal bound. No significant Cp hydrolysis occurred as evidenced by the absence

of multiplets corresponding to cyclopentadiene or dicyclopentadiene, or the appearance of any other signals in the  $^1\text{H}$  NMR spectrum.

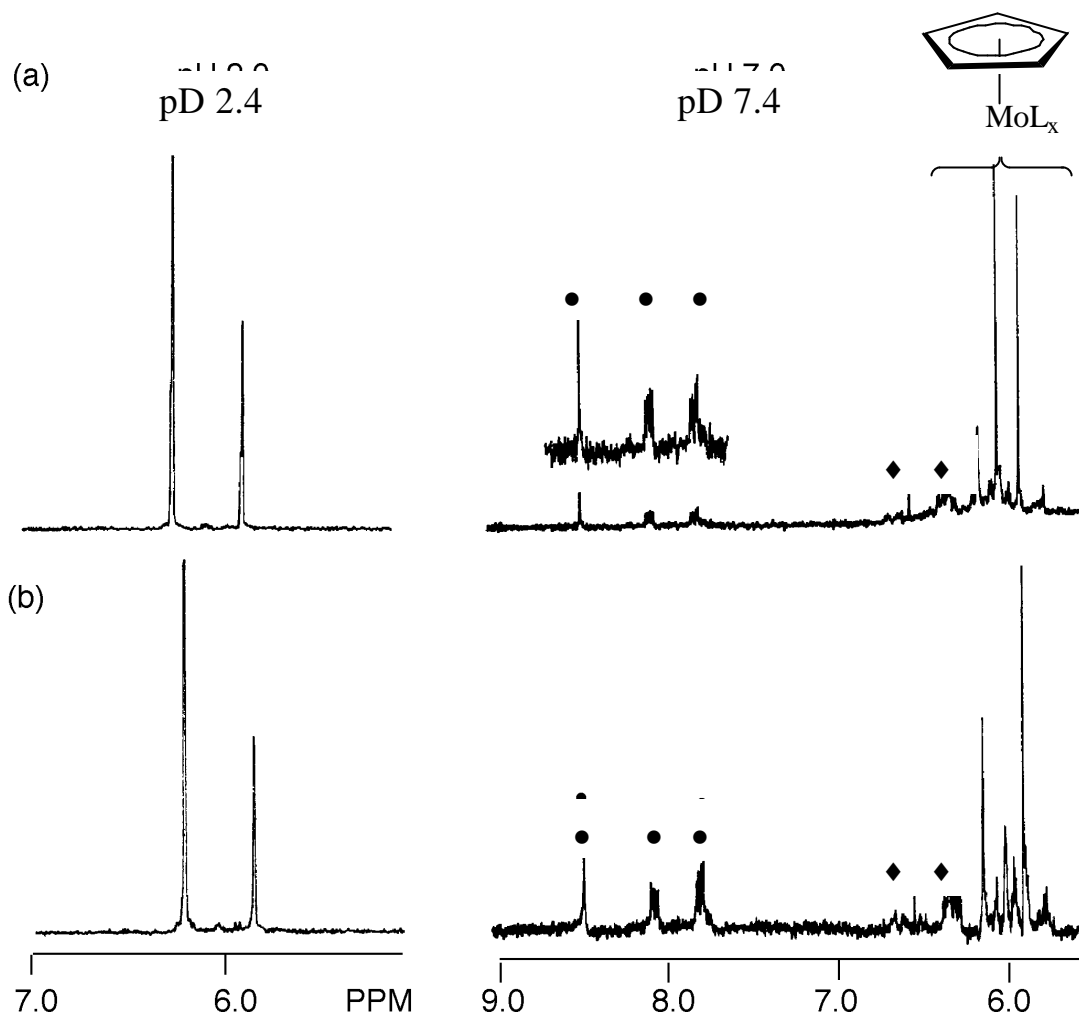


**Figure 2.1:**  $^1\text{H}$  NMR spectra (200 MHz, 50 mM NaCl,  $\text{D}_2\text{O}$ , 25  $^\circ\text{C}$ ) showing the aromatic region of  $\text{Cp}_2\text{MoCl}_2(\text{aq})$  at pD 2.4 and pD 7.4 at times (a) 10 min (b) 24 h after dissolution, • = peaks assigned to hydrolysis product(s), ◆ = cyclopentadiene and dicyclopentadiene

In contrast, at higher pD values in 50 mM NaCl,  $\text{Cp}_2\text{MoCl}_2$  **4** undergoes some Cp hydrolysis. The pD values of freshly prepared samples (pD 1.4-1.9) was raised to either pD 7.4 - 7.9 or pD 9.4 - 9.9, and NMR spectra were recorded over a 24 h period. The relative intensities of the signals in these spectra varied with each sample, but a typical example

is shown in Figure 2.1. At pD ~ 7.4, in addition to two sharp signals around 6 ppm (Figure 2.1a), assigned to metal-bound Cp rings, signals assigned as arising from cyclopentadiene and dicyclopentadiene were observed (indicated by  $\blacklozenge$ ). Some precipitate was also visually observed in these samples. In addition, an unusual set of resonances, not previously observed in related hydrolysis experiments,<sup>58-61</sup> appeared at around 8 ppm and 8.5 ppm (Figure 2.1, indicated by  $\bullet$ ). After 24 h (Figure 2.1b), the relative intensities of the metal-bound Cp signals changed to give two major singlets (5.9, 6.1 ppm) with the singlet at 6.0 ppm reduced in intensity compared to the initial spectrum. In addition, the relative intensities of the downfield signals increased with time. By integration of all signals (Figure 2.1b) it was estimated that ~70% of the species in solution contained metal bound Cp rings. Increasing the pD to ~9.4-9.9 gave very similar results to those observed at pD 7.4 (data not shown).

At high pD in 50 mM NaCl, the exact nature of the species present is difficult to determine as the chloride ion concentration is expected to have a significant influence on the initial rates of hydrolysis of the two chloride ligands as compared to the hydrolysis in pure water. The sharp singlets at ~6.0 ppm were tentatively assigned to increased amounts of species containing a bound chloride ligand eg.,  $\text{Cp}_2\text{Mo}(\text{H}_2\text{O})\text{Cl}^+$ ,  $\text{Cp}_2\text{Mo}(\text{OH})\text{Cl}$ . The signals at 8.0-8.5 ppm have not been assigned, but the sharp downfield singlet (8.5 ppm) is consistent with a metal-bound Cp ring, possibly an intermediate hydrolysis product in which only one Cp ring is bound to the metal centre. Similar signals have not been observed in any of the previous studies of  $\text{Cp}_2\text{MoCl}_2$  **4** (or other metallocenes) with nucleic acid constituents,<sup>59,60,65,66</sup> but these experiments were all carried out at lower pH values and in the absence of salt. As all samples were handled in air, it is possible that these peaks arise due to oxidation of  $\text{Cp}_2\text{MoCl}_2$  **4** at higher pH. While the oxidation chemistry of  $\text{Cp}_2\text{MoCl}_2$  **4** has not

been fully characterised, a number of molybdenum containing species have been reported<sup>83,84</sup> which could arise from oxidation and/or hydrolysis of  $\text{Cp}_2\text{MoCl}_2$  **4**. The precipitate that formed could also arise from oxidation in addition to hydrolysis of the halide and Cp rings of the metallocene. Due to the uncertainty in defining the halide or pseudohalide ligands bound at different pD values, and the presence of minor unidentified hydrolysis products at pD 7.4, the notation  $\text{Cp}_2\text{MoCl}_2(\text{aq})$  is used in this chapter to refer to an aqueous solution of  $\text{Cp}_2\text{MoCl}_2$  **4** in 50 mM salt.

## 2.2. Oligonucleotide Titrations

NMR spectroscopy was used to monitor titration experiments with three different oligonucleotides. The self-complementary 10-base pair sequence  $\text{d}(\text{CGCATATGCG})_2$ , was used as a model of double-stranded DNA. These results were compared with the non-self complementary sequence  $\text{dATGGTA}$ , which was used as a model for single-stranded DNA. Titration experiments with the dinucleotides  $\text{dAT}$  and  $\text{dCG}$ , the nucleotide 5'- $\text{dAMP}$ , and the nucleosides adenosine and guanosine were also carried out in order to assist in the interpretation of spectra with the oligonucleotides. The oligonucleotides and dinucleotides selected in this work lacked terminal phosphates in order to preclude the possible formation of complexes involving sterically accessible terminal phosphate groups. These had been reported previously to be the primary mode of binding between  $\text{Cp}_2\text{MoCl}_2$  **4** and calf thymus DNA.<sup>70</sup> Furthermore, terminal phosphate groups are not present in chromosomal DNA. Formation of adducts involving relatively non-labile binding of a molybdocene species to coordination sites other than a terminal phosphate would provide more conclusive evidence for DNA being a feasible target *in vivo*.

Titration experiments were carried out by adding 0.5, 1.0, and 2.0 equiv. of a salt solution of  $\text{Cp}_2\text{MoCl}_2(\text{aq})$  to each of the oligonucleotides d(ATGGTA), d(CGCATATGCG)<sub>2</sub>, dAT and dCG. All spectra were recorded by Dr. Joel Mackay from the Department of Biochemistry at the University of Sydney.<sup>85</sup> The pD was adjusted to 6.4-7.9 after each addition, and one dimensional <sup>1</sup>H and <sup>31</sup>P NMR spectra were recorded. Phosphate buffer, which is generally used for the study of drug-oligonucleotide complexes, was not used as blank experiments showed that  $\text{Cp}_2\text{MoCl}_2$  **4** binds significantly to this buffer. As complete dissolution of  $\text{Cp}_2\text{MoCl}_2$  **4** did not generally occur (see Experimental), the quoted equiv. refer to the theoretical equiv. present in a completely homogeneous solution.

### 2.2.1. Duplex DNA

Figure 2.2 shows the spectra obtained on titration of 1.0 and 2.0 equiv. of  $\text{Cp}_2\text{MoCl}_2(\text{aq})$  into the duplex 10-mer d(CGCATATGCG)<sub>2</sub>. Preliminary experiments were carried out by Prodigalidad and Lucas.<sup>85</sup> The spectra showed the appearance of several new sharp resonances (indicated by ●). The relative intensities of these resonances, which correspond to the peaks observed in the hydrolysis experiments of  $\text{Cp}_2\text{MoCl}_2(\text{aq})$  under identical experimental conditions (Figure 2.1), increased on addition of each equiv. of  $\text{Cp}_2\text{MoCl}_2(\text{aq})$ .

Two sets of symmetrical pairs of multiplets centred at ~ 6.5 ppm were also detected (indicated by ◆). These signals are characteristic of deuterocyclopentadiene and were assigned to cyclopentadiene and dicyclopentadiene, arising from some

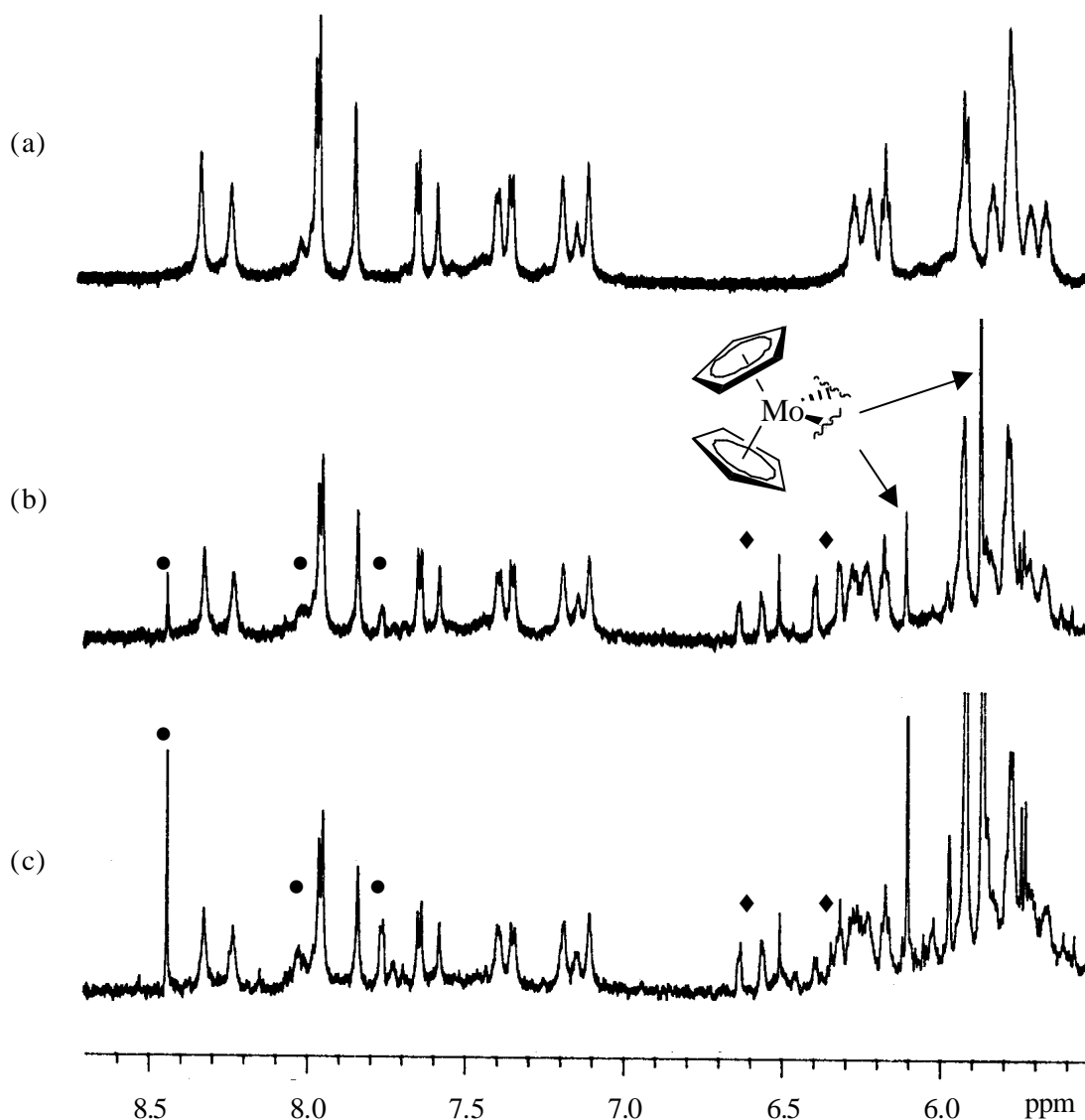


**Figure 2.2:**  $^1\text{H}$  NMR spectra (600 MHz, 50 mM NaCl,  $\text{D}_2\text{O}$ , pD 6.9-7.4, 25  $^\circ\text{C}$ ) showing the aromatic region of  $\text{d}(\text{CGCATATGCG})_2$  on titration of  $\text{Cp}_2\text{MoCl}_2(\text{aq})$  (a) 0 equiv. (b) 1.0 equiv. (c) 2.0 equiv; ● = peaks assigned to hydrolysis product(s), ◆ = cyclopentadiene and dicyclopentadiene

hydrolysis of the Cp rings and assigned previously in related experiments.<sup>60,66</sup> Two sharp singlets at 5.9 and 6.1 ppm were assigned to the Cp protons of the uncomplexed molybdocene  $\text{Cp}_2\text{MoCl}_2(\text{aq})$  (Figure 2.2b).  $^{31}\text{P}$  NMR spectra recorded after each addition,

showed no evidence of formation of a phosphate (O)-centred complex. In particular, a  $^{31}\text{P}$  signal approximately 35-40 ppm downfield of the backbone phosphorus resonances, which is characteristic of Mo phosphate (O) coordination,<sup>60</sup> was not observed (data not shown). Addition of further equiv. of  $\text{Cp}_2\text{MoCl}_2(\text{aq})$  increased the amount of hydrolysed metallocene present, and resulted in formation of dark precipitate which was not characterised, but assumed to be hydrolysed metallocene.

### 2.2.2. Single-Stranded DNA

Figure 2.3 shows the spectra obtained on titration of 1.0 and 2.0 equiv. of  $\text{Cp}_2\text{MoCl}_2(\text{aq})$  with the 6-mer single-stranded oligonucleotide d(ATGGTA), under identical conditions to those used in the titration experiment carried out with the duplex d(CGCATATGCG)<sub>2</sub>. The spectra obtained with d(ATGGTA) (Figure 2.3) showed similar trends to those observed with d(CGCATATGCG)<sub>2</sub>, notably the appearance of downfield signals at 8.5 and 8.0 ppm (indicated by ●). Signals due to cyclopentadiene were also observed (6.4- 6.6 ppm) (data not shown- see Figure 2.2 for similar characteristic peaks). As in the case of d(CGCATATGCG)<sub>2</sub>, there was no change in the  $^{31}\text{P}$  NMR spectra (data not shown), indicating no interaction with the phosphate backbone.

In order to assess the effect of pD on the interaction of  $\text{Cp}_2\text{MoCl}_2$  **4** with oligonucleotides, a second experiment was carried out in which the solution pD was not adjusted to pD 7.4 after each titration (Figure 2.4). Due to the highly acidic nature of freshly dissolved  $\text{Cp}_2\text{MoCl}_2(\text{aq})$  (pD ~1) addition of 1.0 equiv. of  $\text{Cp}_2\text{MoCl}_2(\text{aq})$  to a solution of d(ATGGTA) resulted in a solution of pD 3.4 (Figure 2.4c). For comparison, a reference

spectrum was also recorded of d(ATGGTA) at the same pD values by addition of a solution of DCl (Figure 2.4b).

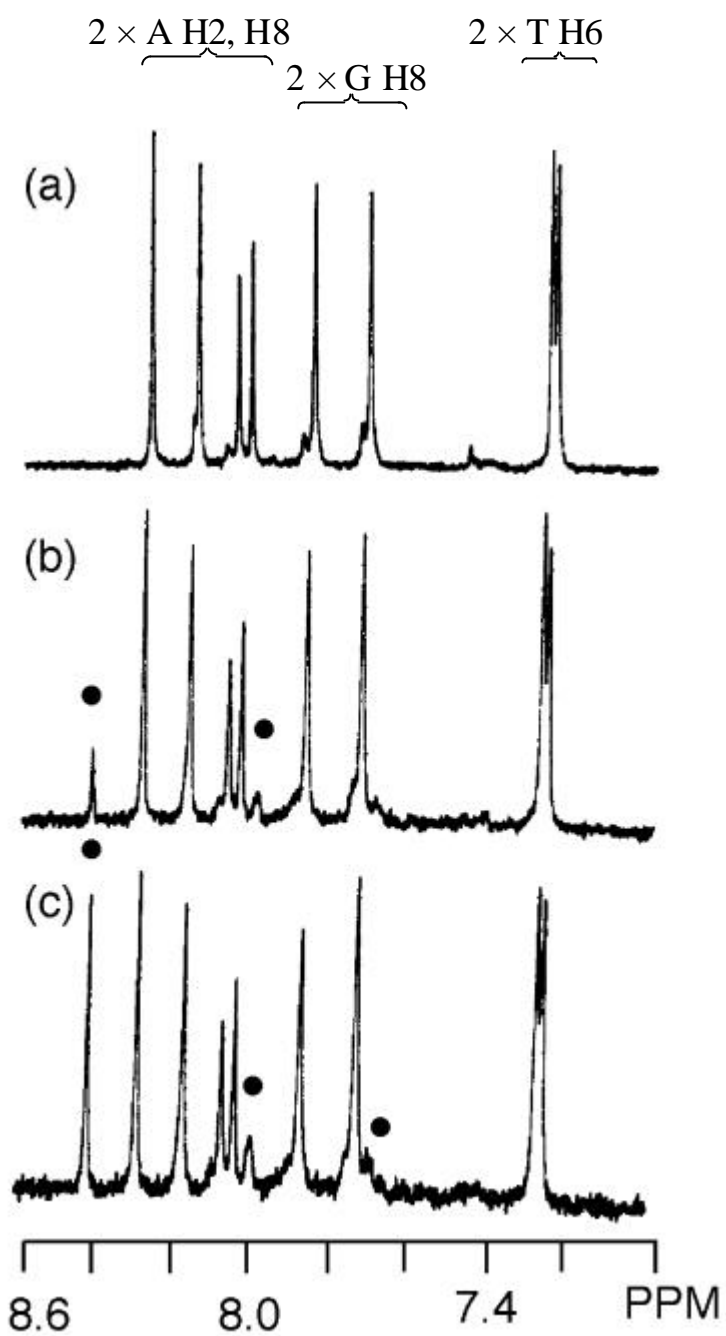


**Figure 2.3:**  $^1\text{H}$  NMR spectra (600 MHz, 50 mM NaCl,  $\text{D}_2\text{O}$ , pD 7.2-7.6, 25  $^\circ\text{C}$ ) showing the aromatic region of d(ATGGTA) on titration of  $\text{Cp}_2\text{MoCl}_2(\text{aq})$  (a) 0 equiv. (b) 1.0 equiv. (c) 2.0 equiv;  $\bullet$  = peaks assigned to hydrolysis product

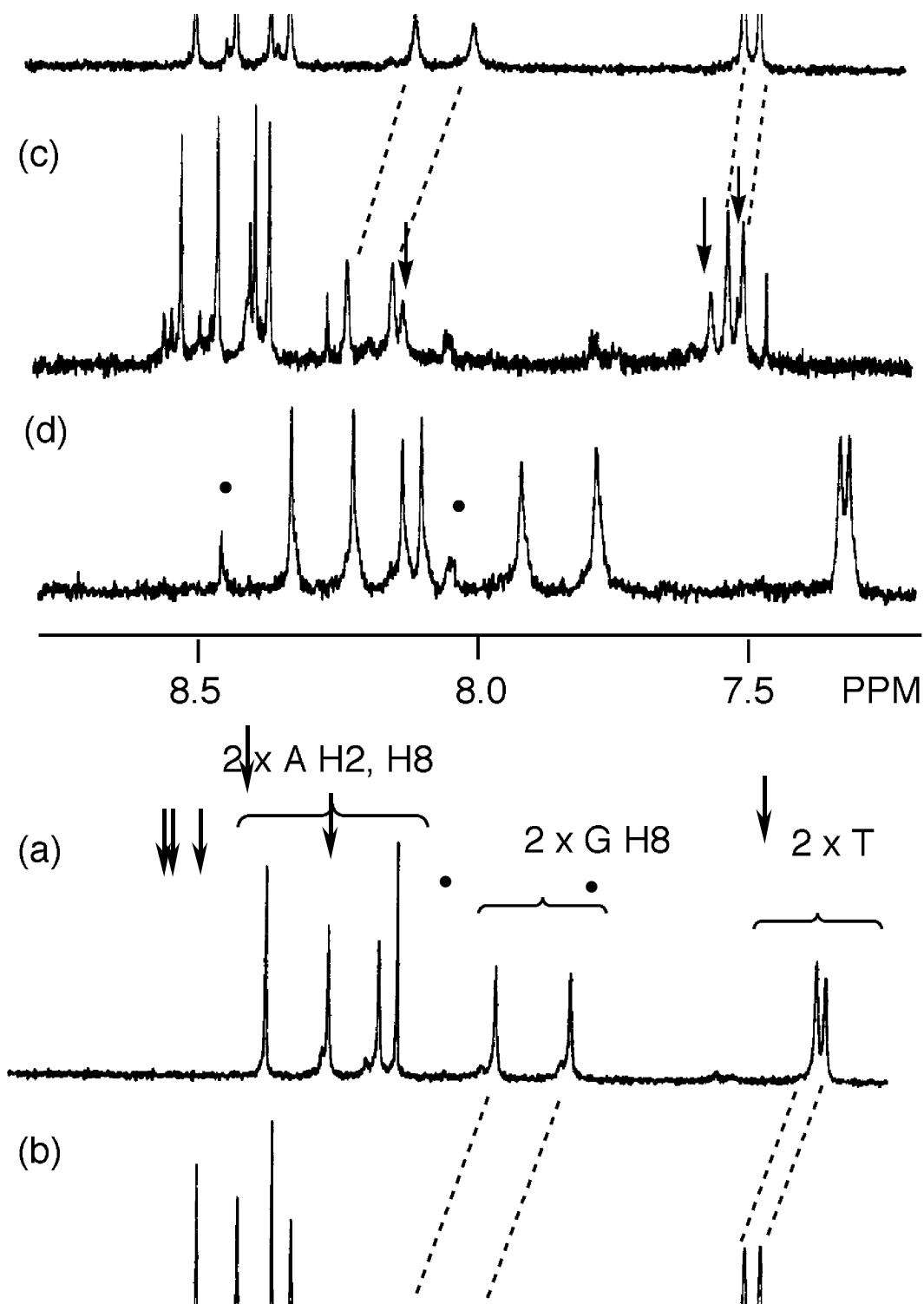


**Figure 2.4:**  $^1\text{H}$  NMR spectra (600 MHz, 50 mM NaCl,  $\text{D}_2\text{O}$ , 25  $^\circ\text{C}$ ) showing the aromatic region of d(ATGGTA) at (a) pD 7.5 and (b) pD 3.4 and following the addition of  $\text{Cp}_2\text{MoCl}_2(\text{aq})$  (c) 1.0 equiv. pD 3.4 (d) 2.0 equiv. pD 7.6; • = peak assigned to hydrolysis product(s); arrows indicate signals assigned to adduct

Figures 2.4a and 2.4b show the 600 MHz  $^1\text{H}$  NMR spectra of d(ATGGTA) at pD 7.5 and pD 3.4 respectively. In addition to some changes in chemical shift that occur on lowering the solution pD, some broadening of the 2 guanine H8 protons was observed (Figure 2.4b). Upon addition of 1.0 equiv. of  $\text{Cp}_2\text{MoCl}_2(\text{aq})$ , several new resonances were observed (Figure 2.4c, indicated with arrows). The relative intensities of these new peaks increased upon addition of a second equiv. of  $\text{Cp}_2\text{MoCl}_2(\text{aq})$  (data not shown). While it was not possible to unequivocally assign all of the new resonances as arising specifically from one oligonucleotide-metalocene complex, the new thymine and guanine signals (Figure 2.4c, indicated with arrows) were consistent with binding of  $\text{Cp}_2\text{MoCl}_2(\text{aq})$  to the oligonucleotide. The formation of new adenine resonances was also consistent with formation of a complex (Figure 2.4c). Upon addition of another equiv. of  $\text{Cp}_2\text{MoCl}_2(\text{aq})$  and raising the solution pD to 7.6, the new peaks disappeared and only signals due to the oligonucleotide d(ATGGTA) and hydrolysis products were observed (Figure 2.4d; indicated by ●)

### 2.2.3. Dinucleotides

In order to confirm the peak assignments made with the oligonucleotide d(ATGGTA), a similar set of titration experiments were carried out with the dinucleotides dCG and dAT. Titration of  $\text{Cp}_2\text{MoCl}_2(\text{aq})$  to either dAT or dCG (Figure 2.5c) and maintaining the pD at ~7.4 showed no evidence for formation of any complexes by either  $^{31}\text{P}$  or  $^1\text{H}$  NMR spectroscopy, and the only new signals were assigned to hydrolysis products (Figure 2.5c, indicated by ●). However, in the case of dCG at low pD values, new signals were observed consistent with the formation of a metallocene-dinucleotide complex (Figure 2.5b, indicated by arrows). In particular a

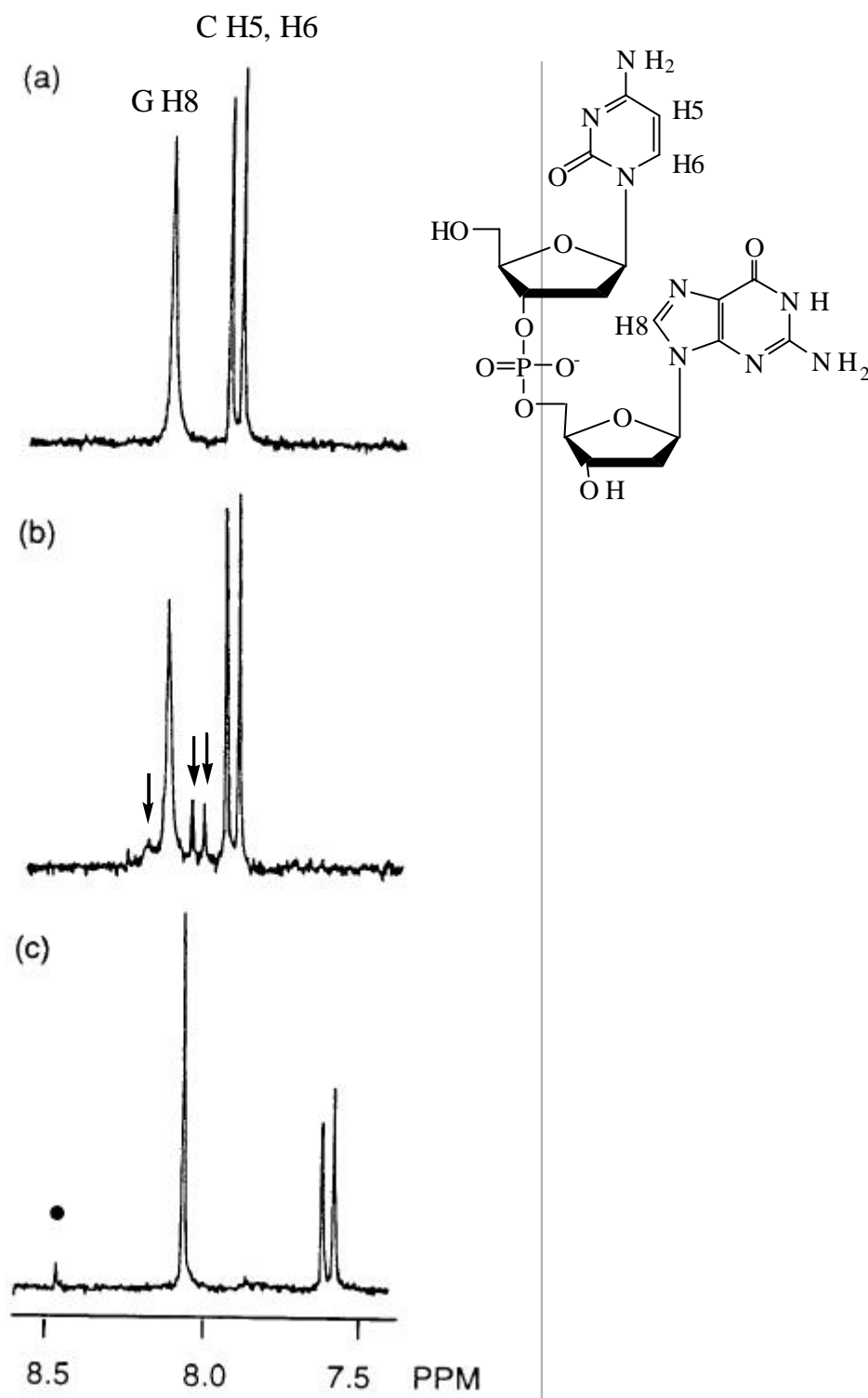


**Figure 2.5:**  $^1\text{H}$  NMR spectra (200 MHz, 50 mM NaCl,  $\text{D}_2\text{O}$ , 25  $^\circ\text{C}$ ) showing the aromatic region of dCpG on titration of  $\text{Cp}_2\text{MoCl}_2(\text{aq})$  (a) 0 equiv, pD 3.4 (b) 1.0 equiv, pD 3.4, and (c) 1.0 equiv, pD 7.4; • = peak assigned to hydrolysis product(s), arrows indicate signals assigned to adduct

new downfield doublet, assigned to H6 of cytosine in the complex appeared and persisted over 24 h. This complex was only stable at low pD values, as increasing the pD to 7.4 resulted in disappearance of these new signals, and formation of minor amounts (<5%) of hydrolysed metallocene (Figure 2.5c, indicated by ●) and some cyclopentadiene. Lowering the pH again resulted in reappearance of the signals assigned to the complex, and confirmed the labile and pH dependent nature of the molybdocene-dCG complex. In contrast, no new signals were observed in titration experiments carried out with dAT under identical conditions.

#### 2.2.4. Nucleotides and Nucleosides

In order to establish the relative importance of the phosphate group in the formation of complexes observed with the oligonucleotides and dinucleotides, titration experiments of  $\text{Cp}_2\text{MoCl}_2(\text{aq})$  with 5'-dAMP, adenosine and guanosine were carried out. Formation of complexes between  $\text{Cp}_2\text{MoCl}_2(\text{aq})$  and nucleotides have been reported previously (Figure 2.6).<sup>60,66</sup> However, as these complexes were formed under different conditions it was necessary to characterise molybdocene-nucleotide adducts under the same conditions used with the oligonucleotide titration experiments (i.e. 50 mM NaCl, pH~7).

Addition of 1 equiv. of  $\text{Cp}_2\text{MoCl}_2(\text{aq})$  to 5'-dAMP at pD 7.4-7.7 produced new H8 and H2 signals in the NMR spectrum (Figure 2.7b, indicated by ◆) due to the formation of the adduct  $\text{Cp}_2\text{Mo}(5'\text{-dAMP})$  which has been previously reported (Figure 2.6).<sup>60</sup> This adduct was stable over 24 h (Figure 2.7c). The small resonances at 8.5 ppm and 8 ppm (Figure 2.6b and c, indicated by ●) are characteristic of the hydrolysis products observed when  $\text{Cp}_2\text{MoCl}_2$  4 hydrolyses in 50 mM NaCl at pD 7.4 and as in the binding studies with the oligonucleotides.

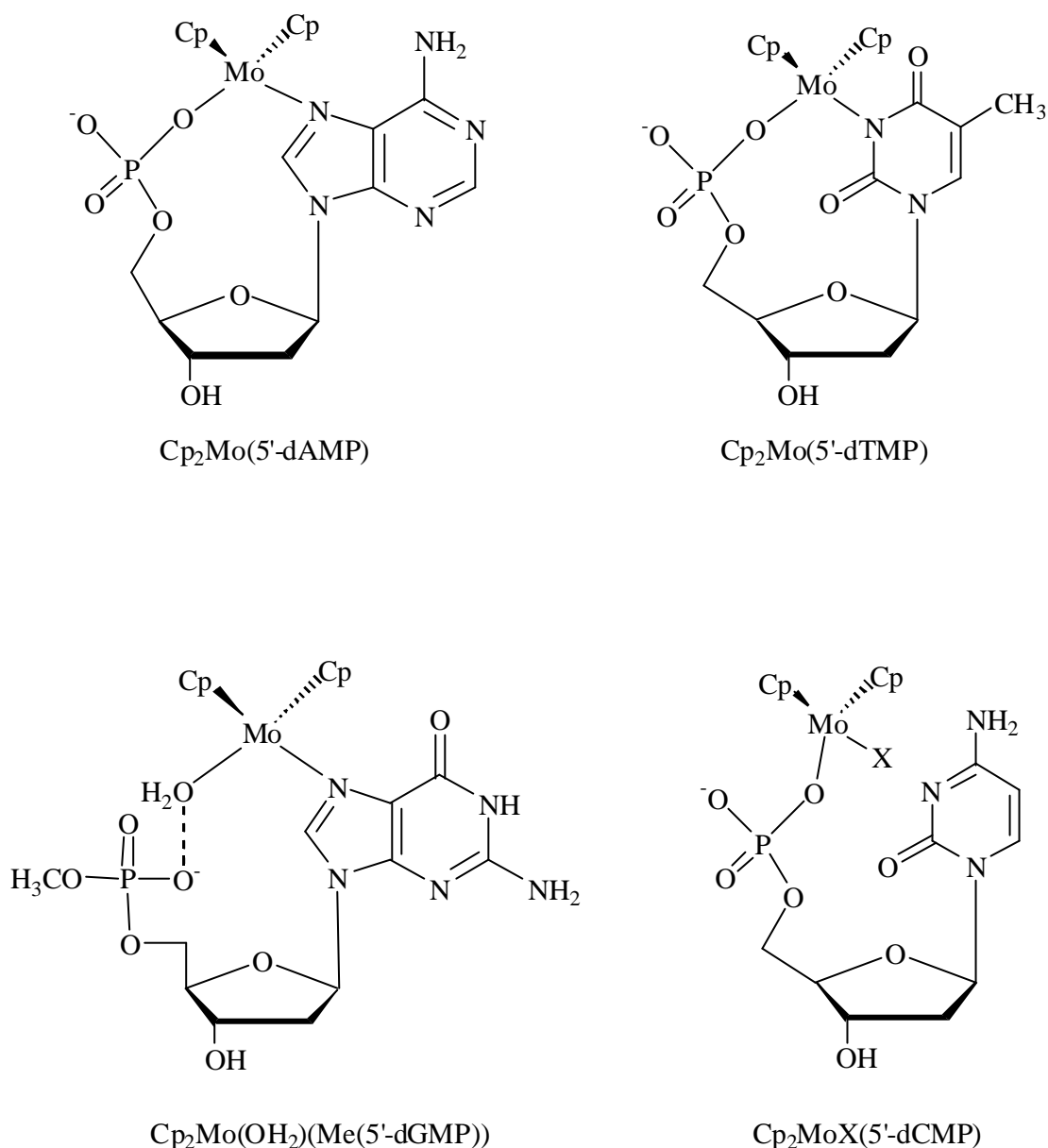


**Figure 2.6:** Types of adducts formed with Cp<sub>2</sub>MoCl<sub>2</sub>(aq) and nucleotides<sup>60</sup>

The interaction of Cp<sub>2</sub>MoCl<sub>2</sub> **4** with the nucleosides adenosine and guanosine was studied at both low pD ~3 and physiological pD ~7.4, in order to compare the results with those obtained with the single strand oligonucleotide at pD 3.4 and pD ~7.4 and the oligonucleotide at pD ~7.4.

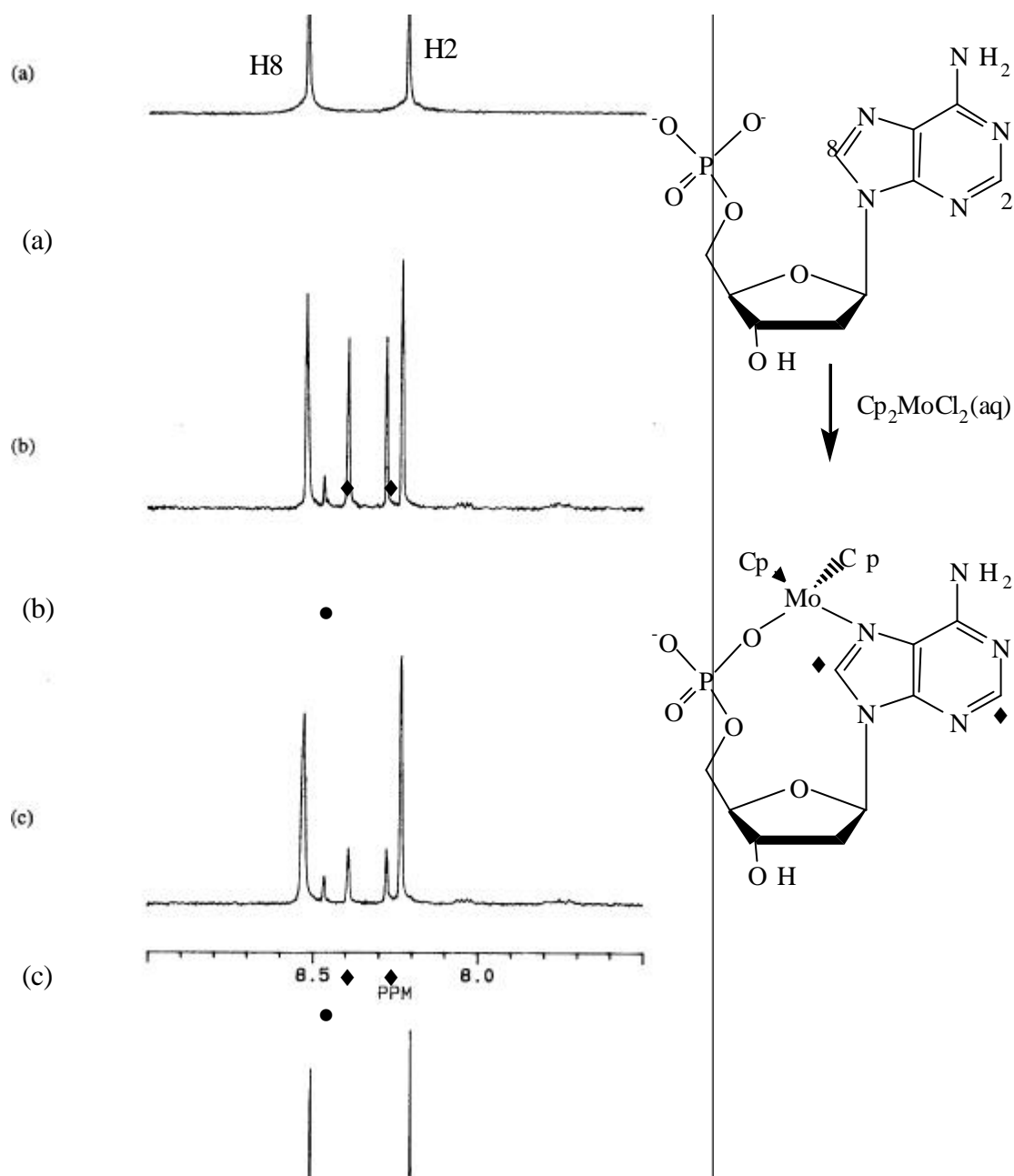


**Figure 2.7:**  $^1\text{H}$  NMR spectra (200 MHz, 50 mM NaCl,  $\text{D}_2\text{O}$ , pD 7.4–7.7, 25 °C) showing the aromatic region of 5'-dAMP on titration of  $\text{Cp}_2\text{MoCl}_2(\text{aq})$  (a) 0 equiv. (b) 1 equiv. after 30 min, (c) 1equiv. after 24 h. • = peak assigned to hydrolysis product(s), ♦ indicate signals assigned to adduct

Figure 2.8 shows the aromatic region of the NMR spectra on addition of 1 equiv. of  $\text{Cp}_2\text{MoCl}_2(\text{aq})$  to adenosine at low pD 3.3-3.4 and physiological pD 7.3-7.4. Adduct formation with adenosine was only observed at pD 7.3-7.4, as evident by the appearance of new H8 and H2 signals due to molybdocene complexed adenosine (Figure 2.8ii, as indicated by arrows). No molybdocene adducts were observed with adenosine at pD 3.3-3.4 (Figure 2.8i). The adduct formed at pD 7.3-7.4 probably involves coordination to the N7 nitrogen and is possibly assisted by a water bridge to the 5'OH group in a similar manner to that reported previously with the methyl-phosphate ester of 5'-dGMP where a water bridge is also involved (Figure 2.6).<sup>60</sup>

Figure 2.9 shows similar titration experiment carried out with guanosine. As with adenosine, adduct formation with guanosine was only observed at pD 7.2-7.7, as evident by the appearance of new H6 signals due to molybdocene complexed guanosine (Figure 2.9ii, as indicated by arrows). No molybdocene adducts were observed with guanosine at pD 3.2-3.3 (Figure 2.9i).

These results are in contrast to those observed with the oligonucleotides and dinucleotides where adduct formation was only observed at low pD and not at physiological pD (Figure 2.2-2.5).

### **2.3. Molybdocene-Nucleic Acid Complexes**

The formation of molybdocene-nucleic acid complexes was dependent on several factors including the length of the oligonucleotide, whether the oligonucleotide was single or double stranded, the presence of a terminal phosphate group and the solution pD. These

factors determine the nature of the donor atom of the nucleic acid as well as its steric accessibility to the molybdenum metal center.

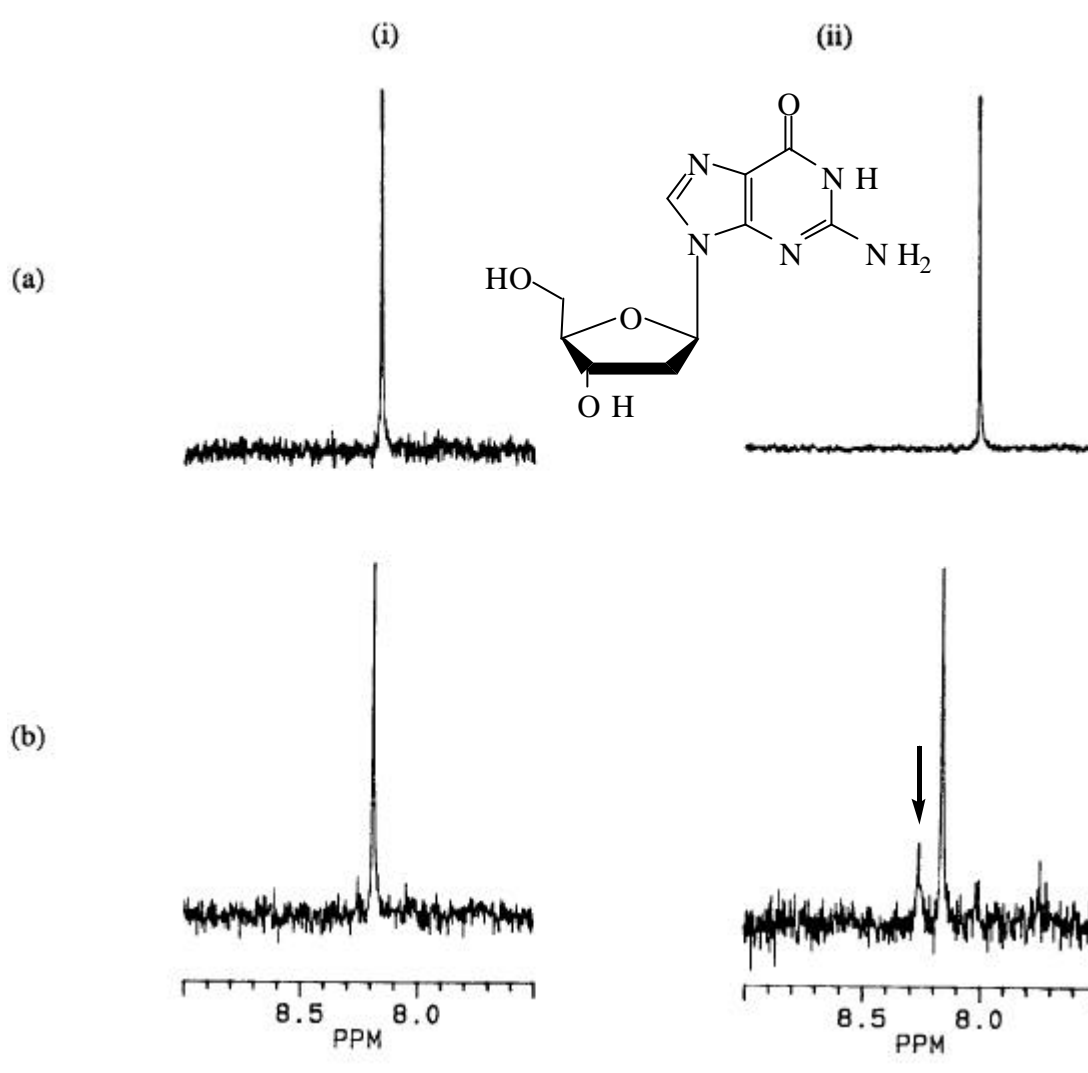


**Figure 2.8:**  $^1\text{H}$  NMR spectra (200 MHz, 50 mM NaCl,  $\text{D}_2\text{O}$ , 25  $^\circ\text{C}$ ) showing the aromatic region of adenosine at (i) pD = 3.3-3.4 and (ii) 7.3-7.4 and following the addition of  $\text{Cp}_2\text{MoCl}_2(\text{aq})$  (a) 0 equiv. (b) 1 equiv. after 30 min. • = peak assigned to hydrolysis product(s), arrows indicate signals assigned to adduct

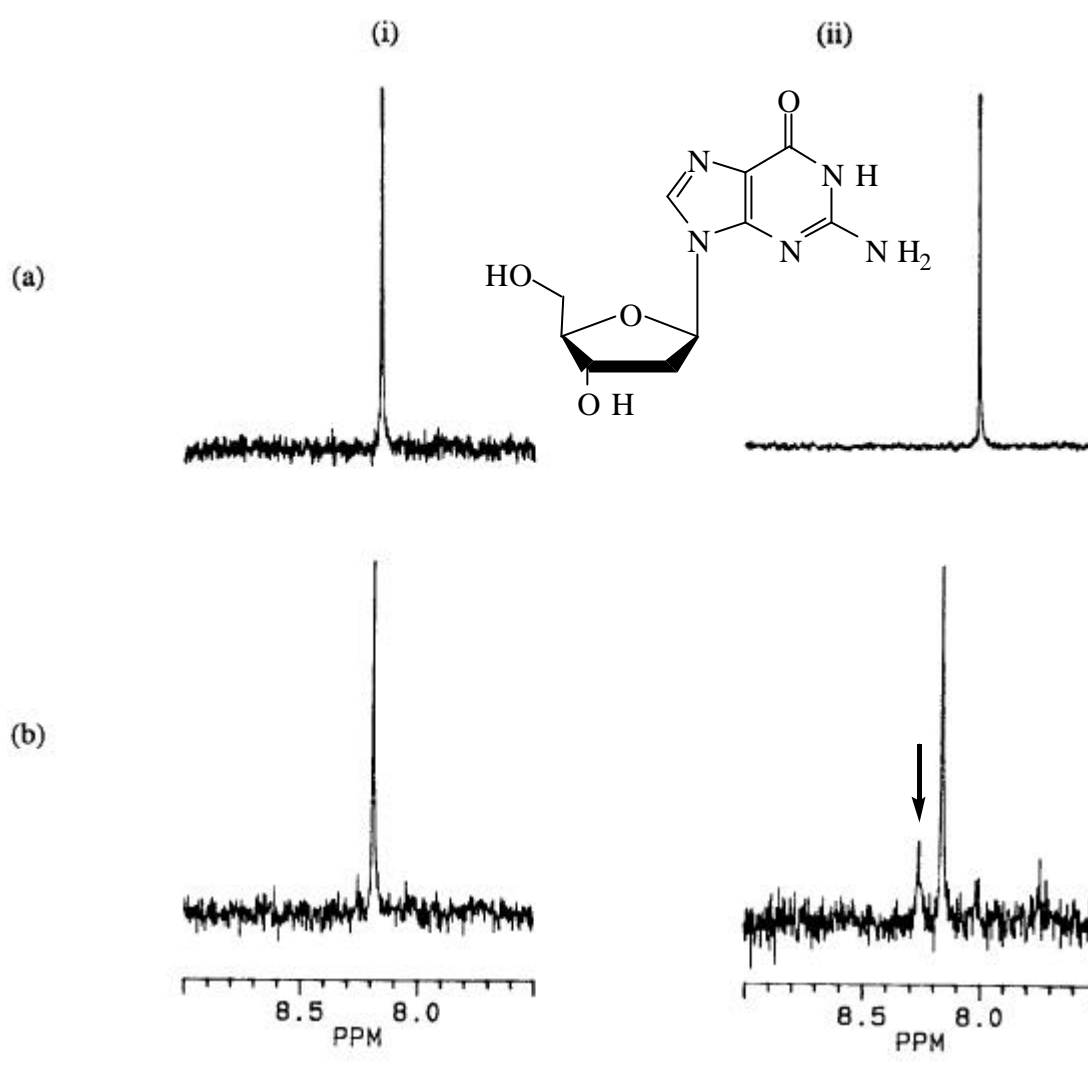


**Figure 2.9:**  $^1\text{H}$  NMR spectra (200 MHz, 50 mM NaCl,  $\text{D}_2\text{O}$ , 25 °C) showing the aromatic region of guanosine at (i) pD = 3.2-3.3 and (ii) 7.2-7.7 and following the addition of  $\text{Cp}_2\text{MoCl}_2(\text{aq})$  (a) 0 equiv. (b) 1 equiv. after 30 min; arrows indicate signals assigned to adduct

Analysis of the  $^1\text{H}$  and  $^{31}\text{P}$  NMR spectra obtained from titration of  $\text{Cp}_2\text{MoCl}_2(\text{aq})$  into  $\text{d}(\text{CGCATATGCG})_2$  and  $\text{d}(\text{ATGGTA})$  showed no evidence for the formation of metallocene-oligonucleotide adducts in 50 mM salt at pD 7.4 (Figures 2.2 and 2.3). However, at low pD values, new signals were observed, consistent with the formation of a complex between  $\text{Cp}_2\text{MoCl}_2(\text{aq})$  and  $\text{d}(\text{ATGGTA})$ . Full characterisation of this complex was not possible, but formation of molybdocene-phosphate (O) adducts, which give a characteristic downfield shift

in the  $^{31}\text{P}$  NMR spectra,<sup>59,60,66</sup> was ruled out as no new signals were observed in  $^{31}\text{P}$  NMR spectra. Comparison of the spectra with those obtained from titrations carried out with dAT and dCG, where adduct formation was only observed with dCG, suggests that coordination of " $\text{Cp}_2\text{Mo}^{2+}$ " occurs with one of the central two guanine bases in d(ATGGTA) (Figure 2.10). Given that there is no interaction with the phosphate backbone, adducts in which the molybdenum is coordinated to N7 of the guanine bases (Figure 2.10), in a similar fashion to that observed with the methyl phosphate ester of 5'-dGMP (Figure 2.6), are most likely.<sup>60</sup> Adduct formation at high pD is less favoured due to competition from the hydrolysis pathway, which increases at higher pD (Figure 2.1). The absence of adduct formation with the double stranded oligonucleotide d(CG CATATGCG)<sub>2</sub> is difficult to explain from the results reported in this chapter. However, adduct formation between the tetrahedral  $\text{Cp}_2\text{Mo}^{2+}$  species and the N7 group of the purine residues is more restricted in the case of double stranded oligonucleotides as compared to single stranded oligonucleotides. This arises due to the double-helical shape of DNA, shown schematically in Figure 2.11, which prevents formation of adducts similar to those shown in Figure 2.10.

The results obtained with the oligonucleotides and dinucleotides are quite different to those obtained with the mononucleotides 5'-dAMP, 5'-dGMP, 5'-dCMP and 5'-dUMP where immediate complexation to the nucleobase (N) and phosphate (O) occurs in a non-labile manner (Figure 2.6).<sup>59,60,66</sup> It has also been reported that adduct formation with mononucleotides does not appear to disrupt Watson-Crick hydrogen bonding in mixtures of complementary nucleotides.<sup>59,60</sup> There are two major differences between this work with d(CG CATATGCG)<sub>2</sub>, d(ATGGTA), dAT and dCG, and previous

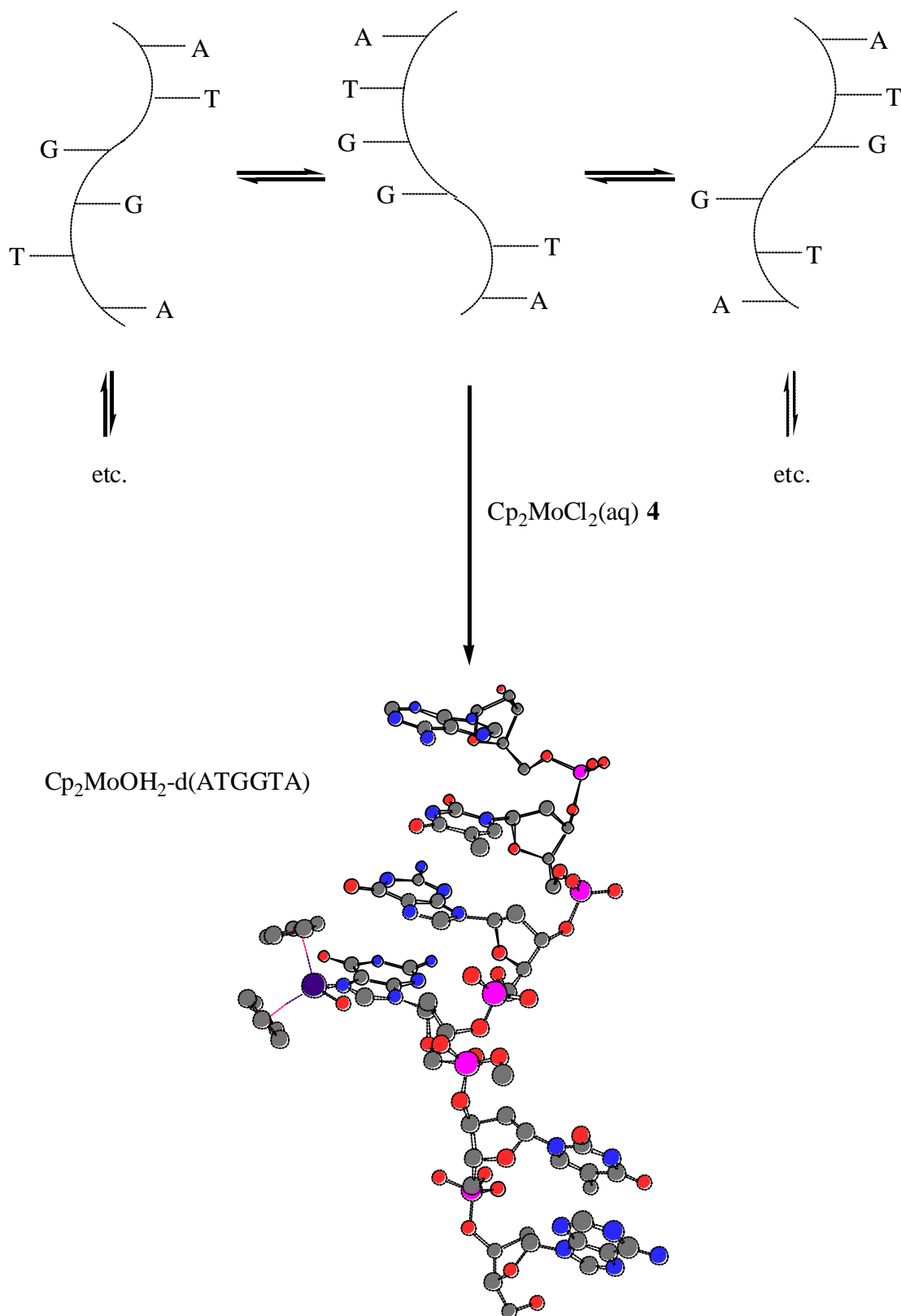


**Figure 2.10:** Proposed adduct formed between  $\text{Cp}_2\text{MoCl}_2(\text{aq})$  and  $\text{d}(\text{ATGGTA})$ ; only one possible conformation of bound oligonucleotide shown

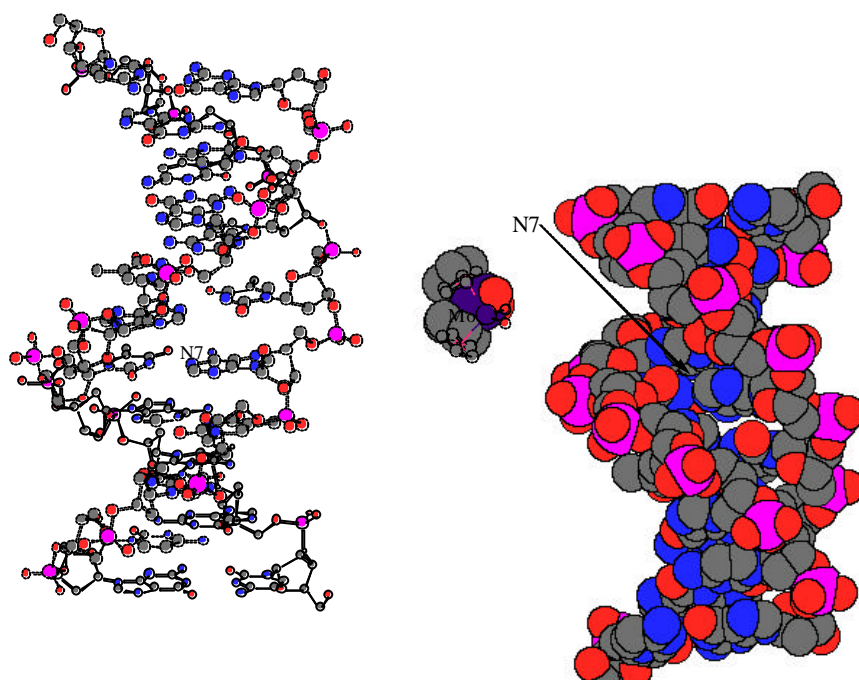


**Figure 2.11:** Computer generated structure of  $d(\text{CG CATATG CG})_2$  showing N7 of A6 in major groove and tetrahedral shape of  $\text{Cp}_2\text{Mo}^{2+}$  moiety

studies with nucleotides. Firstly, the oligonucleotides studied in this work lack terminal phosphate groups, which stabilise and promote formation of the chelates, shown in Figure 2.6, involving phosphate (O) coordination. Indeed, recent preliminary studies of the interaction of  $\text{Cp}_2\text{MoCl}_2(\text{aq})$  with the self complementary 6-mer  $d(\text{AGGCCT})$  and the 5'-phosphorylated analogue  $d(\text{pAGGCCT})$  in  $\text{D}_2\text{O}$  in the absence of salt were reported.<sup>57</sup> As expected, significant perturbations of resonances at the 5'-end of the phosphorylated analogue were detected, consistent with simultaneous  $\text{Cp}_2\text{MoCl}_2(\text{aq})$  coordination at the adenine N7 and phosphate (O) of the 5'-terminal adenosine, but only minor changes were observed in the non-phosphorylated sequences.

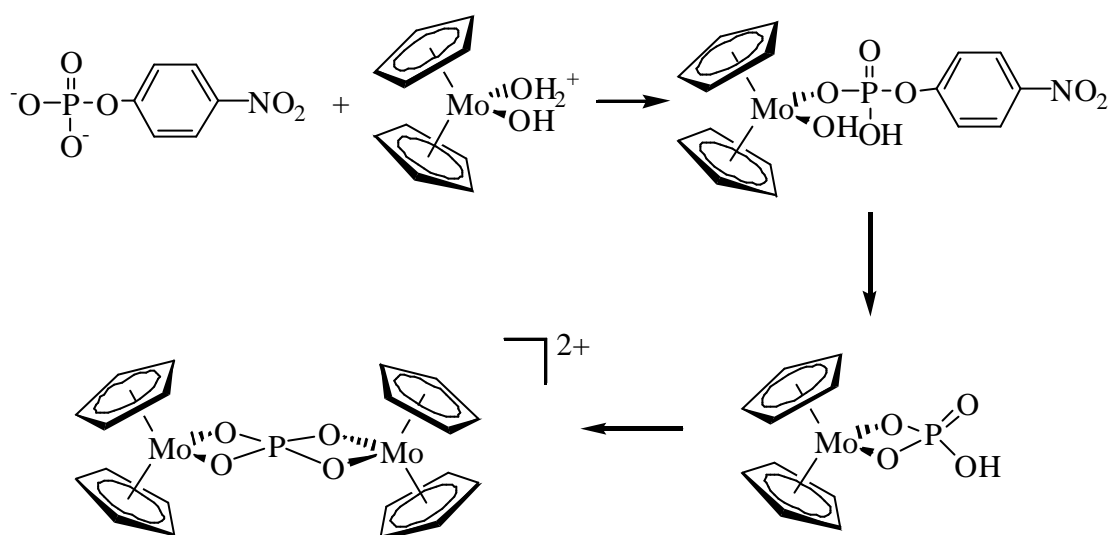
Secondly, different experimental conditions were used in this study; the pD of the solution was kept above 6.4 throughout the titrations, by careful addition of  $\text{Cp}_2\text{MoCl}_2(\text{aq})$

and adjustment of the pD as required. This condition has a major effect on the formation of complexes, since at pD < 4.4, complex(es) with d(ATGGTA) were formed which were stable in solution over 24 h. Even though adduct formation with dAT was not observed at pD~7.4 in 50 mM salt, adduct formation with 5'-dAMP under the same conditions is evident.

At pD~7.4 in salt solution, the only new products formed between oligonucleotides and Cp<sub>2</sub>MoCl<sub>2</sub>(aq) were those arising from hydrolysis of the Cp rings of Cp<sub>2</sub>MoCl<sub>2</sub> **4** as in the control hydrolysis experiments (Figure 2.1, indicated by ●). While the exact species that gives rise to these new peaks was not assigned, the sharp downfield singlet (8.5 ppm) is consistent with a metal-bound Cp ring, and most probably arises from an intermediate hydrolysis product in which only one Cp ring is bound to the metal centre. The relative amounts of the hydrolysis signals (Figures 2.1-2.9, indicated by ●) and their rate of formation were variable in different experiments, but they were consistently detected. However, after several hours, the predominant molybdocene species in each of the titration experiments contained metal bound Cp rings (Cp<sub>n</sub>MoX<sub>2</sub>) that gave rise to sharp singlets at around 6 ppm as in Figure 2.1 and 2.2.

The lack of adduct formation with oligonucleotides at pD ~7.4 was not observed when the same titration experiment was carried out with the nucleosides adenosine (Figure 2.8ii) and guanosine (Figure 2.9ii) which do not have a phosphate ester. This result indicates that adduct formation, most likely through the N7 of the nucleoside bases, is possible at pD ~7.4 and not at lower pD. Formation of adducts at low pD may be prevented due to protonation of the coordination site. The absence of adduct formation at low pD with either adenosine (Figure 2.8i) or guanosine (Figure 2.9i) suggests that adduct formation at low pD could be highly dependent on coordination to the phosphate oxygen.

Kuo *et al*<sup>86</sup> have recently reported that  $\text{Cp}_2\text{MoCl}_2$  **4** promotes cleavage of the phosphodiester bond of activated phosphodiester and phosphomonoesters in aqueous solution (Scheme 2.1). A similar reaction was considered with the oligonucleotides, as a mechanism whereby DNA damage could occur. However, no new signals arising from fragmentation of the oligonucleotides with time, were observed. This is not unexpected, as the phosphates are inactivated to this type of hydrolysis, and furthermore, the reported catalysis was optimal at pD 3.4 and negligible at pD 7.4.



Scheme 2.1

#### 2.4. Conclusions

The results of a comparison of the interaction of  $\text{Cp}_2\text{MoCl}_2(\text{aq})$  with duplex DNA, single-stranded DNA and nucleic acid constituents in salt at pH~7 have important implications for the mechanism of antitumour action of  $\text{Cp}_2\text{MoCl}_2$  **4**. In particular, while adduct formation was evident with the single stranded oligonucleotide at low pH < 4.4, the lack of adduct formation with the double strand oligonucleotide at either low or high pH suggest that formation of the double helix effects the steric accessibility of the coordination sites. The

importance of the phosphate (O) in formation of stable adducts with the nucleotide 5'-dAMP is also apparent, as formation of adducts with oligonucleotides and dinucleotides is limited in the absence of this coordinating group. The formation of adducts at low pH < 4.4 with the dinucleotide dCG and not with dAT indicates that there is selectivity for the bases cytosine and/or guanosine. While the results suggest that adducts may be formed at pH < 4.4 with single-strand DNA or RNA through coordination to the base nitrogens, the formation of stable metallocene-DNA adducts *in vivo* with either double or single strand DNA at pH > 6.4 is unlikely.

Despite the lack of adduct formation observed with the oligonucleotides at pH ~7, the possibility that blood constituents could stabilise complexes with proteins and/or DNA cannot be ruled out. Further work on the effect of Cp<sub>2</sub>MoCl<sub>2</sub> **4** on DNA and RNA synthesis and other possible protein targets is required in order to clarify the mechanism of action of the drug. This interpretation is supported by recent preliminary results<sup>57</sup> that have identified protein kinase C and topoisomerase II as potential targets of Cp<sub>2</sub>MoCl<sub>2</sub> **4** *in vivo*. This study also highlights the importance of contrasting results with nucleic acid constituents with larger fragments of DNA, where steric effects can be significant and where the same binding sites are not necessarily available.

An understanding of the mechanism of antitumour activity of  $\text{Cp}_2\text{TiCl}_2$  **1** requires identification of the active species *in vivo*. The hydrolytic stability of  $\text{Cp}_2\text{TiCl}_2$  **1** in aqueous solutions has been studied *in vitro* (see Section 1.5) in order to determine what species are likely to form under physiological conditions. The hydrolysis of the halide ligands is rapid at low pH to give aquated titanocene complexes with bound Cp ligands.<sup>58</sup> However, Cp hydrolysis is accelerated at  $\text{pH} > 4.5$  to give polymeric and insoluble hydrolysis products,<sup>58</sup> which has prevented studies being carried out under approximately physiological conditions, and also administration of samples at physiological pH. Hence, samples have been administered in 9:1 saline:DMSO solutions at low pH<sup>17,38,46</sup> as preparation of aqueous solutions at  $\text{pH} > 4.5$  is not possible due to rapid Cp hydrolysis to give insoluble precipitates. Special formulations have also been developed and used for clinical trials so as to avoid problems associated with hydrolysis of  $\text{Cp}_2\text{TiCl}_2$  **1** at  $\text{pH} > 4.5$ .<sup>14-16,20,87</sup>

The administration of aqueous solutions of  $\text{Cp}_2\text{TiCl}_2$  **1** at low pH is not desirable due to side-effects associated with injection of acidic solutions,<sup>46</sup> and the uncertainty as to the species formed when the solution transfers to blood serum at pH 7. Indeed, a reduction in side-effects associated with treatment has been observed in solutions of  $\text{Cp}_2\text{TiCl}_2$  **1** in which the pH was buffered at 4.2-5.9 and the samples rapidly injected prior to precipitation of the hydrolysis products.<sup>46</sup> Specifically, the dosage range at which toxicity was observed was elevated upon buffering of solutions.<sup>46</sup> Furthermore, the incidence of peritoneal (abdominal lining) thickening and adhesions were reduced significantly when buffered solutions were administered.<sup>46</sup>

This chapter outlines the design and synthesis of water soluble titanocene derivatives, which are relatively stable to Cp hydrolysis at pH ~7 and hence are suitable for administration in water at physiological pH. In addition to improving the bioavailability of the metallocene, along with possible reduction or modification of side-effects associated with  $\text{Cp}_2\text{TiCl}_2$  **1**, complexes of this type would allow hydrolysis and binding studies to be carried out at pH 7 and thus contribute to the understanding of the mechanism of antitumour action of  $\text{Cp}_2\text{TiCl}_2$  **1**.

### **3.1. Methyl Substituted Titanocene Derivatives**

Methyl substitution of the Cp rings has been reported to significantly modify the electronic effects of the Cp rings leading to increased stability of the Cp-metal bond in metallocene complexes.<sup>88,89</sup> This result is consistent with stabilisation of the Cp-Ti bond by the electron donating alkyl group. However, the hydrolysis of metallocene complexes with alkyl substituted Cp rings has not been investigated in aqueous solutions. Hence, in this work, the preparation and hydrolytic stability of the methyl substituted derivative  $(\text{MeCp})_2\text{TiCl}_2$  **34** was initially investigated.

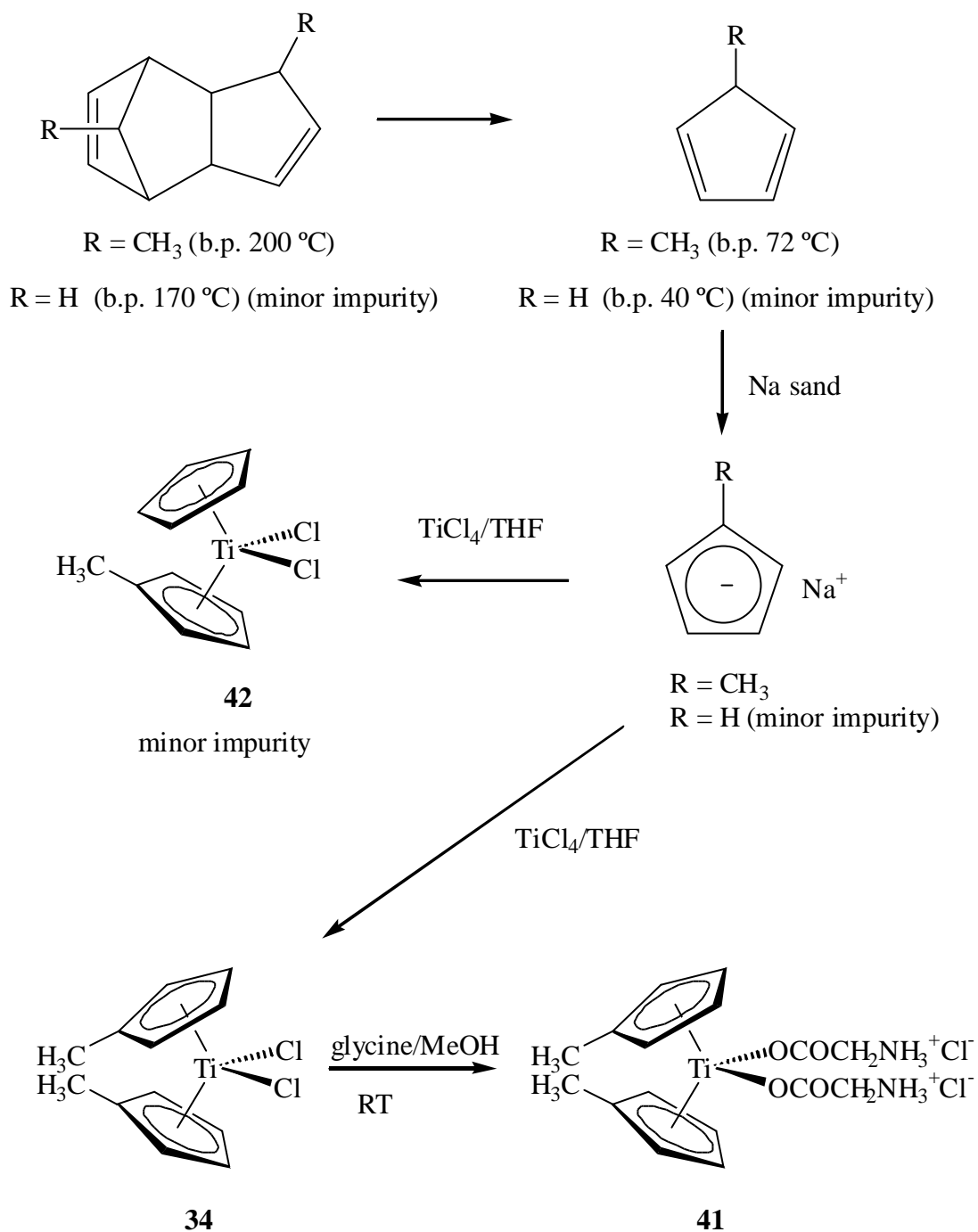
The complex  $(\text{MeCp})_2\text{TiCl}_2$  **34** has been tested previously against EAT in mice and shown to have no activity and high toxicity when administered at low pH in 10%DMSO/90%saline (Table 1.5).<sup>54</sup> The poor activity of this derivative as well as other related alkyl substituted derivatives led to the conclusion that any substitution of the Cp rings results in a loss of activity. It was proposed that modification of the chemical characteristics of the Cp rings interferes with the possible "carrier" function of the Cp rings.<sup>17,18,54</sup> However, the poor activity of the alkyl substituted titanocene derivatives could also be related to the reduced

aqueous solubility, which results from the introduction of hydrophobic alkyl groups, and the administration conditions.

In this work, the complex  $(\text{MeCp})_2\text{TiCl}_2$  **34** was synthesised and its solubility, hydrolytic stability, binding to nucleotides and biological activity were investigated. As introduction of hydrophobic methyl groups is expected to decrease the aqueous solubility of the drug, the bisglycine analogue  $(\text{MeCp})_2\text{Ti}(\text{OCOCH}_2\text{NH}_3\text{Cl})_2$  **41** was also prepared as it has been reported previously that replacement of the chloride ligands of  $\text{Cp}_2\text{TiCl}_2$  **1** with glycine ligands greatly improves the aqueous solubility of the drug.<sup>50,51</sup>

### 3.1.1. Synthesis of $(\text{MeCp})_2\text{TiX}_2$

The complex,  $(\text{MeCp})_2\text{TiCl}_2$  **34**, was prepared using a similar procedure to that reported in the literature,<sup>90</sup> as shown in Scheme 3.1. Thus, methylcyclopentadiene, generated from freshly cracked di(methylcyclopentadiene), was treated with sodium sand followed by titanium(IV) tetrachloride to give  $(\text{MeCp})_2\text{TiCl}_2$  **34** in 25% yield. As reported previously, considerable difficulty was experienced in obtaining  $(\text{MeCp})_2\text{TiCl}_2$  **34** in high purity due to the presence of significant amounts of dicyclopentadiene (b.p.  $\sim 170^\circ\text{C}$ ) in commercially available methylcyclopentadiene dimer (b.p.  $\sim 200^\circ\text{C}$ ).<sup>90</sup> Careful, multiple distillations were employed to obtain pure methylcyclopentadiene, which could be used to make highly pure  $(\text{MeCp})_2\text{TiCl}_2$  **34** suitable for biological testing (Scheme 3.1). In cases where contamination with the mixed complex  $\text{Cp}(\text{MeCp})\text{TiCl}_2$  **42** was evident, recrystallisation to obtain analytically pure  $(\text{MeCp})_2\text{TiCl}_2$  **34** was not successful as complexes **34** and **42** both have very similar properties.<sup>90</sup> The complex **34** was characterised by microanalysis, mass spectroscopy and NMR spectroscopy.



Scheme 3.1

The glycine analogue  $(\text{MeCp})_2\text{Ti}(\text{OCOCH}_2\text{NH}_3\text{Cl})_2$  **41** was prepared in 75% yield using a similar procedure to that reported for the preparation of  $\text{Cp}_2\text{Ti}(\text{OCOCH}_2\text{NH}_3\text{Cl})_2$  **27** (Scheme 3.1).<sup>50,51</sup> Thus, treatment of  $(\text{MeCp})_2\text{TiCl}_2$  **34** with glycine (2 eq.) in methanol at

room temperature afforded the orange complex  $(\text{MeCp})_2\text{Ti}(\text{OCOCH}_2\text{NH}_3\text{Cl})_2$  **41**. The crude product was washed with chloroform to remove any unreacted starting material to give  $(\text{MeCp})_2\text{Ti}(\text{OCOCH}_2\text{NH}_3\text{Cl})_2$  **41**, which was characterised as the hydrate by microanalysis and NMR spectroscopy. The success of the reaction was highly variable and frequently material was isolated that co-crystallised with unreacted glycine. Attempts to further purify such material were generally unsuccessful.

### 3.1.2. Solubility Properties

$\text{Cp}_2\text{TiCl}_2$  **1** has limited solubility in water, but sonication in water results in complete dissolution after 5-10 min to give a clear yellow solution. In comparison, introduction of the two methyl groups to give derivative **34**, not surprisingly, reduces the aqueous solubility significantly and sonication for 2-3 h is required to give a saturated yellow solution that frequently contains undissolved material. In the case of **41**, the charged glycine ligands greatly improve aqueous solubility and the complex dissolves immediately in water with no sonication required. Replacement of the halide ligands of metallocenes with charged or hydrophilic ligands in order to improve aqueous solubility, including the synthesis and improved solubility of  $\text{Cp}_2\text{Ti}(\text{OCOCH}_2\text{NH}_3\text{Cl})_2$  **27**, has been reported previously.<sup>47,50,51</sup>

### 3.1.3. Hydrolysis Studies

The rate of halide and Cp ring hydrolysis in  $\text{Cp}_2\text{TiCl}_2$  **1** has been well characterised (Section 1.5.2). Rapid hydrolysis of the two halide ligands occurs in a series of equilibrium reactions to give a solution at pH ~ 2 in which the Cp rings remain metal bound for >24 h.<sup>58</sup> However, at higher pH values protonolysis of the Cp rings occurs to give cyclopentadiene and dicyclopentadiene as well as insoluble, uncharacterised hydrolysis products.<sup>58</sup> The exact

nature of the ligands in solution have not been identified, with  $\text{Cp}_2\text{TiCl}_2(\text{aq})$  likely to contain a number of species such as  $\text{Cp}_2\text{Ti}(\text{H}_2\text{O})\text{Cl}^+$ , or  $\text{Cp}_2\text{Ti}(\text{H}_2\text{O})_x(\text{OH})_y^{(2-y)+}$ .<sup>58</sup>

While the synthesis of  $\text{Cp}_2\text{Ti}(\text{OCOCH}_2\text{NH}_3\text{Cl})_2$  **27** has been reported,<sup>50</sup> complete hydrolysis studies in water have not been carried out. The complex crystallises from water to give the bisglycine complex **27** in which the glycine carboxylates are coordinated to the metal.<sup>50</sup> This fact, taken with the downfield chemical shift of the glycine methylene in the  $^1\text{H}$  NMR spectrum of **27** (3.68 ppm) compared with unbound glycine (3.38 ppm), was taken as evidence that the glycine ligands are directly coordinated to the metal centre in solution as well as the solid state.<sup>50</sup> The reported changes in chemical shift on coordination of the glycine carboxylate to the metal centre do not appear to have taken into account the change in solution pD. A careful comparison of the NMR spectra of free glycine at pD 2-8 with a solution of  $\text{Cp}_2\text{Ti}(\text{OCOCH}_2\text{NH}_3\text{Cl})_2$  **27** at the same pD values shows that there is no change in chemical shift of free glycine and the glycine resonances in complex **27** at the same pD value (Table 3.1). While there is no doubt that in the solid state the complex crystallises with the amino acid directly coordinated to the metal,<sup>50</sup> pD titration experiments plus binding and competition studies described below are consistent with only a weak interaction between the glycines and metal centre in aqueous solution.

There is limited data on the hydrolytic stability of any substituted titanocene derivative and no studies have been carried out in water. The hydrolysis of  $(\text{MeCp})\text{CpTiCl}_2$  **42** has been studied in aqueous dioxane solutions and was reported to give aquated complexes where the halides are replaced in a similar fashion to that observed with  $\text{Cp}_2\text{TiCl}_2$  **1**.<sup>91</sup>

**Table 3.1:** The effect of pD on the chemical shift of the methylene peak of glycine.

pD of 0.13 M glycine solution in D <sub>2</sub> O	CH <sub>2</sub> peak $\delta$ ppm (referenced to TSP)
7.9	3.56
3.9	3.58
3.6	3.60
3.2	3.63
3.0	3.69
2.0	3.86

In this work the rate of Cp hydrolysis in Cp<sub>2</sub>TiX<sub>2</sub> (X = Cl **1** and OCOCH<sub>2</sub>NH<sub>3</sub>Cl **27**) or MeCp hydrolysis in (MeCp)<sub>2</sub>TiX<sub>2</sub> (X = Cl **34** and OCOCH<sub>2</sub>NH<sub>3</sub>Cl **41**) was measured using <sup>1</sup>H NMR spectroscopy at different pD values in D<sub>2</sub>O at 25 °C (Table 3.2; Figure 3.1 and 3.2). In the case of Cp<sub>2</sub>TiX<sub>2</sub> (X = Cl **1** and OCOCH<sub>2</sub>NH<sub>3</sub>Cl **27**), the rate of Cp ring hydrolysis at 3 different pD values was found to be very similar. While hydrolysis of Cp<sub>2</sub>TiX<sub>2</sub> (X = Cl **1** and OCOCH<sub>2</sub>NH<sub>3</sub>Cl **27**) was accompanied by formation of only a minor amount of insoluble precipitate at pD ~2.4, precipitation increased at higher pD values, with >90% of the metallocene hydrolysed at pD 7.4 (Figure 3.1b). In the case of Cp<sub>2</sub>TiCl<sub>2</sub> **1**, the amount of precipitate (and hence hydrolysis) was estimated visually or by isolation and weighing of the precipitate. However, in the case of the glycine analogue **27**, a more accurate independent estimate was obtained by integration of the glycine CH<sub>2</sub> peak versus the signal arising from the bound cyclopentadienyl protons (Table 3.2; Figure 3.1ii). The glycine analogue **27** gives by integration a ratio of

**Table 3.2:** Hydrolysis of aromatic rings in complexes **1**, **27**, **34**, **41** at various pD values over 24 h.

Complex	X = Cl				X = gly			
	pD <sup>a</sup>	Time (h) <sup>b</sup>	% Precipitated	% Cp Hydrolysis	pD <sup>a</sup>	Time (h) <sup>b</sup>	% <sup>c</sup> Precipitated	% Cp Hydrolysis
Cp <sub>2</sub> TiX <sub>2</sub>  X = Cl <b>1</b> or X = OCOCH <sub>2</sub> NH <sub>3</sub> Cl <b>27</b>	2.0-2.1	1	-	0	3.0-3.1	1	0	0
		24	-	< 2 <sup>d</sup>		24	4	< 2 <sup>d</sup>
	6.1-6.2	0.25	-	15	5.8-6.3	0.25	60	2
		24	-	> 90 <sup>e</sup>		24	> 90	> 90 <sup>e</sup>
	> 6.4	-	> 95 <sup>f</sup>	-	> 6.4	-	> 95 <sup>f</sup>	-
(MeCp) <sub>2</sub> TiX <sub>2</sub>  X = Cl <b>34</b> or X = OCOCH <sub>2</sub> NH <sub>3</sub> Cl <b>41</b>	1.8-2.0	1	-	0	2.5-2.7	1	0	0
		24	-	< 2 <sup>d</sup>		24	12	< 2 <sup>d</sup>
	5.9-6.0	0.25	-	0	5.3-5.6	0.25	21	0
		24	-	< 2 <sup>d</sup>		24	56	< 2 <sup>d</sup>
	7.5-7.9	0.25	-	< 2 <sup>d</sup>	7.1-7.4	0.25	43	< 2 <sup>d</sup>
		24	-	< 5 <sup>g</sup>		24	88	< 5 <sup>g</sup>

<sup>a</sup>For pD 1.8-3.1: pD values were monitored with time and did not drop by more than 0.3 units over 24 h. For pD > 5.4: pD values were monitored with time and adjusted to the required pD range prior to recording NMR spectrum; a drop of 1 pD unit over 24 h was typical.

<sup>b</sup>Time = 0 h refers to when all the sample had dissolved and the pD was adjusted to required value.

<sup>c</sup>Calculated on the ratio of bound Cp signal to CH<sub>2</sub> signal of glycine when compared to the ratio at t = 1 h.

<sup>d</sup>Estimated by integration of the signals from protonated Cp or MeCp dimer/monomer; < 2 when the amount of signal was too small to be integrated accurately.

<sup>e</sup>Hydrolysis was estimated to be > 90 % since the amount of bound Cp signal was negligible.

<sup>f</sup>Above pD values of about 6.4 complexes **1** and **27** were hydrolysed and precipitated completely giving no signal in the NMR spectra and so the % precipitated was estimated at > 95 %.

<sup>g</sup>Estimated at < 5 % based on the amount of dimer and monomer peaks.

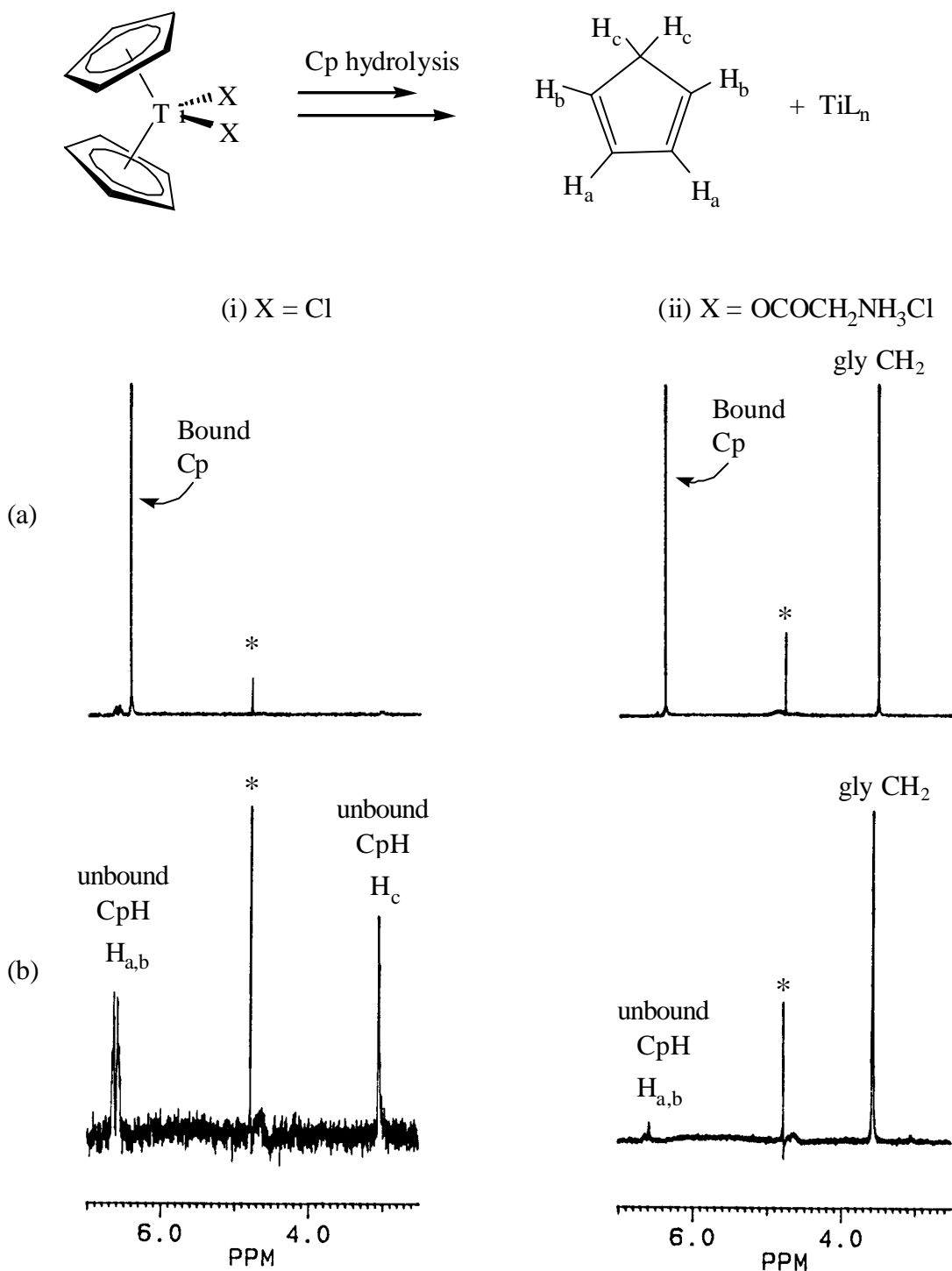


**Figure 3.1:** <sup>1</sup>H NMR spectra (200 MHz, D<sub>2</sub>O, 25 °C) showing hydrolysis of (i) Cp<sub>2</sub>TiCl<sub>2</sub> **1** at pD 6.1-6.2 and (ii) Cp<sub>2</sub>Ti(O<sub>2</sub>CCH<sub>2</sub>NH<sub>3</sub>Cl)<sub>2</sub> **27** at pD 5.8-6.3 after (a) 0.25 h and (b) 24 h. \* residual water. Vertical axis is not to scale.

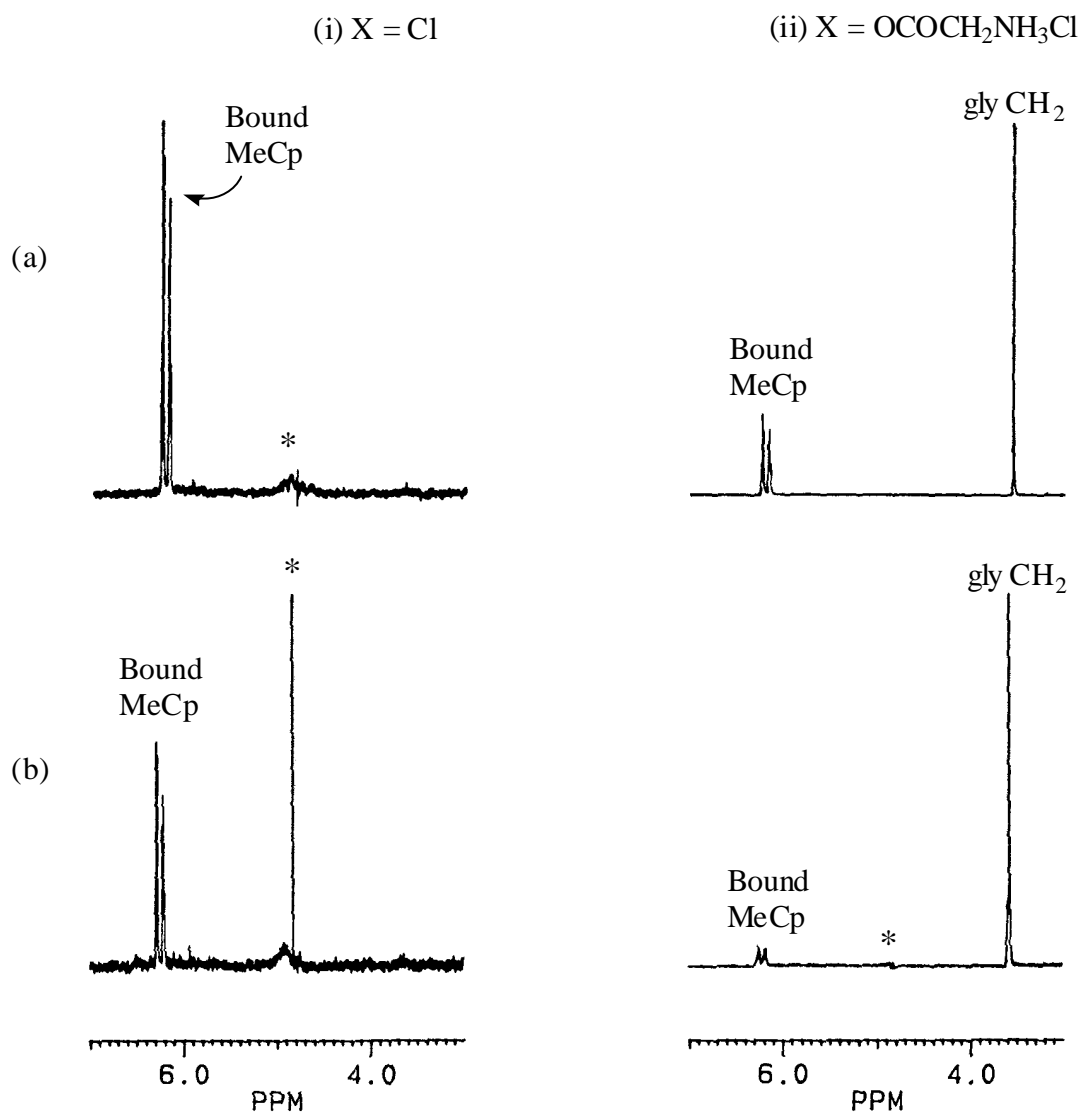
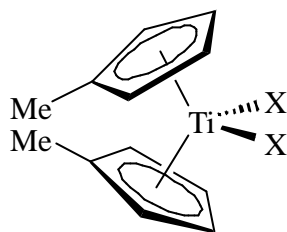


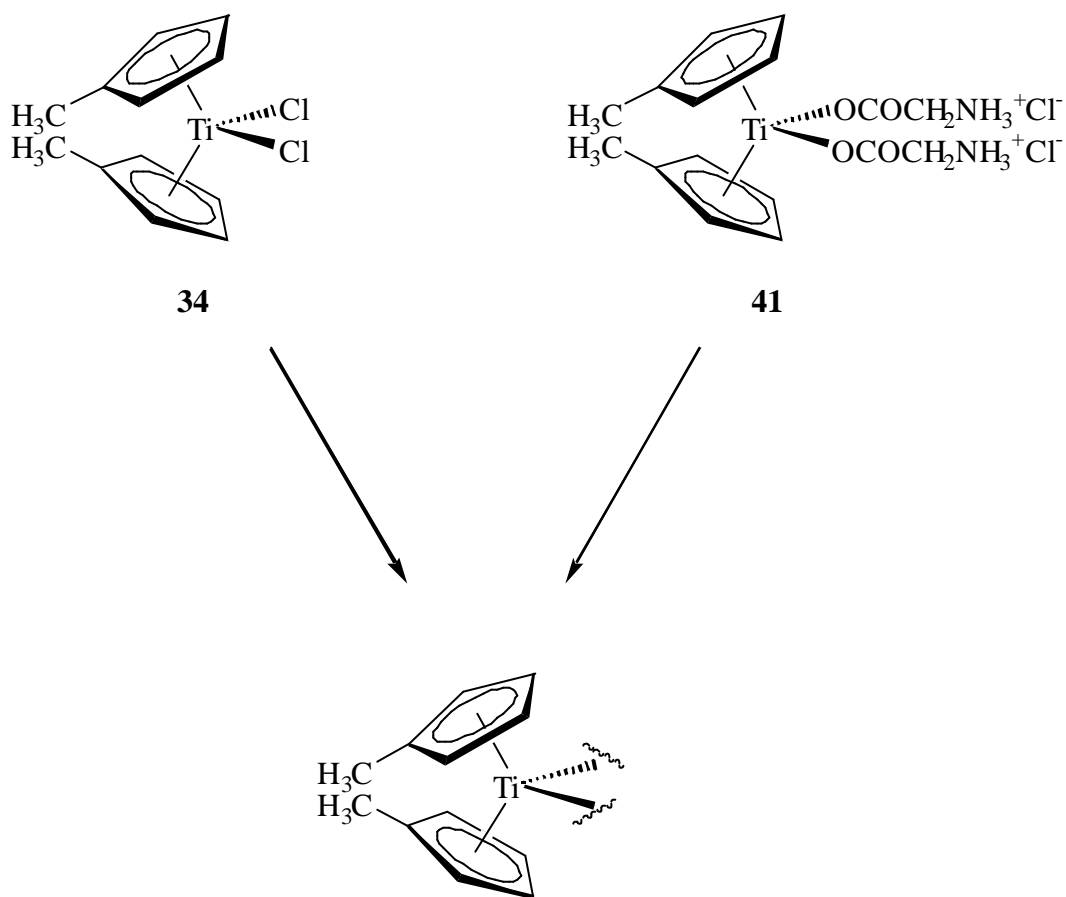
**Figure 3.2:** <sup>1</sup>H NMR spectra (200 MHz, D<sub>2</sub>O, 25 °C) showing hydrolysis of (i) (MeCp)<sub>2</sub>TiCl<sub>2</sub> **34** at pD 7.5-7.9 and (ii) (MeCp)<sub>2</sub>Ti(O<sub>2</sub>CCH<sub>2</sub>NH<sub>3</sub>Cl)<sub>2</sub> **41** at pD 7.5-7.8 after (a) 0.25 h and (b) 24 h. \* residual water

10:4 for Cp:CH<sub>2</sub> when fully dissolved. As precipitation occurs the Cp signal decreased relative to the glycine peak consistent with formation of hydrolysis products derived from the Cp rings. The Cp rings of Cp<sub>2</sub>TiX<sub>2</sub> (X = Cl **1** and OCOCH<sub>2</sub>NH<sub>3</sub>Cl **27**) are hydrolysed rapidly at pD > 5.5 (Table 3.2, Figure 3.1) and no signal from metal bound Cp was observed over pD > 5.5 after 24 h (Figure 3.1b).

The effect of the methyl group on the rate of ring hydrolysis was determined by carrying out similar experiments on (MeCp)<sub>2</sub>TiX<sub>2</sub> (X = Cl **34** and OCOCH<sub>2</sub>NH<sub>3</sub>Cl **41**). An estimate of the MeCp hydrolysis can be calculated from the relative intensities of the new multiplets due to MeCpH (6.5 and 6.6 ppm at pD ~7.4), which appear downfield of the metal-bound MeCp multiplet (6.4 ppm at pD ~7.4) and from the new methyl resonances, which appeared at ~2 ppm in the spectrum. As expected, the halide ligand had little effect on the hydrolysis experiments and similar results were obtained for (MeCp)<sub>2</sub>TiCl<sub>2</sub> **34** and (MeCp)<sub>2</sub>Ti(OCOCH<sub>2</sub>NH<sub>3</sub>Cl)<sub>2</sub> **41** at similar pD values (Table 3.2). At low pD values, a minor amount of precipitate formed with time; the amount of precipitate increased when the solution pD was raised to ~7 and was estimated as described above (Table 3.2). Analysis of the supernatant by NMR spectroscopy showed that the MeCp rings remain metal bound at pD~7.4 (Figure 3.2). The yellow precipitated solid was isolated but due to poor solubility could not be fully characterised.

The hydrolysis studies of both **34** and **41** are consistent with loss of the halide and glycine ligands respectively in water to give the same species, in which both MeCp rings are bound to the metal, i.e., "(MeCp)<sub>2</sub>Ti<sup>2+</sup>" (Scheme 3.2). In order to confirm this interpretation, equimolar amounts of **34** and **41** were dissolved and spectra recorded at different pD values. In all cases only one set of MeCp signals was observed consistent with formation of the same

(or very similar) species in solution, presumably an aquated species such as  $[(\text{MeCp})_2\text{Ti}(\text{H}_2\text{O})_2]^{2+}$  or  $[(\text{MeCp})_2\text{Ti}(\text{H}_2\text{O})_x(\text{OH})_y]^{(2-y)+}$ , at pH  $\sim 7$ . A similar result was obtained on a mixed experiment with **1** and **27**.



Scheme 3.2

### 3.1.4. Nucleotide Binding Studies

A major aim of this work was to prepare water soluble, hydrolytically stable titanocene derivatives that interact with nucleic acid constituents in the same way as  $\text{Cp}_2\text{TiCl}_2$  **1**, and hence may be studied (and administered) in preparations at pH 7.4. To this end, nucleotide binding studies were carried out with  $(\text{MeCp})_2\text{TiX}_2$  ( $\text{X} = \text{Cl}$  **34** and

OCOCH<sub>2</sub>NH<sub>3</sub>Cl **41**) and the stabilities and types of complexes formed with nucleotides compared with those formed by Cp<sub>2</sub>TiX<sub>2</sub> (X = Cl **1** and OCOCH<sub>2</sub>NH<sub>3</sub>Cl **27**).

Complexes **34** and **41** were used in separate titration experiments with the nucleotides 5'-dAMP and 5'-dGMP at different pD values. In each case, new signals were detected, and the percentage complexation determined by integration of the resonances in the region 7.5-9 ppm corresponding to either the purine or pyrimidine protons at pD ~4 or pD ~7. The results are summarised in Table 3.3.

**Table 3.3:** % Complexation between Cp<sub>2</sub>TiX<sub>2</sub> and (MeCp)<sub>2</sub>TiX<sub>2</sub> and nucleotides determined by integration of the purine aromatic resonances in the <sup>1</sup>H NMR spectra

Complex	+ 1 eq. nucleotide	X = Cl			X = gly		
		t (h)	pD	% complex	t (h)	pD	% complex
(MeCp) <sub>2</sub> TiX <sub>2</sub> X = Cl <b>34</b> X = OCOCH <sub>2</sub> NH <sub>3</sub> Cl <b>41</b>	5'-dAMP	0.5	4.9	70	0.5	4.7	60
		0.5	7.9	62	0.5	7.7	50
		24	7.8	40	24	7.5	30
	5'-dGMP	0.5	4.7	60	0.5	3.4	60
		0.5	10.1	14	0.5	7.8	30
		24	7.5	14	24	7.5	20
Cp <sub>2</sub> TiX <sub>2</sub> X = Cl <b>1</b> X = OCOCH <sub>2</sub> NH <sub>3</sub> Cl <b>27</b>	5'-dAMP	0.5	5.0	40	0.5	4.0	50
	5'-dGMP	0.5	5.0	45	0.5	4.6	55

Figure 3.3 compares the complexes formed between 5'-dAMP and either 1 equiv. of (MeCp)<sub>2</sub>TiX<sub>2</sub> (X = Cl **34** and OCOCH<sub>2</sub>NH<sub>3</sub>Cl **41**) (Figure 3.3b) or 1 equiv. of Cp<sub>2</sub>TiX<sub>2</sub> (X = Cl **1** and OCOCH<sub>2</sub>NH<sub>3</sub>Cl **27**) (Figure 3.3c). In all four spectra, signals assigned to

uncomplexed nucleotide (Figure 3.3a) were present (indicated by dashed lines), and new signals assigned to the formation of metallocene-nucleotide complex(es) are detected.  $^{31}\text{P}$  NMR spectra of  $(\text{MeCp})_2\text{TiCl}_2$  **34** (Figure 3.3b inset) also showed the appearance of three new signals, consistent with interaction of the metal centre with the

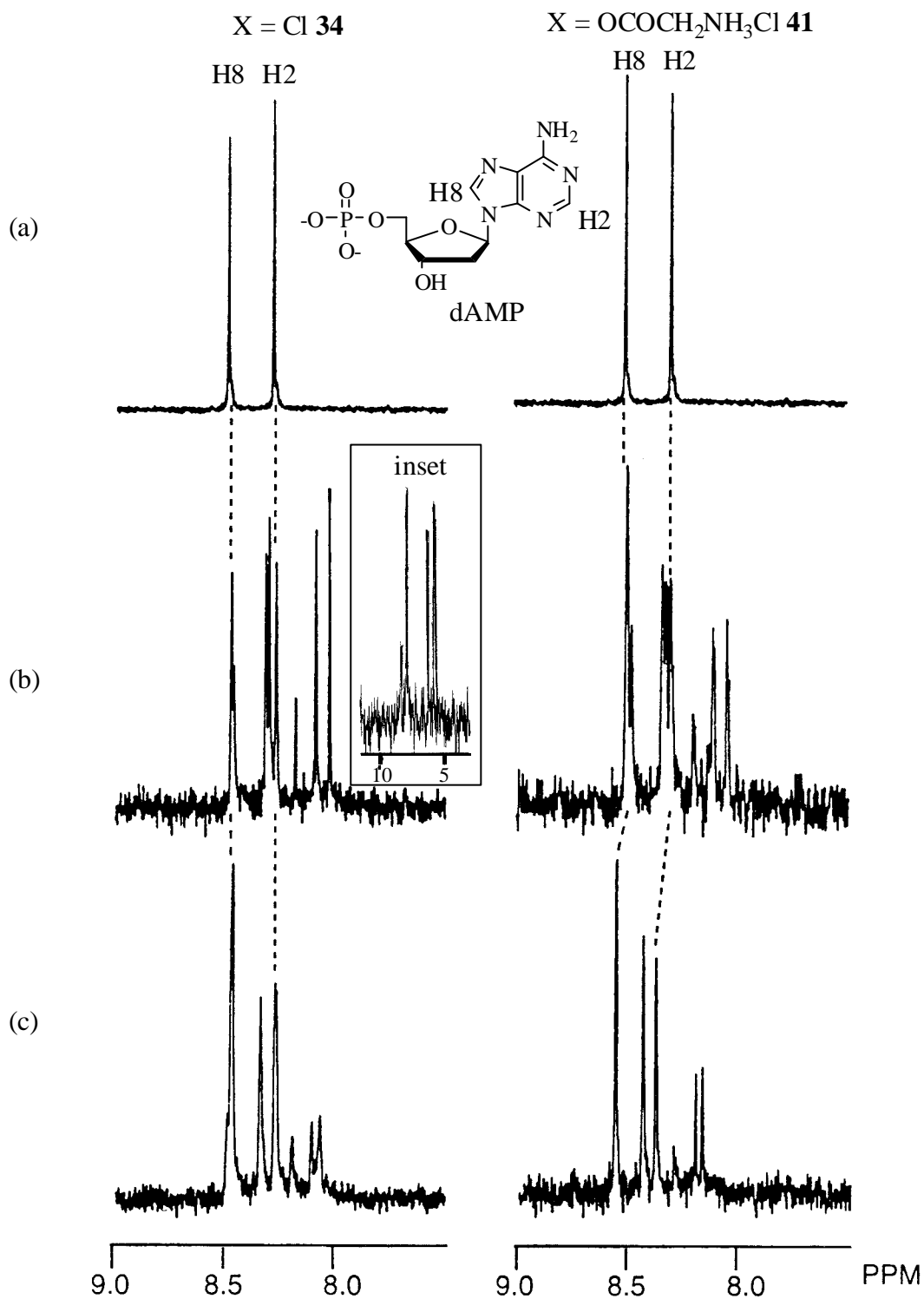


**Figure 3.3:** Aromatic region of <sup>1</sup>H NMR spectra (200 MHz, D<sub>2</sub>O, 25 °C) of (a) 5'-dAMP, pD 4.9 (b) 5'-dAMP + 1 equiv. (MeCp)<sub>2</sub>TiX<sub>2</sub> t = 0.5 h, pD 4.9 (X=Cl), 4.3 (X=gly) (c) 5'-dAMP + 1 equiv. Cp<sub>2</sub>TiX<sub>2</sub>, t = 0.5 h, pD 5.0 (X=Cl), 4.0 (X=gly). Inset: <sup>31</sup>P NMR spectra of 5'-dAMP with 1 equiv. (MeCp)<sub>2</sub>TiCl<sub>2</sub> **34** (t = 0.5 h, pD 4.9)

phosphate (O) of the nucleotide. While the relative intensities of the signals due to the complex(es) in the  $^1\text{H}$  NMR spectra (Figure 3.3b) were slightly different in each spectrum, when one takes into account the slight variations in solution pD, the spectra are remarkably similar which strongly supports the formation of the same types of complex(es) in each case.

Figure 3.4 shows the effect of increasing the solution pD to  $\sim 7.4$  on the relative stabilities of the complexes formed by **34** and **41** at low pD. Spectra are not presented for  $\text{Cp}_2\text{TiX}_2$ , because as soon as the pD is raised above 5.5 both  $\text{Cp}_2\text{TiCl}_2$  **1** (Figure 3.1(i); see also Section 1.5.2) and  $\text{Cp}_2\text{Ti}(\text{OCOCH}_2\text{NH}_3\text{Cl})_2$  **27** (Figure 3.1(ii)) undergo complete hydrolysis and concomitant precipitation and only signals due to the nucleotide (ie., as in Figure 3.4a) are detected. In contrast to this result, clear evidence for formation of stable adducts between  $(\text{MeCp})_2\text{TiX}_2$  and 5'-dAMP (Figure 3.4) at pD  $\sim 7.4$  were obtained. Figure 3.4b shows the spectra obtained on titration of 1 equiv. of  $(\text{MeCp})_2\text{TiX}_2$  into a solution of 5'-dAMP followed by immediate adjustment of the solution pD to  $\sim 7.4$ . Figure 3.4c shows the  $^1\text{H}$  NMR spectra obtained on the same samples after 24 h. Raising the solution pD from 4.9 to 7.4 is accompanied by some precipitation, but distinct signals assigned to metallocene complexes are clearly present at pD 7.4 (Figure 3.4b). After 24 h, the amount of hydrolysis increased, as evidenced by increased precipitation, and the relative amount of complex(es) was reduced (Figure 3.4c). Furthermore, when 1 equiv. of  $(\text{MeCp})_2\text{TiX}_2$  at pD  $\sim 7$  was added to 5'-dAMP at pD  $\sim 7.4$  adduct formation was reduced, but still observed (Figure 3.5). This result shows that the metallocenes **34** and **41** can be administered at elevated pD while maintaining some of the complexing moiety, " $\text{MeCpTi}^{2+}$ ".

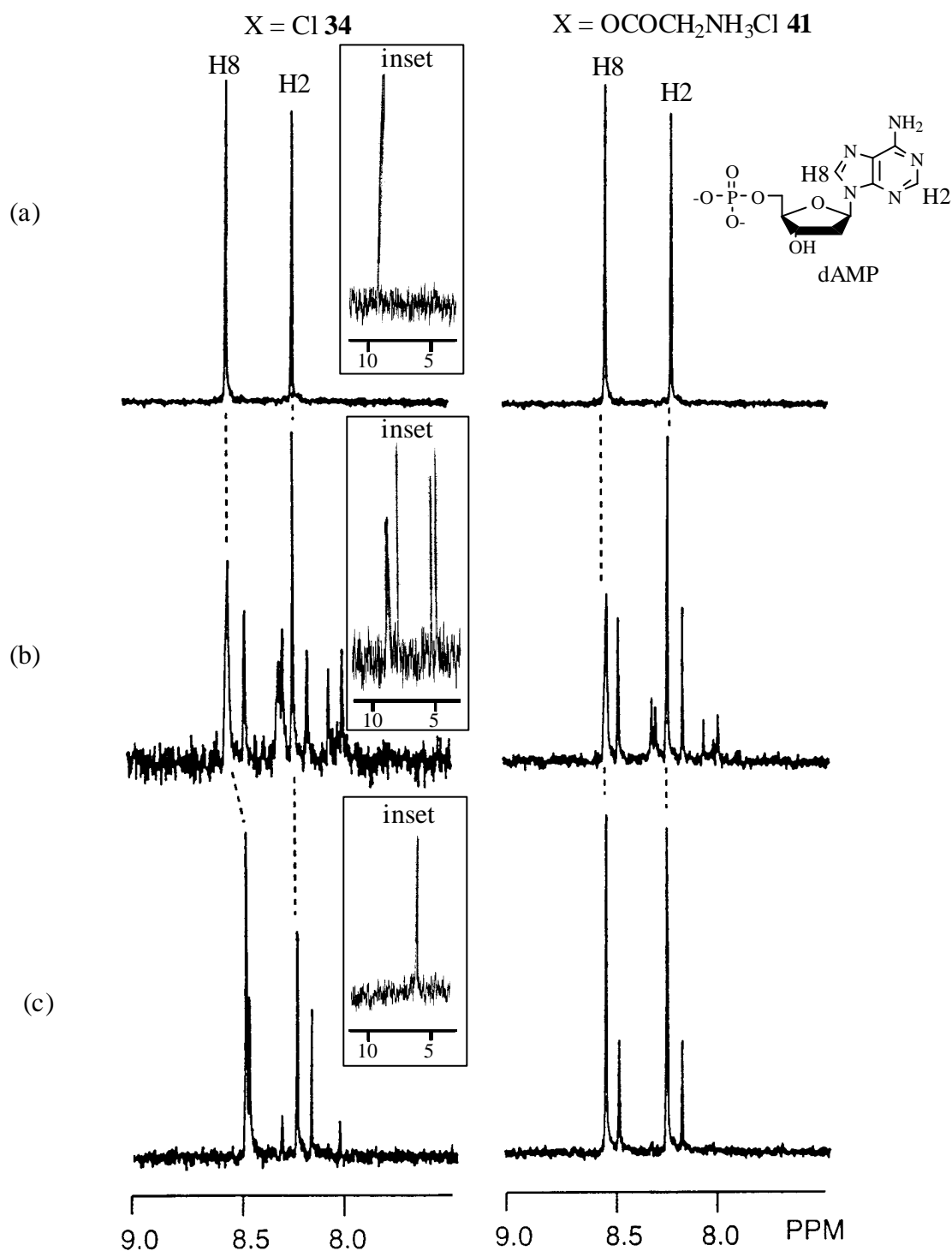


**Figure 3.4:** Aromatic region of  $^1\text{H}$  NMR spectra (200 MHz,  $\text{D}_2\text{O}$ , 25 °C) of (a) 5'-dAMP, pD 7.7 (a) 5'-dAMP + 1 equiv.  $(\text{MeCp})_2\text{TiX}_2$   $t = 0.5$  h, pD 7.9 (X=Cl **34**), 7.7 (X=gly **41**) (c) 5'-dAMP + 1 equiv.  $(\text{MeCp})_2\text{TiX}_2$ ,  $t = 24$  h, pD 7.8 (X=Cl **34**), 7.5 (X=gly **41**). Inset:  $^{31}\text{P}$  NMR spectra of 5'-dAMP with 1 equiv.  $(\text{MeCp})_2\text{TiCl}_2$  **34**

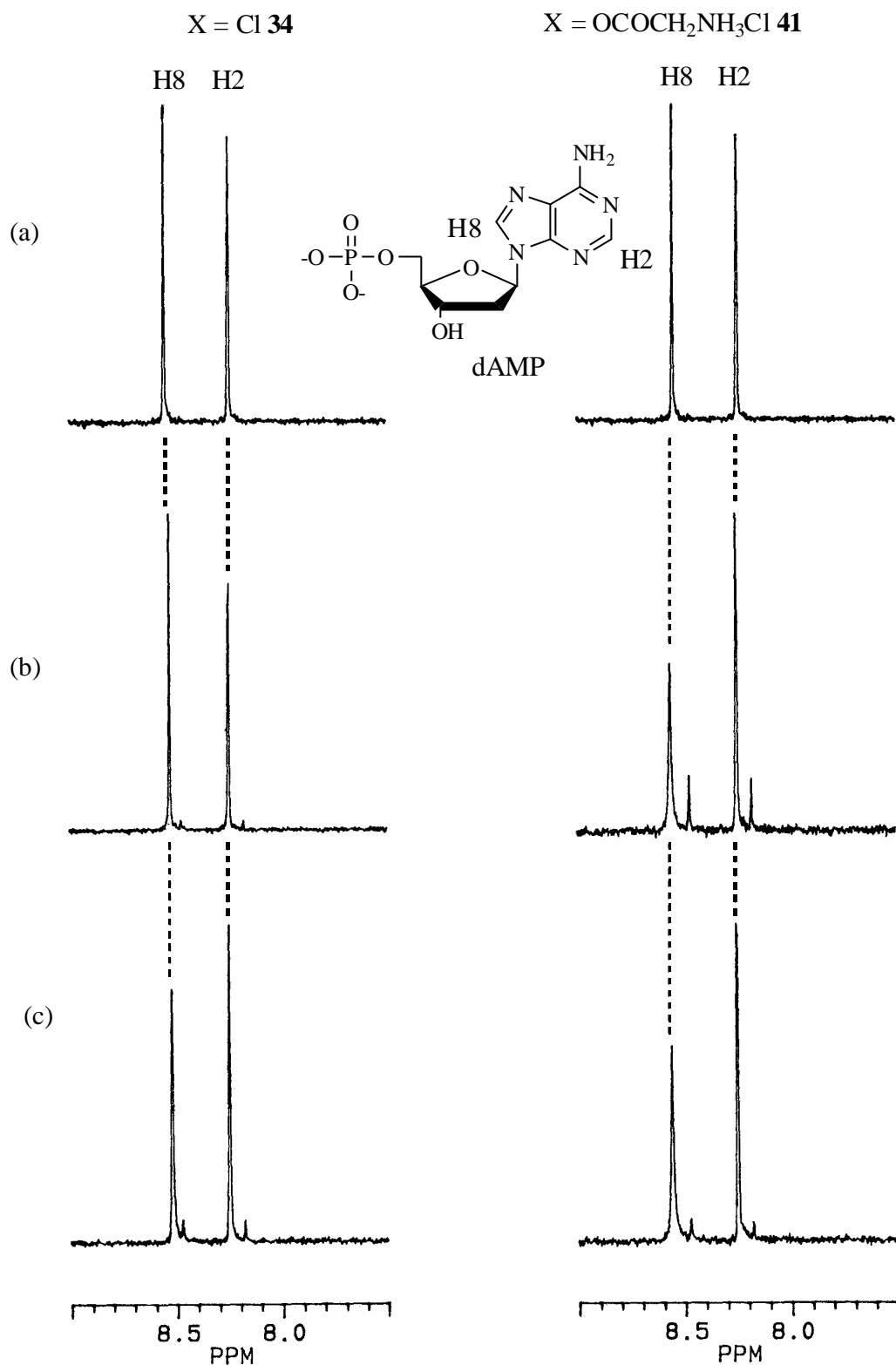


**Figure 3.5:** Aromatic region of  $^1\text{H}$  NMR spectra (200 MHz,  $\text{D}_2\text{O}$ , 25  $^\circ\text{C}$ ) of (a) 5'-dAMP, pD 7.7 (b) 5'-dAMP + 1 equiv.  $(\text{MeCp})_2\text{TiX}_2$  (initially at pD 7.7) at  $t = 0.5$  h, pD 7.7 ( $X = \text{Cl}$  **34**), pD 7.7 ( $X = \text{gly}$  **41**) (c) 5'-dAMP + 1 equiv.  $(\text{MeCp})_2\text{TiX}_2$  at  $t = 24$  h, pD 7.5 ( $X = \text{Cl}$  **34**), 7.6 ( $X = \text{gly}$  **41**)

The effect of the X ligand on complexation is apparent by comparison of the pair of spectra in either Figure 3.3 or in Figure 3.4. Very similar spectra were obtained at each pD value consistent with the conclusions of the hydrolysis studies that indicate that in solution, both the chloride and glycine ligands dissociate to generate either " $\text{Cp}_2\text{Ti}^{2+}$ " in the case of **1** and **27** or " $(\text{MeCp})_2\text{Ti}^{2+}$ " in the case of **34** and **41**. Similar results were obtained from titration experiments with 5'-dGMP (Table 3.3; Figure 3.6 and 3.7). As was noted for the spectra of 5'-dAMP in Figure 3.3 and 3.4, the slight differences between the relative intensities of the signals in the spectra are within the experimental limits of fluctuation of pD with time.

Analogous studies with 5'-dCMP and 5'-dUMP were carried out, but due to signal overlap between the signals of metal bound and unbound pyrimidine protons, accurate integration and assignment of signals was not possible. For this reason, quantitative data for the pyrimidines are not included in Table 3.3. The exact structures of the species formed in solution by  $(\text{MeCp})_2\text{TiX}_2$  ( $X = \text{Cl}$  **34**,  $\text{OCOCH}_2\text{NH}_3\text{Cl}$  **41**) and the nucleotides 5'-dAMP and 5'-dGMP cannot be unambiguously assigned from the NMR spectral data. However, comparison of the chemical shifts of the new aromatic resonances observed in the  $^1\text{H}$  NMR spectra with those observed previously with  $\text{Cp}_2\text{TiX}_2$ ,<sup>60,66</sup> as well as new signals in the  $^{31}\text{P}$  NMR spectra, are consistent with phosphate (O) complexation along with base (N) coordination and the complexes are most probably analogous to the well-characterized Mo-adducts (eg., Figure 2.6).<sup>60,66</sup> The methyl groups in **34** or **41** do not appear to impede complex formation or alter the binding mode compared to  $\text{Cp}_2\text{TiCl}_2$  **1**.



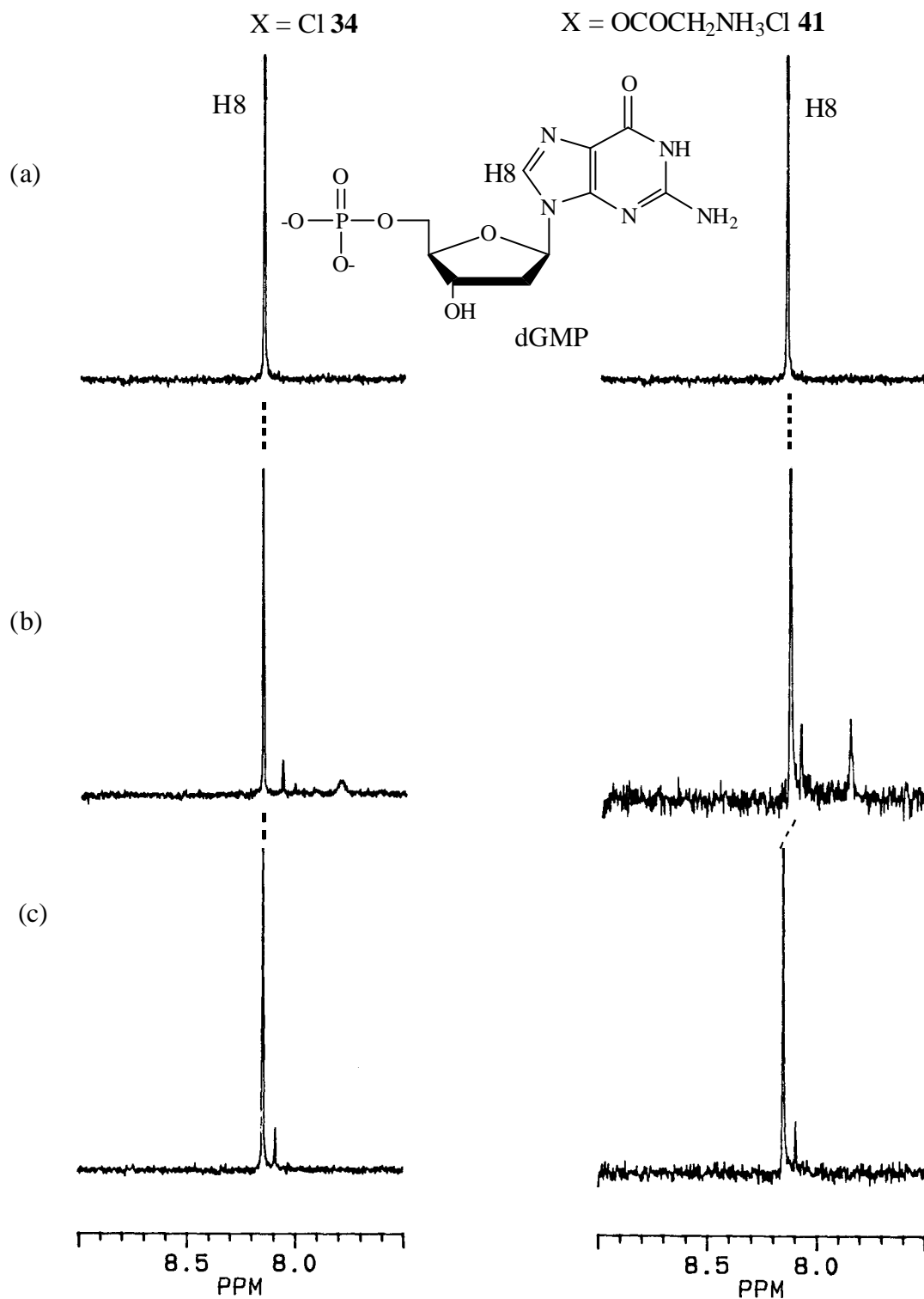


**Figure 3.7:** Aromatic region of  $^1\text{H}$  NMR spectra (200 MHz,  $\text{D}_2\text{O}$ , 25  $^\circ\text{C}$ ) of (a) 5'-dGMP, pD 7.6 (b) 5'-dGMP + 1 equiv. (MeCp)<sub>2</sub>TiX<sub>2</sub> at t = 0.5 h, pD 10.1 (X=Cl **34**), pD 7.8 (X=gly **41**) (c) 5'-dGMP + 1 equiv. (MeCp)<sub>2</sub>TiX<sub>2</sub> at t = 24 h, pD 7.5 (X=Cl **34**), pD 7.5 (X=gly **41**)

### 3.1.5. Biological Properties of Methyl Substituted Titanocene Complexes

The alkyl substituted titanocene complexes  $(\text{MeCp})_2\text{TiCl}_2$  **34** and  $(\text{MeCp})_2\text{Ti}(\text{OOCCH}_2\text{NH}_3\text{Cl})_2$  **41** were tested for antitumour activity *in vivo* by Professor P. Köpf-Maier at the Frei Universität Berlin. Two administration conditions were tested (i) 10% DMSO/90% saline at low pH i.e, the standard conditions that have been used for testing of almost all metallocenes by Köpf and Köpf-Maier;<sup>17,46</sup> and (ii) water at pH 6-6.5. The second set of conditions were used as  $(\text{MeCp})_2\text{TiCl}_2$  **34** could be dissolved in water by sonication for 3-4 h and  $(\text{MeCp})_2\text{Ti}(\text{OCOCH}_2\text{NH}_3\text{Cl})_2$  **41** could be dissolved in water by shaking. The pH was adjusted to 6.2-6.4 with sodium hydroxide solution (1% or 5%) as these complexes are stable to Cp hydrolysis (Section 3.1.3) and form complexes with nucleotides (Section 3.1.4) in this pH range. The elevated pH was also used to minimise toxic effects as is expected from previous reports.<sup>46</sup> The pH was carefully adjusted to 6.2-6.4 without increasing the pH over 7 and therefore Cp hydrolysis processes, which are increased at elevated pH values, were minimised.

The results from the antitumour testing (Table 3.4 and 3.5) showed that neither of the complexes **34** and **41** had any antitumour activity when administered in water at pH 6-6.5 or when administered at low pH in saline/DMSO (9:1) mixtures. These results are quite surprising if interaction with DNA by a " $(\text{MeCp})_2\text{Ti}^{2+}$ " species is a key process in the mechanism of antitumour action. The hydrolysis and nucleotide binding studies outlined in previous sections show that a species in which both of the Cp rings are metal bound " $(\text{MeCp})_2\text{Ti}^{2+}$ " is stable at pH ~7 for at least 24 hours, and can form stable adducts with nucleotides under these conditions.

A reduction in the toxicity of the substituted complexes **34** and **41** was observed when the pH was elevated. The LD<sub>50</sub> can be calculated from the number of toxic deaths in Table 3.4 and 3.5 and is the dose required to kill 50% of the tested mice (i.e. 3/6). For complexes **34** (Table 3.4) and **41** (Table 3.5) the LD<sub>50</sub> increased from 35 mg kg<sup>-1</sup> and 70 mg kg<sup>-1</sup> respectively when administered in saline/DMSO (9:1, low pH) to 80 mg kg<sup>-1</sup> and >160 mg kg<sup>-1</sup> respectively when administered in water (pH 6.2-6.4). It is also interesting that the LD<sub>50</sub> was improved for complex **41** compared to **34** suggesting that the improved aqueous solubility of **41** aids in the reduction of toxicity.

**Table 3.4:** Antitumour activity of (MeCp)<sub>2</sub>TiCl<sub>2</sub> **34** against EAT in mice.

Complex (CH <sub>3</sub> Cp) <sub>2</sub> TiX <sub>2</sub>	Dose (mg/kg)	Number of animals	Tumor deaths	Number of toxic deaths	Cures
X = Cl <b>34</b> 10% DMSO/90% H <sub>2</sub> O	10	6	6	-	-
	20	6	6	-	-
	30	6	4	2	-
	40	6	2	4	-
	50	6	1	5	-
	60	6	-	6	-
X = Cl <b>34</b> H <sub>2</sub> O (pH 6.2-6.4)	20	6	6	-	-
	40	6	6	-	-
	60	6	4	2	-
	80	6	3	3	-
	100	6	2	4	-
	120	6	-	6	-

**Table 3.5:** Antitumour activity of  $(\text{MeCp})_2\text{Ti}(\text{OCOCH}_2\text{NH}_3\text{Cl})_2$  **41** against EAT in mice.

Complex $(\text{CH}_3\text{Cp})_2\text{TiX}_2$	Dose (mg/kg)	Number of animals	Tumour deaths	Number of toxic deaths	Cures
X = $\text{OCOCH}_2\text{NH}_3\text{Cl}$ <b>41</b> 10% DMSO/90% $\text{H}_2\text{O}$	10	6	6	-	-
	20	6	6	-	-
	40	6	6	-	-
	60	6	4	2	-
	80	6	2	4	-
	100	6	-	6	-
	120	6	-	6	-
X = $\text{OCOCH}_2\text{NH}_3\text{Cl}$ <b>41</b> $\text{H}_2\text{O}$ (pH 6.2-6.4)	20	6	6	-	-
	40	6	6	-	-
	60	6	6	-	-
	80	6	6	-	-
	100	6	6	-	-
	120	6	6	-	-
	140	6	6	-	-
	160	6	6	-	-
	200	6	-	6	-

The absence of any biological activity for complexes **34** and **41** suggests that the steric and/or electronic changes in these complexes compared to  $\text{Cp}_2\text{TiCl}_2$  **1** have had a detrimental effect on the mechanism of action. Firstly, the steric bulk of the methyl group may impede interaction of the complex with DNA and/or proteins *in vivo* even though binding is observed *in vitro* with the nucleotides. Secondly, in contrast to  $\text{Cp}_2\text{TiCl}_2$  **1**, the improved hydrolytic

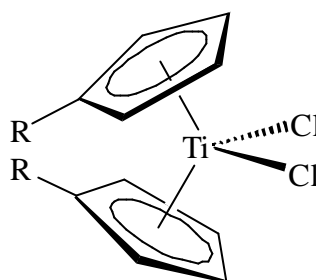
stability of the Cp rings in **34** and **41** may prevent loss of the Cp rings *in vivo*. Thus, the lability of the Cp-Ti bond in  $\text{Cp}_2\text{TiCl}_2$  **1** may be a crucial feature of the drug, which allows release of a  $\text{Ti}^{4+}$  species *in vivo*.

### 3.2. Design of Titanocene Derivatives with Modified Hydrolytic Stability

In order to test the hypothesis that the reduced antitumour activity of the methylsubstituted derivatives **34** and **41** is related to hydrolytic stability, the design and synthesis of a range of Cp-substituted titanocene derivatives with modified hydrolytic stability was investigated. The overall aim was to prepare a derivative in which the hydrolytic stability of the Cp-Ti bond was improved compared to  $\text{Cp}_2\text{TiCl}_2$  **1** but reduced compared with  $(\text{MeCp})_2\text{TiCl}_2$  **34**, ie., Cp hydrolysis would occur in a range which was faster than  $(\text{MeCp})_2\text{TiCl}_2$  **34** but slower than  $\text{Cp}_2\text{TiCl}_2$  **1** to generate a  $\text{Ti}^{4+}$  species similar to that generated by  $\text{Cp}_2\text{TiCl}_2$  **1** *in vivo*.

In this work the design and synthesis of Cp substituted derivatives of  $\text{Cp}_2\text{TiCl}_2$  **1** which showed a reduced Cp hydrolysis rate compared to  $\text{Cp}_2\text{TiCl}_2$  **1**, but were not as stable as the methyl substituted derivatives  $(\text{MeCp})_2\text{TiCl}_2$  **34** and  $(\text{MeCp})_2\text{Ti}(\text{OCOCH}_2\text{NH}_3\text{Cl})_2$  **41**, were investigated (Figure 3.8). The substituted groups were chosen on the basis of electron donating ability.<sup>92</sup> Derivatives  $(\text{CpCH}_2\text{Y})_2\text{TiCl}_2$  where Y = -CHO **43**, -CONMe<sub>2</sub> **44**, -NO<sub>2</sub> **45** were designed to be less Cp stabilising than a methyl group by incorporating an electron withdrawing group (Y) on the CH<sub>2</sub> group attached to the Cp ring (Figure 3.8). For completeness, the design and synthesis of derivatives  $(\text{RCp})_2\text{TiCl}_2$  where R = -COMe **46**, -COOMe **47** or -CONMe<sub>2</sub> **48**, which contain electron withdrawing groups directly attached to the Cp ring, were also investigated (Figure 3.8).

A range of monosubstituted Cp (RCp) ligands have been reported in the literature and complexed to various transition metals. The synthesis of many of these titanocene complexes has been undertaken in studies where the complexes are investigated for their catalytic properties in various reactions.<sup>93,94</sup> For example, titanium complexes incorporating alkyl substitution such as (RCp)<sub>2</sub>TiCl<sub>2</sub>, where R = -CH<sub>3</sub>, -CH<sub>2</sub>CH<sub>3</sub>, -<sup>i</sup>Pr, -<sup>t</sup>Bu, or -CO<sub>2</sub>Me, have



R electron donating	R weak effect	R electron withdrawing
-NMe <sub>2</sub> <b>62</b>	-CH <sub>2</sub> CH <sub>2</sub> <sup>+</sup> NHMe <sub>2</sub> <b>65</b>	-COMe <b>46</b>
-CH <sub>2</sub> CH <sub>2</sub> NMe <sub>2</sub> <b>63</b>	- <sup>+</sup> NHMe <sub>2</sub> <b>64</b>	-COOMe <b>47</b>
-CH <sub>3</sub> <b>34</b>	-CH <sub>2</sub> CONMe <sub>2</sub> <b>44</b>	-CONMe <sub>2</sub> <b>48</b>
	-CH <sub>2</sub> CHO <b>43</b>	
	-CH <sub>2</sub> NO <sub>2</sub> <b>45</b>	

been prepared to study the influence of steric and electronic effects on the behaviour of these complexes as catalysts in ethene polymerisation.<sup>93</sup>

**Figure 3.8:** Cp substituted titanocene complexes with electron donating or withdrawing R groups

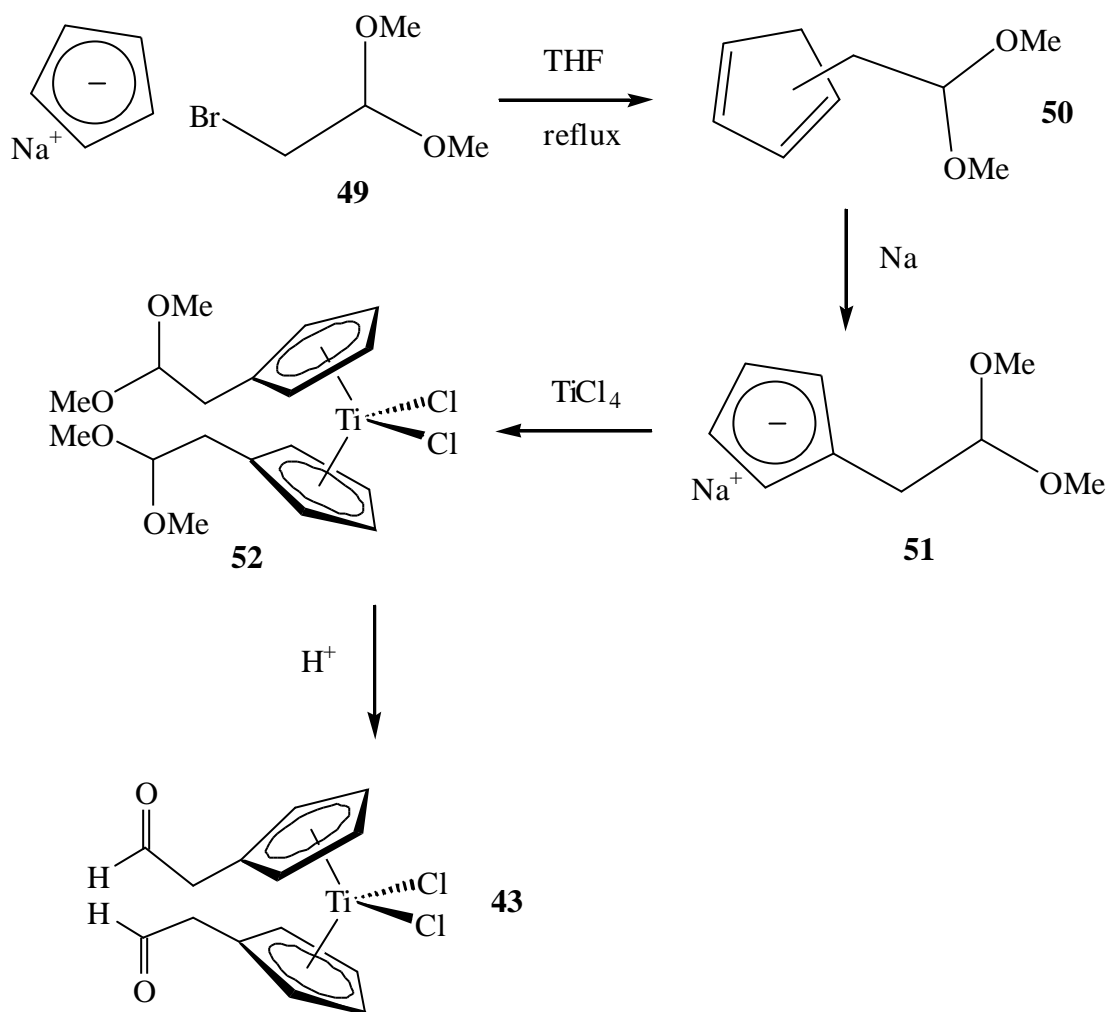
### 3.2.1. Synthesis of Titanocene Derivatives with Cp-CH<sub>2</sub>Y ligands

The preparation of complexes of the type (Cp-CH<sub>2</sub>Y)<sub>2</sub>TiCl<sub>2</sub>, where Y = -CHO **43**, -CONMe<sub>2</sub> **44** or -NO<sub>2</sub> **45** was investigated. In general the required Cp substituted ligand was prepared by direct nucleophilic substitution of the appropriately functionalised bromide with sodium cyclopentadienyl. In the case of compound **43**, the Cp substituted ligand required

was not prepared from sodium cyclopentadienyl and 2-bromoacetaldehyde directly, as the carbonyl group present in 2-bromoacetaldehyde is also susceptible to nucleophilic attack. Therefore, the protected dimethyl acetal **49** was used, with the intention of hydrolysing the acetal group to the corresponding aldehyde at a later stage in the synthesis.

Treatment of the dimethyl acetal of 2-bromoacetaldehyde,  $\text{BrCH}_2\text{CH}(\text{OMe})_2$  **49**, with sodium cyclopentadienyl at reflux for 2-3 h in THF afforded a mixture of the isomeric Cp substituted derivatives  $\text{CpCH}_2\text{CH}(\text{OMe})_2$  **50** (Scheme 3.3). Formation of these isomers was confirmed by the downfield multiplets at 6-6.5 ppm corresponding to the olefinic protons in the  $^1\text{H}$  NMR spectrum. The isomers **50**, which are susceptible to further cycloaddition reactions were not separated and isolated, but were reacted *in situ* with sodium in THF to give the anion **51** (Scheme 3.3). Formation of the required anion was confirmed by the appearance of doublets at 6.15 and 6.25 ppm in  $d_8$ -THF corresponding to the 4 aromatic protons, and the downfield shift of the  $\text{CH}_2$  protons, from 4.5 ppm in the unreacted monomer **50** to 4.7 ppm in the deprotonated anion **51**. Reaction of the anion with titanium tetrachloride produced a crude orange/red product which was dissolved in chloroform, filtered and the solvent removed. The resultant orange/red complex **52** gave a sharp singlet at 6.5 ppm consistent with formation of bound aromatic Cp rings, and aliphatic signals at 4.5 ppm ( $\text{CH}_2$ ) and 3.4 ppm (OMe). However, the singlet at 6.5 ppm broadened significantly over time, and multiple new broad peaks appeared. Simultaneously, an uncharacterised, insoluble amorphous solid precipitated. These results are consistent with polymerisation, and probably arise due to the presence of coordinating groups in substituents on the Cp rings which result in intermolecular displacement of the chlorides via the carbonyl and/or acetyl(O) atoms. The

lack of success of this reaction did not permit deprotection of the acetal group in complex **52** to afford the desired aldehyde substituted complex **43**.



Nucleophilic substitution reactions were also attempted with *N,N*-dimethylbromoacetamide ( $\text{BrCH}_2\text{CONMe}_2$ ), which was prepared from dimethylamine and the acid chloride of bromoacetic acid, and also with the commercially available bromonitromethane ( $\text{BrCH}_2\text{NO}_2$ ). Treatment of each bromide with sodium cyclopentadienyl in THF at room temperature failed to give the required substituted derivatives. In the case of the amide derivative the failure of the reaction may be attributed to the carbonyl group being much less electrophilic compared to  $\text{CH}_2$  in  $\text{BrCH}_2\text{CH}(\text{OMe})_2$  **49**. Further NMR spectroscopic

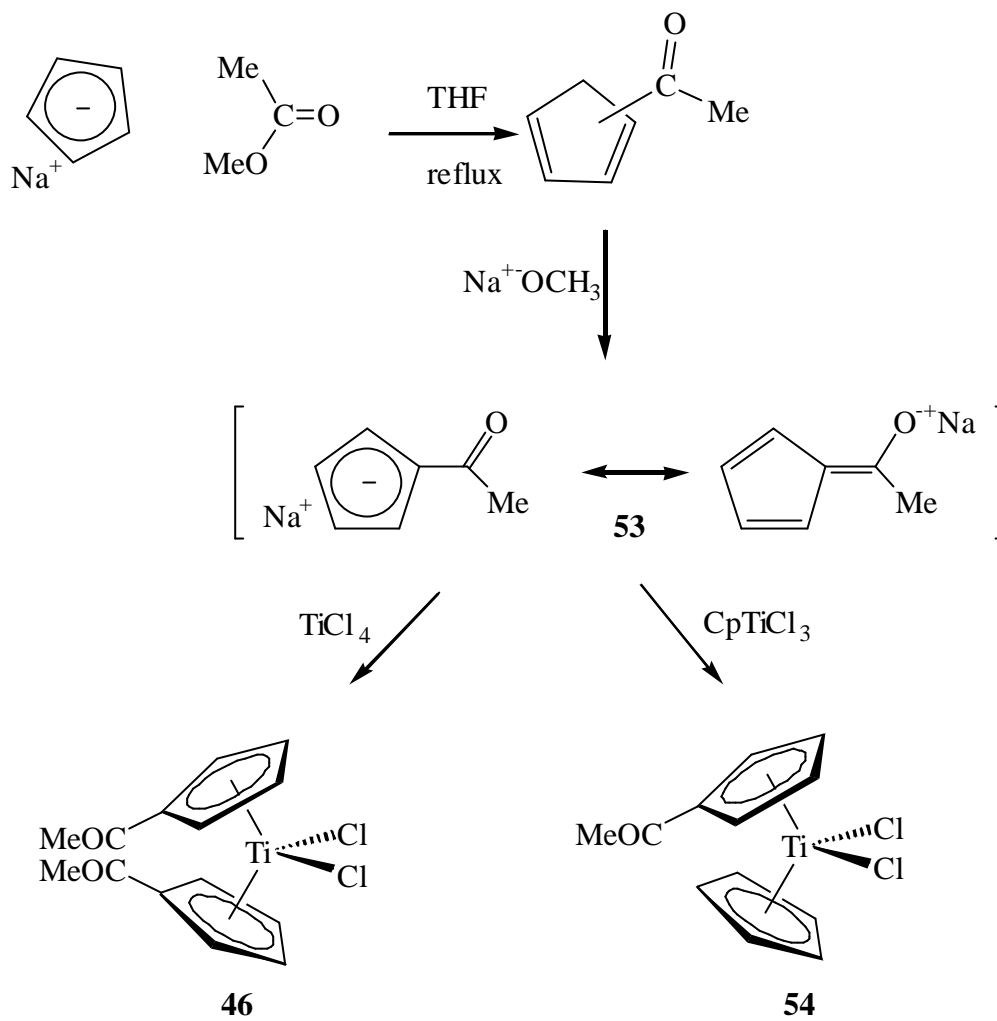
investigation of the nucleophilic substitution reaction to give  $\text{CpCH}_2\text{CON}(\text{Me})_2$  confirmed the lack of reactivity. Addition of 1 equiv. of  $\text{BrCH}_2\text{CON}(\text{Me})_2$  to sodium cyclopentadienyl in  $d_8$ -THF in an NMR sample tube resulted in formation of a brown precipitate, and signals for cyclopentadiene and the starting material  $\text{BrCH}_2\text{CON}(\text{Me})_2$  were detected in the NMR spectra. In the case of bromonitromethane, a competing acid base reaction between the cyclopentadienyl anion and the acidic  $\text{CH}_2$  protons of the bromide ( $\text{pK}_a$  of  $\text{RCH}_2\text{NO}_2$  is  $\sim 10$  while the  $\text{pK}_a$  of cyclopentadiene is 16)<sup>92</sup> precluded formation of  $\text{CpCH}_2\text{NO}_2$ .

### 3.2.2. Synthesis of R-Cp Derivatives with Electron Withdrawing Groups

A limited number of substituted titanocene derivatives with electron withdrawing groups have been reported, incorporating monosubstituted ligands such as  $\text{CpCF}_3$ ,<sup>95,96</sup>  $\text{CpCl}$ ,<sup>97</sup> and  $\text{CpCO}_2\text{Me}$ .<sup>98</sup> In this work, the introduction of the acetyl group was investigated by nucleophilic addition of the cyclopentadienyl anion to methyl acetate (Scheme 3.4). Thus, methyl acetate was added to sodium cyclopentadienyl and refluxed for 2 h in THF to give acetylcyclopentadienylsodium **53** in 35% yield, in agreement with the literature (Scheme 3.4).<sup>99</sup> The anion **53** is stabilised by the electron withdrawing substituent as the negative charge is not only delocalised around the ring but also through the carbonyl group (Scheme 3.4).<sup>100</sup>

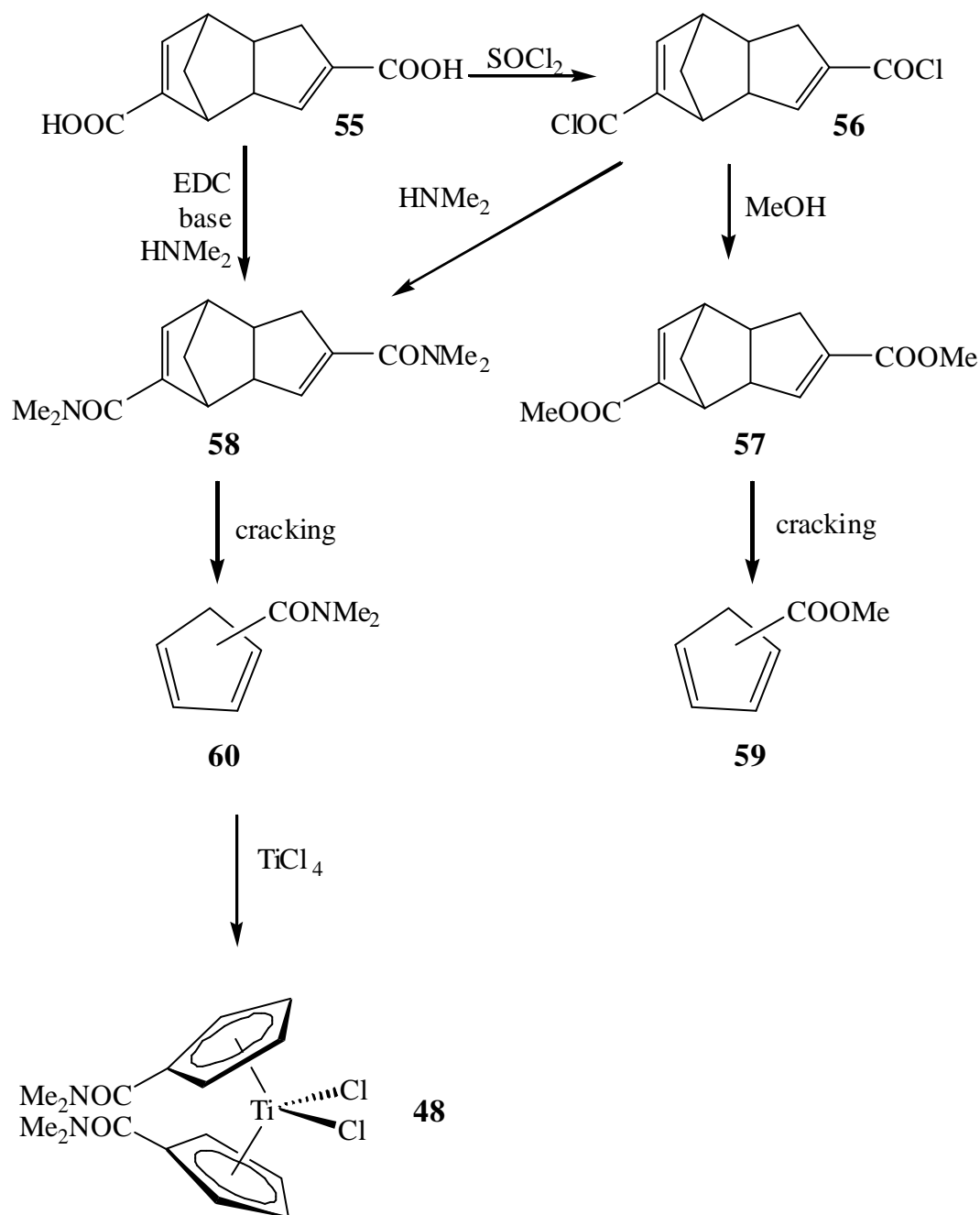
Attempts to complex the ligand **53** to titanium were unsuccessful with either titanium tetrachloride to give **46**, or cyclopentadienetitanium trichloride to give **54**. In the case of the bisubstituted derivative **46**, the NMR spectrum of the crude product in  $\text{CDCl}_3$  showed a broad signal at 6.7 ppm, consistent with formation of a polymeric Cp containing species. However, this product rapidly decomposed to give a brown/black solid. NMR spectroscopic

analyses of this solid in  $\text{CDCl}_3$ ,  $\text{D}_2\text{O}$ ,  $d_6$ -DMSO and MeOD showed no signals that were consistent with formation of the required product. Further characterisation and purification were not pursued due to the lack of solubility of the brown solid in either organic or aqueous solvents. The rapid decomposition of the resulting product was attributed to the presence of coordinating groups on the Cp rings, which can compete for coordination to the Ti metal center. It is also expected that the presence of the electron-withdrawing group on the Cp ring destabilises the Ti-Cp bond and so would also have contributed to the lack of stability of the product, or to the reactivity of the anion. The anion **53** is also expected to be less nucleophilic due to the delocalisation of its negative charge, which would contribute to the lack of reactivity of the anion **53**.



Scheme 3.4

An alternative route to substituted Cp derivatives, starting with commercially available Thiele's acid **55**, was investigated. Thiele's acid **55** was reported in 1901 by Thiele<sup>101</sup> and has been used to prepare a variety of substituted cyclopentadienyl derivatives.<sup>102</sup> In this work, Thiele's acid **55** was used as a starting material to incorporate functionality onto the Cp rings, according to the literature method (Scheme 3.5).



Scheme 3.5

Thiele's acid **55** was heated with thionyl chloride for 2 h to give the corresponding acid chloride **56** in 80% yield. The acid chloride was reacted with methanol or dimethylamine to give the dicyclopentadiene substituted methyl ester **57** in 65% yield and the dimethylamine derivative **58** in 47% yield respectively (Scheme 3.5).<sup>102</sup> The next step required cracking of these dimers to produce the cyclopentadiene monomers **59** and **60**. However, attempts to crack the dimers to the respective monomers resulted in isolation of only minor amounts of pure material in insufficient quantities to allow formation of the final metallocene complexes. Therefore, this route to the substituted Cp derivatives was abandoned.

A more efficient, one-step procedure was employed to produce the dimethylamine substituted dicyclopentadiene derivative **58** (Scheme 3.5). Thiele's acid **55** was coupled directly to dimethylamine using (1-3-dimethylaminopropyl)-3-ethylcarbodiimide hydrochloride (EDC), to give **58** in 80% yield (Scheme 3.5). The dimer **58** was cracked to the monomer **60** at 200 °C under pressure (~20 mm), and formation of pure monomer was confirmed by NMR spectroscopy. Deprotonation of the monomer **60** with *n*-BuLi gave the corresponding anion **61**, as indicated by the appearance of multiplets from the aromatic protons at 5.7 and 6.2 ppm. However, all attempts to prepare the disubstituted titanium complex **48** from titanium tetrachloride and the amide substituted anion **61** were unsuccessful, giving a black/brown solid, which decomposed when characterisation was attempted. The product decomposed in CDCl<sub>3</sub> to give an uncharacterised white precipitate, and showed no signals which were consistent with formation of the product. The mass spectrum showed neither the expected molecular ion peak nor fragment ions of the required product. The failure to form the complex is most likely due to the presence of the electron withdrawing amide group on the Cp rings, which destabilises the metal-Cp bond in the titanocene complex **48**. Polymerisation

of the product **48** is also possible due to the presence of coordinating groups in the Cp side chain. In either case, such complexes are not appropriate candidates for further investigation as antitumour drugs.

### 3.2.3. Synthesis of Aminoalkyl Substituted Derivatives

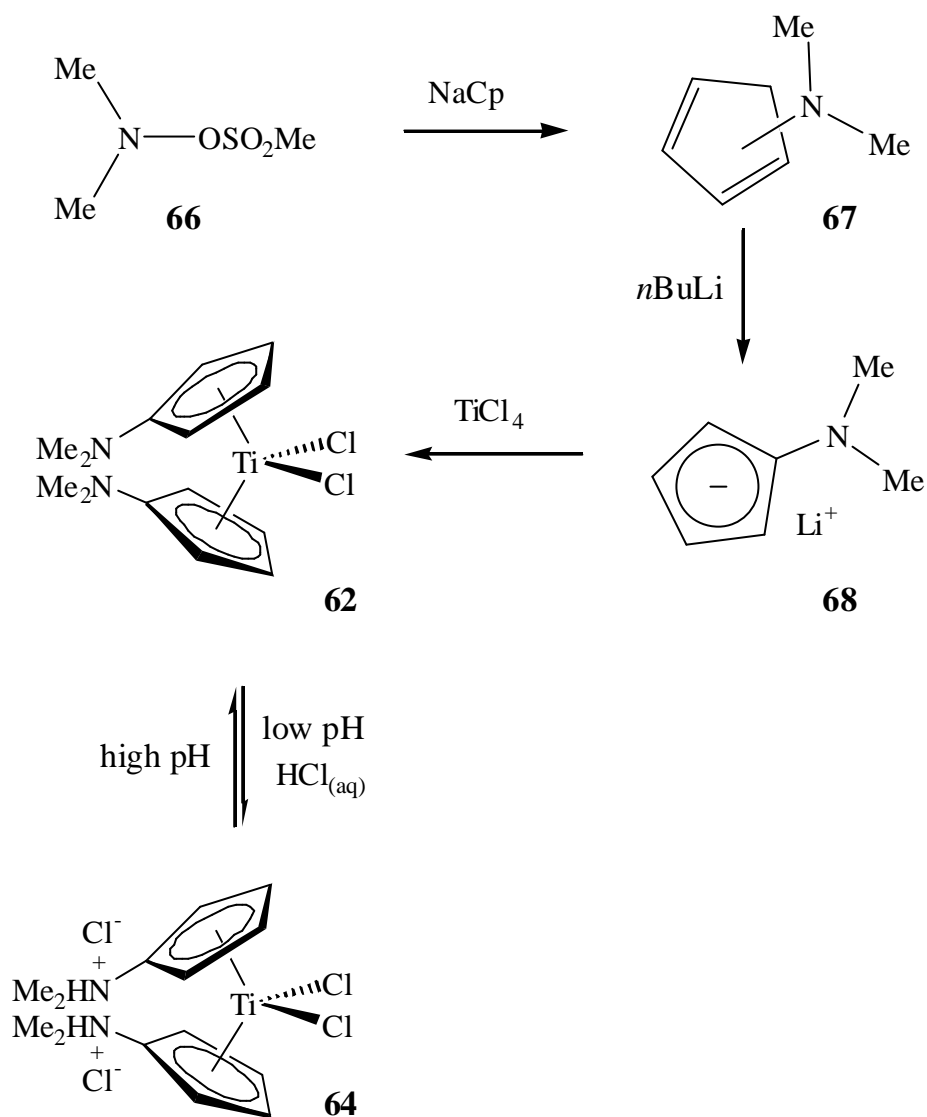
The synthetic investigations from Sections 3.2.1 and 3.2.2 suggested that the presence of Ti-coordinating side-chains in the complex led to decomposition/polymerisation which prevented isolation of pure complex. Therefore, introduction of aminoalkyl group was investigated, as this group can be protected as the ammonium salt at low pH (Scheme 3.6). Furthermore, upon deprotonation, the electronic character of the side-chain would be modified, changing the hydrolytic stability of the Cp ring.

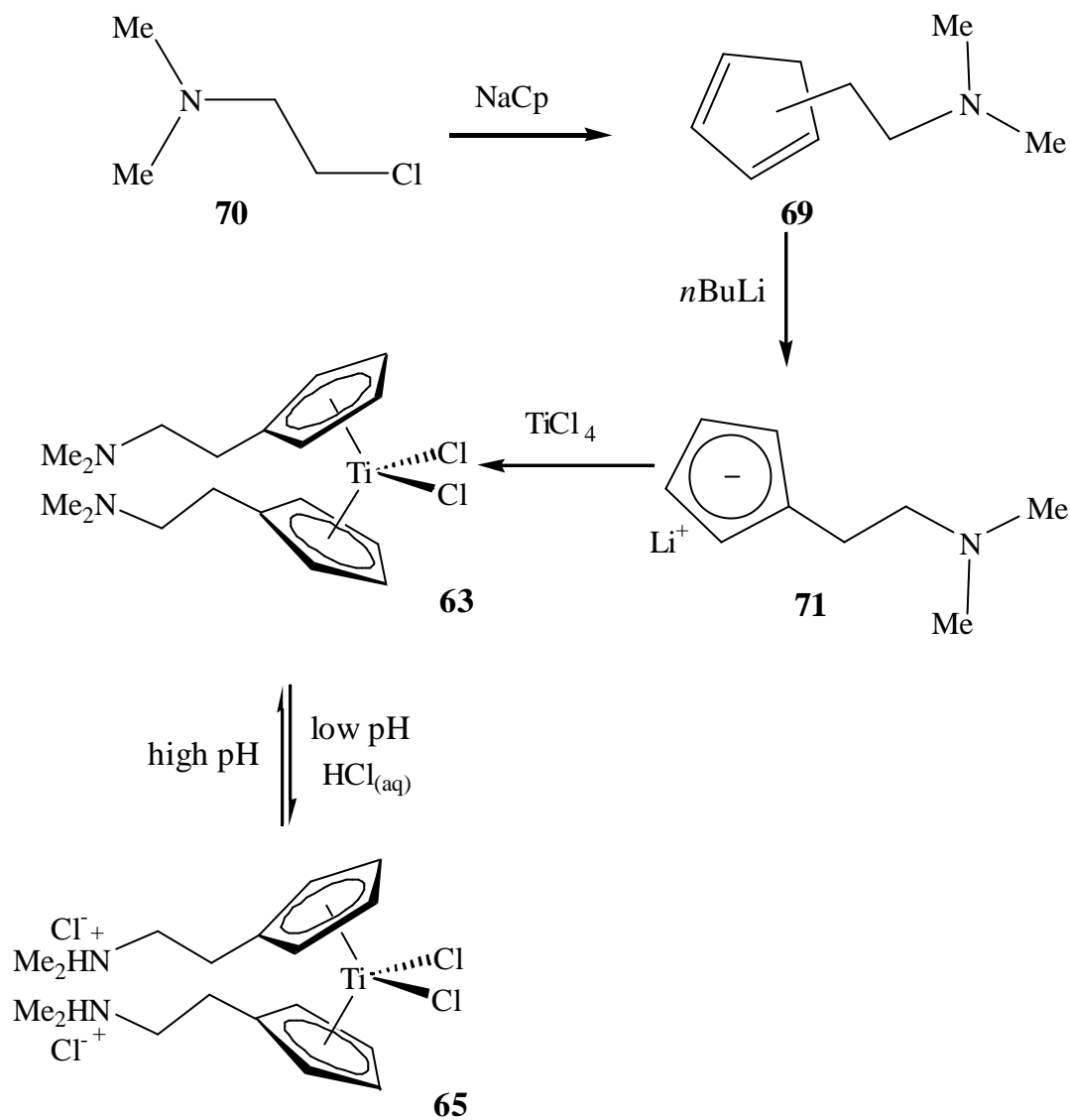
Amino-functionalised Cp substituted (e.g.  $\text{Cp}(\text{CH}_2)_n\text{NR}_2$ ) complexes of titanium,<sup>103-107</sup> molybdenum,<sup>108</sup> rhodium,<sup>109</sup> iron,<sup>106,110,111</sup> vanadium,<sup>103,110</sup> zirconium<sup>104,112</sup> and chromium<sup>103</sup> have been reported.

In this work, synthesis of the amine substituted titanocene derivatives  $(\text{CpNMe}_2)_2\text{TiCl}_2$  **62** and  $(\text{Cp}(\text{CH}_2)_2\text{NMe}_2)_2\text{TiCl}_2$  **63** was investigated. Complexes incorporating the ligands  $\text{CpNMe}_2$ <sup>106</sup> and  $\text{Cp}(\text{CH}_2)_2\text{NMe}_2$ <sup>103,104</sup> have been reported previously. The reported synthesis of the ligand  $\text{CpNMe}_2$  **67** involves nucleophilic substitution of the leaving group  $-\text{OSO}_2\text{CH}_3$  with Cp (Scheme 3.6).<sup>113</sup> The reported synthesis of  $\text{Cp}(\text{CH}_2)_2\text{NMe}_2$  **69** involves nucleophilic substitution of  $-\text{Cl}$  with Cp (Scheme 3.7).<sup>108,109</sup> It was anticipated that these ligands would provide electron donating side chains, which would allow formation of the hydrolytically stable bis-substituted titanocene complexes **62** (Scheme 3.6) and **63** (Scheme 3.7). The electronic character of the Cp side chain could then be altered in water, by lowering the pH, to give the

corresponding complexes **64** (Scheme 3.6) and **65** (Scheme 3.7) as the ammonium salts, and therefore allow an investigation of the electron donating character of the side chain on the hydrolytic stability of these complexes.

Scheme 3.6





Scheme 3.7

In this work,  $N,N$ -dimethyl- $O$ -(methylsulfonyl)hydroxylamine ( $\text{Me}_2\text{NOSO}_2\text{Me}$ ) **66** was prepared from  $N,N$ -dimethylhydroxylamine hydrochloride and methylsulfonyl chloride in the presence of base.<sup>108</sup> The Cp substituted derivative **67** was generated *in situ* following the reported procedure,<sup>113</sup> and deprotonation with  $n\text{-BuLi}$  gave  $\text{NaCpNMe}_2$  **68** (Scheme 3.6). The anion **68** was not isolated but was treated directly with titanium tetrachloride, in an attempt to generate the desired complex **62** (Scheme 3.6). However, all attempts to isolate

the bis-substituted complex  $(\text{CpNMe}_2)_2\text{TiCl}_2$  failed. Typically, a brown oil, which was not fully characterised, was isolated, and the NMR spectrum of this crude product in  $\text{CDCl}_3$  did not show any signals consistent with formation of the product.

The synthesis of the complex  $(\text{Cp}(\text{CH}_2)_2\text{NMe}_2)_2\text{TiCl}_2$  **63** proved to be problematic (Scheme 3.7). Successful formation of the complex has been reported to be solvent dependent, with polymerisation occurring in some solvents, especially THF.<sup>103,104</sup> However, protonation of the amines stabilises the complex and prevents polymerisation reactions.<sup>103</sup>

The ligand  $\text{Cp}(\text{CH}_2)_2\text{NMe}_2$  **69** was prepared in 56% yield by nucleophilic substitution of 2-dimethylaminoethyl chloride hydrochloride **70** with sodium cyclopentadienyl in THF according to the literature procedure (Scheme 3.7).<sup>103</sup> The ligand **69** was deprotonated with *n*-BuLi to give the anion **71**, which was characterised by NMR spectroscopy (Scheme 3.7). The anion **71** was added to  $\text{TiCl}_4$  in either THF or toluene to form the complex **63**. In contrast to the literature reports, the complex **63** appeared to undergo polymerisation in all solvents tested, including THF and toluene. Attempts to form the monomer by the addition of  $\text{HCl}(\text{aq})$  to the polymer as reported by Enders, *et. al.*<sup>103</sup> (Scheme 3.7), gave a brown homogeneous solution. When the polymer was dissolved in  $\text{D}_2\text{O}$  with  $\text{DCl}$ , the NMR spectrum showed signals characteristic of the impure ionic complex  $(\text{Cp}(\text{CH}_2)_2\text{NHMe}_2^+\text{Cl}^-)_2\text{TiCl}_2$  **65**. The problems encountered in the synthesis of  $(\text{Cp}(\text{CH}_2)_2\text{NMe}_2)_2\text{TiCl}_2$  **63**, and its poor stability, excluded this complex from further investigation as a hydrolytically stable antitumour drug.

### 3.3. Conclusions

The rate of hydrolysis of the Cp rings in  $(\text{MeCp})_2\text{TiX}_2$  ( $\text{X} = \text{Cl}$  **34**,  $\text{OCOCH}_2\text{NH}_3\text{Cl}$  **41**) in water at pH 7 is significantly improved in comparison to the corresponding unsubstituted metallocenes  $\text{Cp}_2\text{TiX}_2$ . While methyl substitution of the Cp rings decreases aqueous solubility, replacement of the halide ligands with charged glycine ligands gives the highly water soluble complex **41**, in which the Cp rings remain metal bound at physiological pH. The methyl substituted complexes **34** and **41** both form adducts with nucleotides which are stable for 24 h at pH 7.4.

Substitution of the Cp rings in  $\text{Cp}_2\text{TiCl}_2$  **1** with alkyl groups has been reported to generally decrease the antitumour activity of the drug.<sup>54</sup> However, the reduced aqueous solubility of the complexes, as well as administration of the compounds in DMSO/saline at low pH, needs to be taken into account in the interpretation of biological data. Screening of complexes **34** and **41**, which were administered in aqueous solution at pH 7.4, as well as at low pH in saline/DMSO (9:1) mixtures, confirmed that these substituted complexes had no antitumour activity for reasons other than poor aqueous solubility. Reduced toxicity associated with administration at elevated pH values (6.2-6.4) was also confirmed, in line with previous studies.<sup>46</sup>

While the preparation of Cp substituted derivatives of  $\text{Cp}_2\text{TiCl}_2$  **1** with modified hydrolytic stability was unsuccessful, largely due to purification and formation of byproducts, the results with  $(\text{MeCp})_2\text{CpTiX}_2$  ( $\text{X} = \text{Cl}$  **34** and  $\text{X} = \text{OCOCH}_2\text{NH}_3\text{Cl}$  **41**) nevertheless provide some important information regarding the importance of lability of the Cp-Ti bond on antitumour activity. The lack of activity of the Cp substituted derivatives suggests that the moiety " $\text{Cp}_2\text{Ti}^{2+}$ " is required to release the biologically active species (e.g. a " $\text{Ti}^{4+}$ " species) *in*

*vivo*. This result is supported by recent studies published during the course of this work, which suggest that a "Ti<sup>4+</sup>" species is released from the complex *in vivo*, to bind the blood transport protein transferrin.<sup>76,78,80,81,114,115</sup> These studies also suggest that a "Ti<sup>4+</sup>" species is then delivered specifically to tumour cells and the site of action.

The design of a range of substituted titanocene derivatives would confirm the relationship between the electronic character of the ligands bound to the metal and antitumour activity, however, the synthesis of Cp substituted derivatives is problematic in terms of their reactivity and stability.

Structure-activity studies on  $\text{Cp}_2\text{TiCl}_2$  **1**, in which both the halide ligands and the Cp rings have been modified (see Section 1.2.), are consistent with the formation of a hydrolysed species (" $\text{Cp}_2\text{Ti}^{2+}$ ") as the active species *in vivo*. This species is assumed to form a complex with DNA and interfere with normal cell replication processes.  $\text{Cp}_2\text{TiCl}_2$  **1** undergoes rapid halide and cyclopentadienyl (Cp) hydrolysis to form cyclopentadiene (CpH) and dicyclopentadiene,<sup>58</sup> particularly at pH >4.0 (see Section 1.4.). However, these hydrolysis products cause non-specific, local tumour inhibiting effects and do not exhibit the systemic antitumour activity of  $\text{Cp}_2\text{TiCl}_2$  **1**.<sup>18,116</sup> The partially hydrolysed derivative,  $\text{CpTiCl}_3$  **30**, which lacks one of the Cp rings, exhibits reduced activity (Table 1.3),<sup>53</sup> while substitution of the Cp rings, or bridging of the two Cp rings resulted in significant loss of antitumour activity (see Section 1.3.3. and 3.1.4.).<sup>18,54</sup> Thus, the unsubstituted Cp rings are an important structural feature required in maintaining antitumour activity.

In contrast to modification of the Cp ligands, modification of the halide ligands is possible, provided the Ti-X bond remains labile in aqueous solution. Thus, derivatives  $\text{Cp}_2\text{TiX}_2$  (eg., X = F **16**, Cl **1**, Br **17**, I **18**, NCS **19**,  $\text{N}_3$  **20**, Y see Table 1.1) retain antitumour activity, whereas the reduced activity observed in several cases (eg., X = *p*- $\text{OC}_6\text{H}_4\text{NO}_2$  **24**) is attributed to pseudohalide ligands that are too strongly bound to the titanium centre thus preventing dissociation in aqueous systems.<sup>18,48</sup> Introduction of hydrophilic and charged X ligands (eg.,  $\text{SC}_6\text{H}_4\text{NH}_3\text{Cl}$  **21**,  $\text{OCOCCl}_3$  **22**, *cis*  $\text{OCOCHCHCO}_2\text{H}$  **23**) has been proposed as a method whereby the aqueous solubility of complexes  $\text{Cp}_2\text{TiX}_2$  may be improved, without significant perturbation of antitumour properties.<sup>47</sup> While the aqueous solubility of  $\text{Cp}_2\text{Ti}(\text{SC}_6\text{H}_4\text{NH}_3\text{Cl})_2$  **21** and

$\text{Cp}_2\text{Ti}(\text{OCOCHCO}_2\text{H})_2$  **23** was improved compared to  $\text{Cp}_2\text{TiCl}_2$  **1**, the aqueous solubility of  $\text{Cp}_2\text{Ti}(\text{OCOCCl}_3)_2$  **22** was not quantified. The synthesis and biological activity of the highly water soluble amino acid derivative  $\text{Cp}_2\text{Ti}(\text{OCOCH}_2\text{NH}_3\text{Cl})_2$  **27** and  $\text{Cp}_2\text{Ti}(\text{OCOCHCH}_3\text{NH}_3\text{Cl})_2$  **28** has also been reported.<sup>49-51</sup> While in the solid state, the complex  $\text{Cp}_2\text{Ti}(\text{OCOCH}_2\text{NH}_3\text{Cl})_2$  **27** crystallises with the carboxylate groups coordinated to the metal centre, in solution the studies reported in Chapter 3 showed that the glycine ligands are only weakly coordinated to the metal centre, and that, as in the case of  $\text{Cp}_2\text{TiCl}_2(\text{aq})$  **1**, the predominant species present in aqueous solutions of  $\text{Cp}_2\text{Ti}(\text{OCOCH}_2\text{NH}_3\text{Cl})_2$  **27** in the range pH 2-5 is " $\text{Cp}_2\text{Ti}^{2+}$ " (see Section 3.1.). However, in contrast to all previously studied titanocenes containing weakly coordinating halide or pseudohalide ligands, antitumour testing of this derivative against EAT did not show the expected 100% cure rates and activity levels of only 50% were achieved (see Section 1.4.2.; Table 1.3).

In an effort to further define the key structural elements required in  $\text{Cp}_2\text{TiX}_2$  to retain antitumour activity, this chapter reports a study of the hydrolysis chemistry of titanocene derivatives  $\text{Cp}_2\text{TiX}_2$  ( $X = \text{Cl}$  **1**,  $\text{OCOCCl}_3$  **22** and  $\text{OCOCH}_2\text{NH}_3\text{Cl}$  **27**) in water and aqueous DMSO mixtures. Particular attention was paid to the therapeutic conditions of 10% DMSO/90% saline.

The rate of Cp hydrolysis of  $\text{Cp}_2\text{TiCl}_2$  **1** in water has been reported previously (see Section 1.5.2.) and the Cp hydrolysis of  $\text{Cp}_2\text{Ti}(\text{OCOCH}_2\text{NH}_3\text{Cl})_2$  **27** in water at different pH values is discussed in Section 3.1.2. Preliminary data for the hydrolysis of a number of carboxylate complexes in water, including  $\text{Cp}_2\text{Ti}(\text{OCOCCl}_3)_2$  **22**, have been reported.<sup>62</sup> However, no details of the aqueous solubility of  $\text{Cp}_2\text{Ti}(\text{OCOCCl}_3)_2$  **22** have been reported.

Furthermore, there are no systematic studies of the hydrolysis of  $\text{Cp}_2\text{TiCl}_2$  **1**,  $\text{Cp}_2\text{Ti}(\text{OCOCCl}_3)_2$  **22** or  $\text{Cp}_2\text{Ti}(\text{OCOCH}_2\text{NH}_3\text{Cl})_2$  **27** in aqueous DMSO or neat DMSO.

Due to the use of DMSO in therapeutic mixtures, the relative stabilities of metallocenes  $\text{Cp}_2\text{TiX}_2$  ( $\text{X} = \text{Cl}$  **1**,  $\text{OCOCCl}_3$  **22**,  $\text{OCOCH}_2\text{NH}_3\text{Cl}$  **27**) in three different solutions was examined in this work. Complex **1** was studied as the parent metallocene undergoing clinical trials. The bis glycine analogue **27** was studied due to the unexpected, reduced antitumour activity of this complex,<sup>49</sup> and the trichloroacetate analogue **22** was selected as a representative of the hydrophilic carboxylate series<sup>47</sup> which has been screened against a number of tumour types.<sup>28</sup>

#### **4.1. Hydrolysis Experiments**

The hydrolysis of  $\text{Cp}_2\text{TiX}_2$  can involve Cp hydrolysis and/or hydrolysis of the X ligand. In this work, NMR spectroscopy was used to monitor the rate of Cp hydrolysis in  $\text{Cp}_2\text{TiX}_2$  ( $\text{X} = \text{Cl}$  **1**,  $\text{OCOCCl}_3$  **22** and  $\text{OCOCH}_2\text{NH}_3\text{Cl}$  **27**). It was also possible in some cases to gain information regarding the hydrolysis of the X ligand. The rate of Cp hydrolysis in  $\text{Cp}_2\text{TiX}_2$  ( $\text{X} = \text{Cl}$  **1**,  $\text{OCOCCl}_3$  **22** and  $\text{OCOCH}_2\text{NH}_3\text{Cl}$  **27**) was measured using  $^1\text{H}$  NMR spectroscopy at regular time intervals in  $\text{D}_2\text{O}$ , DMSO and 10% DMSO/ $\text{D}_2\text{O}$  at 25 °C, using similar methods to those reported in Chapter 2 and 3. Thus, an estimate of the Cp hydrolysis may be calculated from the relative intensities of the new multiplets due to cyclopentadiene and dicyclopentadiene in solution. In addition, hydrolysis is also apparent by formation of precipitates which accumulates with time. As in previous studies,<sup>58,62,63</sup> full characterisation of these precipitates has not been possible due to their poor aqueous solubility, but formation of oligomers and bridged species containing Cp rings cannot be ruled out. Hence the amount of

precipitate formed was also used as an indicator of the amount of hydrolysis occurring in solution. In the case of  $\text{Cp}_2\text{TiCl}_2$  **1** and  $\text{Cp}_2\text{Ti}(\text{OCOCCl}_3)_2$  **22** the amount of precipitate (and hence hydrolysis) could only be estimated visually or by isolation and weighing the precipitate. However, in the case of  $\text{Cp}_2\text{Ti}(\text{OCOCH}_2\text{NH}_3\text{Cl})_2$  **27**, a more accurate estimate was possible by integration of the glycine  $\text{CH}_2$  peak versus the Cp protons. Fully dissolved  $\text{Cp}_2\text{Ti}(\text{OCOCH}_2\text{NH}_3\text{Cl})_2$  **27** gives by integration a ratio of 10:4 = Cp:CH<sub>2</sub>. As the precipitate accumulated, the Cp signal decreased relative to the glycine peak. This change in signals is consistent with formation of hydrolysis products derived from the Cp rings.

#### **4.1.1. Cp Hydrolysis in Water**

The rate of Cp hydrolysis of complexes  $\text{Cp}_2\text{TiCl}_2$  **1** and  $\text{Cp}_2\text{Ti}(\text{OCOCH}_2\text{NH}_3\text{Cl})_2$  **27**, including mixed experiments containing equal amounts of both complexes, have been reported and discussed in Chapter 3, and the results are summarised in Table 4.1. While the hydrolysis of both  $\text{Cp}_2\text{TiCl}_2$  **1** and  $\text{Cp}_2\text{Ti}(\text{OCOCH}_2\text{NH}_3\text{Cl})_2$  **27** is accompanied by formation of a minor amount of insoluble precipitate at pD ~2, all of the dissolved material contains the Cp rings bound to the metal. Attempts to carry out similar experiments with  $\text{Cp}_2\text{Ti}(\text{OCOCCl}_3)_2$  **22** confirmed previous reports of poor aqueous solubility of the complex. While the solubility was not quantified, the trichloroacetate derivative **22** appeared to be less soluble than  $\text{Cp}_2\text{TiCl}_2$  **1**.

#### **4.1.2. Hydrolysis<sup>†</sup> in 100% DMSO**

Table 4.1 summarises the results obtained for the complexes  $\text{Cp}_2\text{TiX}_2$  (X = Cl **1**,  $\text{OCOCCl}_3$  **22**,  $\text{OCOCH}_2\text{NH}_3\text{Cl}$  **27**; 10  $\mu\text{mol}$ ) in 100% DMSO. All complexes readily dissolved in DMSO but small amounts of precipitate formed over a 24 h period. There are 2

competing hydrolysis pathways that could be occurring (i) halide hydrolysis, and (ii) Cp hydrolysis.

**Table 4.1:** Effect of solvent on rates of hydrolysis of aromatic rings in Cp<sub>2</sub>TiX<sub>2</sub>.

Complex Cp <sub>2</sub> TiX <sub>2</sub>	DMSO		10%DMSO/90%D <sub>2</sub> O		D <sub>2</sub> O (pD ~2-3)	
	Reaction time (h) <sup>a</sup>	% Cp hydrolysis	Reaction time (h) <sup>a</sup>	% Cp hydrolysis	Reaction time (h) <sup>a</sup>	% Cp hydrolysis
Cl <b>1</b>	0.25	<5	0.25	<2	-	-
	3	7	3	<2	1	0
	24	30	24	<2	24	<2
OCOCCl <sub>3</sub> <b>22</b>	0.25	>99	0.25	<2	- <sup>b</sup>	-
	3	>99	3	<2	- <sup>b</sup>	-
	24	>99	24	<2	- <sup>b</sup>	-
OCOCH <sub>2</sub> NH <sub>3</sub> Cl <b>27</b>	0.25	>99	0.25	<2	-	-
	3	>99	3	<2	1	0
	24	>99	24	20	24	<2
Cl <b>1</b> + 2 equiv. HOCOCH <sub>2</sub> NH <sub>2</sub>	0.25	40	-	-	-	-
	3	80	-	-	-	-
	24	>99	-	-	-	-

<sup>a</sup> The time taken after complete dissolution was achieved; <sup>b</sup> Insoluble

In the case of Cp<sub>2</sub>TiCl<sub>2</sub> **1**, negligible Cp hydrolysis occurred after 0.25 h and a sharp singlet for the aromatic protons was observed (Figure 4.1(i), (a) X = Cl **1**). After 24 h, by integration of the newly formed multiplets from cyclopentadiene, it was estimated that approximately 30% of the Cp rings in the complex had hydrolysed (Figure 4.1(iii), (a) X = Cl **1**). A new downfield multiplet at ~3 ppm also appeared corresponding to the aliphatic H<sub>c</sub> protons of unbound cyclopentadiene (data not shown). This signal increased in intensity at

<sup>†</sup> the term hydrolysis is used to indicate solvolysis in DMSO in this section

approximately the same rate as the signals due to the unbound vinylic cyclopentadiene protons.

In the case of complexes  $\text{Cp}_2\text{Ti}(\text{OCOCCl}_3)_2$  **22** and  $\text{Cp}_2\text{Ti}(\text{OCOCH}_2\text{NH}_3\text{Cl})_2$  **27**, rapid Cp and X ligand hydrolysis occurred within 0.25 h (Figure 4.1(i); (b) X =  $\text{OCOCCl}_3$  **22** and (c)  $\text{OCOCH}_2\text{NH}_3\text{Cl}$  **27** and Figure 4.2(i); (a) X =  $\text{OCOCCl}_3$  **22** and (b)  $\text{OCOCH}_2\text{NH}_3\text{Cl}$  **27**). After 24 h the singlets due to the metal bound Cp rings had completely disappeared and only the characteristic (CpH) multiplets remained after 24 h (Figure 4.1(iii); (b) X =  $\text{OCOCCl}_3$  **22** and (c)  $\text{OCOCH}_2\text{NH}_3\text{Cl}$  **27**). Solutions of  $\text{Cp}_2\text{Ti}(\text{OCOCCl}_3)_2$  **22** also darkened after 24 h and a new resonance also appeared in the spectra at around 8.4 ppm (Figure 4.1(b), (c) and (d)) and was tentatively assigned as a binuclear degradation species similar to those reported previously (eg.,  $[\text{Cp}_2\text{Ti}(\text{X})(\text{O})(\text{X})\text{TiCp}_2]^{2+}$ ).<sup>62</sup> This resonance was sharp in solutions of  $\text{Cp}_2\text{Ti}(\text{OCOCCl}_3)_2$  **22** and broad in solutions where glycine was present (Figure 4.1(c) and (d)).

In order to establish whether glycine, which appears to rapidly dissociate from the metal when  $\text{Cp}_2\text{Ti}(\text{OCOCH}_2\text{NH}_3\text{Cl})_2$  **27** is dissolved in DMSO, promotes the Cp hydrolysis reaction, glycine ( $\text{HO}_2\text{CCH}_2\text{NH}_2$ , 2 mol equivalents) was added to a solution of  $\text{Cp}_2\text{TiCl}_2$  **1** and  $^1\text{H}$  NMR spectra were recorded over 24 h. After 15 min, approximately 40% Cp hydrolysis had occurred, while after 3 h significant Cp hydrolysis (80%) was observed (Figure 4.1(d), Table 4.1). Thus, free glycine does promote the Cp hydrolysis reaction, but the rate is slower than in the case of the bisglycine derivative **27** in which the glycine ligands are initially coordinated to the metal centre in the zwitterionic form.

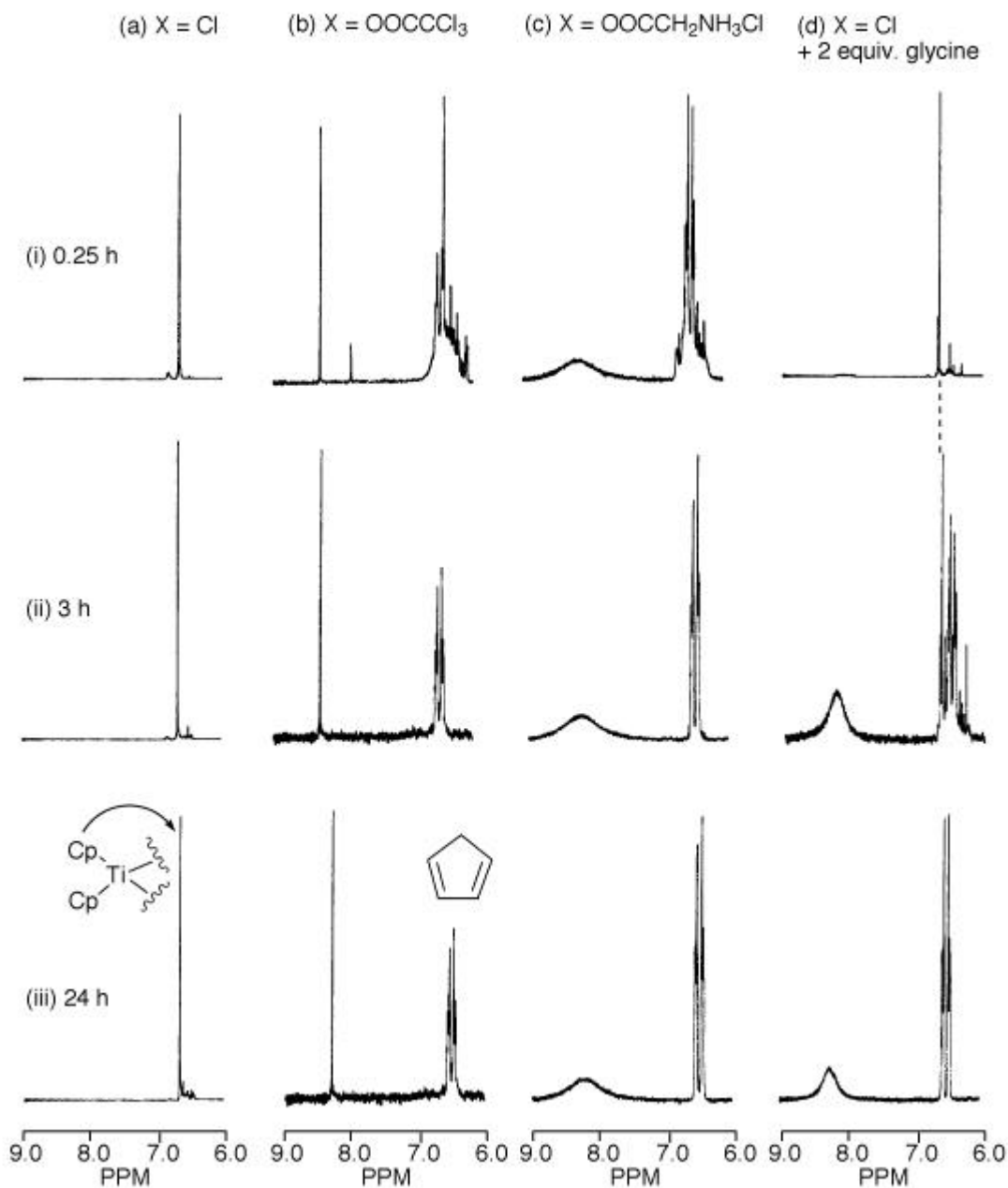


**Figure 4.1:** Aromatic region of  $^1\text{H}$  NMR spectra (200 MHz,  $d_6$ -DMSO, 25 °C) of  $\text{Cp}_2\text{TiX}_2$  complexes (a)  $\text{X} = \text{Cl}$  **1**, (b)  $\text{X} = \text{OCOCCl}_3$  **22**, (c)  $\text{X} = \text{OCOCH}_2\text{NH}_3\text{Cl}$  **27**, (d)  $\text{X} = \text{Cl}$  **1** with 2 equiv.  $\text{HOCOCH}_2\text{NH}_2$ . Spectra recorded at (i)  $t = 0.25$  h, (ii) 3 h and (iii) 24 h after complexes dissolved.

### 4.1.3. Hydrolysis in 10%DMSO/90%D<sub>2</sub>O

Two different methods were used to prepare titanocene derivatives in

10%DMSO/90%D<sub>2</sub>O, (i) the sample was dissolved directly in 10%DMSO/90%D<sub>2</sub>O solution and (ii) the sample was dissolved in DMSO and then diluted with D<sub>2</sub>O (ie., the method used for sample administration<sup>46</sup>) with accurate recording of the time the sample was allowed to stand in DMSO before dilution with water.

Firstly the rate of Cp hydrolysis of the complexes Cp<sub>2</sub>TiX<sub>2</sub> (X = Cl **1**, OCOCCl<sub>3</sub> **22**, OCOCH<sub>2</sub>NH<sub>3</sub>Cl **27**; 10 μmol) directly dissolved in 10%DMSO/90%D<sub>2</sub>O solutions was measured and the results are summarised in Table 4.1. The Cp hydrolysis was estimated to be < 2% over 24 h for Cp<sub>2</sub>TiCl<sub>2</sub> **1** and Cp<sub>2</sub>Ti(OCOCCl<sub>3</sub>)<sub>2</sub> **22** as the amount of signal from CpH in the NMR spectra was negligible. In the case of Cp<sub>2</sub>Ti(OCOCH<sub>2</sub>NH<sub>3</sub>Cl)<sub>2</sub> **27** the amount of bound Cp signal was reduced by 20% compared to the CH<sub>2</sub> signal of glycine after 24 h and was attributed to Cp hydrolysis which resulted in precipitation of a Cp containing species. For all complexes, the amount of precipitate was negligible within 3 h and 20% for Cp<sub>2</sub>Ti(OCOCH<sub>2</sub>NH<sub>3</sub>Cl)<sub>2</sub> after 24 h. The results confirm that the solvent mixture of 10%DMSO/90%D<sub>2</sub>O does not have a significant effect on Cp hydrolysis over several hours when this preparation method is employed, and the results are very similar to those obtained in water.

Secondly the rate of Cp hydrolysis was measured when the complexes Cp<sub>2</sub>TiX<sub>2</sub> (X = Cl **1**, OCOCCl<sub>3</sub> **22**, OCOCH<sub>2</sub>NH<sub>3</sub>Cl **27**; 10 μmol) were initially dissolved in 50 μL DMSO and left to stand for 0.5, 3 and 10 min before addition of 450 μL of D<sub>2</sub>O. The results are summarised in Table 4.2. In the case of Cp<sub>2</sub>TiCl<sub>2</sub> **1**, minimal precipitation was detected with time and there was no evidence of free CpH in solution or the presence of any dicyclopentadiene (spectra not shown).

**Table 4.2:** Hydrolysis of titanocene complexes dissolved in DMSO and left standing for various lengths of time before adding D<sub>2</sub>O to give a 10%DMSO/90%D<sub>2</sub>O solution.

Complex	Time in DMSO (min) <sup>a</sup>	Reaction Time (h) <sup>b</sup>	% Cp Hydrolysis
Cp <sub>2</sub> TiCl <sub>2</sub> <b>1</b>	0.5	0.25	<2
		3	<2
		24	<2
	3	0.25	<2
		3	<2
		24	<2
	10	0.25	<2
		3	<2
		24	<2
Cp <sub>2</sub> Ti(OCOCH <sub>2</sub> NH <sub>3</sub> Cl) <sub>2</sub> <b>27</b>	0.5	0.25	10
		3	10
		24	10
	3	0.25	25
		3	25
		24	40
	10	0.25	35
		3	40
		24	40

<sup>a</sup> t = 0 is the time taken when DMSO was added; <sup>b</sup> t = 0 is the time taken when D<sub>2</sub>O was added

In the case of Cp<sub>2</sub>Ti(OCOCH<sub>2</sub>NH<sub>3</sub>Cl)<sub>2</sub> **27**, precipitation was observed to increase with time. The % Cp hydrolysis was estimated by comparing the integral of the bound Cp resonances to that for the CH<sub>2</sub> resonance of the glycine ligand (spectra not shown). The

results show that the % Cp hydrolysis increased when  $\text{Cp}_2\text{Ti}(\text{OCOCH}_2\text{NH}_3\text{Cl})_2$  **27** was allowed to stand in DMSO for greater lengths of time (Table 4.2). Further Cp hydrolysis was almost completely inhibited upon dilution with  $\text{D}_2\text{O}$ .

Hydrolysis with  $\text{Cp}_2\text{Ti}(\text{OCOCCl}_3)_2$  **22** was evident due to the formation of precipitate and darkening of solutions. The initial concentration of complex dissolved in DMSO was also important; lowering the concentration of the complex (10  $\mu\text{mol}$  to 6  $\mu\text{mol}$ ) followed by dilution with  $\text{D}_2\text{O}$  showed only a very weak Cp signal in the NMR spectrum. Cp hydrolysis was estimated at >90% with the lower concentration (6  $\mu\text{mol}$ ) of the complex.

#### **4.2. Effect of Solvent on Rate of Cp Hydrolysis in $\text{Cp}_2\text{TiX}_2$**

Due to the limited aqueous solubility of  $\text{Cp}_2\text{TiCl}_2$  **1**, and the formation of precipitates at high pH,  $\text{Cp}_2\text{TiCl}_2$  **1** has been administered in 10% DMSO/90% saline solutions at low pH. The complex is typically dissolved in DMSO and then diluted to the required volume with saline.<sup>46</sup> In order to overcome potential problems associated with precipitation upon intravenous administration and to increase the bioavailability of the drug, a number of active derivatives with improved aqueous solubility have been reported.<sup>47,50,51</sup> In the case of the complexes  $\text{Cp}_2\text{Ti}(\text{SC}_6\text{H}_4\text{NH}_3\text{Cl})_2$  **21**,  $\text{Cp}_2\text{Ti}(\text{OCOCCl}_3)_2$  **22** and  $\text{Cp}_2\text{Ti}(\text{OCOCHCHCO}_2\text{H})_2$  **23**, the introduction of hydrophilic ligands resulted in (i) diminution of toxic properties (ii) widening of the therapeutic range and (iii) an increase in aqueous solubility for  $\text{Cp}_2\text{Ti}(\text{SC}_6\text{H}_4\text{NH}_3\text{Cl})_2$  **21** and  $\text{Cp}_2\text{Ti}(\text{OCOCHCHCO}_2\text{H})_2$  **23** which allowed the complexes to be administered in pure saline.<sup>47</sup> Moreover, a further reduction in toxic properties was attained by elevation of the pH of the injected solution of the complex  $\text{Cp}_2\text{Ti}(\text{SC}_6\text{H}_4\text{NH}_3\text{Cl})_2$  **21** in a manner similar to  $\text{Cp}_2\text{TiCl}_2$  **1**.<sup>46</sup> However, in contrast to other carboxylated

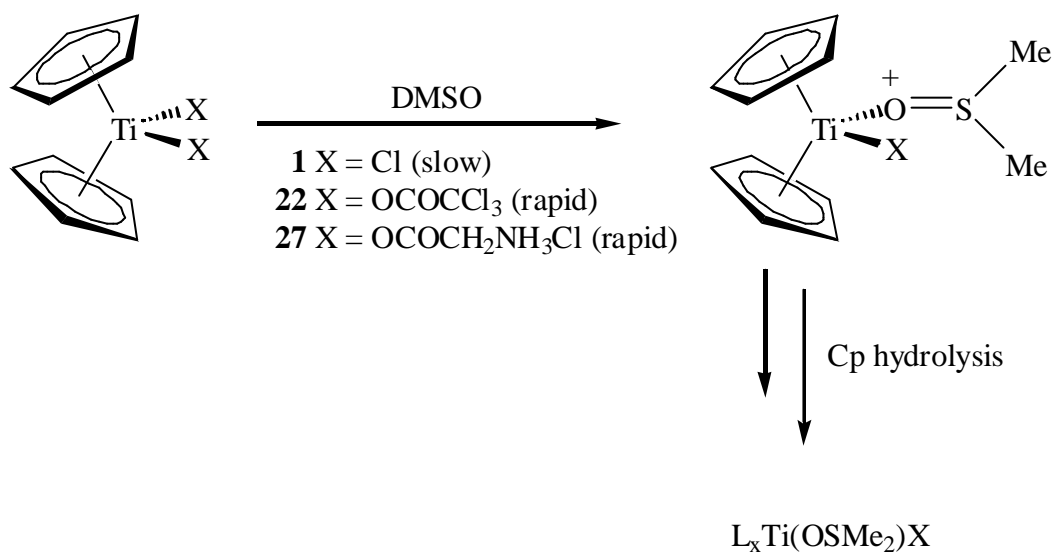
complexes, the trichloroacetate derivative **22** did not exhibit improved aqueous solubility, and hence administration was carried out in 10% DMSO.<sup>47</sup> The bisglycine derivate **27**, while exhibiting excellent aqueous solubility, was tested in 10% DMSO, presumably to allow comparison of the results with all previous studies.<sup>49</sup>

Comparison of the rate of Cp hydrolysis of derivative **1**, **22** and **27** in water, DMSO and 10%DMSO/90%D<sub>2</sub>O showed several distinct trends. Firstly, the rate of hydrolysis of Cp<sub>2</sub>TiX<sub>2</sub> (X = OCOCCL<sub>3</sub> **22**, OCOCH<sub>2</sub>NH<sub>3</sub>Cl **27**) is accelerated in DMSO compared with the parent compound Cp<sub>2</sub>TiCl<sub>2</sub> **1**. Secondly, the hydrolysis reactions in DMSO to give inactive titanocene species are highly concentration dependent, as diluting the DMSO to ~10% with water effectively prevents further degradation from occurring. Thus, for samples prepared in 10%DMSO, the amount of time between when the sample is dissolved and then diluted with water is significant; after several minutes as much as 40% of the species present in DMSO no longer contains the "Cp<sub>2</sub>Ti<sup>2+</sup>" moiety in which the Cp rings remain coordinated to the titanium metal centre.

The rate of halide and Cp ring hydrolysis in Cp<sub>2</sub>TiCl<sub>2</sub> **1** in water has been well characterised.<sup>58</sup> Rapid hydrolysis of the two halide ligands occurs in a series of equilibrium reactions to give a solution at pH ~1 in which the Cp rings remain metal bound for >24 h. However, at higher pH values protonolysis of the Cp rings occurs to give cyclopentadiene and dicyclopentadiene as well as insoluble, uncharacterised hydrolysis products. The exact nature of the pseudohalide ligands have not been identified with Cp<sub>2</sub>TiCl<sub>2</sub>(aq) **1** likely to contain a number of species such as Cp<sub>2</sub>Ti(H<sub>2</sub>O)Cl<sup>+</sup>, or Cp<sub>2</sub>Ti(H<sub>2</sub>O)<sub>x</sub>(OH)<sub>y</sub><sup>(2-y)+</sup>. If the effect of DMSO on this equilibrium is considered, then the results presented in this chapter (Figure 4.1,

Table 4.1) show that the rate of Cp hydrolysis is slightly faster in the presence of DMSO than in pure water at low pH.

It is not clear how DMSO is able to accelerate the Cp hydrolysis, however, a possible mechanism may involve coordination of DMSO to the metal center via displacement of the carboxylate ligands or halide ligands (Scheme 4.1). It can then be speculated that the coordinated DMSO may then activate the complex towards Cp hydrolysis (Scheme 4.1). A slow displacement of the Cl ligands in Cp<sub>2</sub>TiCl<sub>2</sub> **1** and rapid displacement of the carboxylate ligands in **22** and **27** provides a possible explanation for the difference in the degradation process of these complexes (Scheme 4.1). However, further studies are required to confirm this.



**Scheme 4.1**

### 4.3. Correlation with Biological Activity

As the major focus of this thesis on antitumour metallocenes has been to correlate the chemical stability and coordination chemistry of these complexes with their observed antitumour properties, and thus provide the basis for rational drug design, this work provides a

comparison of the hydrolysis results with the antitumour data in the literature. In the case of the glycine derivative **27**, the results reported in this chapter suggest that administration of the complex in pure water should give improved results compared to those in 10%DMSO. As the time between dissolving the complex in DMSO and dilution with water has not been specified<sup>49</sup> (and was generally not expected to be important), it is impossible to state unequivocally that Cp hydrolysis was responsible for the very surprising reduced activity observed (Table 1.3). However, partial Cp hydrolysis in DMSO does offer a simple explanation for the results and still supports the general hypothesis that the biologically active species generated *in vivo* is "Cp<sub>2</sub>Ti<sup>2+</sup>". A unique feature of the amino acid complexes, which may play a role in the biological activity, is that they are zwitterionic and are present as the hydrochloride salt in the complex. However, the thiophenol derivative **21** was also tested as the hydrochloride salt and found to have maximum activity against EAT tumours (Table 1.3). It is interesting that only sporadic cure rates, and the absence of strong dose-activity relationships was observed for the corresponding ortho derivative **33** (Table 1.4) in which the same amine is present in neutral form, hinting that these sidechains may affect the subsequent chemistry.

The antitumour results obtained with the trichloroacetate derivative **22** are more difficult to rationalise on a chemical basis (Table 1.3). This derivative **22** retains the activity of the parent derivative Cp<sub>2</sub>TiCl<sub>2</sub> **1** (Table 1.1) but the dose required to achieve an optimal cure rate is significantly increased compared to other titanocene derivatives (Table 1.3). Partial decomposition in DMSO could contribute to the increased dosage required but further comparative tests on a range of related titanocene would be required to confirm this hypothesis.

#### **4.4. Conclusions**

The hydrolysis studies reported in this chapter suggest certain carboxylate ligands such as in  $\text{Cp}_2\text{TiX}_2$  ( $\text{X} = \text{OCOCCH}_3$  **22** and  $\text{OCOCH}_2\text{NH}_3\text{Cl}$  **27**) promote hydrolysis/degradation reactions to biologically inactive species in DMSO, where the process is DMSO concentration dependent. These results are consistent with the reduced activity observed for the bisglycine analogue and suggest that administration in the absence of DMSO (as the complex is highly water soluble) or direct dissolution in 10%DMSO/90%saline may result in modified cure rates and optimum doses. The results also emphasise that examination of the effect of coordinating solvents on the stability of metallocene complexes is important.

In terms of medicinal chemistry and the design of new transition metal containing drugs based on the titanocene framework, previous structure-activity studies indicate that a range of X substituents, with the exception of certain carboxylate ligands, may be incorporated into the  $\text{Cp}_2\text{TiX}_2$  structure without loss of activity (see Chapter 1). The results reported in this chapter suggest that the reduced activity of titanocene complexes containing carboxylate ligands is due to the reduced stability of these complexes in DMSO and hence carboxylate ligands need not be excluded in the design of new antitumour metallocenes. However, the chemical hydrolysis reactions that occur in water at both low and elevated pH as well as the effect of DMSO on new titanocene based anticancer drugs needs to be taken into account in derivatives that contain functional groups in the X ligands.

As outlined in Chapter 1, it has been assumed that formation of DNA-metallocene adducts *in vivo* is related to the antitumour activity of all metallocenes since  $\text{Cp}_2\text{TiCl}_2$  **1** and  $\text{Cp}_2\text{VCl}_2$  **2** have been reported to inhibit DNA and RNA synthesis<sup>22,24</sup> and titanium and vanadium have been found to accumulate in nucleic acid-rich regions of tumour cells.<sup>23,24</sup> Hence a large number of studies have focused on characterisation of the interaction of metallocenes with nucleic acid constituents,<sup>59-61,66</sup> oligonucleotides (see Chapter 2) and DNA.<sup>57,70,71</sup> However, in contrast to  $\text{Cp}_2\text{TiCl}_2$  **1** and  $\text{Cp}_2\text{VCl}_2$  **2**, the lack of interaction of  $\text{Cp}_2\text{MoCl}_2$  **4** with oligonucleotides as models of DNA at pH 7.0 (see Chapter 2) does not support DNA as the main target *in vivo*. Similarly, there is no biological evidence to support formation of niobocene-DNA interactions *in vivo*, and  $\text{Cp}_2\text{NbCl}_2$  **3** does not form coordination complexes with nucleotides or amino acids.<sup>65</sup> Hence more recent studies on metallocenes have addressed proteins and amino acids as potential biological targets *in vivo*.<sup>50,51,57,76,78,114,115</sup>

Almost all detailed chemical and biological studies to date have focused on  $\text{Cp}_2\text{TiCl}_2$  **1**,<sup>19</sup> but experiments designed to establish the precise mechanism of action have been hampered by the hydrolytic instability of this drug under physiological conditions.<sup>58</sup> While  $\text{Cp}_2\text{TiCl}_2$  **1** does inhibit DNA synthesis,<sup>22,24</sup> and Ti-DNA adducts have been characterised,<sup>71</sup> implicating titanocene-DNA interactions in the mechanism of action, Ti-protein interactions are also important. Several very recent papers published during the course of this work have reported that Ti(IV) derived from titanium(IV) citrate or  $\text{Cp}_2\text{TiCl}_2$  **1** forms a strong complex with human serum transferrin and hence the active species may be transported into tumour cells via formation of a Ti-transferrin complex.<sup>76,78,80,114,115</sup> In addition to blood plasma

proteins, proteins involved in cellular replication have also been implicated in the mechanism of action of several metallocenes. Preliminary studies have shown that both protein kinase C, an enzyme involved in cellular proliferation, and bacterial topoisomerase II, are significantly inhibited by  $\text{Cp}_2\text{VCl}_2$  **2** and  $\text{Cp}_2\text{MoCl}_2$  **4**.<sup>57</sup> However, full details of these studies have not been published.

Studies on diacetyl and dicarboxaldoxime derivatives of ferrocene,<sup>117</sup> several cobalt salicylaldoxime complexes<sup>118</sup> and aryl substituted ruthenium complexes<sup>119</sup> (Figure 5.1) have shown that topoisomerase II is a potential target of small metal complexes and that the mechanism of action depends critically on substituents present in the metal complexes. In order to further clarify the mechanism of antitumour action of the metallocene dihalides, this chapter reports a study of the interaction of a range of metallocene dihalides with human topoisomerase II. The study included both biologically active and inactive drugs (Figure 5.2) and complements preliminary studies with complexes **2** and **4** and bacterial topoisomerase II.<sup>57</sup>

### **5.1. Topoisomerases and DNA Topology**

Human topoisomerases play a major role in DNA replication and consequently are essential for cellular survival.<sup>120</sup> The enzymes are able to catalyse changes in the topology of DNA which are necessary for a number of cellular processes, including DNA replication, chromosome segregation, and transcription.<sup>120</sup> The enzymes topoisomerase I and II, which are classified based on their mechanism of action, are both expressed in human cells.<sup>120</sup>

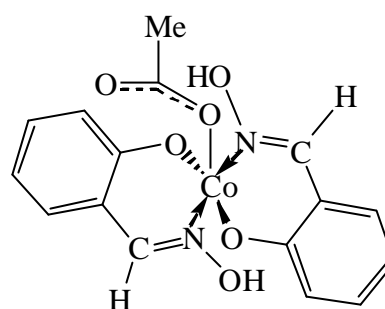
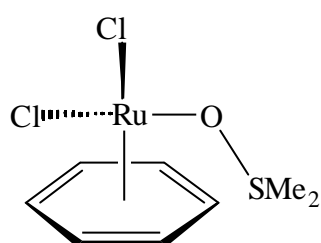
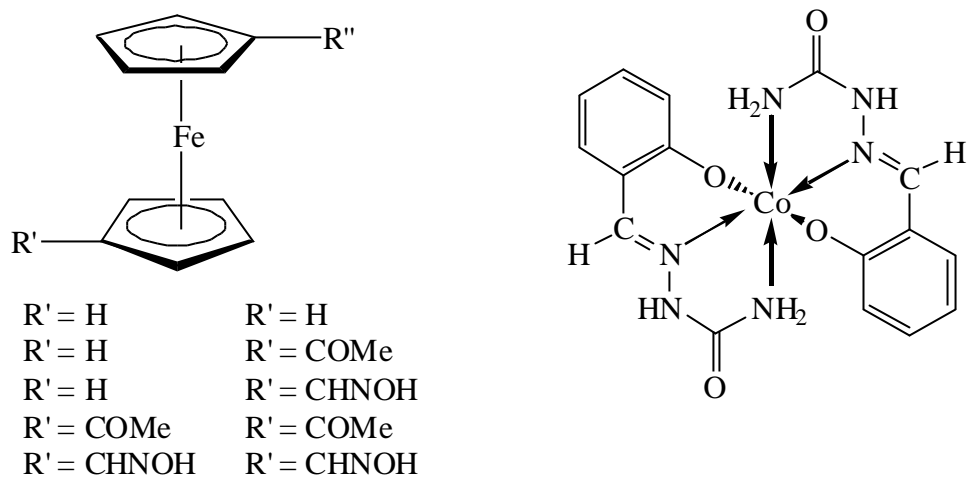


**Figure 5.1:** Metal complexes that have shown topoisomerase II inhibition activity

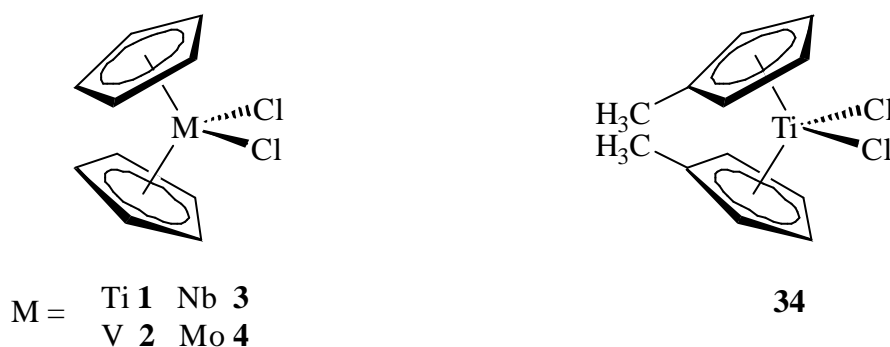


**Figure 5.2:** Structures of biologically active **1-4** and inactive **34** metallocenes studied

The type I topoisomerases differ from the type II topoisomerases by the way in which they are able to alter the topology of DNA. The type I topoisomerases transiently cleave one DNA strand at a time to allow passage of another strand through the break.<sup>120</sup> The type II enzymes alter the topology of DNA by transiently cleaving both strands of complementary

DNA (gated helix) and then allowing passage of a second double stranded DNA segment (transported helix) through the break in an ATP dependent mechanism (Figure 5.3).<sup>120</sup>

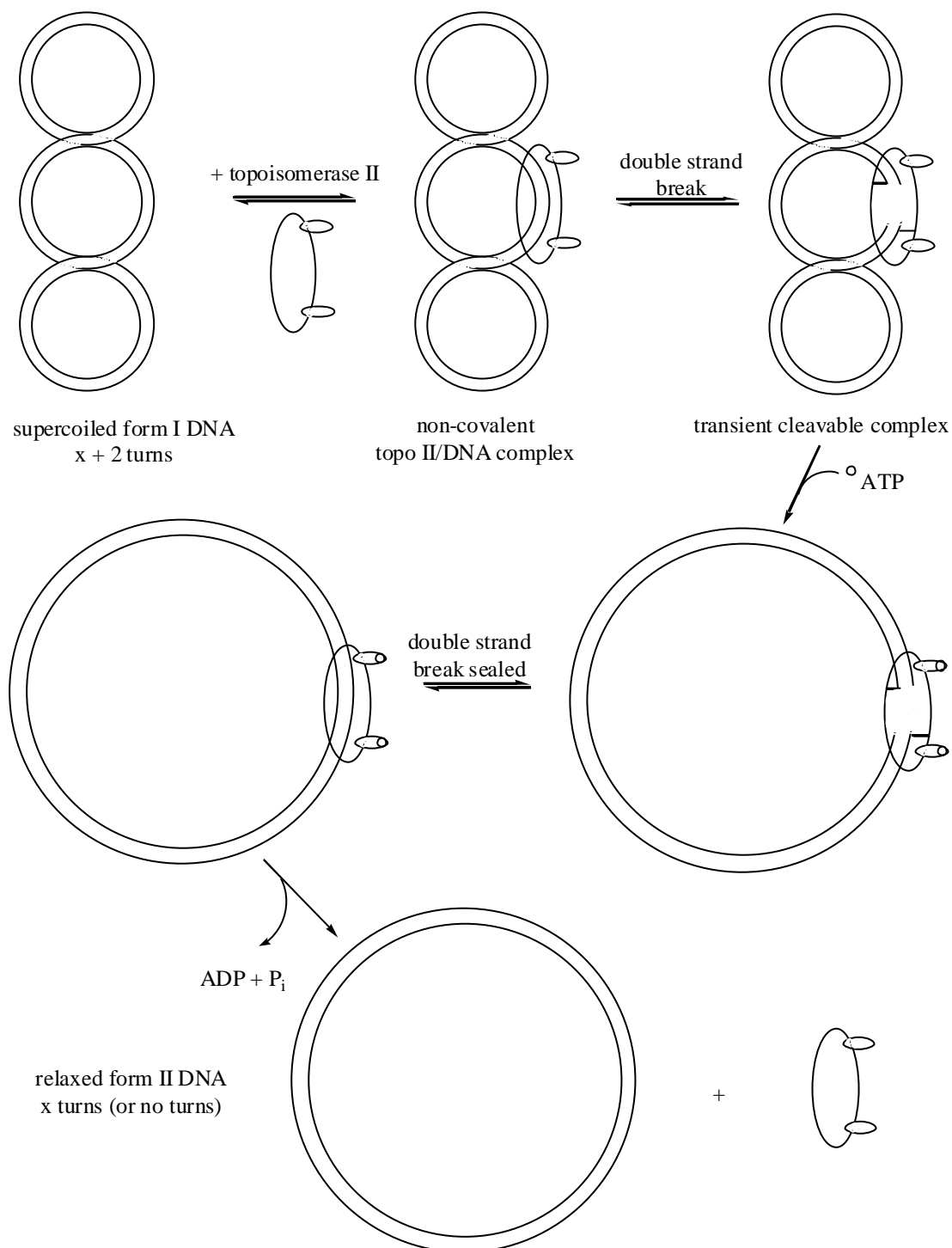


**Figure 5.3:** Schematic illustration of the key steps in the ATP dependent mechanism of topoisomerase II relaxation of circular DNA; 2 turns shown in the circular DNA

Topoisomerase II is of most relevance to the work described in this chapter. Human cells express at least two forms of the type II topoisomerase. Human topoisomerase II $\alpha$  form is a dimeric enzyme and has a molecular weight of 172 kDa (p170) while the  $\beta$  form has a molecular weight of 180 kDa (p180).<sup>121</sup> While both forms of the type II enzyme are known to work by the same mechanism of action *in vitro*, it has been reported that human topoisomerase II $\alpha$  is responsible for processes necessary for cell proliferation and the type II $\beta$  form is responsible for processes necessary for cell differentiation.<sup>122</sup> Since the type II $\alpha$  form is involved more closely with cell proliferation its activity may be more important in rapidly dividing tumour cells. However, as both forms are inhibited/poisoned by drugs *in vitro*, both are potential drug targets *in vivo*.<sup>121</sup>

The mechanism of catalytic activity of the type II DNA topoisomerases involves binding of the dimeric enzyme to the DNA strand to give a non-covalent complex (Figure 5.3). A covalent complex is then formed when a tyrosine residue in the active site of each monomer becomes covalently linked to a 5'-phosphate group of each DNA strand, which results in a double strand break. The topoisomerase bridged DNA complex, referred to as the transient cleavable complex, allows the movement of the transported DNA helix through the gated helix. The passing of the transported DNA helix through the gated helix results when ATP binds to the dimeric enzyme causing a conformational change. The enzyme religates the gated helix under equilibrium conditions and is then released from the DNA when the bound ATP is hydrolysed to ADP. Each catalytic cycle results in the removal of two knots of the supercoiled DNA.

## 5.2. Human Topoisomerase II as a Drug Target

The inhibition or poisoning of human topoisomerases has been implicated in the mechanism of activity of several antitumour drugs.<sup>120-124</sup> Since tumours utilise an increase in topoisomerase activity, the inhibition of topoisomerases becomes an important target in achieving antitumour activity.<sup>121,124</sup> While topoisomerase I activity is almost equal in all cell cycle phases, topoisomerase II has highest activity during the log phase of the cell cycle. Therefore, in fast growing tumours, the inhibition of topoisomerase I should intensify the effect of topoisomase II inhibitors.<sup>120,124</sup>

Topoisomerase II targeting antitumour drugs are referred to as either topoisomerase II inhibitors or poisons. The anticancer agents etoposide, doxorubicin, *m*AMSA and ellipticine have been classed as topoisomerase II poisons.<sup>121</sup> These drugs are able to stabilise the transient cleavable topoisomerase-DNA complex, altering the equilibrium to give an increased amount of complexes in which the DNA is cleaved to give linear or form III DNA (Figure 5.4). These drugs are able to form such complexes since they have both DNA and protein binding domains. For example *m*AMSA is a DNA intercalator as well as having protein binding functional groups (Figure 5.5).<sup>125</sup>

Drugs that are termed topoisomerase II inhibitors inhibit or alter the activity of topoisomerase II without being able to stabilise the cleavable complex.<sup>121</sup> These include merbarone, suramin, and the bisdioxopiperazines.<sup>121</sup> Since topoisomerase II inhibitors alter the activity of topoisomerase II, they are generally found to also antagonise the effect of drugs classed as topoisomerase II poisons.<sup>121</sup>

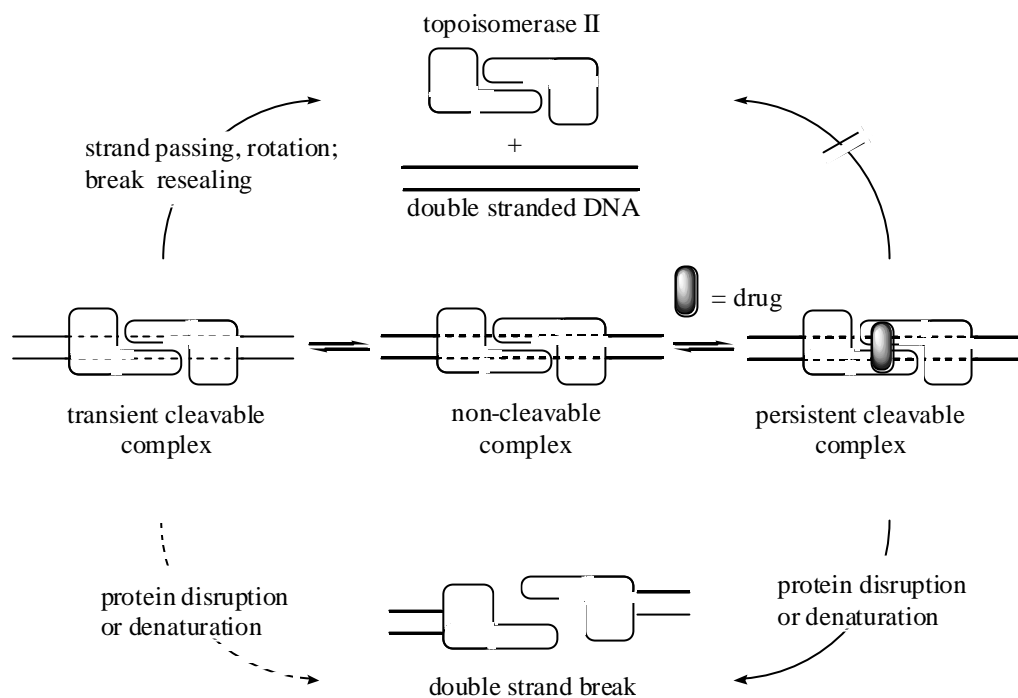


**Figure 5.4:** DNA damage induced by poisoning of topoisomerase II (adapted from W.B. Pratt<sup>6</sup>)

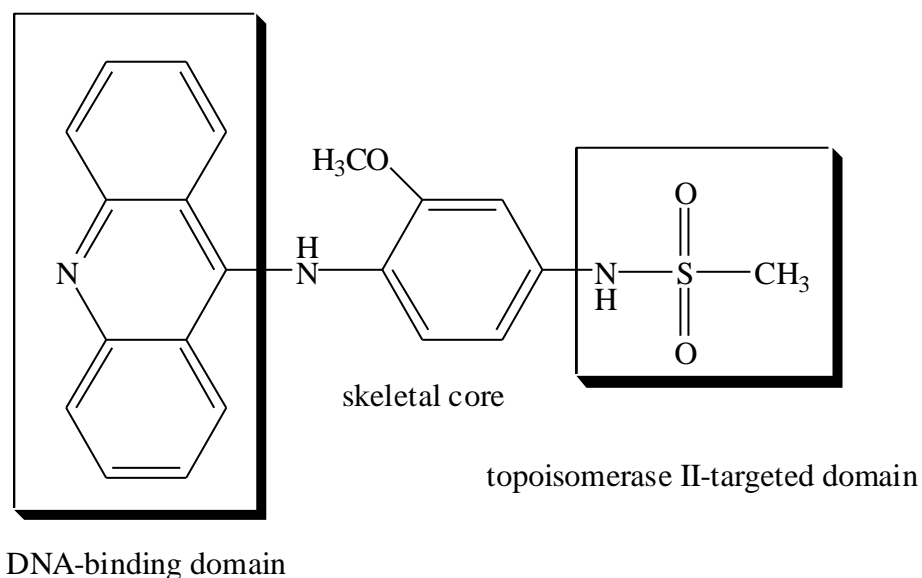


**Figure 5.5:** mAMSA a topoisomerase II poison with DNA and protein binding domains

The metallocene dihalides are structurally unique compared to all other metal complexes that have been previously studied as potential topoisomerase II inhibitors. There is no evidence to support intercalation of the Cp rings of any of the metallocenes with DNA (see Chapter 2)<sup>18,57</sup> (indeed the tetrahedral shape of the complex would prevent intercalation), and recent studies suggest that the Cp rings of  $\text{Cp}_2\text{TiCl}_2$  **1** may not even be present when the active species enters the cell.<sup>78,80,114,115</sup> Substituted ferrocene derivatives (Figure 5.1) have been proposed to form drug-DNA-enzyme complexes via the interaction of the ring substituents with the enzyme and/or DNA.<sup>117</sup> However, these metallocenes are overall neutral, are not tetrahedral in shape, and lack the vacant coordination sites that are present in the antitumour metallocenes upon rapid hydrolysis of the chloride ligands in water. Thus, formation of a stabilised DNA-drug-topoisomerase II complex with any of the antitumour metallocenes (Figure 5.2) seems unlikely. Hence this study focused on a topoisomerase II inhibition assay rather than a cleavage assay which is typically used with topoisomerase II poisons where a stable cleavable complex is formed.

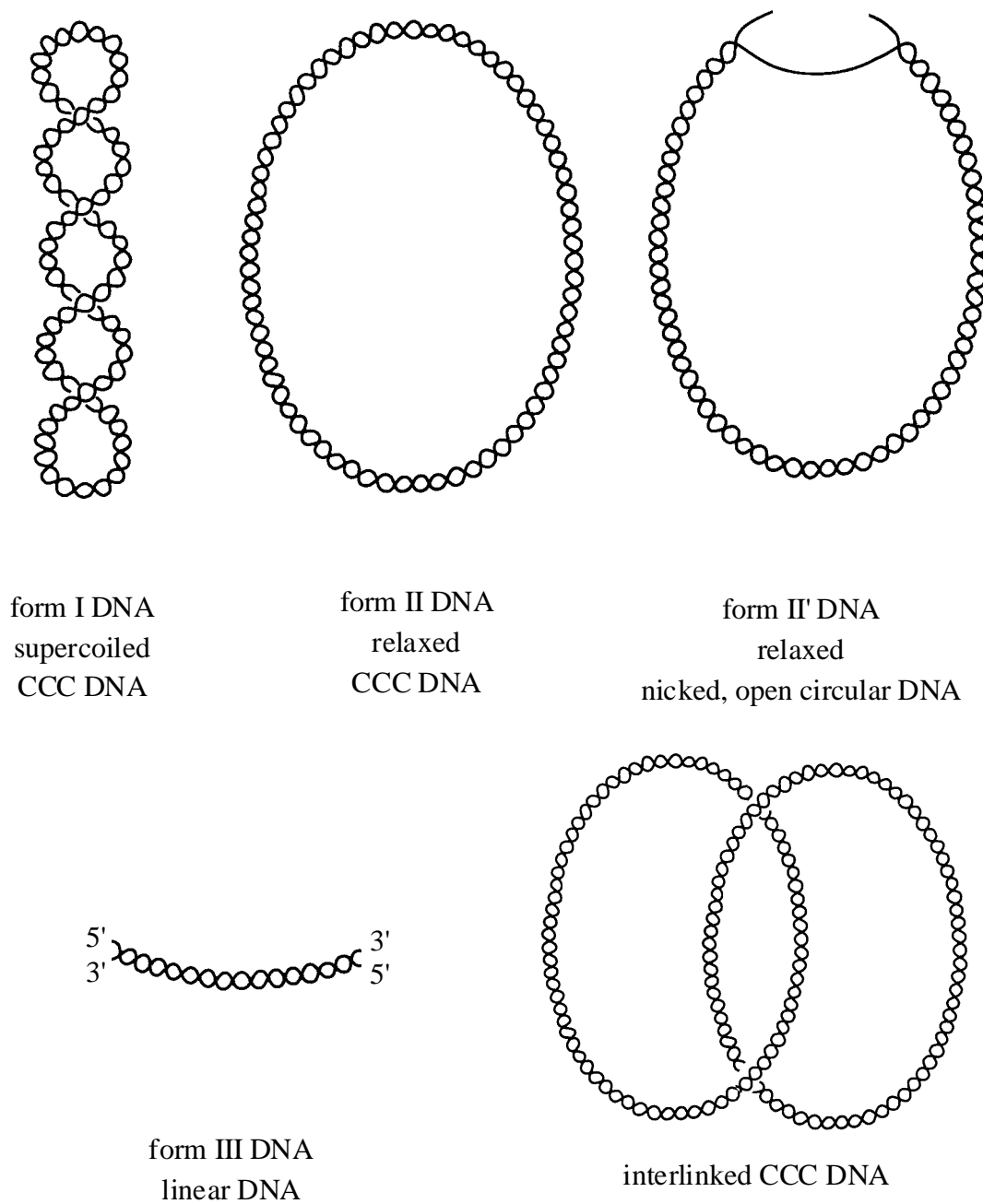
### **5.3. General Topoisomerase II Inhibition Assay**

Human topoisomerase II is commonly used to relax supercoiled closed circular DNA *in vitro*. Supercoiled closed circular DNA refers to the twisted form of the closed circular DNA that inherently results due to the double helical secondary structure of DNA. This is also referred to as form I DNA (Figure 5.6) and allows DNA to be tightly packed within a cell where space is limited. The term relaxation is used to refer to essentially two processes (i) decatenation and (ii) unwinding. Decatenation refers to the unlinking of interlinked or intertwined closed circular DNA molecules (Figure 5.6). A catenane network of interlinked

closed circular DNA segments commonly exists, as in supercoiled kDNA (kinetoplast DNA).<sup>126</sup> Unwinding refers to the sequential removal of each twisted coil or unknotting of the twisted coils. In both processes of relaxation, the mechanism of catalytic activity of topoisomerase II is the same and involves the described gated mechanism. Complete relaxation of supercoiled kDNA with human topoisomerase II results in decatanation and unwinding of the individual monomers to give monomeric relaxed circular DNA (also referred to as minicircles or form II or II' DNA, Figure 5.6).<sup>126</sup>

Topoisomerase II-drug inhibition screening assays involve detection of topoisomerase II relaxation of supercoiled DNA in the presence and absence of the test drug. The different forms of DNA resulting from the reaction are detected by gel electrophoresis. Circular plasmid DNA vectors such as pBR322 are generally used as they allow a simple analysis of the amount of supercoiled, relaxed and linear DNA present following reaction with topoisomerase II in the presence and absence of a drug.

The relaxation assay involves a comparison between the control reaction of topoisomerase II with supercoiled DNA to give predominantly relaxed DNA and the reaction which also includes the inhibitor where the formation of relaxed DNA is inhibited (Figure 5.7). Incomplete relaxation is evident when several DNA topoisomers are observed on the gel (Figure 5.7). Topoisomers differ from each other by the number of supercoils present and hence migrate at different rates through the gel. The more supercoils that are incorporated into the DNA the more compact the DNA is and so the electrophoretic mobility is improved. The presence of the different topoisomers results in a laddering effect on the gel (Figure 5.7).

**Figure 5.6:** Different forms of DNA

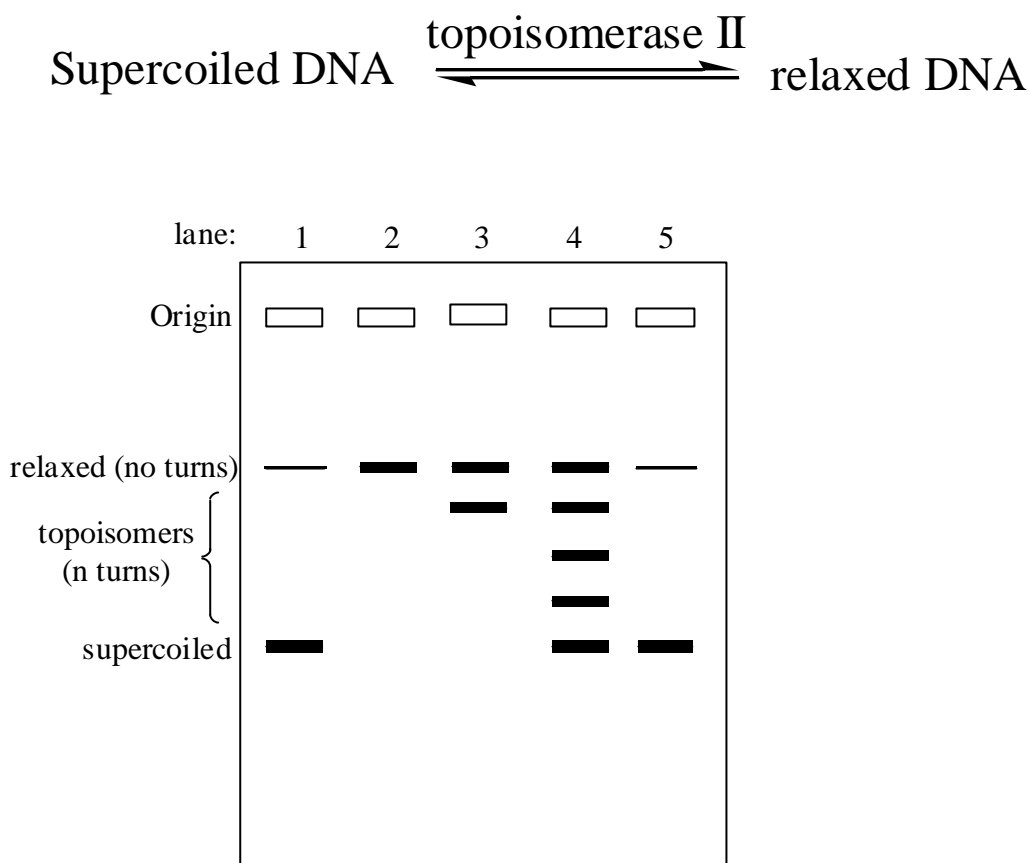


**Figure 5.7:** Typical gel showing effect of topoisomerase II on supercoiled DNA in the presence and absence of an inhibitor. Lane 1: supercoiled DNA; lane 2: DNA + topoisomerase II; lane 3: DNA + topoisomerase II + low [inhibitor]; lane 4: DNA + topoisomerase II + medium [inhibitor]; lane 5: DNA + topoisomerase II + high [inhibitor]

#### 5.4. Inhibition Assay with the Antitumour Metalloenes

The inhibition of topoisomerase II by  $\text{Cp}_2\text{VCl}_2$  **2** and  $\text{Cp}_2\text{MoCl}_2$  **4** has been considered in one study by Marks *et. al.*<sup>57</sup> Topoisomerase II was investigated as a potential target since antitumour metalloenes were observed to inhibit cellular DNA synthesis *in vitro* by arresting cells preferentially at the G2 or at the G1/G2 phases of the cell cycle,<sup>41</sup> a phenomenon observed for other antitumour drugs that target topoisomerase II.<sup>74,127</sup> It was reported that electrophoretic experiments revealed a concentration-dependent inhibition of

bacterial DNA topoisomerase II (winding) activity on relaxed DNA plasmid treated with  $\text{Cp}_2\text{VCl}_2$  **2** or  $\text{Cp}_2\text{MoCl}_2$  **4**,<sup>57</sup> but no further details or experimental data have been published.

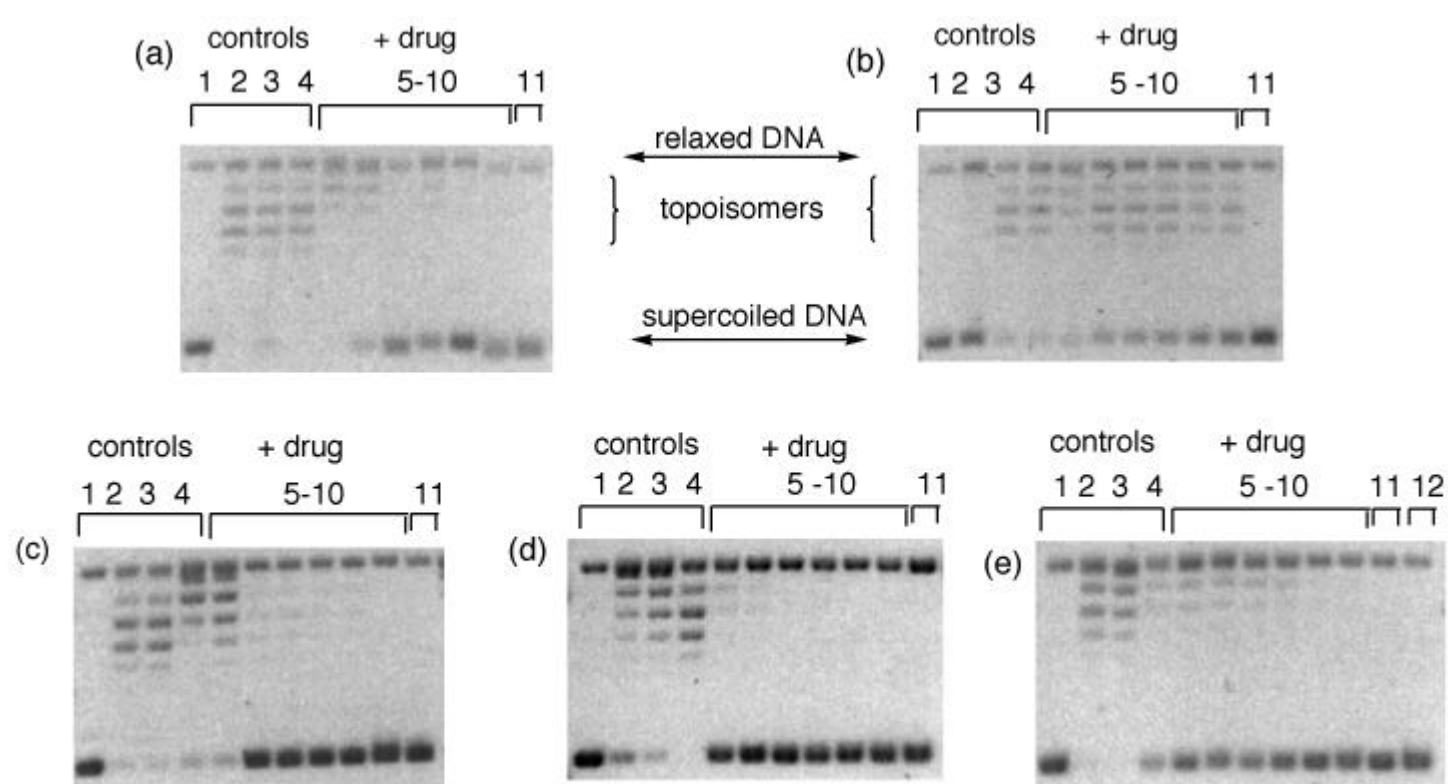
The metallocenes  $\text{Cp}_2\text{MCl}_2$  (M = Ti **1**, V **2**, Nb **3**, Mo **4**), which all exhibit 100% OCRs against EAT tumours,<sup>19</sup> as well as the methyl substituted titanocene derivative  $(\text{MeCp})_2\text{TiCl}_2$  **34** which is inactive against the same tumour line,<sup>54</sup> were tested for their ability to inhibit topoisomerase II relaxation of supercoiled pBR322. Due to hydrolysis reactions,<sup>58,60,61,65,86</sup> freshly dissolved aqueous samples of the metallocenes are quite acidic (pH 1-2, see section 2.2) which is not desirable for biological assays. At low pH, Cp hydrolysis is minimal,<sup>58,60,61,65,86</sup> and hence aqueous solutions contain a number of species including  $[\text{Cp}_2\text{M}(\text{OH})(\text{OH}_2)]^+$  and  $[\text{Cp}_2\text{M}(\text{OH}_2)\text{Cl}]^+$  with the metal in the +IV oxidation state. In the case of  $\text{Cp}_2\text{NbCl}_2$  **3**, oxidation to Nb(V) accompanies dissolution to generate  $\text{Cp}_2\text{NbCl}_2(\text{OH})$ .<sup>65</sup> While the pH of aqueous solutions of  $\text{Cp}_2\text{MoCl}_2$  **4** (see Chapter 2) and  $(\text{MeCp})_2\text{TiCl}_2$  **34** (see Chapter 3) can be adjusted to close to pH 7 without significant Cp hydrolysis or precipitation,<sup>60</sup> in the case of  $\text{Cp}_2\text{TiCl}_2$  **1** and  $\text{Cp}_2\text{NbCl}_2$  **3**, rapid hydrolysis to give insoluble precipitates prevents administration and handling of these samples at physiological pH. Hence, for consistency, aqueous low pH solutions of all metallocenes were added to the topoisomerase II assay mixture which buffered the solutions to give a final incubation solution of pH ~ 7.0. Previous independent studies have shown that the presence of biomolecules stabilizes the metallocenes to hydrolysis<sup>70,71</sup> and hence precipitation is prevented at pH 7.0 in the presence of DNA. In order to show that the initial addition of these low pH solutions did not affect the activity of the enzyme or the assay, appropriate blank experiments were carried out by addition of water at the relevant pH value.

Figure 5.8 shows typical gels obtained with metallocenes **1-4** and **34**. The control experiments (lanes 2-4) show the relaxation activity of 2 units of topoisomerase II over a 30 min incubation period. Compared to lane 1 which contains pBR322 (supercoiled plus a minor amount of relaxed), lane 2 shows the presence of fully relaxed pBR322 plus several topoisomers. Lanes 3 and 4 containing the solvent controls, where 4 and 6  $\mu\text{L}$  of water (pH 1.7) were added, show no significant effect of the solution pH on the activity of topoisomerase II, and give bands very similar in appearance to lane 2. mAMSA, an established topoisomerase II inhibitor,<sup>120</sup> was also included on most gels (eg, Figure 5.8e, lane 12) and gave the expected inhibition pattern.

Lanes 5-10 (Fig. 5.8a) show the effect of increasing concentrations (0.5-3.0 mM) of  $\text{Cp}_2\text{TiCl}_2$  **1** on topoisomerase II mediated relaxation of DNA. At low concentration (0.5 mM, lane 5), inhibition was not significant, while in the presence of 1.0 mM drug (lane 6) and 1.5 mM (lane 8), some supercoiled DNA as well as some topoisomers can be detected. At drug concentrations of 2 mM (lane 7) or higher (lanes 9-10) maximum activity was observed and only supercoiled DNA plus a minor amount of relaxed DNA (comparable to the control in lane 1) were observed. Lane 11 shows that  $\text{Cp}_2\text{TiCl}_2$  **1** (3.0 mM) does not affect the electrophoretic mobility of relaxed or supercoiled pBR322 in the absence of topoisomerase II.

Similar results were obtained for all other metallocenes tested (Figure 5.8b-e). Some minor variation in the relative amount of topoisomers formed in the controls was observed in each experiment. However, relative to these controls, inhibition of the enzyme activity was clearly apparent in the presence of a metallocene dichloride by the appearance of increasing amounts of supercoiled DNA (eg., lanes 5-10, Figure 5.8) The concentration at which maximum enzyme inhibition was achieved varied considerably,





**Figure 5.8:** Agarose gel electrophoresis showing the effect of  $\text{Cp}_2\text{MCl}_2$  on the relaxation of pBR322 by human topoisomerase II. Lane 1: pBR322; lane 2: pBR322 + topoisomerase II; lanes 3 and 4: pBR322 + topoisomerase II + 4  $\mu\text{L}$  and 6  $\mu\text{L}$   $\text{H}_2\text{O}$ . (a)  $\text{M} = \text{Ti}$  **1**; lane 5-10: pBR322 + topoisomerase II + 0.5, 1.0, 2.0, 1.5, 2.5 and 3.0 mM  $\text{Cp}_2\text{TiCl}_2$  **1**; lane 11: pBR322 + 3.0 mM  $\text{Cp}_2\text{TiCl}_2$  **1**; (b)  $\text{M} = \text{Mo}$  **4**; lanes 5-10: pBR322 + topoisomerase II + 0.5, 1.0, 1.5, 2.0, 2.5 and 3.0 mM  $\text{Cp}_2\text{MoCl}_2$  **4**; lane 11: pBR322 + 3.0 mM  $\text{Cp}_2\text{MoCl}_2$  **4** (Note : topoisomerase II inactive in lane 2); (c)  $\text{M} = \text{Nb}$  **3**: lanes 5-10: pBR322 + topoisomerase II + 0.05, 0.1, 0.15, 0.2, 0.25 and 0.5 mM  $\text{Cp}_2\text{NbCl}_2$  **3**; lane 11: pBR322 + 0.5 mM  $\text{Cp}_2\text{NbCl}_2$  **3**. (d)  $\text{M} = \text{V}$  **2**: lanes 5-10: pBR322 + topoisomerase II + 0.125, 0.25, 0.375, 0.5, 0.615 and 0.75 mM  $\text{Cp}_2\text{VCl}_2$  **2**; lane 11: pBR322 + 0.75 mM  $\text{Cp}_2\text{VCl}_2$  **2**. (e)  $(\text{MeCp})_2\text{TiCl}_2$  **34**: lane 5-10: pBR322 + topoisomerase II + 0.5, 1.0, 1.5, 2.0, 2.5 and 3.0 mM  $(\text{MeCp})_2\text{TiCl}_2$  **34**; lane 11: pBR322 + 3.0 mM  $(\text{MeCp})_2\text{TiCl}_2$  **34**; lane 12: pBR322 + topoisomerase II + 10  $\mu\text{M}$  *m*AMSA

and  $\text{Cp}_2\text{NbCl}_2$  **3** and  $\text{Cp}_2\text{VCl}_2$  **2** inhibited at significantly lower concentrations than  $\text{Cp}_2\text{TiCl}_2$  **1**. The results are summarised in Table 5.1. All experiments were repeated in triplicate and gave reproducible inhibition patterns at comparable concentrations to those presented in Figure 5.8.

**Table 5.1** : Summary of drug concentrations (mM) at which inhibition of topoisomerase II was observed and biological activity against EAT as reported in the literature.

No.	drug	Maximum <sup>a</sup> (mM)	OCR (%)	LD <sub>50</sub> (mg kg <sup>-1</sup> )	ref
<b>1</b>	$\text{Cp}_2\text{TiCl}_2$	> 2.0	100	100	38
<b>2</b>	$\text{Cp}_2\text{VCl}_2$	> 0.25	100	110	40
<b>3</b>	$\text{Cp}_2\text{NbCl}_2$	> 0.2	100	35	43
<b>4</b>	$\text{Cp}_2\text{MoCl}_2$	> 3.0	100	175	42
<b>34</b>	$(\text{MeCp})_2\text{TiCl}_2$	> 2.0	0	30	54

<sup>a</sup>drug concentration to achieve maximum inhibition

### 5.5. Correlation with Antitumor Activity

Table 5.1 includes the previously published OCRs and LD<sub>50</sub> values for the drugs tested *in vivo* against EAT along with the results of the topoisomerase II inhibition assays. Kuo *et al* have reported a concentration dependent inhibition of bacterial DNA topoisomerase II (winding) activity on relaxed DNA plasmid treated with  $\text{Cp}_2\text{MCl}_2(\text{aq})$  (M = V **2**, Mo **4**).<sup>57</sup> The concentrations at which drug inhibition was observed and the exact experimental conditions used have not been published and hence direct comparison with the results in Table 5.1, obtained with human topoisomerase II, is not possible. Qualitatively,

$\text{Cp}_2\text{MCl}_2$  (M=V **2**, Mo **4**) inhibit both human topoisomerase II (Figure 5.8) and bacterial topoisomerase II.<sup>57</sup> While all antitumour active metallocenes did inhibit topoisomerase II, the biologically inactive derivative  $(\text{MeCp})_2\text{TiCl}_2$  **34** also showed inhibition at comparable concentrations to the other metallocenes. Thus there is no direct correlation between inhibition and activity. However,  $\text{Cp}_2\text{VCl}_2$  **2** and  $\text{Cp}_2\text{NbCl}_2$  **3** inhibited topoisomerase II at lower concentrations than metallocenes **1**, **4** and **34** (Table 5.1). These results parallel the higher activity of  $\text{Cp}_2\text{VCl}_2$  **2** in inhibiting cell proliferation *in vitro* compared to other metallocenes<sup>39</sup> as well as inhibition of nucleic acid metabolism at a lower concentration than  $\text{Cp}_2\text{TiCl}_2$  **1**.<sup>21</sup>

It should be noted that DNA-binding of  $\text{Cp}_2\text{MX}_2$  *in vitro*, monitored by ICP spectroscopy,<sup>71</sup> has also not correlated with antitumour activity. While distinct adducts were observed with the antitumor active metallocene dichlorides  $\text{Cp}_2\text{TiCl}_2$  **1** and  $\text{Cp}_2\text{MoCl}_2$  **4**, DNA adducts were also detected with  $\text{Cp}_2\text{ZrCl}_2$  **7** and  $\text{Cp}_2\text{HfCl}_2$  **8**, which show no anticancer activity. Furthermore adducts were not detected with  $\text{Cp}_2\text{VCl}_2$  **2** which is the most active metallocene *in vitro*. These results, along with the vastly different stabilities and coordination chemistry of each metallocene dihalide, points to a unique mechanism of action for each compound.

## 5.6. Implications for the Mechanism of Antitumour Action

The inhibition or poisoning of human topoisomerase II has been implicated in the mechanism of activity of numerous antitumour drugs.<sup>120,124</sup> The most common class of drugs are topoisomerase II poisons which have typically both DNA and topoisomerase II binding domains allowing the drug to stabilize the DNA-topoisomerase II cleavable complex.<sup>124</sup>

Topoisomerase II inhibitors include non-DNA binding drugs or drugs that inhibit the ATP hydrolysis reaction that is required for the enzyme to function.

The antitumour metallocenes would not be expected to have any topoisomerase II poisoning effect as they lack the structural complexity which would enable them to bind to DNA via a DNA intercalating domain and also to topoisomerase II via a protein binding domain to stabilise the transient cleavable complex. As a consequence, the focus of this study was to determine whether the metallocenes  $\text{Cp}_2\text{MCl}_2$  ( $\text{M} = \text{Ti}$  **1**,  $\text{V}$  **2**,  $\text{Nb}$  **3**,  $\text{Mo}$  **4** and  $(\text{MeCp})_2\text{TiCl}_2$  **34**) inhibited topoisomerase II relaxation of supercoiled pBR322 and whether this correlated with their antitumour activity *in vivo*.

All of the metallocenes tested were able to inhibit the relaxation of supercoiled DNA by human topoisomerase II but at different concentrations. These compounds all undergo rapid halide hydrolysis *in vitro* to form similar species at low pH (" $\text{Cp}_2\text{M}^{n+}$ ") which can form coordination complexes, and are stable to Cp hydrolysis in the presence of DNA and proteins. Thus, a possible common mechanism could involve inhibition of topoisomerase II via binding of " $\text{Cp}_2\text{M}^{n+}$ " to accessible coordinating groups on the surface of the protein, with resultant reduction in the activity of the enzyme. As discussed above, there is no evidence to implicate direct binding of the metallocenes to DNA. Hence, initial metallocene-DNA binding, stabilisation of a ternary metallocene-DNA-enzyme complexes or interaction of an initial metallocene-enzyme complex with DNA seem highly unlikely as key steps responsible for topoisomerase II inhibition. However, extension of *in vitro* results to *in vivo* activity must be treated with caution. The active species *in vivo* has not been identified for any of the metallocene dihalides. A number of roles for the Cp ligands have been proposed, including a function where the hydrophobic Cp ligands facilitate transport and subsequent release of the

active metal species into the cell.<sup>18</sup> It is also possible that the Cp ligands act as a delivery agent to a blood transport protein such as transferrin.<sup>78,80,114,115</sup> The results of this work suggest that if a species such as " $\text{Cp}_2\text{M}^{n+}$ " was transported into cancer cells, then inhibition of topoisomerase II is possible, most probably by direct interaction with the enzyme. Recent studies<sup>78,80,114,115</sup> suggest that this is unlikely to be the case for  $\text{Cp}_2\text{TiCl}_2$  **1**, but may be feasible with metallocenes **2**, **3** and **4**. As topoisomerase II inhibition is ATP dependent, formation of metallocene-ATP complexes could also lead to reduced enzyme activity. However,  $\text{Cp}_2\text{NbCl}_2$  **3** does not interact with nucleotides and  $\text{Cp}_2\text{VCl}_2$  **2** forms only weak complexes with nucleotides.

### **5.7. Conclusions**

The results of this study confirm that the mechanism of all of the antitumour metallocenes is most likely a complex pathway, involving a number of different species in the transport and delivery of the active species into cancer cells and subsequent interactions with nucleic acids and/or proteins (including topoisomerases) and/or other potential coordinating species present in the intracellular environment. Inhibition of topoisomerase II is a possible mechanism that may be related to anticancer activity, but the precise mechanism whereby this occurs requires further study to establish the biologically active species that is formed for each of the metallocenes *in vivo*.

As discussed in Section 1.6, DNA has been implicated in the mechanism of action of several antitumour metallocenes. However, more recent studies have suggested that the interactions of metallocenes with proteins and enzymes also need to be considered.<sup>57</sup> Furthermore, during the course of the work reported in this thesis, studies on the blood transport protein transferrin have implicated this protein in the delivery of "Ti<sup>4+</sup>", derived from Cp<sub>2</sub>TiCl<sub>2</sub> **1**, to tumour cells.<sup>76,80,114,115</sup>

In order to further clarify the molecular basis for the mechanism of action of the antitumour metallocenes, this Chapter reports a study of the interaction of several metallocenes with calf thymus DNA and HSA using UV spectroscopy and ICP-AES. These techniques were used in order to gain qualitative information regarding the relative binding affinity of the metallocenes for calf thymus DNA versus HSA and provide complementary information to studies reported in Chapters 2 and 3 on short oligonucleotides and nucleic acid constituents. HSA was studied as this is the major protein present in blood and in addition to transferrin, is one of the few blood proteins that has been implicated in the transport of metal ions *in vivo*.<sup>128,129</sup>

The binding studies with calf thymus DNA and HSA focused on Cp<sub>2</sub>TiCl<sub>2</sub> **1** and Cp<sub>2</sub>MoCl<sub>2</sub> **4**. The interaction of Cp<sub>2</sub>TiCl<sub>2</sub> **1** with small molecules cannot be studied under physiological conditions, however, the formation of complexes with bulk DNA has been reported.<sup>71</sup> While Cp<sub>2</sub>MoCl<sub>2</sub> **4** forms discrete complexes with nucleotides (Section 2.2.4.), the absence of complexation with oligonucleotides under physiological conditions (Chapter 2) suggests that DNA may not be the principal cellular target. However, the lack of complexation with short oligonucleotides does not rule out interaction with bulk DNA and

hence these experiments were designed to provide complementary information to that reported in Chapter 2.

The use of titanium NMR spectroscopy as a tool to monitor the interaction of  $\text{Cp}_2\text{TiCl}_2$  **1** with biomolecules was also investigated. Potentially, this technique would allow the formation and subsequent chemistry of Ti species formed from  $\text{Cp}_2\text{TiCl}_2$  **1** in cellular mixtures to be monitored. The interaction of several antitumour metallocenes with glutathione, a tripeptide that is present at high concentration (mM) inside cells and has been implicated in the intracellular transport and detoxification of cisplatin,<sup>130-133</sup> was also studied using  $^1\text{H}$  NMR spectroscopy.

### **6.1. UV Studies**

UV spectroscopy is a technique commonly used to study the interaction of a substrate (e.g. a drug) with biomolecules including DNA and proteins.<sup>72,73,76,134,135</sup> The advantage of the technique is that it can be carried out at low sample concentrations with solutions that approximate physiological conditions, provided the sample contains a suitable chromophore that absorbs light at a wavelength that can be monitored. Typically, an interaction or association is apparent when there is a shift in the maximum absorbance wavelength or when there is a change in the absorbance at a selected wavelength. As each spectrum can be recorded in a relatively short period of time, a range of sample concentrations can be screened. These experiments, which can be carried out with large molecular weight proteins and DNA, provide complementary information to that obtained with X-ray crystallography and NMR spectroscopy, which are restricted to smaller molecular weight species. The

limitation of the technique is that the molecular level detail of any interaction cannot be determined.

In this work UV spectroscopy was used to study the interaction of  $\text{Cp}_2\text{TiCl}_2$  **1** and  $\text{Cp}_2\text{MoCl}_2$  **4** with calf thymus DNA or HSA. Previously, it has been reported that metallocenes interact with the nucleic acids DNA or RNA leading to an alteration in the secondary structure.<sup>17</sup> UV spectroscopy has been used to monitor the interaction of titanocene complexes with DNA.<sup>72,73,134</sup> The UV absorbance of  $\text{Cp}_2\text{TiCl}_2$  **1** in 0.1 M NaCl at pH 7.2 was reported to decrease rapidly over 48 h at 258 nm due to hydrolysis processes. While in the presence of DNA the decrease in the UV absorbance at 258 nm was less prominent implying that there was an interaction with DNA.<sup>72</sup>

### **6.1.1. DNA Binding**

In order to determine whether  $\text{Cp}_2\text{TiCl}_2$  **1** and  $\text{Cp}_2\text{MoCl}_2$  **4** show any interaction or association with DNA, the UV spectra of aqueous solutions of each metallocene (0.07 mM and 0.3 mM respectively) at pH 7 was recorded at regular intervals in the absence (Figure 6.1a and 6.2a) and presence (Figure 6.1b and 6.2b) of calf thymus DNA (0.05 mM). The absorbance of calf thymus DNA (0.05 mM) was independently measured over the same time frame and subtracted from the UV absorbance measured in presence of  $\text{Cp}_2\text{TiCl}_2$  **1** (Figure 6.1b) and  $\text{Cp}_2\text{MoCl}_2$  **4** (Figure 6.2b).

The UV spectrum of  $\text{Cp}_2\text{TiCl}_2$  **1** (0.07 mM) in water at pH 7 (pale yellow solution) shows a maximum absorbance at 244 nm and a shoulder peak at 316 nm after 0.25 h (Figure 6.1a). These peaks are rapidly diminished with time due to rapid hydrolysis of the Cp rings to give a precipitate and loss of the pale yellow colour of the solution (see Section 1.5.2.) (Figure

6.1a). In contrast, the absorbance of  $\text{Cp}_2\text{TiCl}_2$  **1** in the presence of calf thymus DNA (Figure 6.1b) is significantly altered compared to the control experiment (Figure 6.1a). Firstly, the shift in the maximum absorbance to

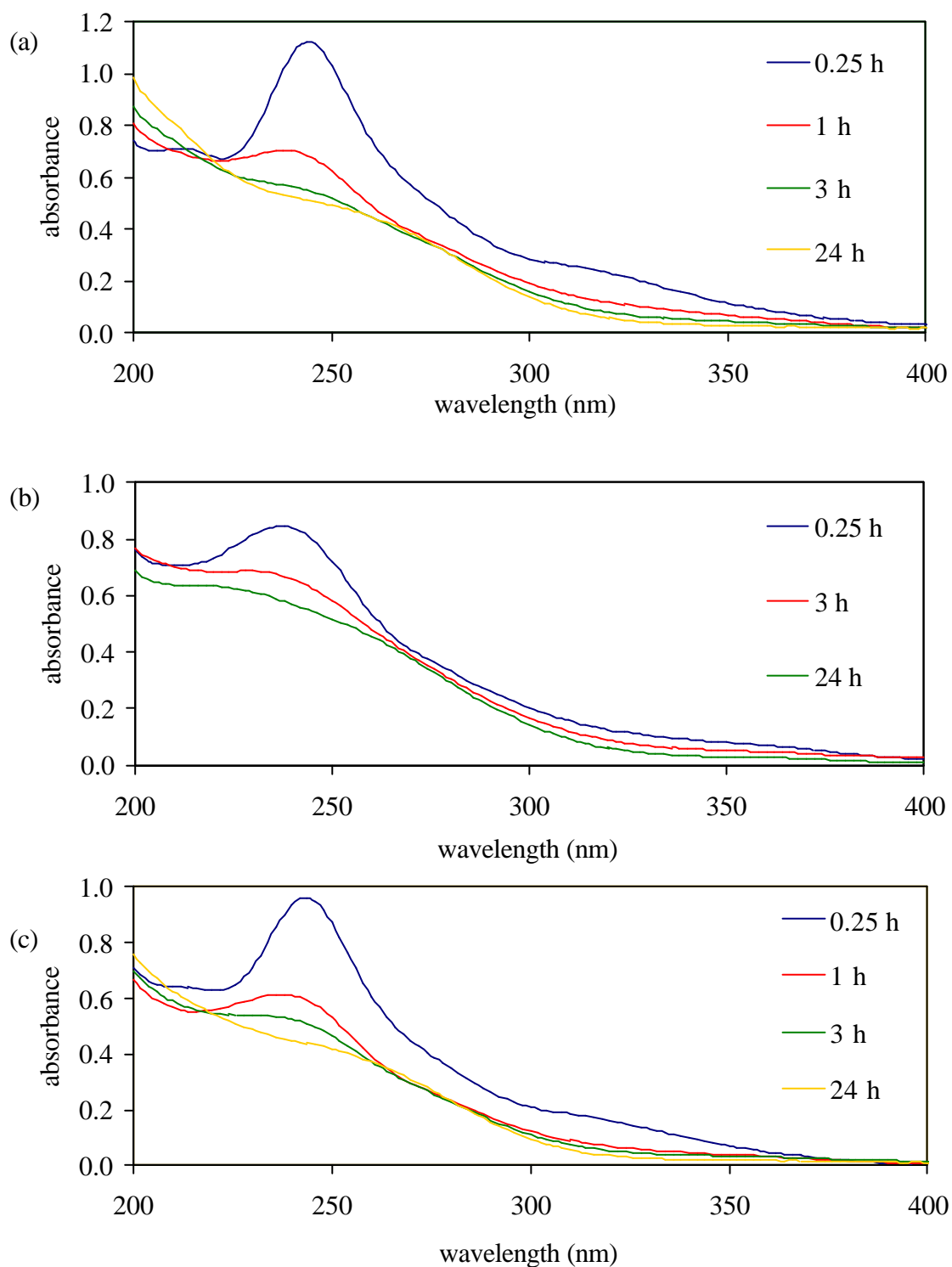


**Figure 6.1:** UV absorbance of Cp<sub>2</sub>TiCl<sub>2</sub> **1** (0.07 mM, pH 7) over 24 h at 25 °C in water with (a) no biomolecules, (b) calf thymus DNA (0.05 mM), (c) HSA (0.16 μM)

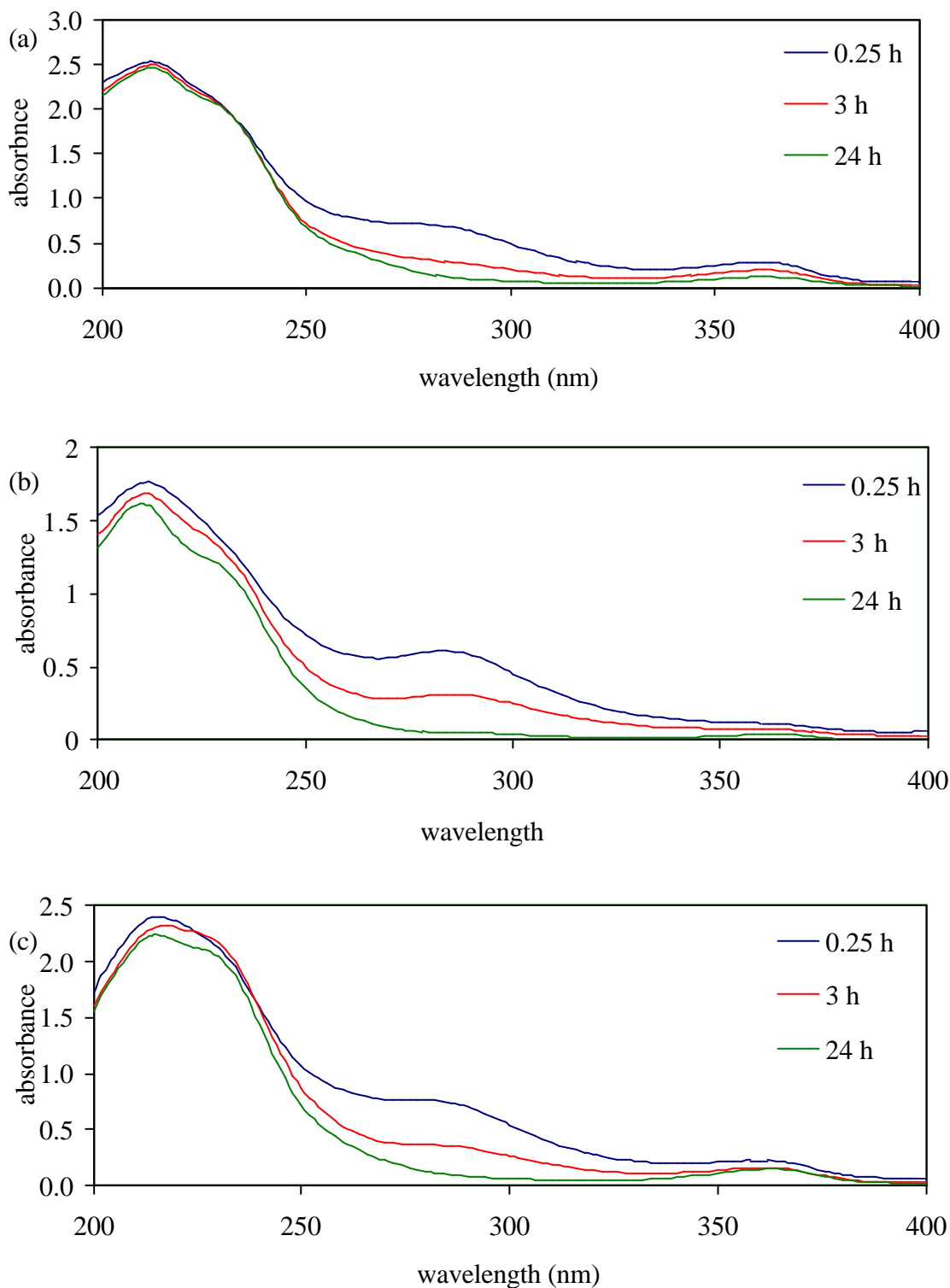


**Figure 6.2:** UV absorbance of  $\text{Cp}_2\text{MoCl}_2 \mathbf{4}$  (0.3 mM, pH 7) over 24 h at 25 °C in water with (a) no biomolecules, (b) calf thymus DNA (0.05 mM), (c) HSA (0.16  $\mu\text{M}$ )

234 nm from 244 nm implies that the Cp ligands are in a different environment, consistent with formation of a metallocene-DNA complex. The UV absorbance is also decreased initially by approximately 20%. Secondly, no precipitation occurred in solutions of  $\text{Cp}_2\text{TiCl}_2$  **1** in the presence of calf thymus DNA at pH 7 over 72 h. This observation indicates that Cp hydrolysis processes are altered in the presence of calf thymus DNA at pH 7 and supports the UV data, which indicate that there is an interaction or association of  $\text{Cp}_2\text{TiCl}_2$  **1** with calf thymus DNA.

Similar experiments were carried out with  $\text{Cp}_2\text{MoCl}_2$  **4**. The UV spectrum of  $\text{Cp}_2\text{MoCl}_2$  **4** (0.3 mM) in water at pH 7 (mauve coloured solution) shows peaks at 214 nm and 360 nm and a shoulder peak at 286 nm. The absorbance at 286 nm decreases significantly with time (Figure 6.2a) with some decreases also noted at 214 nm and 360 nm. As in the case of  $\text{Cp}_2\text{TiCl}_2$  **1**, in the presence of calf thymus DNA (Figure 6.2b), the absorbance of  $\text{Cp}_2\text{MoCl}_2$  **4** is significantly altered compared to the control experiment (Figure 6.2a). This is evident by the decrease in absorbance at 214 nm and 360 nm. The altered absorbance is consistent with an interaction between  $\text{Cp}_2\text{MoCl}_2$  **4** and calf thymus DNA.

### **6.1.2. HSA Binding**

In order to determine whether  $\text{Cp}_2\text{TiCl}_2$  **1** or  $\text{Cp}_2\text{MoCl}_2$  **4** show any interaction or association with HSA the UV spectra of each metallocene in the presence of HSA in water at pH 7 was recorded at certain intervals (Figure 6.1c and 6.2c) and compared to the UV spectra recorded for the metallocenes in water at pH 7 (Figure 6.1a and 6.2a). The absorbance of HSA (0.13  $\mu\text{M}$ ) was independently measured over the same time frame and

subtracted from the UV absorbance measured in the presence of  $\text{Cp}_2\text{TiCl}_2$  **1** (0.07 mM) (Figure 6.1c) and  $\text{Cp}_2\text{MoCl}_2$  **4** (0.3 mM) (Figure 6.2c).

The absorbance of  $\text{Cp}_2\text{TiCl}_2$  **1** (0.07 mM) in the presence of HSA (0.13  $\mu\text{M}$ ) (Figure 6.1c) was not significantly altered compared to the control experiment (Figure 6.1a), with the changes in the spectra over time showing that the protein was not preventing hydrolysis of the metallocene to any significant extent. This interpretation was supported by the formation of a precipitate in solutions of  $\text{Cp}_2\text{TiCl}_2$  **1** (0.07 mM) and HSA (0.13  $\mu\text{M}$ ) at pH 7.

A similar result was obtained with  $\text{Cp}_2\text{MoCl}_2$  **4**. The absorbance of  $\text{Cp}_2\text{MoCl}_2$  **4** (0.3 mM) in the presence of HSA (0.13  $\mu\text{M}$ ) (Figure 6.2c) was not significantly altered compared to the control experiment (Figure 6.2a).

## **6.2. Inductively Coupled Plasma Spectroscopy/Dialysis Studies**

ICP-AES is a powerful technique that allows the detection of a range of metals at low concentrations.<sup>136-138</sup> ICP provides the source for analysis by AES and involves introduction of the sample into the plasma torch using a nebuliser.<sup>136</sup> The sample is introduced into the nebuliser in solution, following strong acid digestion to give a homogenous solution in order to avoid interference by the matrix. The technique is highly sensitive, allowing detection limits of typically  $1\ \mu\text{g L}^{-1}$  (0.001 ppm) to be measured, depending on the metal ion, ie., about 1-2 order(s) of magnitude better than atomic absorption methods.<sup>136,138,139</sup> ICP also has the advantage of lower matrix interference compared to atomic absorption methods.<sup>136</sup>

ICP-AES has been used successfully to measure metal concentration in samples taken from biological sources.<sup>138</sup> For example, Ti and Zr levels in serum<sup>140</sup> and Ca levels in the

bone<sup>141</sup> have been analysed by ICP-AES. ICP-AES has also been used to measure the amount of Ti derived from  $\text{Cp}_2\text{TiCl}_2$  **1** and titanium(IV) citrate bound to transferrin.<sup>76</sup> Various sample preparation techniques have been applied for samples from biological sources so as to reduce and/or eliminate interference.<sup>128,141</sup> For example carbon interference in Ti and Zr determination has been eliminated by pressurised digestion with mixtures of nitric and hydrochloric acid.<sup>140</sup>

ICP has been used previously to show that the metallocenes  $\text{Cp}_2\text{MCl}_2$  ( $\text{M} = \text{Ti}$  **1**, Nb **3**, Zr **7**, Hf **8**), form adducts with salmon testes DNA or calf thymus DNA at pH 5-6.<sup>71</sup> Studies using tritium-labelled  $\text{Cp}_2\text{TiCl}_2$  **1** showed that  $\text{Cp}_2\text{Ti}$ -DNA adducts are formed at pH 5.3 and  $\text{CpTi}$ -DNA adducts are formed at pH 7.0.<sup>71</sup> The binding studies were carried out in solutions of sodium perchlorate by incubating the metallocene with DNA followed by precipitation of the DNA and DNA-metallocene complex(es) with 95% ethanol saturated with sodium acetate. The precipitated pellets were analysed by ICP following digestion in 5% ammonium hydroxide.

In this work, dialysis was used instead of ethanol precipitation to isolate metallocene-DNA adducts from small unbound metallocene species. The use of dialysis was employed so as to avoid possible coprecipitation of unbound hydrolysed metallocene, which could occur during the ethanol DNA precipitation and to allow different conditions to be used in the initial preparation of the DNA-adducts (40 mM NaCl, pH 5-6.5). In addition, formation of molybdocene-DNA adducts, which has not been previously reported, was investigated.

Figure 6.3 shows a schematic of the dialysis experiment used to prepare samples for ICP-AES analysis. In the general assay, the metallocene  $\text{Cp}_2\text{MCl}_2$  ( $\text{M} = \text{Ti}$  **1**, Nb **3**, Mo **4**)

(0.25 mM) was incubated with a solution of DNA in saline (40 mM) in the pH range of 5.0-6.5 (Figure 6.3a and b). Three different concentrations of DNA (2.5, 0.25 and 0.025 mM nucleotide) were selected, i.e., a metal:nucleotide ratio of 1:10, 1:1 and 10:1 respectively. With the nucleotide concentration at 2.5 mM, an excess number of binding sites are available, while at 0.25 mM, the metallocene and nucleotide concentrations are equal. In the third experiment, the metallocene was in excess and hence all DNA binding sites would be predicted to be saturated.

After incubation with DNA for typically 72 h, the samples were centrifuged, if required, to remove any precipitate (Figure 6.3c), and 1 mL of the DNA-metallocene solution was dialysed in a 20 mL saline solution for 48 h (Figure 6.3d). A 30,000 molecular weight cut-off membrane was used in the dialysis tubing as this would retain the calf thymus DNA (MW ~66,000) plus any metallocene-DNA complex. In the absence of formation of a metallocene-DNA complex, hydrolysis of the metallocene occurs to give small MW species that would equilibrate in the solution. After dialysis was complete, an accurate volume of the contents of compartments 1 and 2 (Figure 6.3e) was analysed for the concentration of metal present. The samples were lyophilised in glass vials and digested with concentrated nitric acid (1 mL) and diluted to a standard volume (10 mL) for analysis. ICP-AES of these samples was carried out by the Warwick Analytical Service, University of Warwick. The metal content measured was recorded in ppm and was corrected to give the concentration of metal in compartments 1 and 2 (Figure 6.3f).

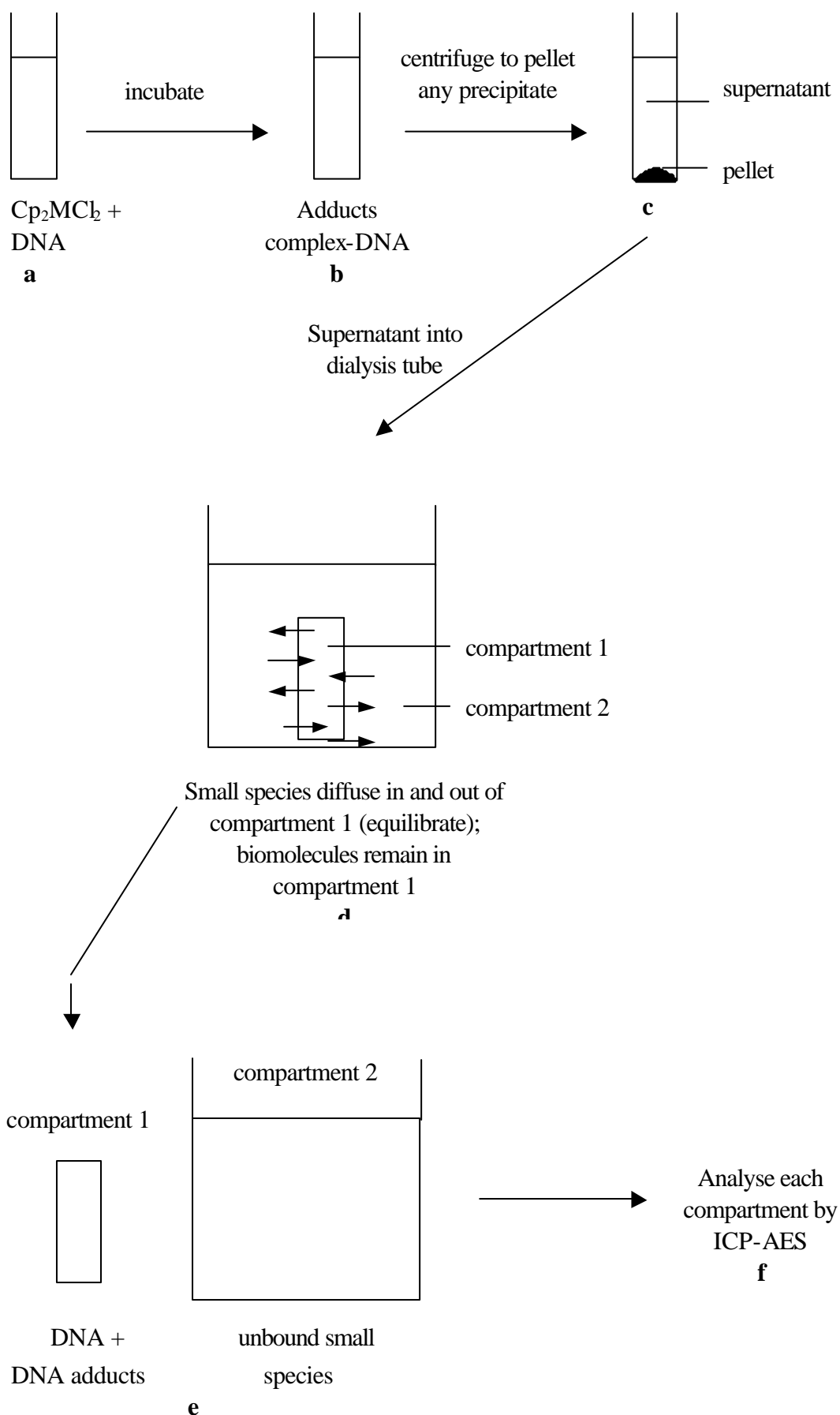


**Figure 6.3:** Schematic of the procedure for the ICP/dialysis assays

Table 6.1a summarises the results obtained with  $\text{Cp}_2\text{TiCl}_2$  **1**. In experiment 1, assuming all the metallocene bound to the DNA and was retained in the dialysis tube, a calculated Ti concentration of 0.25 mM would result (column a, Expt. 1). If none of the metallocene bound to the DNA, then equilibrium between the two compartments would be established to give a calculated Ti concentration of 0.012 mM in each compartment (column b, Expt. 1). The measured concentration of Ti (column c, Expt. 1) was found to be 0.20 mM in compartment 1, which corresponds to 79% of the metal initially present. While this result supports formation of a titanocene-DNA complex under the conditions used, the metal concentration in compartment 2, showed that the results are only qualitative, and errors in either sample handling and/or analysis methods were present. Specifically, the metal concentration in compartment 2 was found to be 0.012 mM indicating that 99% of the Ti is unbound and has equilibrated, which does not agree with the metal concentration found in compartment 1.

**Table 6.1a:** Analysis by ICP-AES of titanium associated with calf thymus DNA after 72 h incubation with  $\text{Cp}_2\text{TiCl}_2$  **1** and 48 h dialysis time in 40 mM NaCl at 25 °C

Expt.	Compartment	a Initial		b Calculated maximum if		c After 48 h dialysis	
		[Ti] (mM)	DNA [nucleotide] (mM)	100% Ti bound (mM)	0% Ti bound (equilibrium) (mM)	[Ti] found (mM)	% of maximum calculated Ti
1	1	0.25	2.5	0.25	0.012	0.20	79
	2	0	0	0	0.012	0.012	99
2	1	0.25	0.25	0.25	0.012	0.18	74
	2	0	0	0	0.012	0.008	67
3	1	0.25	0.025	0.25	0.012	0.14	55
	2	0	0	0	0.012	0.006	54

**Table 6.1b:** Analysis of titanium content in the supernatant and pellet by ICP-AES after 120 h incubation of  $\text{Cp}_2\text{TiCl}_2$  **1** in 40 mM NaCl at 25 °C

Expt.	Supernatant/ pellet	Calculated maximum if		After 120 h incubation	
		100% of Ti precipitates (mg)	0% of Ti precipitates (mg)	Ti found (mg)	% of maximum calculated Ti
$\text{Cp}_2\text{TiCl}_2$ <b>1</b>	pellet	0.025	0	0.015	63
(control)	supernatant	0	0.025	0.0011	5

Experiments 2 and 3 gave similar results taking into account the different DNA concentrations, but as in the case of experiment 1, there is a discrepancy in the metal concentration that was found in compartment 2 compared to compartment 1 (Table 6.1a, column c). However, qualitatively, the metal concentrations in compartment 1 were consistently higher than the equilibrium concentration and these results support binding of the metal to DNA, which has been independently observed using other techniques.<sup>71-73,134</sup> Furthermore, the amount of Ti found to be complexed to DNA decreased as the number of available binding sites is decreased.

The reasons for the errors are not easily rationalised as the metal content was sometimes found to be higher than what was expected theoretically. Errors associated with the ICP-AES analysis technique, either in the digestion method or in the actual recording of the metal content cannot be ruled out. Incomplete digestion has been reported to be a source of error with ICP analysis, for example titanium dioxide, if present, is not digested in nitric acid.<sup>142</sup> Incomplete digestion of the biological material can also lead to errors due to interference from the matrix.<sup>136,138</sup> The precision of the detection technique can also be

compromised near the detection limit as is the case for the concentrations expected in the compartment 2.<sup>136</sup> Complicated matrices are also known to increase the detection limits.<sup>136</sup>

Control experiments were also carried out with  $\text{Cp}_2\text{TiCl}_2$  **1** (0.25 mM) in 40 mM saline (2 mL) in the absence of DNA. The formation of insoluble precipitates due to Cp hydrolysis processes was visually evident in the control experiment containing  $\text{Cp}_2\text{TiCl}_2$  **1** over a 120 h incubation period. Due to formation of the precipitate, the control experiments were not dialysed. This is in contrast to the DNA-binding experiments in which no precipitate was observed during the 72 h of incubation and 48 h of dialysis (this was also observed in the UV binding studies; see Section 6.1.1). Hence, control solutions were centrifuged to concentrate the precipitate into a pellet. In order to obtain a measure of the amount of metal that precipitated out of solution, half of the volume of supernatant was taken and analysed by ICP-AES. The remaining half of the supernatant together with the precipitated pellet was also analysed by ICP-AES. ICP-AES analysis confirmed that most of the Ti precipitated out of solution (Table 6.1b; 63%). However, only 68% of the Ti was accounted for. This result confirms that further optimisation of the digestion assay is required to give quantitative results.

The results obtained from the dialysis studies were supported using ethanol precipitation of DNA instead of dialysis, as a means of isolating the titanocene-DNA adduct. The precipitated DNA was found to contain a significantly increased concentration of titanium (~70% of the total available titanium).

Dialysis experiments with  $\text{Cp}_2\text{NbCl}_2$  **3** (Table 6.2a) and  $\text{Cp}_2\text{MoCl}_2$  **4** (Table 6.3a) with calf thymus DNA gave similar results to those obtained with  $\text{Cp}_2\text{TiCl}_2$  **1**. The metal content was consistently found to be higher than the equilibrium concentration and these results

support binding of the metal to DNA. As with  $\text{Cp}_2\text{TiCl}_2$  **1** the total concentrations found in compartments 1 and 2 indicated significant errors in the assay. For example, in one experiment the concentration in compartment 2 exceeded the maximum equilibrium concentration that is theoretically possible. Furthermore, the control experiments showed that only 14% of the total theoretical Nb was recovered (Table 6.2b) and 36% of the total theoretical Mo was recovered (Table 6.3b). The discrepancies can be attributed to errors similar to those discussed for  $\text{Cp}_2\text{TiCl}_2$  **1**. The controls also show that significant precipitation does not occur in solutions of  $\text{Cp}_2\text{NbCl}_2$  **3** (Table 6.2b; 2%) and  $\text{Cp}_2\text{MoCl}_2$  **4** (Table 6.3b; 0%).

**Table 6.2a:** Analysis by ICP-AES of niobium be associated with calf thymus DNA after 72 h incubation with  $\text{Cp}_2\text{NbCl}_2$  **3** and 48 h dialysis time in 40 mM NaCl at 25 °C

Expt.	Compartment	a Initial		b Calculated maximum if		c After 48 h dialysis	
		[Nb] (mM)	DNA [nucleotide] (mM)	100% Nb bound (mM)	0% Nb bound (equilibrium) (mM)	[Nb] found (mM)	% of maximum calculated Nb
4	1	0.25	2.5	0.25	0.010	0.040	16
	2	0	0	0	0.010	0.001	12
5	1	0.25	0.25	0.25	0.010	0.056	22
	2	0	0	0	0.010	0	0
6	1	0.25	0.025	0.25	0.010	0.009	3
	2	0	0	0	0.010	0.001	10

**Table 6.2b:** Analysis of niobium content in the supernatant and pellet by ICP-AES after 120 h incubation of  $\text{Cp}_2\text{NbCl}_2$  **3** in 40 mM NaCl at 25 °C

	Calculated maximum if	After 120 h incubation

Expt.	Supernatant/ pellet	100% of Nb precipitates (mg)	0% of Nb precipitates (mg)	Nb found (mg)	% of maximum calculated Nb
Cp <sub>2</sub> NbCl <sub>2</sub> <b>3</b> (control)	pellet	0.046	0	0.001	2
	supernatant	0	0.046	0.0054	12

**Table 6.3a:** Analysis by ICP-AES of molybdenum associated with calf thymus DNA after 72 h incubation with Cp<sub>2</sub>MoCl<sub>2</sub> **4** and 48 h dialysis time in 40 mM NaCl at 25 °C

Expt.	Compartment	a Initial		b Calculated maximum if		c After 48 h dialysis	
		[Mo] (mM)	DNA [nucleotide] (mM)	100% Mo bound (mM)	0% Mo bound (equilibrium) (mM)	[Mo] found (mM)	% of maximum calculated Mo
7	1	0.25	2.5	0.25	0.012	0.061	26
	2	0	0	0	0.012	0.017	144
8	1	0.25	0.25	0.25	0.012	0.054	21
	2	0	0	0	0.012	0.013	113
9	1	0.25	0.025	0.25	0.012	0.032	13
	2	0	0	0	0.012	0.003	26

**Table 6.3b:** Analysis of molybdenum content in the supernatant and pellet by ICP-AES after 120 h incubation of Cp<sub>2</sub>MoCl<sub>2</sub> **4** in 40 mM NaCl at 25 °C

Expt.	Supernatant/ pellet	Calculated maximum if		After 120 h incubation	
		100% of Mo precipitates (mg)	0% of Mo precipitates (mg)	Mo found (mg)	% of maximum calculated Mo
Cp <sub>2</sub> MoCl <sub>2</sub> <b>4</b> (control)	pellet	0.048	0	0	0
	supernatant	0	0.048	0.0175	36

The results obtained from the dialysis studies with  $\text{Cp}_2\text{NbCl}_2$  **3** and  $\text{Cp}_2\text{MoCl}_2$  **4** were supported using ethanol precipitation of DNA instead of dialysis, as a means of isolating the metallocene-DNA adduct. The precipitated DNA was found to contain significantly increased concentration of niobium or molybdenum (~70% of the total available niobium and ~55% of the total available molybdenum).

### 6.3. Titanium NMR

Few studies involving  $^{49}\text{Ti}$  or  $^{47}\text{Ti}$  nuclei as NMR probes have been reported.<sup>143-146</sup> Both nuclei are magnetically active and their natural abundance is high enough to allow direct observation by NMR spectroscopy ( $^{47}\text{Ti}$ - I = 5/2, 7.28% and  $^{49}\text{Ti}$ - I = 7/2, 5.51%).<sup>147</sup> The quadrupole moment for the  $^{47}\text{Ti}$  ( $Q = 0.29 \times 10^{28} \text{ m}^2$ ) and  $^{49}\text{Ti}$  ( $Q = 0.24 \times 10^{28} \text{ m}^2$ ) is also relatively high which means that very broad peaks result when the complex is not symmetrical.<sup>147</sup> In general,  $\text{TiCl}_4$  which is highly symmetrical is used as an external standard and the sharp  $^{49}\text{Ti}$  peak is referenced as  $\delta$  0.00 ppm and the  $^{47}\text{Ti}$  peak appears at -266 ppm (Figure 6.4a).<sup>146</sup> NMR spectra of  $^{49}\text{Ti}$  nuclei in complexes of the form  $\text{Cp}_2\text{TiX}_2$ , where X is a halogen, show that the chemical shift lies in a broad range of about 1000 ppm.<sup>144</sup> This provides a powerful means of characterisation which can clearly identify the type of ligand present in titanocene complexes. As an example the  $^{49}\text{Ti}$  resonance appears at -1051 ppm for  $\text{Cp}_2\text{TiF}_2$  **16**, -773 ppm for  $\text{Cp}_2\text{TiCl}_2$  **1** and -671 ppm for  $\text{Cp}_2\text{TiBr}_2$  **17**.<sup>146</sup> These results also show that there is an inverse dependence between the electronegativity of the ligand and the chemical shift. That is that the chemical shift moves upfield as the electronegativity of the ligand is increased, which is the reverse of what is expected in proton NMR.

In this work, the use of Ti NMR as a technique to monitor the interaction of  $\text{Cp}_2\text{TiCl}_2$  **1** with biomolecules, as well as to provide further information on the biologically active species, was investigated. Experiments were initially carried out on  $\text{Cp}_2\text{TiCl}_2$  **1** in chloroform. In this organic solvent, both the Cp and halide ligands are metal bound and hence the fully symmetrical complex should give rise to one Ti signal in the NMR spectrum. Figure 6.4b shows the  $^{49}\text{Ti}$  NMR spectrum obtained on a saturated solution of  $\text{Cp}_2\text{TiCl}_2$  **1** (10 mg) in  $\text{CDCl}_3$  (0.5 mL) acquired over 24 h. A signal was detected at  $-773$  ppm in agreement with the literature.<sup>146</sup>

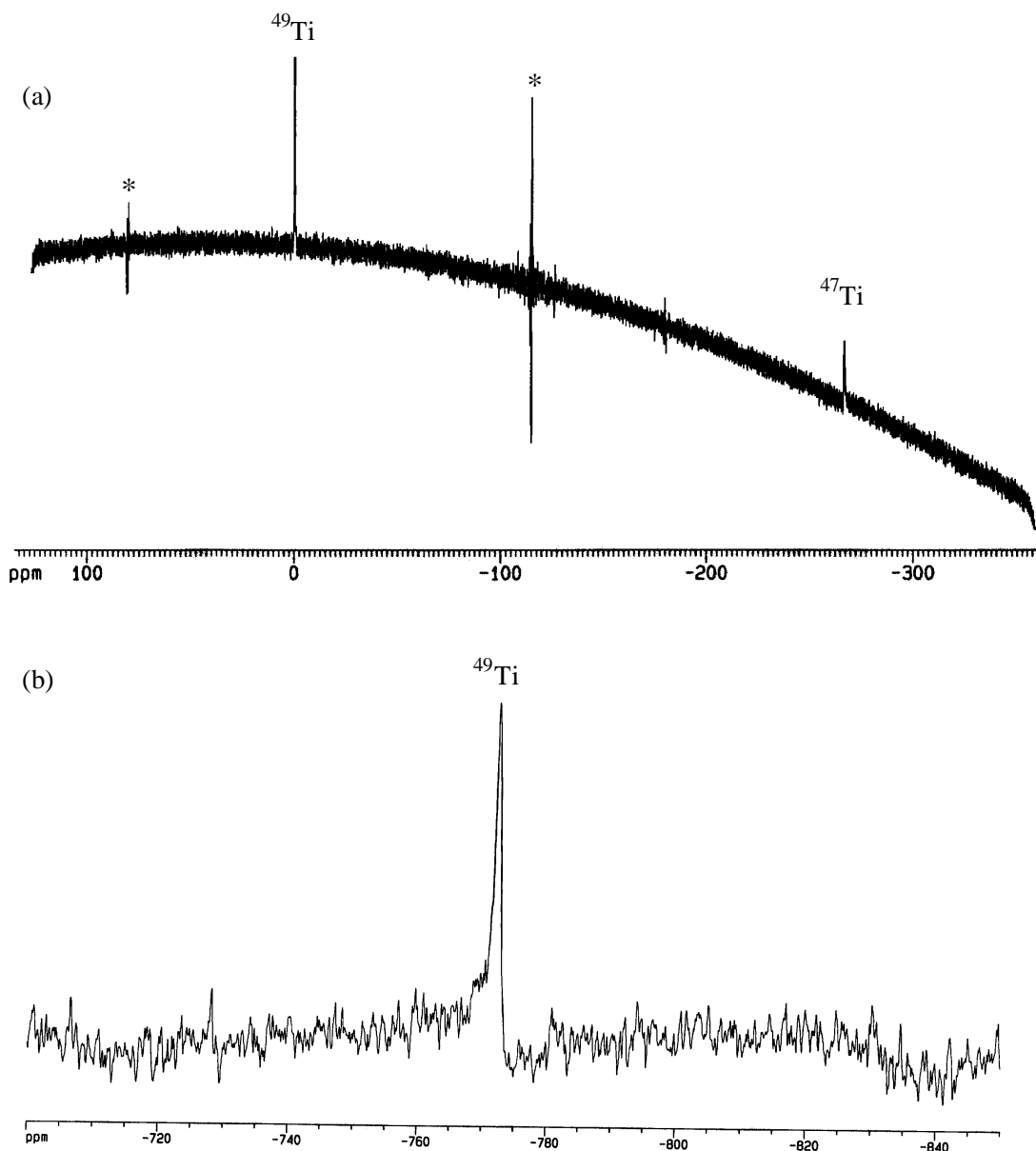


**Figure 6.4:** 22.565 MHz Ti NMR of (a) neat  $\text{TiCl}_4$  and (b)  $\text{Cp}_2\text{TiCl}_2$  **1** in  $\text{CDCl}_3$  (saturated; 10 mg in 0.5 mL); \* spikes which are not real peaks

In contrast to chloroform, the solubility of  $\text{Cp}_2\text{TiCl}_2$  **1** in water is significantly reduced ( $\sim 7 \text{ mg ml}^{-1}$ ). An attempt to record a  $^{49}\text{Ti}$  spectrum of this solution gave no detectable signal after 48 h due to the low sample concentration and an increased number of Ti-containing species present in the aqueous solution (Section 1.5.). Given that higher sample concentrations could not be achieved, further studies were not carried out.

#### 6.4. Glutathione 72 Binding Studies



3-7. Figure 6.5(i) shows the aliphatic region of the  $^1\text{H}$  NMR spectra of glutathione **72** upon titration of 1 equiv.  $\text{Cp}_2\text{TiCl}_2$  **1** with time at pD 2.4 or 7.1. At pD 2.4 or pD 7.1, the chemical shifts and appearance of the glutathione **72** resonances are similar in the absence and presence of 1 equiv of  $\text{Cp}_2\text{TiCl}_2$  **1** (Figure 6.5(i)). It is evident from the spectra that  $\text{Cp}_2\text{TiCl}_2$  **1** does not interact or bind to glutathione **72** at pD 2.4 or 7.1 after 0.25 h (Figure 6.5(i) b and c) as the NMR signals are not significantly changed compared to glutathione **72** alone (Figure 6.5(i) a). The lack of binding at pD 7.1 can be attributed to the rapid hydrolysis of  $\text{Cp}_2\text{TiCl}_2$  **1** in this pD range (see Section 1.5.). At pD 2.4 50% of the carboxylate groups of glutathione are protonated ( $\text{pK}_a$  of  $\alpha$ -COOH in gly or glu is  $\sim 2.2$ - $2.3$ ) and therefore restricts coordination of the metal center to  $\text{COO}^-$ . In contrast, at pD 6 after 2 h and 24 h a new cys  $\beta$ - $\text{CH}_2$  signal was observed (Figure 6.5(ii) c and d; indicated by  $\bullet$ ). At this pH, the competing hydrolysis reaction is slow compared to pD 7.3, allowing formation of a stable complex. These changes are consistent with interaction of  $\text{Cp}_2\text{TiCl}_2$  **1** with glutathione **72** via binding to the sulfur donor group of glutathione **72** and possibly assisted by simultaneous coordination to the  $\text{COO}^-$  group. The lack of binding at low pD 2.4 suggests that the  $\text{COO}^-$  groups may be important in complexation of  $\text{Cp}_2\text{TiCl}_2$  **1** to glutathione **72** at pD 6.

Figure 6.6(i) shows the aliphatic region of the  $^1\text{H}$  NMR of glutathione **72** upon titration of 1 equiv.  $\text{Cp}_2\text{NbCl}_2$  **3** with time at pD 2.7 or 7.4. The appearance of new cysteine and glutamate signals was observed at pD 2.7 or 7.4 after 0.25 h (Figure 6.6(i) b and d; indicated by  $\bullet$ ). At pD 6 after 2 h and 24 h the relative intensities of the new cysteine and glutamate signals increased (Figure 6.6(ii) c and d; indicated by  $\bullet$ ). These changes are consistent with interaction of  $\text{Cp}_2\text{NbCl}_2$  **3** with glutathione **72** via binding to the sulfur donor group.

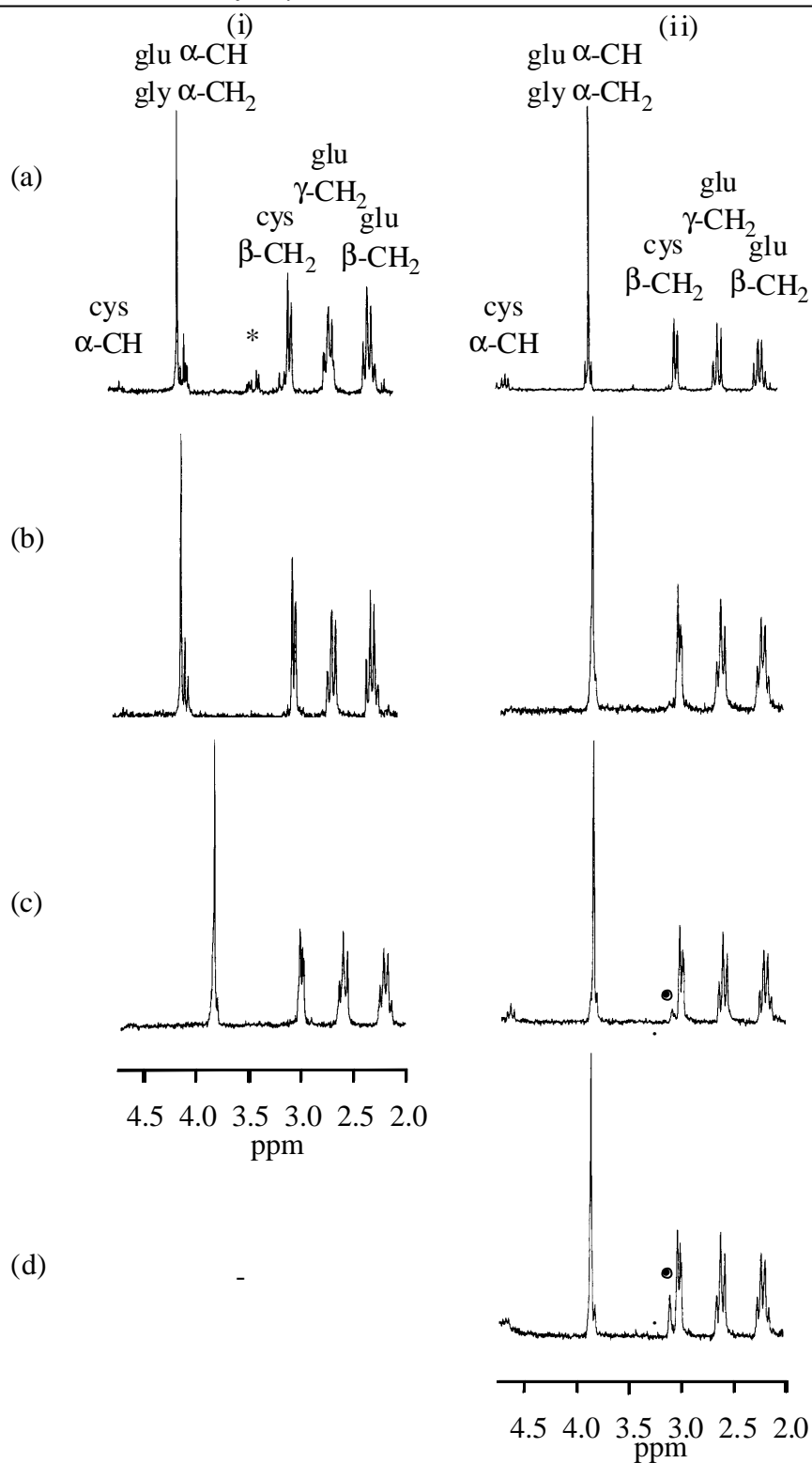


**Figure 6.5:** Aliphatic region of  $^1\text{H}$ -NMR spectra (200 MHz,  $\text{D}_2\text{O}$ ,  $25^\circ\text{C}$ ) of (i) glutathione **72** with (a) 0 equiv.  $\text{Cp}_2\text{TiCl}_2$  **1** at pD 2.7; (b) 1 equiv.  $\text{Cp}_2\text{TiCl}_2$  **1** at pD 2.4 after 0.25 h; (c) 1 equiv.  $\text{Cp}_2\text{TiCl}_2$  **1** at pD 7.1 after 0.25 h and (ii) glutathione **72** with (a) 0 equiv.  $\text{Cp}_2\text{TiCl}_2$  **1** at pD 6.0; (b) 1 equiv.  $\text{Cp}_2\text{TiCl}_2$  **1** at pD 6.1 after 0.25 h; (c) 1 equiv.  $\text{Cp}_2\text{TiCl}_2$  **1** at pD 6.1 after 2 h; (d) 1 equiv.  $\text{Cp}_2\text{TiCl}_2$  **1** at pD 5.7 after 24 h. \* oxidised glutathione.

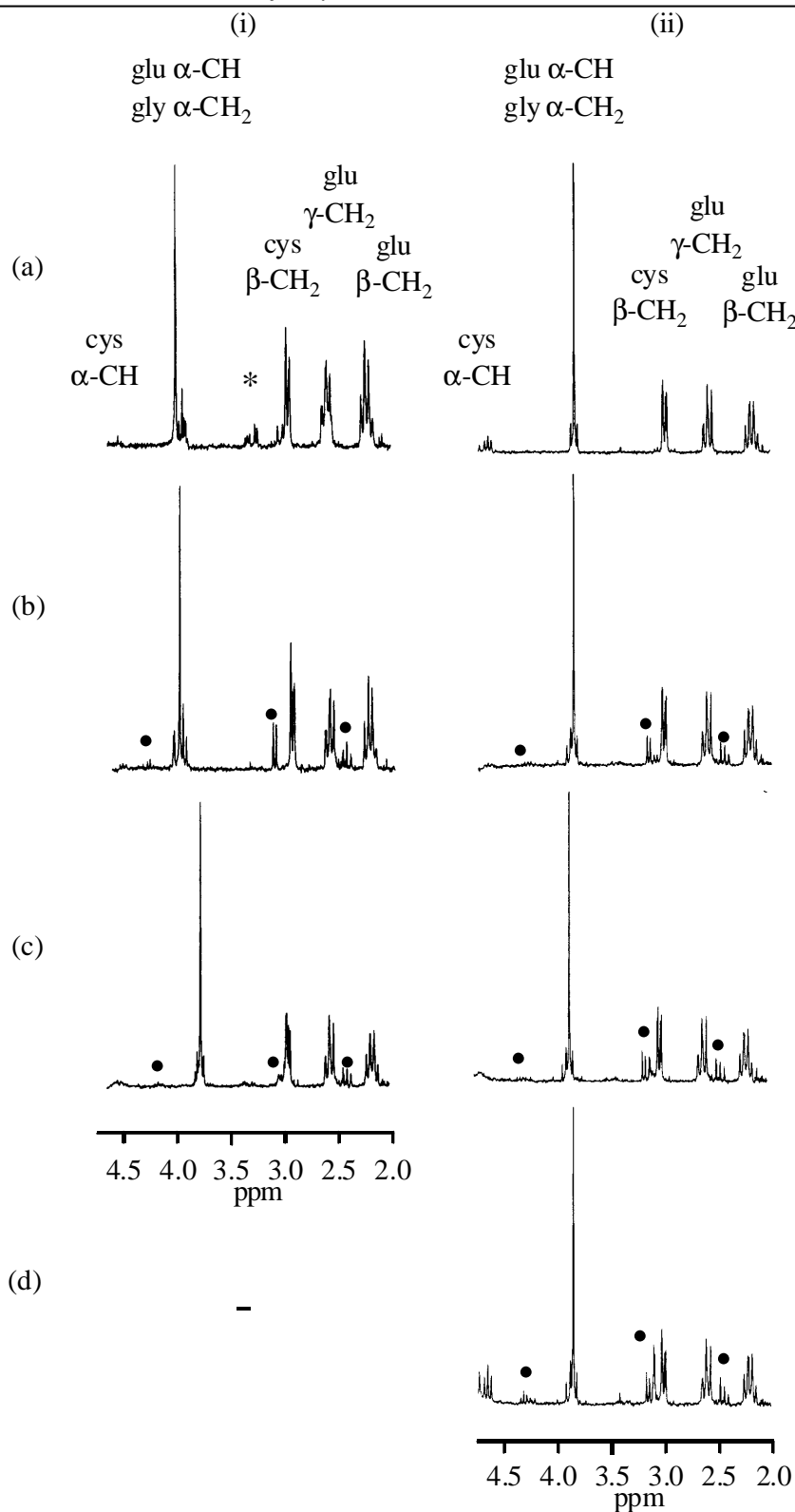


**Figure 6.6:** Aliphatic region of  $^1\text{H-NMR}$  spectra (200 MHz,  $\text{D}_2\text{O}$ , 25  $^\circ\text{C}$ ) of (i) glutathione **72** with (a) 0 equiv.  $\text{Cp}_2\text{NbCl}_2$  **3** at pD 2.7; (b) 1 equiv.  $\text{Cp}_2\text{NbCl}_2$  **3** at pD 2.7 after 0.25 h; (c) 1 equiv.  $\text{Cp}_2\text{NbCl}_2$  **3** at pD 7.4 after 0.25 h and (ii) glutathione **72** with (a) 0 equiv.  $\text{Cp}_2\text{NbCl}_2$  **3** at pD 6.0; (b) 1 equiv.  $\text{Cp}_2\text{NbCl}_2$  **3** at pD 5.8 after 0.25 h; (c) 1 equiv.

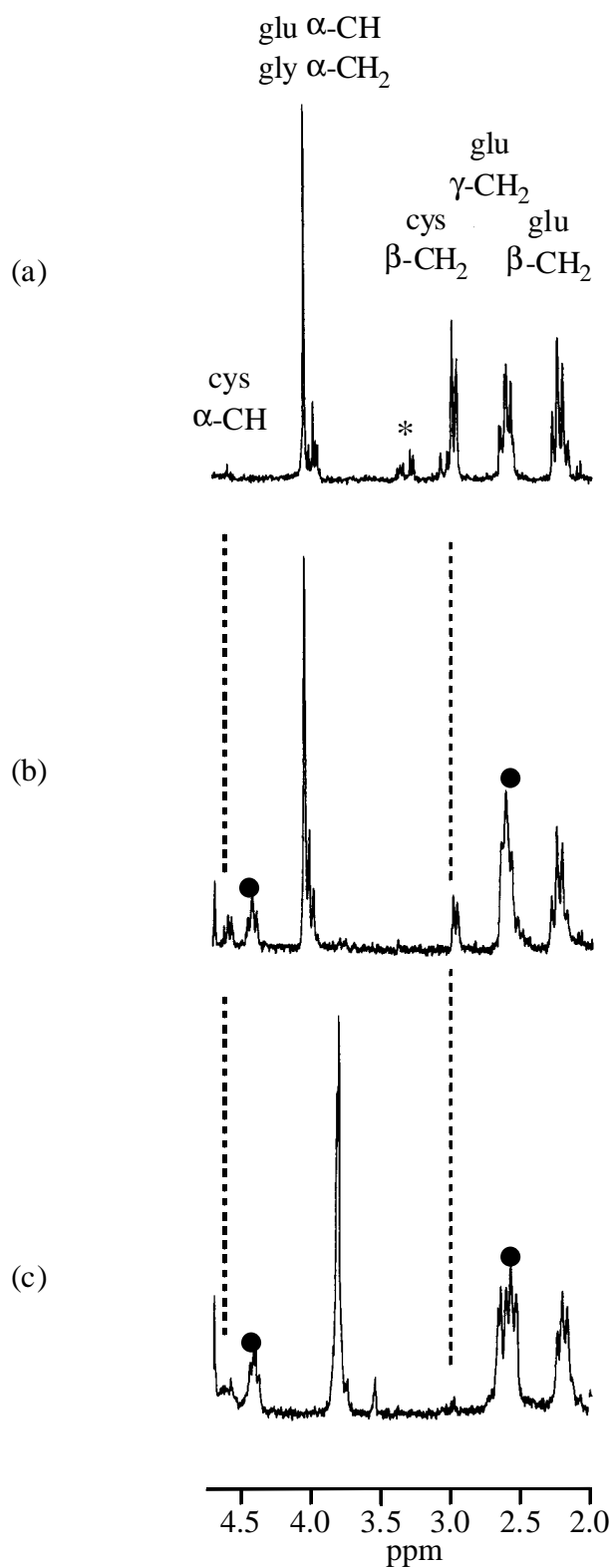
Cp<sub>2</sub>NbCl<sub>2</sub> **3** at pD 5.8 after 2 h; (c) 1 equiv. Cp<sub>2</sub>NbCl<sub>2</sub> (**3**) at pD 5.9 after 24 h. \* oxidised glutathione

Figure 6.7 and Figure 6.8 shows the aliphatic region of the <sup>1</sup>H NMR of glutathione **72** upon titration of 1 equiv. Cp<sub>2</sub>MoCl<sub>2</sub> **4** with time at pD 2.7-7.3. New resonances assignable to the α-CH and β-CH<sub>2</sub> protons of the cysteine residue were observed upfield of the corresponding unbound glutathione **72** resonances upon titration of 1 equiv. Cp<sub>2</sub>MoCl<sub>2</sub> **4** at pD 2.7 after 0.25 h and 24 h (Figure 6.7i b and c; indicated by • where the new cys β-CH<sub>2</sub> signal coincides with the glu γ-CH<sub>2</sub> signal as determined by integration). These signals were also shifted upfield upon titration of 1 equiv. Cp<sub>2</sub>MoCl<sub>2</sub> **4** at pD 6 or 7 over 24 h (Figure 6.8; indicated by •). These changes are consistent with interaction of Cp<sub>2</sub>MoCl<sub>2</sub> **4** to glutathione via binding to the sulfur donor group. Sulfur coordinating is supported by the shifting of cysteine signals (α and β- CH<sub>2</sub>) closest to the sulfur donor where binding to the Mo center occurs.

These results show that, under the conditions studied, glutathione-metalocene adducts are formed between metallocenes Cp<sub>2</sub>MCl<sub>2</sub> (M = Ti **1**, Nb **3**, Mo **4**) and glutathione **72**. However, the relative stabilities and amounts of complexes formed varied with the central metal ion. The greatest complexation was observed with Cp<sub>2</sub>MoCl<sub>2</sub> **4** and was estimated to be > 95% at pD~6, by integration. The relative amount of complexation with Cp<sub>2</sub>TiCl<sub>2</sub> **1** or Cp<sub>2</sub>NbCl<sub>2</sub> **3** was not able to be measured by integration due to signal overlap and incomplete assignment of signals. However, qualitatively Cp<sub>2</sub>TiCl<sub>2</sub> **1** showed the least complexation at pD 6, while complexation with Cp<sub>2</sub>NbCl<sub>2</sub> **3** was moderate in comparison, judging by the intensity of the new glutathione **72** signals. This trend of binding affinity to the sulfur group parallels the Lewis character of the metal center. Titanium(IV) is the hardest metal while molybdenum(IV)

is a softer metal and so would have the strongest affinity for the sulfur donor group of glutathione.

While extrapolation of the results obtained *in vitro* to *in vivo* conditions must be



**Figure 6.7:** Aliphatic region of  $^1\text{H-NMR}$  spectra (200 MHz,  $\text{D}_2\text{O}$ , 25  $^\circ\text{C}$ ) of glutathione **72** with (a) 0 equiv.  $\text{Cp}_2\text{MoCl}_2$  **4** at pD 2.7; (b) 1 equiv.  $\text{Cp}_2\text{MoCl}_2$  **4** at pD 2.7 after 0.25 h; (c) 1 equiv.  $\text{Cp}_2\text{MoCl}_2$  **4** at pD 7.3 after 0.25 h. \* oxidised glutathione

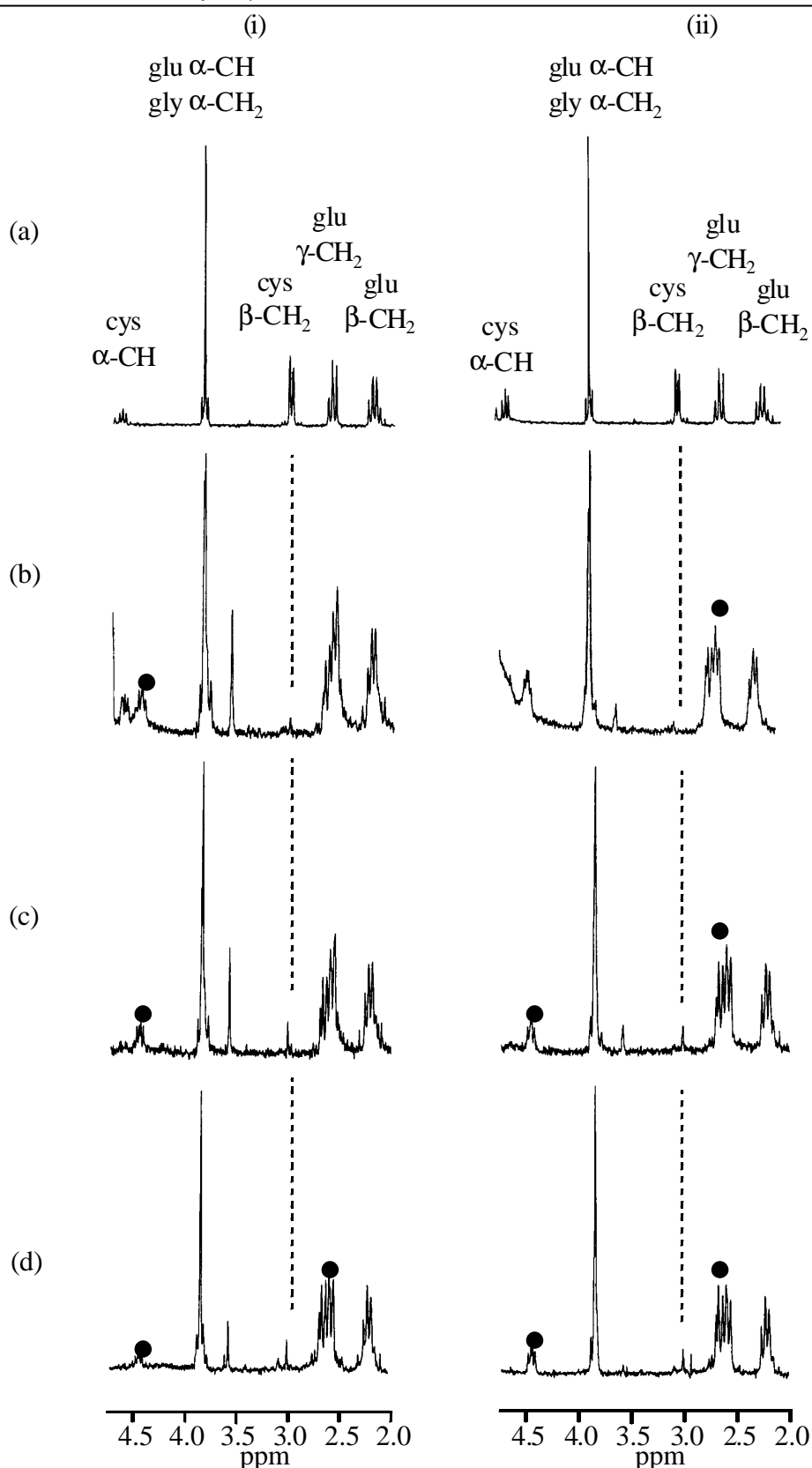


**Figure 6.8:** Aliphatic region of  $^1\text{H-NMR}$  spectra (200 MHz,  $\text{D}_2\text{O}$ , 25  $^\circ\text{C}$ ) of glutathione **72** at (i) pD 6.3-5.9 and (ii) pD 7.3-6.1 with (a) 0 equiv.  $\text{Cp}_2\text{MoCl}_2$  **4**; (b) 1 equiv.  $\text{Cp}_2\text{MoCl}_2$  **4** after 0.25 h; (c) 1 equiv.  $\text{Cp}_2\text{MoCl}_2$  **4** after 3 h; (d) 1 equiv.  $\text{Cp}_2\text{MoCl}_2$  **4** after 24 h

approached with caution, these results have implications for the mechanism of antitumour activity of the metallocenes. The results suggest that  $\text{Cp}_2\text{TiCl}_2$  **1** is not likely to be deactivated by glutathione **72** in tumour cells that have developed resistance to antitumour drugs by increasing the concentration of glutathione **72**. It would be of interest to study whether the lack of cross-resistance of  $\text{Cp}_2\text{TiCl}_2$  **1** with cisplatin, reported previously,<sup>12,33-35</sup> is related to the binding affinity of each drug with glutathione **72**. The cross-resistance of  $\text{Cp}_2\text{NbCl}_2$  **3** and  $\text{Cp}_2\text{MoCl}_2$  **4** with cisplatin has not been investigated but would also be of interest in view of the relative affinities of these metallocenes with glutathione **72**.

The role of glutathione as a carrier for  $\text{Cp}_2\text{MoCl}_2$  **4** inside cells was also investigated in this work, by carrying out a number of model competition experiments with 5'-dAMP. A solution of  $\text{Cp}_2\text{MoCl}_2$  **4** (1 equiv.) was titrated into a solution of 5'-dAMP (1 equiv.) with glutathione **72** (1 equiv.) in  $\text{D}_2\text{O}$ , 4 mM NaCl at pD 5.3-5.8. Independent titration experiments where 5'-dAMP (1 equiv.) was titrated into solutions of  $\text{Cp}_2\text{MoCl}_2$  **4** (1 equiv.) and glutathione **72** (1 equiv.) were also carried out. These experiments were designed to determine whether  $\text{Cp}_2\text{MoCl}_2$  **4** preferably bound 5'-dAMP or glutathione and whether  $\text{Cp}_2\text{MoCl}_2$  **4** would be displaced by 5'-dAMP if it was initially complexed to glutathione **72**.

Figure 6.9 shows the aromatic and aliphatic region of the  $^1\text{H}$  NMR spectra of a mixture of glutathione and 5'-dAMP upon titration of 0 and 1 equiv. of  $\text{Cp}_2\text{MoCl}_2$  **4** with time at pD 5.3-5.4. The addition of 1 equiv. of  $\text{Cp}_2\text{MoCl}_2$  **4** to a mixture of 5'-dAMP and glutathione **72** resulted in the appearance of new H8 and H2 signals of 5'-dAMP (indicated by ●) and shifting of the  $\beta\text{-CH}_2$  of cysteine after 0.25 and 2 h (Figure 6.9b and

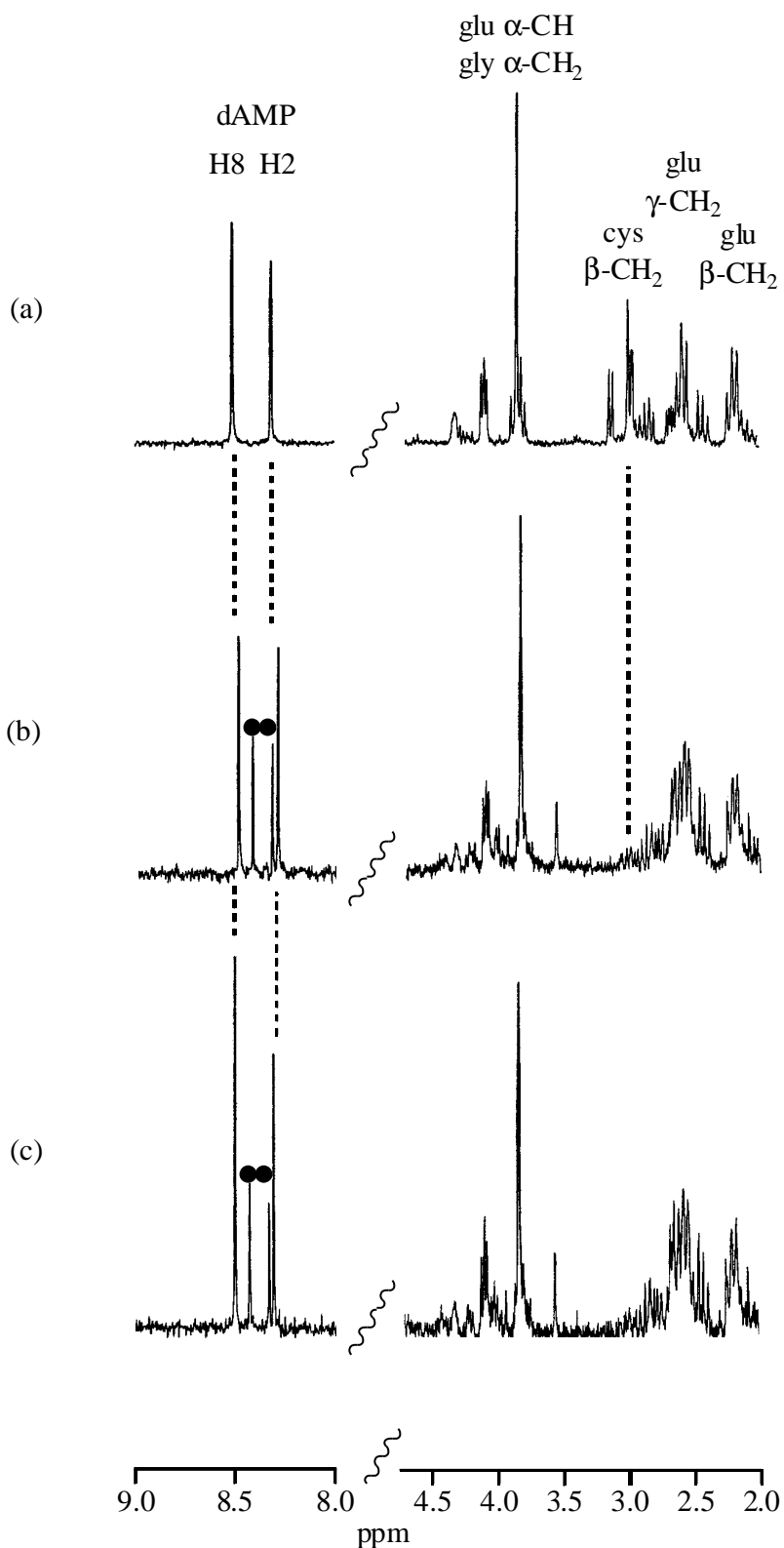


**Figure 6.9:** Aromatic and aliphatic regions of  $^1\text{H-NMR}$  spectra (200 MHz,  $\text{D}_2\text{O}$ , 25  $^\circ\text{C}$ ) of glutathione **72** + 5'-dAMP with (a) 0 equiv.  $\text{Cp}_2\text{MoCl}_2$  **4** at pH 5.4; (b) 1 equiv.  $\text{Cp}_2\text{MoCl}_2$  **4** at pH 5.4 after 0.25 h; (c) 1 equiv.  $\text{Cp}_2\text{MoCl}_2$  **4** at pH 5.4 after 2 h

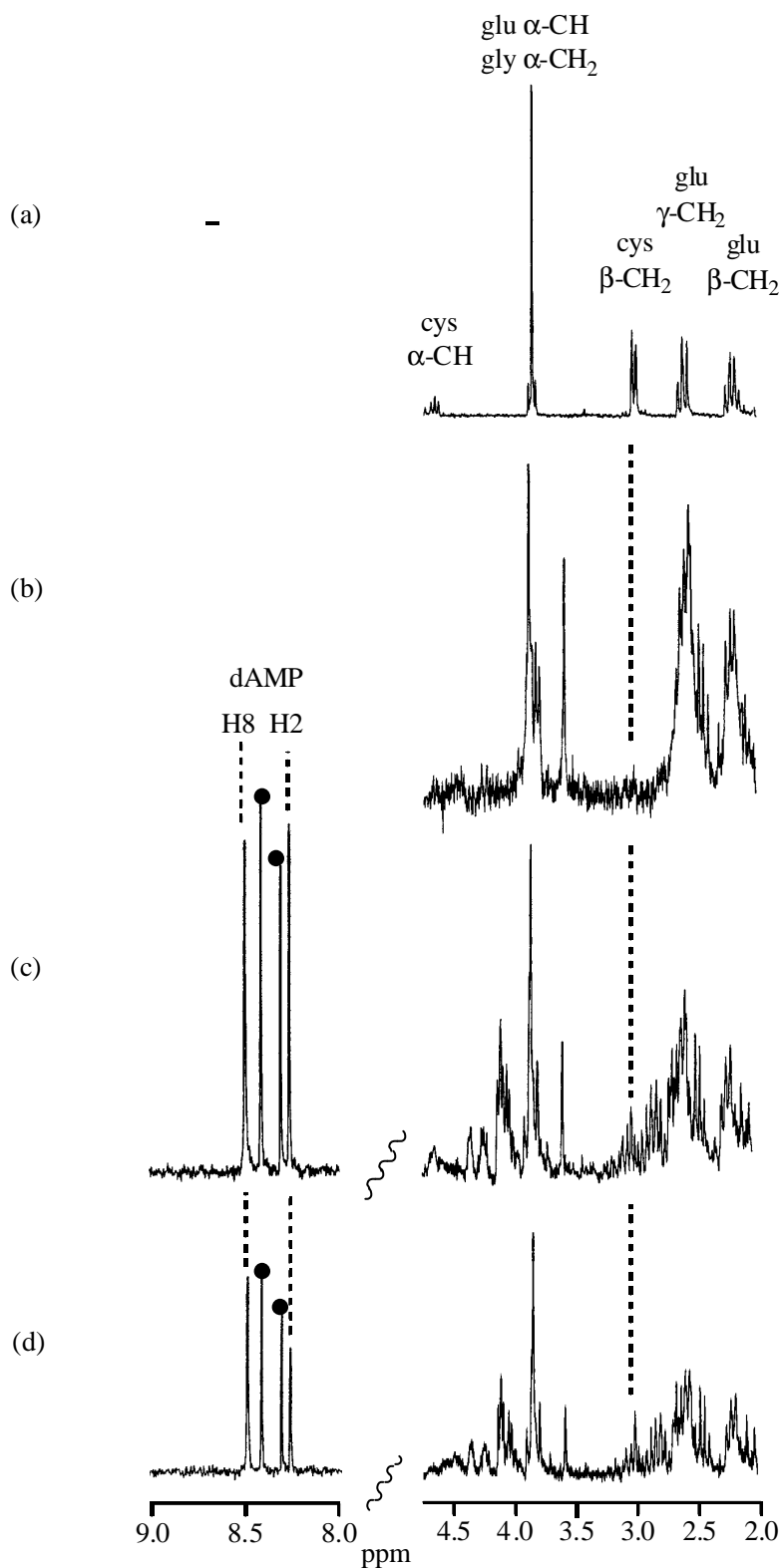
c). These changes are consistent with adduct formation between  $\text{Cp}_2\text{MoCl}_2$  **4** and both 5'-dAMP and glutathione **72**.

Figure 6.10 shows the aromatic and aliphatic region of the  $^1\text{H}$  NMR spectra upon titration 1 equiv. of 5'-dAMP into a solution of  $\text{Cp}_2\text{MoCl}_2$  **4** with glutathione at pD 5.4-5.7. The addition of 1 equiv. of  $\text{Cp}_2\text{MoCl}_2$  **4** to a solution of glutathione gave the expected molybdocene-glutathione adduct as evident by the shift in the  $\alpha$ -CH and  $\beta$ -CH<sub>2</sub> signals of cysteine (Figure 6.10b). The addition of 1 equiv. 5'-dAMP to this solution resulted in the appearance of new H8 and H2 signals consistent with the formation of a molybdocene-dAMP adduct (Figure 6.10c; indicated by •). The reappearance of unbound  $\beta$ -CH<sub>2</sub> cysteine signals is consistent with dissociation of the molybdocene-glutathione adducts to give back free glutathione (Figure 6.10c and d). This suggests that the complexed glutathione **72** can be displaced by 5'-dAMP to give molybdocene-dAMP adducts. Thus, this process may be possible inside a cell allowing molybdocene to be released from glutathione **72** to bind nucleic acid sites (Scheme 6.1).

## 6.5. Conclusions

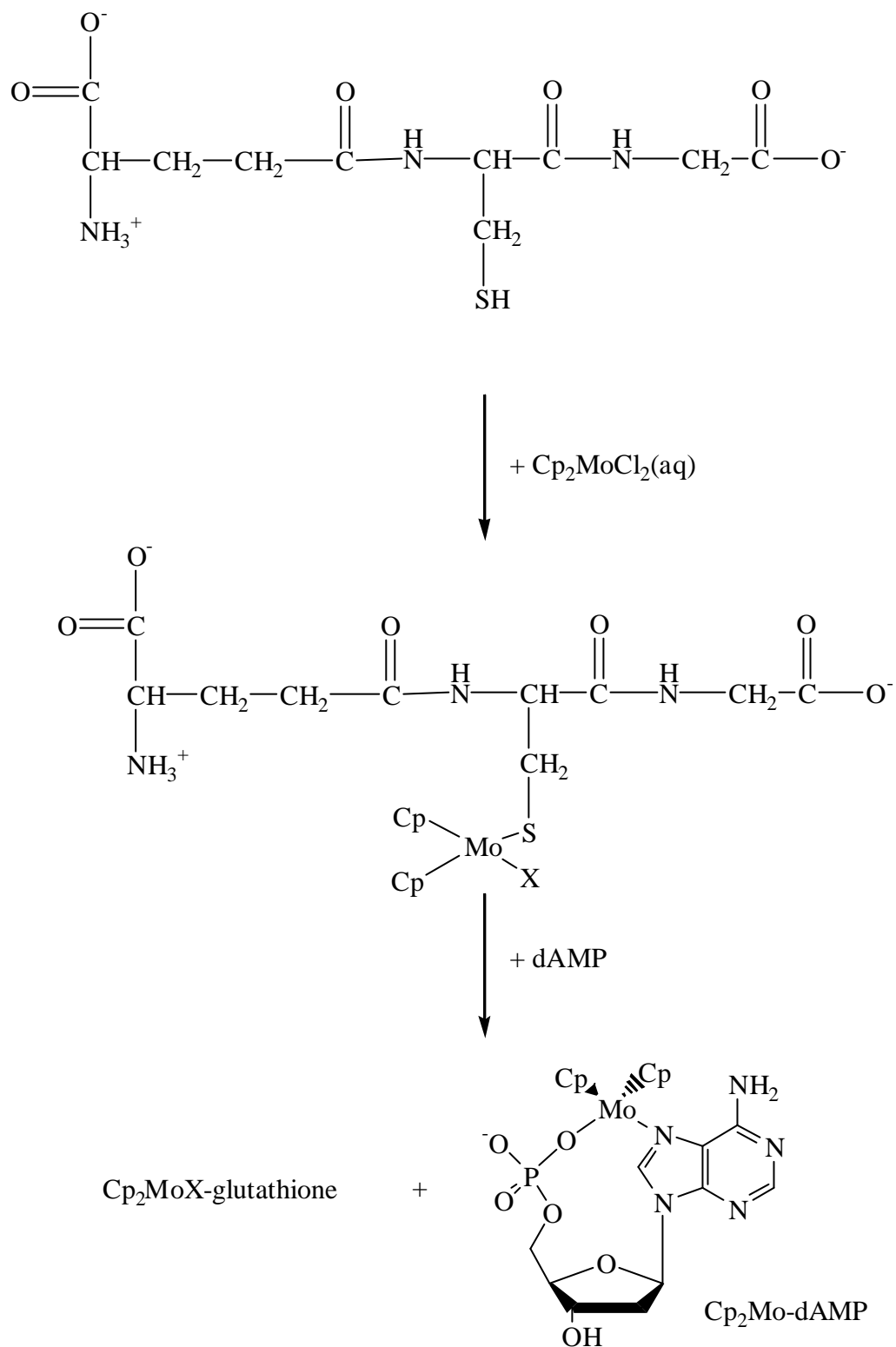
The UV binding studies with calf thymus DNA indicated that an interaction or association occurs with  $\text{Cp}_2\text{TiCl}_2$  **1** and  $\text{Cp}_2\text{MoCl}_2$  **4** at pH 7. In contrast, there was no evidence for stabilisation of the complexes by HSA, a major metal transport protein (52% of the total weight of human plasma proteins). HSA is known to bind and transport metals such as copper(II), nickel(II), calcium(II) and zinc(II) in the blood.<sup>75</sup> HSA has also been implicated in the transport of gold(I) derived from anti-arthritis drugs based on this metal. In

general HSA preferentially binds soft metals through soft nitrogen donors in a square-planar geometry.<sup>75</sup> Therefore, the results in this chapter



**Figure 6.10:** Aromatic and aliphatic regions of  $^1\text{H-NMR}$  spectra (200 MHz,  $\text{D}_2\text{O}$ , 25  $^\circ\text{C}$ ) of glutathione **72** with (a) 0 equiv.  $\text{Cp}_2\text{MoCl}_2$  **4** at pD 6.0; (b) 1 equiv.  $\text{Cp}_2\text{MoCl}_2$  **4** at pD 5.7 after 0.25 h; (c) 1 equiv.  $\text{Cp}_2\text{MoCl}_2$  **4** + 1 equiv. 5'-dAMP at pD 5.7 after 0.25 h; (d) 1 equiv.  $\text{Cp}_2\text{MoCl}_2$  **4** + 1 equiv. 5'-dAMP at pD 5.7 after 2 h

## Glutathione 72

 $\gamma$ -L-glutamyl-L-cysteinylglycine

Scheme 6.1

gave expected results, as titanium(IV) and molybdenum(IV) do not prefer a square-planar geometry.

The use of ICP-AES/dialysis as a technique to monitor the interactions of the metallocene dihalides with biomolecules was largely unsuccessful. While qualitatively, adducts containing titanium, niobium or molybdenum with calf thymus DNA were detected, significant errors in the total metal concentration indicate that detailed studies on the digestion of samples are required to obtain meaningful results. Titanium NMR, while potentially a very powerful technique for monitoring the interaction of titanocene species with biomolecules, is not feasible due to the low sensitivity of the nucleus and the poor aqueous solubility of  $\text{Cp}_2\text{TiCl}_2$  **1**.

The formation of complexes with glutathione **72** suggests that glutathione **72** may play an important role in the activity of the antitumour metallocenes. In particular, the binding of glutathione **72** to molydocene species inside tumour cells could effectively detoxify the active species and therefore contribute to the tumour cell's resistance to  $\text{Cp}_2\text{MoCl}_2$  **4**. The co-administration of glutathione **72** with  $\text{Cp}_2\text{MoCl}_2$  **4** could also reduce the toxicity of the drug in normal cells, such as in renal cells, as occurs with cisplatin.<sup>133</sup> The glutathione **72** binding studies also suggest that any biomolecule containing a sulfur donor group could be targeted by the antitumour metallocenes. In particular, the strong complex formation with  $\text{Cp}_2\text{MoCl}_2$  **4** suggest that any protein or enzyme with an exposed sulfur coordination site is a potential target for  $\text{Cp}_2\text{MoCl}_2$  **4**. This implies that targeting of proteins or enzymes involved in cell proliferation could play a significant role in the antitumour activity of  $\text{Cp}_2\text{MoCl}_2$  **4** and is supported by recent reports that  $\text{Cp}_2\text{MoCl}_2$  **4** and  $\text{Cp}_2\text{VCl}_2$  **2** inhibit the enzymes PKC and bacterial topoisomerase II, which was also confirmed in the topoisomerase II inhibition studies reported in Chapter 5.

## 7.1. General Procedures

Metallocene dihalides were purchased from the Aldrich Chemical Company and used without further purification. The UV measurements were carried out on a Hewlett Packard Diode Array UV-Vis spectrophotometer 8452A. pD values were measured using a Beckman  $\Phi$ 11 meter and a Mettler NMR tube pH probe and are related to the pH meter reading by the formula  $pD = pH(\text{meter reading}) + 0.4$ .<sup>150</sup> The pD values were adjusted with DCl and NaOD as required. Measured pD values are  $\pm 0.3$ , due to fluctuations in sample pD which occurred over time. Sonication of samples was carried out using an Elma Transsonic Digital Ultrasound water bath. Melting points were determined on a Gallenkamp heating stage and are uncorrected. Electron Ionisation Mass Spectra (EI MS) were recorded on an A.E.I. MS-920 spectrophotometer at 70 eV (positive ion). Electrospray (ES) mass spectra were recorded at the Australian Government Analytical Laboratories (AGAL) on a Fisons/VG Quatra mass spectrometer. IR spectra were recorded on a Perkin Elmer- 1600 FT-IR spectrophotometer and peaks labelled with the abbreviations: s, strong signal; m, medium signal; w, weak signal.  $^1\text{H}$  NMR spectra were recorded using a Bruker AC 200 spectrometer at 200 MHz and at 300 K or where otherwise stated. Spectra were recorded using the indicated deuterated solvent with the signal locked on solvent deuterium. Chemical shifts are reported as parts per million (ppm) relative to residual solvent protons or tetramethylsilane (TMS, 0.00 ppm) unless the solvent used was  $\text{D}_2\text{O}$ . Samples in  $\text{D}_2\text{O}$  were referenced to 1,4-dioxane (3.73 ppm) or 3-(trimethylsilyl)- $\text{D}_4$ -propionate (TSP, 0.00 ppm). Abbreviations used for multiplicity labeling are: s, singlet; d, doublet; t, triplet; q, quartet; m, multiplet; b, broad.

Solvents were distilled and dried prior to use as required by the experimental conditions. Analytical grade chloroform was used without distillation. THF was dried and stored over sodium wire and benzophenone, distilled under nitrogen and used immediately. Acetonitrile and benzene were distilled and dried over Linde type 4 Å. Ethanol, methanol, ether and carbon tetrachloride were distilled prior to use. Toluene and xylene were dried over sodium wire. Water was deionised by an Alpha Q filter and purifying system, manufactured by Millipore. Chromatography was carried out on Merck silica gel (type 9385, 230-400 mesh).

## **7.2. NMR Studies of Molybdocene Dichloride-Oligonucleotide Interactions**

Nucleotides, nucleosides and the dinucleotides dApT and dCpG were purchased from Sigma Aldrich Chemical Company. Oligonucleotides d(ATGGTA) and d(CGCATATGCG)<sub>2</sub> were supplied as the triethylammonium salts by AUSPEP Pty Ltd, Melbourne, Australia. Samples were purified by ethanol precipitation to remove triethylammonium acetate using the following procedure. The oligonucleotide was dissolved in NaCl solution (300 µL, 1.0 M) then absolute ethanol (1 mL) was added to precipitate the oligonucleotide. The mixture was chilled on ice for 5 min, centrifuged (5 min, 14 000 rpm) and the supernatant removed. This procedure was repeated with NaCl (450 µL, 1.0 M) and ethanol (1.5 mL). The resulting pellet was dissolved in H<sub>2</sub>O (1000 µL) and split into 4 aliquots. Each sample was evaporated to dryness. The concentration of the samples was determined by UV absorbance at 260 nm (1 absorbance unit corresponds to 33 µg of oligonucleotide in a 1.0 mL solution at 20 °C in a 1 cm path-length cuvette).<sup>151</sup> The <sup>1</sup>H and <sup>31</sup>P NMR spectra were recorded on a Bruker AMX600 NMR spectrometer by Dr Joel

Mackay at the Department of Biochemistry, University of Sydney. All 600 MHz  $^1\text{H}$  and  $^{31}\text{P}$  NMR spectroscopy data processing was carried out using Bruker UxNMR software on a Silicon Graphics workstation.

Binding and hydrolysis studies were carried out in  $\text{D}_2\text{O}$  with TSP (0.00 ppm) or dioxane (3.73 ppm) used as a chemical shift reference. NMR spectroscopy experiments with oligonucleotides  $\text{d(ATGGTA)}$  and  $\text{d(CGCATATGCG)}_2$  were carried out on a Bruker AMX600 NMR spectrometer while those with nucleotides, nucleosides and dinucleotides were carried out on a Bruker AC200 NMR spectrometer.

### **7.2.1. Hydrolysis Experiments**

The general procedure involved dissolving  $\text{Cp}_2\text{MoCl}_2$  **4** (0.01-0.02 mmol) in  $\text{D}_2\text{O}$  (500-600  $\mu\text{L}$ ) by sonication for 3h, with heat, to give a deep maroon coloured solution; complete dissolution was generally not achieved. The pD was adjusted to the required value with  $\text{DCl}$  (0.2 - 1.0 M) and  $\text{NaOD}$  (0.2 - 1.0 M), by addition of not more than 5  $\mu\text{L}$  aliquots of either base or acid solution. Addition of 5  $\mu\text{L}$   $\text{NaOD}$  (0.25 M) raised the pD by 3 units. For hydrolysis experiments carried out at pD 7.4, the pD dropped slowly with time, and was readjusted to maintain the pD as required; a solution with initial pD 7.4-7.8 was at pD 5.9-6.4 after 24 h. Measured hydrolysis times were estimated once the pD was adjusted. Measured pD values are  $\pm 0.3$  due to fluctuations in sample pD which occurred over 30 min.  $^1\text{H}$  NMR spectra were recorded at time intervals with any developing precipitate ignored. The rate of Cp hydrolysis was estimated by integration of one of the two multiplets arising from free cyclopentadiene  $\text{C}_5\text{H}_5\text{D}$  (6.5 and 6.6 ppm at pD = 6.2) versus the metal-bound  $\text{C}_5\text{H}_5$  signals.

### 7.2.2. Oligonucleotide Binding Studies.

NMR spectroscopy samples were prepared in deuterated 50 mM NaCl (pD 7.0-8.0).  $\text{Cp}_2\text{MoCl}_2$  **4** (6.0 mg) was suspended in 50 mM NaCl solution in  $\text{D}_2\text{O}$  (600  $\mu\text{L}$ ) and dissolved by vigorous sonication with heat for 3 h to give a saturated deep mauve coloured solution (pD 1.4-1.9). Any precipitate was ignored and hence equiv. added refer to the theoretical amount of  $\text{Cp}_2\text{MoCl}_2$  **4** assuming all the solid had dissolved. For double stranded oligonucleotide  $\text{d}(\text{CGCATATGCG})_2$ , aliquots of this solution were added to the oligonucleotide (pD 7-8) as required such that the pD remained above 5.9, in order to maintain the duplex structure. The pD of the resultant solution was monitored and adjusted to 6.9-7.8 (0.1 M NaOD) after each addition. Typically, for the single-stranded oligonucleotide  $\text{d}(\text{ATGGTA})$ , the dinucleotides, nucleotides and nucleosides the pD of the solution dropped to  $\sim 3.0$  upon addition of 1.0 equiv. of  $\text{Cp}_2\text{MoCl}_2$  **4**; the solution pD was then adjusted back to pD  $\sim 7.4$  using NaOD (0.25 M,  $\sim 40$   $\mu\text{L}$ ). Fluctuations in sample pD occurred with variations of  $\pm 0.3$  pD units occurred over 30 min, and decreased by 1-2 pD units over 24 h. Any precipitate that formed during the titration experiments was ignored.

## 7.3. Hydrolytically Stable Titanocene Derivatives

### 7.3.1. Methyl Substituted Titanocene Derivatives

#### 7.3.1.1. Synthesis of $(\text{MeCp})_2\text{TiCl}_2$ **34**

Methylcyclopentadiene dimer (200 mL) was cracked at  $> 200$   $^\circ\text{C}$  to give methylcyclopentadiene (b.p.  $72$   $^\circ\text{C}$ ) which was collected at  $-78$   $^\circ\text{C}$ . The collected monomer was re-cracked and redistilled several times. The initial low boiling fractions ( $< 70$   $^\circ\text{C}$ ) were

discarded. The methylcyclopentadiene monomer was stored at  $-78\text{ }^{\circ}\text{C}$  until used. Sodium sand was generated by refluxing sodium (4.7 g, 0.20 mol) in toluene (100 mL). The toluene was removed, and the sodium sand was washed with THF ( $3 \times 25\text{ mL}$ ) then THF (50 mL) was added. Methylcyclopentadiene (13 mL, 10.4 g, 0.13 mol) was added dropwise over 5 min to the suspension of sodium sand at  $-10$  to  $-15\text{ }^{\circ}\text{C}$ . The reaction mixture was stirred for 5 h at room temperature. The solution containing sodium methylcyclopentadienyl was filtered under nitrogen. A sample of the filtered reaction mixture containing sodium methylcyclopentadienyl (14 mL, 36 mmol, 2.6 M) was added dropwise to titanium(IV) tetrachloride (1 mL, 9 mmol) in THF (40 mL) at  $-20\text{ }^{\circ}\text{C}$ . The reaction mixture was allowed to stir overnight at room temperature, the solvents were removed under reduced pressure, and the resultant brown/red residue was dissolved in chloroform (70 mL). Flash silica was added to the reaction mixture which was stirred for 40 min, and filtered to remove silica and impurities. The residual flash silica was further extracted with chloroform ( $2 \times 100\text{ mL}$ ). The solvent was removed from the dark, blood-red filtrate to give the crude product as a brown/red precipitate which was dried under vacuum. Recrystallisation from chloroform afforded bis(methylcyclopentadiene) titanocene dichloride **34** (0.35 g, 14%) as a red diamond shaped crystalline solid, m.p. dec.  $> 200\text{ }^{\circ}\text{C}$  (lit.<sup>90</sup> dec.  $217\text{-}218\text{ }^{\circ}\text{C}$ ). Anal. Calcd for  $(\text{MeCp})_2\text{TiCl}_2$  **34**: C, 52.0; H, 5.1; Cl, 25.6. Found: C, 52.3; H, 5.0; Cl, 25.5.  $^1\text{H}$  NMR 200 MHz ( $\text{D}_2\text{O}$ )  $\delta$  6.3-6.4 (m, 8H, Cp), 2.3 (s, 6H,  $2\text{CH}_3$ ). EI MS  $m/z$  276  $(\text{MeCp})_2\text{TiCl}_2^+$ , 29%); 241  $(\text{MeCp})_2\text{TiCl}^+$ , 31%); 204  $(\text{MeCp})_2\text{Ti}^+$ , 69%); 197  $(\text{MeCp})\text{TiCl}_2^+$ , 97%); 161  $(\text{MeCp})\text{TiCl}^+$ , 100%); 126  $(\text{MeCp})\text{Ti}^+$ , 37%).

### 7.3.1.2. Synthesis of (MeCp)<sub>2</sub>Ti(gly)<sub>2</sub> **41**

Bis(methylcyclopentadiene) titanocene dichloride **34** (0.28 g, 1.0 mmol) and glycine (0.15 g, 2.0 mmol) were stirred in methanol (20 mL) at room temperature under a nitrogen atmosphere for 4 h. The reaction mixture was filtered, and the filtrate evaporated to dryness. The semicrystalline product solidified after 1 day at -17 °C. The solid was washed with chloroform and dried under vacuum to give bis(methylcyclopentadiene) titanocene bis(glycine) **41** (0.34 g, 75%) as an orange crystalline solid, m.p. dec. > 200 °C. Anal. Calcd for (MeCp)<sub>2</sub>Ti(OOCCH<sub>2</sub>NH<sub>3</sub>Cl)<sub>2</sub>·1.5H<sub>2</sub>O **41**: C, 42.1; H, 5.8; N, 6.2. Found: C, 42.1; H, 5.8; N, 6.4. <sup>1</sup>H NMR 200 MHz (D<sub>2</sub>O) δ 6.4 (m, 8H, 2MeCp), 3.68 (s, 4H, 2CH<sub>2</sub>), 2.01 (s, 6H, 2Me).

### 7.3.1.3. Hydrolysis Experiments

The general procedure involved dissolving the complex (5-15 μmol) in D<sub>2</sub>O (500 μL) with TSP added for reference. Dissolution of Cp<sub>2</sub>TiCl<sub>2</sub> **1** and (MeCp)<sub>2</sub>TiCl<sub>2</sub> **34** required sonication for 10 min and 200 min respectively to give a clear yellow solution. Complexes Cp<sub>2</sub>Ti(OOCCH<sub>2</sub>NH<sub>3</sub>Cl)<sub>2</sub> **27** and (MeCp)<sub>2</sub>Ti(OOCCH<sub>2</sub>NH<sub>3</sub>Cl)<sub>2</sub> **41** were dissolved by shaking for 2 min. Hydrolysis time was taken after the pD was adjusted. <sup>1</sup>H NMR spectra were recorded at time intervals with any developing precipitate ignored. The rate of Cp hydrolysis was estimated by integration of one of the two multiplets arising from free cyclopentadiene C<sub>5</sub>H<sub>5</sub>D (6.5 and 6.6 ppm at pD = 6.2) versus the metal-bound C<sub>5</sub>H<sub>5</sub> signals.

#### 7.3.1.4. Nucleotide Binding Studies

Binding studies were carried out in D<sub>2</sub>O with TSP added for reference. Sonication was used where necessary to dissolve the complexes. A typical titration experiment involved dissolving the metallocene in D<sub>2</sub>O (0.002- 0.01 mmol, 0.5 mL) by sonication where necessary. The solution was titrated into a solution of the nucleotide (0.01 mmol, 0.6 mL). The pD, <sup>1</sup>H and <sup>31</sup>P NMR spectra were recorded after the addition of 0.5, 1.0, 2.0 equiv. of the metallocene. The pD was adjusted with DCl and NaOD as required. Any precipitate formation was ignored.

#### 7.3.1.5. Biological Properties of Methyl Substituted Titanocene Derivatives

The antitumour activity of the methyl substituted derivatives **34** and **41** was tested in CF1 mice bearing EAT by Professor P. Köpf-Maier at the Frei Universität Berlin. The experimental conditions employed were similar to those reported previously.<sup>17,46</sup> The methyl substituted derivatives **34** and **41** were administered under the usual conditions in 10%DMSO/90%saline at low pH as reported previously.<sup>17,46</sup>

The methyl substituted derivatives **34** and **41** were also administered in water at pH 6.2-6.4. The methyl substituted chloride derivative **34** was dissolved in water at the required concentration by sonication for 3-4 h as described in Section 7.3.2.1. and the pH adjusted to 6.2-6.4 with NaOH solution (1% or 5% w/v). Typically the compound **34** (11 μmol) in water (500 μL) has an initial pH of 1.5. Addition of NaOH (5% w/v, 5 μL) raises the pH 1-3 units. The pH was carefully adjusted to pH 6.2-6.4 with NaOH (1% w/v) without raising the pH above 7.

The methyl substituted glycine derivative **41** was dissolved in water by shaking for ~2 min. Typically the compound **41** (6  $\mu\text{mol}$ ) in water (500  $\mu\text{L}$ ) has an initial pH of 2. Addition of 5  $\mu\text{L}$  of NaOH (5% w/v) raises the pH by about 1 unit. Careful addition of a 1% solution of NaOH was used to give the required pH of 6.2-6.4 without raising the pH above 7.

### 7.3.2. Synthesis of Titanocene Derivatives with Cp-CH<sub>2</sub>Y Ligands

#### (a) Preparation of NaC<sub>5</sub>H<sub>4</sub>-CH<sub>2</sub>CH(OMe)<sub>2</sub> **51**

Bromoacetaldehyde dimethyl acetal **49** (1.4 g, 8.5 mmol) in THF (5 mL) was added to sodium cyclopentadienyl in THF (2 M, 4.2 mL, 8.5 mmol) at room temperature under a nitrogen atmosphere. The reaction mixture was refluxed for 2 h, allowed to stand at room temperature for 12 h, filtered and the solvent removed under reduced pressure to give the crude product as a brown oil. An aliquot of the reaction mixture was purified by distillation under reduced pressure (40 °C) to give a mixture of the isomers of C<sub>5</sub>H<sub>5</sub>-CH<sub>2</sub>CH(OMe)<sub>2</sub> **50** as a pale yellow oil, which was used directly in the next step. <sup>1</sup>H NMR 200 MHz (CDCl<sub>3</sub>)  $\delta$  6.0-6.5 (m, 3H, vinylic C<sub>5</sub>H<sub>5</sub>), 4.5 (m, 1H, CH), 3.45 (s, 3H, OMe), 3.35 (s, 3H, OMe), 3.4 (d, 2H, CH<sub>2</sub>), 2.95 (m, 2H, aliphatic C<sub>5</sub>H<sub>5</sub>).

The mixture of isomers of C<sub>5</sub>H<sub>5</sub>-CH<sub>2</sub>CH(OMe)<sub>2</sub> **50** (8.5 mmol) in THF (9 mL) was added to a suspension of sodium sand (0.6 g, 26 mmol) in THF (10 mL) at -15 to -20 °C under a nitrogen atmosphere. The reaction mixture was stirred for 1 h then allowed to warm to room temperature to give a blood red solution. An aliquot of the reaction mixture was removed for analysis. The solvent was removed under reduced pressure to give NaCp-CH<sub>2</sub>CH(OMe)<sub>2</sub> **51** as a dark red solid. <sup>1</sup>H NMR 200 MHz (d<sub>8</sub>-THF)  $\delta$  6.15 and 6.25 (2

× d, 4H, aromatic C<sub>5</sub>H<sub>4</sub>), 4.7 (m, 1H, CH), 3.45 (s, 3H, OCH<sub>3</sub>), 3.35 (s, 3H, OCH<sub>3</sub>), 3.4 (d, 2H, CH<sub>2</sub>).

### (b) Attempted Synthesis of (CpCH<sub>2</sub>CH(OMe)<sub>2</sub>)<sub>2</sub>TiCl<sub>2</sub> **52**

Titanium tetrachloride (0.4 mL, 0.6 g, 3.3 mmol) was added to a solution of the anion **51** (~ 8 mmol) in THF at -15 to -20 °C under a nitrogen atmosphere. The reaction mixture was stirred for 4 h then allowed to warm to room temperature to give a dark orange/red solution. The solvent was removed under reduced pressure to give a yellow/orange solid, which was dissolved in chloroform and filtered to give a blood red filtrate. The solvent was removed to give a red oil which degraded rapidly to a black amorphous solid which is not soluble in chloroform. Analysis of the chloroform soluble crude product by <sup>1</sup>H NMR spectroscopy initially showed a sharp signal at around 6.5 ppm, which broadened and decreased in intensity with time.

### (c) Attempted Synthesis of C<sub>5</sub>H<sub>5</sub>-CH<sub>2</sub>CON(CH<sub>3</sub>)<sub>2</sub>

Distilled thionyl chloride (3 mL, 4.9 g, 0.04 mol) was added to bromoacetic acid (2.4 g, 0.017 mol) at room temperature under a nitrogen atmosphere. The reaction mixture was refluxed for 1 h. The excess thionyl chloride was evaporated to give the 1-chloro-2-bromo-acetate (2.7 g, 100%) as a clear oil. <sup>1</sup>H NMR 200 MHz (CDCl<sub>3</sub>) δ 4.35 (s, 2H, CH<sub>2</sub>). Anhydrous dimethylamine (5 mL, 3.4 g, 0.075 mol) was added slowly to the acid chloride (2.7 g, 0.017 mol) at -60 °C under a nitrogen atmosphere. The reaction was stirred for 2 h then allowed to warm to room temperature to give a yellow solid. The product was dissolved in dichloromethane (30 mL) and washed with 3M HCl (20 mL). The organic phase was dried over sodium sulfate and the solvent removed to give

*N,N*-dimethylbromoacetamide (2.2 g, 78%) as a yellow semi-crystalline solid.  $^1\text{H}$  NMR 200 MHz ( $\text{CDCl}_3$ )  $\delta$  4.1 (s, 2H,  $\text{CH}_2$ ), 3.1 (s, 3H,  $\text{NCH}_3$ ), 3.0 (s, 3H,  $\text{NCH}_3$ ). Sodium cyclopentadienyl in THF (2 M, 0.1 mL, 0.2 mmol) was added to *N,N*-dimethylbromoacetamide (7 mg, 0.04 mmol) in  $d_8$ -THF at room temperature. A brown precipitate resulted immediately. The  $^1\text{H}$  NMR spectrum ( $d_8$ -THF) of the filtrate after 15 min showed peaks consistent with the formation of cyclopentadiene as well as the starting materials, cyclopentadienyl anion and *N,N*-dimethylbromoacetamide.

### 7.3.3. Synthesis of R-Cp Derivatives with Electron-Withdrawing Groups

#### (a) Synthesis of NaCp-COMe 53

Sodium cyclopentadienyl in THF (2 M, 6 mL, 12 mmol) was added to methyl acetate (0.8 mL, 8 mmol), which had been distilled from  $\text{P}_2\text{O}_5$ , at room temperature under a nitrogen atmosphere. The reaction mixture was refluxed for 2 h, cooled and the solvent removed under reduced pressure to give a brown solid. The crude product was washed with ether and dried under vacuum (50 °C,  $\text{P}_2\text{O}_5$ ) to give acetylcyclopentadienylsodium **53** (0.3 g, 35%) as a brown solid, which gave NMR spectroscopy data consistent with that reported in the literature.<sup>99</sup>  $^1\text{H}$  NMR 200 MHz ( $\text{D}_2\text{O}$ )  $\delta$  6.65 and 6.20 (m, 4H, aromatic  $\text{C}_5\text{H}_4$ ), 2.30 (s, 3H, Me).

#### (b) Attempted Synthesis of $(\text{Cp-COMe})_2\text{TiCl}_2$ 46

Acetylcyclopentadienylsodium **53** (0.3 g, 2.3 mmol) in THF (20 mL) was added dropwise over 5 min to titanium tetrachloride (0.1 mL, 0.84 mmol) in THF (2 mL) at -10 to -15 °C with rapid stirring. The reaction mixture was allowed to warm to room temperature

and was stirred for a further 24 h. The solvent was removed from the resulting brown solution to give a brown solid, which was dissolved in chloroform and stirred with flash silica for 1 h. The reaction mixture was filtered and the filtrate evaporated to give a brown solid. Analysis of the product by  $^1\text{H}$  NMR spectroscopy ( $\text{CDCl}_3$ ,  $\text{D}_2\text{O}$ ,  $\text{d}_6$ -DMSO,  $\text{d}_4$ -MeOD) did not show any peaks consistent with formation of the desired product.

### (c) Attempted Synthesis of $(\text{Cp-COMe})\text{TiCl}_3$ **54**

Cyclopentadienetitanium trichloride (0.5 g, 2.3 mmol) in THF (10 mL) was added to acetylcyclopentadienylsodium **53** (20 mmol) in THF (10 mL) at room temperature under a nitrogen atmosphere. The reaction mixture was refluxed for 1.5 h, cooled and the solvent was removed to give a brown solid. The residue was dissolved in chloroform then filtered. The solvent was removed from the filtrate to give a brown solid. Analysis of the product by  $^1\text{H}$  NMR spectroscopy ( $\text{CDCl}_3$ ,  $\text{d}_4$ -MeOD) did not show any signals consistent with formation of the desired product and no Cp signals were detected.

## 7.3.4. Synthesis of Derivatives of Thiele's acid **55**

### (a) Preparation of

#### **Endo-tricyclo[5,2,1,0<sup>2,6</sup>]-4,8-dichloroformyldeca-3,8-diene **56****

Thionyl chloride (10 mL, 16.4 g, 137 mmol) was added to Thiele's acid **55** (2 g, 9 mmol) at room temperature under a nitrogen atmosphere. The suspension was refluxed for 2 h to give a dark brown homogenous solution. The solvent was removed under vacuum to give a brown oily residue, which was taken up in light petroleum (20 mL) and filtered. The solvent was removed to give endo-tricyclo[5,2,1,0<sup>2,6</sup>]-4,8-dichloroformyldeca-3,8-

diene **56** (1.9 g, 80%) as a yellow semi-crystalline solid, which gave NMR spectroscopy and MS data consistent with formation of the required product previously reported by Peters.<sup>102</sup>  $^1\text{H}$  NMR 200 MHz ( $\text{CDCl}_3$ )  $\delta$  6.2 (m, 1H, H(9)), 6.3 (m, 1H, H(3)), 3.7 (m, 1H, H(1)), 3.5 (m, 1H, H(7)), 3.1 (m, 1H, H(6)), 2.6 (m, 1H, H(2)), 2.1 (m, 2H, H(5) and H(5')), 1.8 (m, 1H, H(10')), 1.5 (d, 1H, H(10)). EI MS  $m/z$  252 ( $\text{C}_{10}\text{H}_6(\text{COCl})_2^+$ , 3%); 217 ( $\text{C}_{10}\text{H}_6(\text{COCl})\text{CO}^+$ , 8%); 189 ( $\text{C}_{10}\text{H}_6\text{COCl}^+$ , 15%); 157 ( $\text{C}_{10}\text{H}_9\text{CO}^+$ , 8%); 124 ( $\text{C}_{10}\text{H}_4^+$ , 97%); 65 ( $\text{C}_5\text{H}_5^+$ , 100%).

### (b) Preparation of

#### **Endo-tricyclo[5,2,1,0<sup>2,6</sup>]-4,8-dimethylformyldeca-3,8-diene **57****

Methanol (5 mL) was added to the acid chloride **56** (0.8 g, 3.1 mmol) in light petroleum (10 mL) at room temperature under a nitrogen atmosphere, and the reaction mixture was stirred for 10 min. The solvent was evaporated to give endo-tricyclo[5,2,1,0<sup>2,6</sup>]-4,8-dimethylformyldeca-3,8-diene **57** (0.5 g, 65%) as a white/yellow solid, which gave NMR spectroscopy and MS data consistent with formation of the required product previously reported by Peters.<sup>102</sup>  $^1\text{H}$  NMR 200 MHz ( $\text{CDCl}_3$ )  $\delta$  6.8 (m, 1H, H(9)), 6.5 (m, 1H, H(3)), 3.8 (d, 3H,  $\text{CH}_3$ (8)), 3.7 (d, 3H,  $\text{CH}_3$ (4)), 3.5 (m, 1H, H(1)), 3.4 (m, 1H, H(7)), 3.2 (m, 1H, H(6)), 3.0 (m, 1H, H(2)), 2.5 (m, 2H, H(5) and H(5')), 2.0 (m, 1H, H(10')), 1.4 (d, 1H, H(10)). EI MS  $m/z$  248 ( $\text{C}_{10}\text{H}_{10}(\text{COOMe})_2^+$ , 3%); 217 ( $\text{C}_{10}\text{H}_6(\text{COOMe})\text{CO}^+$ , 8%); 189 ( $\text{C}_{10}\text{H}_6\text{COOMe}^+$ , 13%); 157 ( $\text{C}_{10}\text{H}_9\text{CO}^+$ , 5%); 124 ( $\text{C}_5\text{H}_5\text{COOMe}^+$ , 100%); 93 ( $\text{C}_5\text{H}_5\text{CO}^+$ , 85%); 65 ( $\text{C}_5\text{H}_5^+$ , 93%).

**(c) Preparation of****Endo-tricyclo[5,2,1,0<sup>2,6</sup>]-4,8-dimethylamidodeca-3,8-diene 58**

*Method 1:* Dimethylamine in THF (3 M, 5 mL, 15 mmol) was added to the acid chloride **56** (0.8 g, 3.1 mmol) in light petroleum (10 mL) at room temperature under a nitrogen atmosphere. The reaction mixture was stirred for 5 min and the solvent evaporated to give endo-tricyclo[5,2,1,0<sup>2,6</sup>]-4,8-dimethylamidodeca-3,8-diene **58** (0.4 g, 47%) as a cream/brown solid, which gave NMR spectroscopy and MS data consistent with that reported in the literature.<sup>152</sup> <sup>1</sup>H NMR 200 MHz (CDCl<sub>3</sub>) δ 6.1 (d, 1H, H(9)), 5.5 (m, 1H, H(3)), 3.4 (m, 1H, H(1)), 3.2 (d, 1H, H(7)), 3.1 (m, 1H, H(6)), 3.0 (d, 3H, CH<sub>3</sub>(4)), 2.9 (m, 1H, H(2)), 2.8 (d, 3H, CH<sub>3</sub>(8)), 2.5 (m, 2H, H(5) and H(5')), 1.7 (m, 1H, H(10')), 1.4 (d, 1H, H(10)). EI MS *m/z* 274 (C<sub>10</sub>H<sub>10</sub>(CONMe<sub>2</sub>)<sub>2</sub><sup>+</sup>, 3%); 230 (C<sub>10</sub>H<sub>10</sub>(CONMe<sub>2</sub>)CO<sup>+</sup>, 1%); 202 (C<sub>10</sub>H<sub>10</sub>CONMe<sub>2</sub><sup>+</sup>, 3%); 137 (C<sub>5</sub>H<sub>5</sub>CONMe<sub>2</sub><sup>+</sup>, 70%); 93 (C<sub>5</sub>H<sub>5</sub>CO<sup>+</sup>, 84%); 65 (C<sub>5</sub>H<sub>5</sub><sup>+</sup>, 100%).

*Method 2:* Dimethylamine in THF (2.5 M, 4 mL, 10 mmol) was added to a solution of Thiele's acid **55** (0.5 g, 2.3 mmol), 4-(dimethylamino)pyridine (1.1 g, 8.8 mmol) and 1-(3-dimethylaminopropyl)-3-ethylcarbodiimide hydrochloride (1.7 g, 8.8 mmol) in DCM (30 mL) at room temperature under a nitrogen atmosphere. The reaction mixture was stirred for 12 h, diluted with dichloromethane (50 mL) and washed with 2.5% sodium hydrogen carbonate (2 × 50 mL), 1 M HCl (2 × 50 mL) and water (100 mL). The organic phase was dried over anhydrous sodium sulfate and the solvent evaporated to give crude dimeric dimethyl amide (0.5 g, 80%) as a brown oil. Recrystallisation from light petroleum afforded the dimethyl amide **58** as a white solid as before, which gave NMR spectroscopy

and MS data identical to the product isolated in method 1 and consistent with that reported in the literature.<sup>152</sup>

#### (d) Attempted Synthesis of $(\text{CpCONMe}_2)_2\text{TiCl}_2$ **48**

The dimeric dimethyl amide **58** (0.5 g, 1.8 mmol) was cracked at 200 °C under reduced pressure (~20 mm) to give the monomeric dimethyl amide **60** (0.32 g, 66%) as a red/yellow glass, which was used immediately in the next step. <sup>1</sup>H NMR 200 MHz (*d*<sub>8</sub>-THF) δ 6.8-6.6 (m, 3H, vinylic C<sub>5</sub>H<sub>5</sub>), 3.0 (s, 2H, aliphatic C<sub>5</sub>H<sub>5</sub>), 2.7 (s, 3H, NMe), 2.6 (s, 3H, NMe). *n*Butyllithium (1 M, 3 mL, 3 mmol) was added to the monomeric dimethyl amide **60** (0.3 g, 2.2 mmol) in THF (10 mL) at -78 °C under a nitrogen atmosphere. The reaction mixture was stirred for 1 h at -78 °C and a further 12 h at room temperature. Formation of the anion was confirmed by removal of the solvent from an aliquot of the reaction mixture (~0.1 mL). <sup>1</sup>H NMR 200 MHz of residue (*d*<sub>8</sub>-THF) δ 6.2 and 5.7 (m, 4H, aromatic C<sub>5</sub>H<sub>4</sub>), 2.7 (m, 6H, NMe<sub>2</sub>). The anion (~ 2 mmol) in THF (13 mL) was added to a solution of titanium tetrachloride (0.3 mL, 2.7 mmol) in THF (15 mL) at -20 °C. The reaction mixture was stirred for 12 h at room temperature and the solvent was removed to give a brown/black solid. The <sup>1</sup>H NMR spectra (*d*<sub>8</sub>-THF or D<sub>2</sub>O) did not give any signals consistent with formation of the product.

### 7.3.5. Synthesis of Aminoalkyl Substituted Derivatives

#### (a) Synthesis of $(\text{CpNMe}_2)_2\text{TiCl}_2$ **62**

Methylsulfonyl chloride (0.4 mL, 0.59 g, 5 mmol) was added to a solution of *N,N*-dimethylhydroxylamine hydrochloride (0.5 g, 5 mmol) and 1,6-lutidine (1.25 mL, 1.15 g,

10.8 mmol) at -10 to -20 °C under a nitrogen atmosphere. The reaction mixture was stirred for 1 h at -10 to -20 °C and washed with ice-water (2 × 25 mL). The organic phase was dried over anhydrous sodium sulfate and the solvent was removed at -20 °C to give *N,N*-dimethyl-*O*-(methylsulfonyl)hydroxylamine **66** (0.58 g, 83%) as a clear oil, which has been previously reported.<sup>113</sup> <sup>1</sup>H NMR 200 MHz (CDCl<sub>3</sub>) δ 3.2 (s, 3H, SO<sub>2</sub>Me), 2.9 (s, 6H, NMe<sub>2</sub>). Sodium cyclopentadienyl in THF (2 M, 2 mL, 4 mmol) was added to a solution of *N,N*-dimethyl-*O*-(methylsulfonyl)hydroxylamine **66** (0.58 g, 4.2 mmol) in THF (10 mL) at -20 to -30 °C. The reaction mixture was stirred for 30 min at -20 to -30 °C, the solvent was evaporated under reduced pressure at -20 to -30 °C and the residue digested in cold pentane (20 mL). The solution was filtered at -35 °C under a nitrogen atmosphere and the solvent evaporated at -20 to -30 °C. The residual product *N,N*-dimethylaminecyclopentadiene **67** was kept at -30 °C and used immediately without complete characterisation. *n*Butyllithium in hexanes (2 M, 1 mL, 2 mmol) was added to *N,N*-dimethylaminecyclopentadiene **67** (~2 mmol) in THF (10 mL) at -30 °C. The reaction mixture was stirred at -30 °C for 1 h to give a brown solution. Titanium tetrachloride (0.4 mL, 3.6 mmol) was added immediately to the reaction mixture containing the anion at -20 to -30 °C. The reaction mixture was stirred at -20 to -30 °C for 1 h and allowed to warm to room temperature. The solvent was evaporated to give a brown/black residue. The residue was dissolved in chloroform (30 mL) and filtered. The solvent was evaporated to give a brown/black oil. The <sup>1</sup>H NMR spectrum (CDCl<sub>3</sub>) did not show any signals consistent with formation of the product. Broad signals at 6.5 and 4.5 ppm were consistent with formation of a polymeric species.

**(b) Synthesis of (Cp(CH<sub>2</sub>)<sub>2</sub>NMe<sub>2</sub>)<sub>2</sub>TiCl<sub>2</sub> 63**

Sodium cyclopentadienyl in THF (2 M, 60 mL, 120 mmol) was added to a stirred suspension of 2-dimethylaminoethylchloride hydrochloride **70** (6.9 g, 48 mmol) in THF (60 mL) and dimethylformamide (17 mL) at 0 °C over 10 min under a nitrogen atmosphere. The resulting brown/black solution was refluxed for 4 h, and the reaction mixture was concentrated. Water (200 mL) was added to the residue and the resulting solution was extracted with pentane (3 × 150 mL). The organic phase was washed with water (150 mL), dried over anhydrous sodium sulfate and filtered. The solvent was evaporated to give the crude product as a yellow/brown oil. The crude oily product was distilled (Kugelrohr) using a dry ice cooling device under reduced pressure (~20 mm) at 80-100 °C to give (dimethylaminoethyl)cyclopentadiene **69** (3.7 g, 56%) as a clear colourless oil, which gave NMR spectroscopy data consistent with that reported in the literature.<sup>108</sup> <sup>1</sup>H NMR 200 MHz (d<sub>8</sub>-THF) δ 6.0-6.5 (m, 3H, vinylic C<sub>5</sub>H<sub>5</sub>), 3.0 (s, 2H, aliphatic C<sub>5</sub>H<sub>5</sub>), 2.5 (m, 4H, CH<sub>2</sub>CH<sub>2</sub>), 2.2 (s, 6H, NMe<sub>2</sub>).

*n*Butyllithium in hexane (1 M, 50 mL, 50 mmol) was added to a stirred solution of (dimethylaminoethyl)cyclopentadiene **69** (3.7 g, 27 mmol) in THF (70 mL) at 0 °C over 5 min under a nitrogen atmosphere. The reaction mixture was stirred for 10 min at 0 °C and at room temperature for 2 h. The formation of the anion **71** was confirmed by taking an aliquot of the reaction mixture (~0.1 mL), removing the solvent and characterising the resulting residue. <sup>1</sup>H NMR 200 MHz (d<sub>8</sub>-THF) δ 5.5-5.7 (m, 4H, aromatic C<sub>5</sub>H<sub>4</sub>), 2.6 (t, 2H, CH<sub>2</sub>), 2.4 (t, 2H, CH<sub>2</sub>), 2.1 (s, 6H, NMe<sub>2</sub>).

A solution of the anion **71** in THF (60 mL, ~13.5 mmol) or toluene (60 mL, ~13.5 mmol) was added via a cannular to a solution of titanium tetrachloride (0.75 mL, 6.8 mmol)

in THF (40 mL) or toluene (40 mL) at -10 to 0 °. The brown/black reaction mixture was allowed to warm to room temperature. The reaction mixture was refluxed for 30 min and stirred at room temperature for 12 h. The reaction mixture was filtered through a plug of celite. The solvent was evaporated to give a cream/brown solid from the reaction in THF and a brown oil from the reaction in toluene. The solid obtained from the reaction in THF had poor solubility in  $\text{CDCl}_3$  and  $\text{C}_6\text{D}_6$  and the NMR spectra did not show any signals consistent with formation of the required product. The brown oil obtained from the reaction in toluene contained the impure disubstituted complex **63**, which gave NMR spectroscopy data consistent with that reported in the literature.<sup>104</sup>  $^1\text{H}$  NMR 200 MHz ( $\text{CDCl}_3$ )  $\delta$  6.3-6.4 (m, 4H, aromatic  $\text{C}_5\text{H}_4$ ), 3.0 (t, 2H,  $\text{CH}_2$ ), 2.7 (t, 2H,  $\text{CH}_2$ ), 2.4 (s, 6H,  $\text{NMe}_2$ ). The solid filtered out of the reaction mixture from the reaction in toluene was most likely a polymeric species, which was completely soluble in  $\text{D}_2\text{O}$  following addition of DCl. The  $^1\text{H}$  NMR spectra ( $\text{D}_2\text{O}$ ) showed broad signal at 5.0-6.5 and 4 ppm but could not be completely assigned. The excellent solubility in water or methanol suggests that the product is the ammonium salt of the disubstituted complex **65**. When the polymer was dissolved in  $\text{D}_2\text{O}$  with DCl the NMR spectrum showed signals characteristic of the impure ionic complex  $(\text{Cp}(\text{CH}_2)_2\text{NHMe}_2^+\text{Cl})_2\text{TiCl}_2$  **65**.

#### 7.4. Effect of DMSO on the Stability of Titanocene Derivatives

The general procedure involved dissolving the complex (5-15  $\mu\text{mol}$ ) in  $\text{D}_2\text{O}$  (500  $\mu\text{L}$ ) or  $d_6$ -DMSO (500  $\mu\text{L}$ ), or 10%DMSO/ $\text{D}_2\text{O}$  (500  $\mu\text{L}$ ). For samples in 10%DMSO, the solid was first dissolved in DMSO, and then diluted with  $\text{D}_2\text{O}$  to the required volume.

$^1\text{H}$  NMR spectra were recorded at time intervals with any developing precipitate ignored. The rate of Cp hydrolysis was estimated by integration of one of the two multiplets arising from free cyclopentadiene  $\text{C}_5\text{H}_5\text{D}$  (6.5 and 6.6 ppm at  $\text{pD} = 6.2$ ) versus the metal-bound  $\text{C}_5\text{H}_5$  signals. In the case of  $\text{Cp}_2\text{Ti}(\text{gly})_2$  **27** an estimate of the hydrolysis was also made from integration of the unbound glycine peak versus the metal bound-Cp signal.

## 7.5. Topoisomerase II Inhibition Studies

### 7.5.1. Materials

Topo II inhibition studies were carried out with the commercial drug screening kit supplied by TopoGen Inc. USA. The 10 $\times$  topo II relaxation buffer (500 mM Tris-HCl, pH 8, 1200 mM KCl, 100 mM  $\text{MgCl}_2$ , 5 mM ATP, 5 mM dithiothreitol), 10% SDS (2  $\mu\text{L}$ ), 10 $\times$  gel loading buffer (0.25% bromophenol blue and 50% glycerol) were used as supplied in the drug testing kit. Human topo II $\alpha$  (p170, 2 units activity  $\mu\text{L}^{-1}$ ) was purchased from Topogen Inc. USA. The enzyme was stored at  $-70\text{ }^\circ\text{C}$  and the number of freeze-thaw cycles minimized as this resulted in reduction of activity. Supercoiled pBR322, proteinase K, nuclease free agarose and 10 $\times$  or 40 $\times$  TAE buffer were purchased from Promega. mAMSA was purchased from the Sigma Chemical Company.

### 7.5.2. Stock Solutions

Metallocene stock solutions were prepared by dissolving the required metallocene (2-5 mg) in water (1 mL) by sonication with heating until no solid remained (typically 1-3 h). This gave solutions as follows :  $\text{Cp}_2\text{TiCl}_2$  **1**, 10 mM, pale yellow solution, pH 1.9;  $\text{Cp}_2\text{MoCl}_2$  **4**, 10 mM, mauve-brown solution, pH 1.8;  $\text{Cp}_2\text{NbCl}_2$  **3**, 5 mM, yellow solution,

pH 2.1;  $(\text{MeCp})_2\text{TiCl}_2$  **34**, 10 mM, yellow, pH 2.0.  $\text{Cp}_2\text{VCl}_2$  **2** (1 mg/ mL) exhibited very poor aqueous solubility after 3 h sonication and hence the concentration of dissolved solid in the yellow/brown supernatant (1.1 mM, pH 3.0) was estimated based on undissolved solid. The control sample containing no metallocene (pH 1.5-2) was prepared by addition of 0.3 M HCl. mAMSA was dissolved in water to give a yellow solution which was diluted to final concentration of 50  $\mu\text{M}$ .

### **7.5.3. Topoisomerase Inhibition Assays**

The reactions were assembled on ice in autoclaved eppendorf tubes (1.5 mL) to give final reaction volumes of 20  $\mu\text{L}$ . The components of the assay were added in order as follows: (i) sterile water (ii) 10 $\times$  topo II relaxation buffer (2  $\mu\text{L}$ , giving 1 $\times$  topo II relaxation buffer) (iii) plasmid supercoiled pBR322 (2  $\mu\text{L}$ , 0.1  $\mu\text{g } \mu\text{L}^{-1}$ ) (iv) the drug stock solution was added to give the required final concentration (v) topo II (1  $\mu\text{L}$ , 2 units). The reaction mixture was incubated at 37  $^\circ\text{C}$  for 30 min, 10% SDS (2  $\mu\text{L}$ ) was added to stop the reaction, and the mixture was digested with proteinase K (2  $\mu\text{L}$ , 500  $\mu\text{g mL}^{-1}$ ) by incubation at 37  $^\circ\text{C}$  for 15 min. 10 $\times$  Gel loading buffer (2  $\mu\text{L}$ ) was added and the reaction mixture was extracted with chloroform:isoamyl alcohol (24:1, 20  $\mu\text{L}$ ) and centrifuged at 14 000 rpm for 5 s. The blue coloured phase (15  $\mu\text{L}$ ) was loaded onto a 1% agarose gel (0.5 g agarose in 50 mL TAE buffer). The gels were subjected to electrophoresis at 100 V (70 mA) for 5 min then 14-16 V (8-12 mA) for 15- 19 h in TAE buffer (200 mL). The gels were stained with ethidium bromide (15  $\mu\text{L}$  of a 10 mg  $\text{mL}^{-1}$  stock solution) in 200 mL TAE buffer for 1 h, then destained for 10 - 15 min in millipore water and photographed by computer video capture when transilluminated with UV light.

## 7.6. UV Binding Studies

Calf Thymus DNA was purchased from Sigma and used without further purification. A stock solution was prepared by dissolving DNA (~ 1.8 mg) in water (100 mL) by stirring at room temperature for 24 h. The purity of the DNA solution was verified from the ratio  $A_{260\text{nm}}/A_{280\text{nm}}$  which was close to 1.85. The nucleotide concentration (0.05 mM) was determined by UV absorbance ( $A_{260\text{nm}}$ ,  $\epsilon = 6600 \text{ M}^{-1}\text{cm}^{-1}$ ).<sup>151</sup> HSA was purchased from Sigma and used without further purification. A stock solution was prepared by dissolving HSA (MW 68 500, 0.9 mg, 0.013  $\mu\text{mol}$ ) in water (2 mL) by stirring for 1 day. Stock solutions of  $\text{Cp}_2\text{TiCl}_2$  **1** (0.7 mg, 2.8  $\mu\text{mol}$ ) were prepared by sonication for 5-15 min with warming in water (2 mL). Stock solutions of  $\text{Cp}_2\text{MoCl}_2$  **4** (0.9 mg, 3.0  $\mu\text{mol}$ ) were prepared by sonication for 0.5-1 h with warming in water (2 mL). The pH of solutions was adjusted with sodium hydroxide (1% w/v) as required.

The UV spectra of  $\text{Cp}_2\text{TiCl}_2$  **1** (0.07 mM) and  $\text{Cp}_2\text{MoCl}_2$  **4** (0.3 mM) in water at pH 7.0-7.4 was recorded at 0.25, 3 and 24 h at 25 °C. The UV spectra of HSA (0.16  $\mu\text{M}$ ) and calf thymus DNA (0.05 mM) in water were recorded at 0.25, 3 and 24 h at 25 °C so as to provide blank experiments. The UV binding experiment with HSA involved recording the UV spectra over 24 h of solutions HSA (0.16  $\mu\text{M}$ ) with  $\text{Cp}_2\text{TiCl}_2$  **1** (0.07 mM) at pH 7.0-7.5 or with  $\text{Cp}_2\text{MoCl}_2$  **4** (0.3 mM) at pH 7.0-7.1 at 25 °C. The UV absorbance of blank experiments with HSA under identical conditions was subtracted from the UV absorbance recorded in the presence of the metallocenes. The UV binding experiment with calf thymus DNA involved recording the UV spectra over 24 h of solutions of calf thymus DNA (0.05 mM) with  $\text{Cp}_2\text{TiCl}_2$  **1** (0.07 mM) at pH 6.9-7.6 or with

Cp<sub>2</sub>MoCl<sub>2</sub> **4** (0.3 mM) at pH 7.1-7.4 at 25 °C. The UV absorbance of blank experiments with calf thymus DNA under identical conditions was subtracted from the UV absorbance recorded in the presence of the metallocenes.

### **7.7. ICP/dialysis Binding Studies**

A stock solution of calf thymus DNA was prepared by dissolving DNA (~43 mg) in saline (10 mL, 40 mM) by stirring at room temperature for 2 days. The nucleotide the purity of the DNA was verified as outlined in Section 7.6. Stock solutions of Cp<sub>2</sub>TiCl<sub>2</sub> **1** (5.9 mg, 0.024 mmol) were prepared by sonication for 5-15 min with warming in saline (2 mL, 40 mM). Stock solutions of Cp<sub>2</sub>NbCl<sub>2</sub> **3** (2.3 mg, 0.0078 mmol) were prepared by sonication for 1 h with warming in saline (2 mL, 40 mM). Stock solutions of Cp<sub>2</sub>MoCl<sub>2</sub> **4** (2.4 mg, 0.0081 mmol) were prepared by sonication for 1.5 h with warming in saline (2 mL, 40 mM). Dialysis of solutions (1 mL) was carried out with cellulose ester DispoDialysers (MWCO 25 000) supplied by Spectrum. ICP measurements were performed by first digesting the sample by heating and stirring in nitric acid (1 mL) with sonication for up to 1 h and then making up the volume in water (10 mL).

Dialysis experiments were performed with mixtures of DNA and Cp<sub>2</sub>TiCl<sub>2</sub> **1**, or Cp<sub>2</sub>NbCl<sub>2</sub> **3** or Cp<sub>2</sub>MoCl<sub>2</sub> **4**. A solution of Cp<sub>2</sub>TiCl<sub>2</sub> **1** (0.4 mL, 4.7 μmol), Cp<sub>2</sub>NbCl<sub>2</sub> **3** (0.67 mL, 2.6 μmol) or Cp<sub>2</sub>MoCl<sub>2</sub> **4** (0.67 mL, 2.7 μmol) was added to a solution of calf thymus DNA (1.0 mL, 10 μmol nucleotide, 10 mM nucleotide, pH 7.5) and the final volume made up to 2 mL with saline (40 mM). The pH was not allowed to drop below 4 so as to avoid precipitation of the DNA. The final pH was adjusted to 5–6.5. Solutions were incubated for 72 h at 25 °C. The solutions were centrifuged at 12 000 rpm for 5 min after

which no significant precipitate was evident. The solutions (1 mL) were dialysed in a saline bath (20 mL, 40 mM) for 48 h at 25 °C. Samples of the dialysis tube solutions (0.8 mL) and bath solutions (2 mL) were dried under vacuum and analysed by ICP.

DNA precipitation experiments with ethanol were performed with mixtures of DNA and  $\text{Cp}_2\text{TiCl}_2$  **1**, or  $\text{Cp}_2\text{NbCl}_2$  **3** or  $\text{Cp}_2\text{MoCl}_2$  **4** as in the dialysis experiments. After incubation of the samples for 72 h at 25 °C the DNA was isolated by ethanol precipitation. The general procedure involved making up the volume to 1.2 mL in a saline solution with a final NaCl concentration of 0.2 M. The solution was divided into 3 lots of 400  $\mu\text{l}$ . To each aliquot, ethanol (800  $\mu\text{l}$ ) was added and the DNA allowed to precipitate at 0 °C for 15-30 min. The solution was centrifuged at 12 000 g for 10 min. The supernatant was discarded and 70% ethanol was added (1 mL). The solution was centrifuged at 12 000 g for 2 min and the supernatant was discarded. The procedure did not yield any DNA.

Control experiments without any DNA present involved incubation of solutions of  $\text{Cp}_2\text{MCl}_2$  (M = Ti **1**, Nb **3**, Mo **4** (2.5 mM) in 40 mM saline (2 mL) at pH 5-7 for 120 h at 25 °C. Control samples gave considerable amounts of precipitate when centrifuged at 12 000 g for 5 min. Control experiments were not routinely dialysed as dialysis of the supernatant gave no detectable levels of metal. Instead the metal content was analysed in the precipitate with 1 mL of supernatant as well as 1 mL samples of the supernatant which were dried under vacuum.

## **7.8. Titanium NMR**

The  $^{49}\text{Ti}$  and  $^{47}\text{Ti}$  NMR spectra were recorded on a Bruker DP×400 at 22.565 MHz. Spectra were recorded with 25 600 scans at 25 °C and were referenced to neat  $^{49}\text{TiCl}_4$  (at 0.00 ppm).

### **7.9. Glutathione Binding Studies**

Glutathione and 5'-dAMP were purchased from the Sigma Aldrich Chemical Company. Stock solutions of glutathione (0.043 g, 0.14 mmol) were prepared in  $\text{D}_2\text{O}$  (1 mL). Stock solutions of 5'-dAMP (3.3 mg, 0.010 mmol) were prepared in  $\text{D}_2\text{O}$  (0.2 mL). Stock solutions of  $\text{Cp}_2\text{TiCl}_2$  **1** (2.9 mg, 0.012 mmol) were prepared in  $\text{D}_2\text{O}$  (0.5 mL) by sonication for 1 h. Stock solutions of  $\text{Cp}_2\text{NbCl}_2$  **3** (2.9 mg, 0.099 mmol) were prepared in  $\text{D}_2\text{O}$  (0.5 mL) by sonication for 1 h. Stock solutions of  $\text{Cp}_2\text{MoCl}_2$  **4** (3.0 mg, 0.010 mmol) were prepared in  $\text{D}_2\text{O}$  (0.5 mL) by sonication for 2.5 h.

A typical titration experiment involved addition of each metallocene (4  $\mu\text{mol}$ , 1 equiv.) to glutathione (reduced) (4  $\mu\text{mol}$ ) in  $\text{D}_2\text{O}$  (0.5 mL) with 4 mM NaCl. Competition experiments with 5'-dAMP involved addition of 5'-dAMP (4  $\mu\text{mol}$ , 1 equiv.) to solutions containing glutathione (reduced) (1 equiv.) with  $\text{Cp}_2\text{MoCl}_2$  **4** (1 equiv.). Glutathione (reduced) (4  $\mu\text{mol}$ , 1 equiv.) was added to solutions containing 5'-dAMP (1 equiv.) with  $\text{Cp}_2\text{MoCl}_2$  **4** (1 equiv.). Any precipitate formation was ignored. The  $^1\text{H}$  NMR spectra (200 MHz) were recorded where applicable over a 24 h period.

## Conclusions

Titanocene dichloride **1** is the only metallocene currently in clinical trials and further results are required to establish whether this complex will become a clinically useful drug for cancer treatment. The poor solubility and stability of the drug at pH 6-7 are drawbacks in the development of a suitable formulation for administration and in the design of titanocene based drugs with improved and/or modified activity. While the exact mechanism of action is still unknown, the results of Chapters 3-6 support formation of a Ti(IV) species *in vivo* that is stabilised and/or transported into cells under physiological conditions. Interactions with blood plasma proteins have been demonstrated and are important in the mechanism.<sup>14,16,67,76,77</sup> The lability of the Cp-Ti bond (Chapter 3) is also important and interaction with DNA may be due to a simple non-specific electrostatic interaction once a Ti(IV) species is released in the cell.

The very recent reports of formation of Ti-transferrin complexes between titanocene dichloride **1** and human serum transferrin (hTF) is an important breakthrough<sup>76,78,81,114,115</sup> and opens up the possibility of using Ti<sub>2</sub>-hTF complexes as anticancer drugs, in a similar manner to Ru-hTF complexes.<sup>153,154</sup> Furthermore, this suggests that other titanium complexes that release a Ti(IV) species that interacts with transferrin in the same way as aqueous titanocene dichloride **1**, may lead to the same effects, and hence identification of new titanium based antitumour drugs.

In this context, budotitane (Figure 1.3, Section 1.2), a related titanium complex that contains diacido ligands instead of Cp rings, shows antitumour activity comparable to titanocene dichloride **1**.<sup>13,155-157</sup> The hydrolysis chemistry and structure activity studies

suggest that this complex may function in a similar way to titanocene dichloride **1** by releasing a Ti(IV) species *in vivo*. As with titanocene dichloride **1**, dissolution of budotitane in water is accompanied by rapid halide dissociation and hydrolytic ligand cleavage of the diaceto groups,<sup>155</sup> requiring administration in a special galenic formulation for clinical trials.<sup>155</sup> Structure activity studies with budotitane derivatives have shown variation of the leaving ethoxy group with halide ligands such as Cl has no significant affect on antitumour activity. However, in contrast to titanocene dichloride **1**, where Cp substitution results in loss of antitumour activity,<sup>17,54</sup> replacement of the acetylacetonato ligand for lipophilic, bulky alkyl or cycloalkyl substituted aceto ligands increases the antitumour activity of the complex.<sup>155</sup> Although a complete investigation to identify the key structural features required for antitumour activity has not been carried out, the initial results for budotitane suggest that substitution or replacement of the ligands is a viable method for modifying and improving the antitumour activity of titanium based complexes. The hydrolysis and structure activity studies of budotitane and its derivatives suggest that they may also have ligands with just the right hydrolytic stability to release the active species (eg., Ti(IV)) *in vivo* in a similar way to titanocene dichloride **1**.

Table 8.1 summarises the biological and chemical data previously reported (see introduction), as well as the results reported in this thesis, for each of the metallocene dihalides. While the extensive studies on titanocene dichloride **1** have provided some insight into the mechanism of antitumour action discussed above, at the present time, there is insufficient biological and structure-activity data on the other metallocene dihalides to propose mechanisms of action. The vastly different chemical stabilities at physiological pH and different coordination chemistries of each complex point to significantly different mechanisms of antitumour action for each drug. While there is evidence that metals derived from titanocene

*Conclusions*

dichloride **1** and vanadocene dichloride **2**, administered *in vivo*, accumulate in nucleic acid rich regions of EAT cells,<sup>23,24</sup> there is no comparable data for other metallocene complexes. Furthermore, there are limited studies on other metallocenes with potential cellular components that may be related to their antitumour activity (Table 8.1). Opportunities for further research include biological assays to clarify where the metals from each of the different antitumour active metallocenes shown in Table 8.1 accumulate in tumour cells as well as the effects of these complexes on nucleic acid synthesis. Structure activity studies will also be important in clarifying the mechanism of action of each drug and has the potential to identify new lead compounds.

**Table 8.1 :** Summary of coordination chemistry, biological activity and interaction of  $Cp_2MCl_2$  with nucleic acids and peptides.

	antitumour activity			DNA binding			enzyme inhibition		peptide binding	
	<i>in vitro</i> EAT	<i>in vivo</i> fluid EAT	<i>in vivo</i> human xenograft	DNA adducts ICP/UV pH > 5	Nucleo- tide binding pH < 4	oligo binding pH > 5	PKC topo II		hTF	gluta- thione pH > 5
M(IV)										
Ti 1	✓✓	✓✓ ✓	YES	YES	YES			YES	YES	NO
V 2	✓✓✓	✓✓	YES	NO	YES		YES	YES	NO	
Nb 3		✓✓ ✓		YES	NO			YES		NO
Mo 4	✓✓	✓✓		YES	YES	NO	YES	YES		YES
Ta 5		✓								
W 6		✓								
Zr 7	✓			YES	NO					
Hf 8	✓			YES	NO					

**Blue:** results reported in the literature and confirmed in this thesis under different conditions

**Red:** results reported in this thesis

**Black:** results reported in the literature (see introduction for references)

Ticks and crosses give a relative comparison of the concentration of each metallocene required for maximum activity; ✓✓✓ lowest concentration; ✓ highest concentration

**Reference**

- 1) Rang, H. P.; Dale, M. M. *Pharmacology*; 2nd ed.; Churchill Livingstone: Melbourne, 1991.
- 2) Guyton, A. C. *Textbook of Medical Physiology*; 8th ed.; W.B. Saunders Company: Sydney, 1991.
- 3) Hall, E. *Cancer Control in Australia*, Public Affairs and Behavioural Intervention Committee of the Australian Cancer Society, Australian Government Publishing Service, 1995.
- 4) Priestman, T. J. *Cancer Chemotherapy: An Introduction*; 3rd ed.; Springer-Verlag: London, 1989.
- 5) Bishop, J. M. *Cell* **1991**, *64*, 235-248.
- 6) Pratt, W. B.; Rudden, R. W.; Ensminger, W. D.; Maybaum, J. *The Anticancer Drugs*; 2nd Ed. ed.; Oxford University Press: New York, 1994.
- 7) Rosenberg, B.; Van Camp, L.; Grimley, E. B.; Thomson, A. J. *J. Biol. Chem.* **1967**, *242*, 1347-1352.
- 8) Fricker, S. P. Introduction, In *Metal Compounds in Cancer Therapy*; Fricker, S. P., Ed.; Chapman and Hall: London, 1994, pp 1-31.
- 9) Collery, P. Gallium Compounds in Cancer Therapy, In *Metal Compounds in Cancer Chemotherapy*; Fricker, S. P., Ed.; Chapman and Hall: London, 1994, pp 180-197.
- 10) Collery, P.; Morel, M.; Desoize, B.; Millart, H.; Perdu, D.; Prevost, A.; Vallerand, H.; Pechery, C.; Choisy, H.; Etienne, J. C.; Dubois De Montreynaud, J. M. *Anticancer Res.* **1991**, *11*, 1529-1532.
- 11) Collery, P.; Morel, M.; Millart, H. Oral Administration of Gallium in Conjunction with Platinum in Lung Cancer Treatment, In *Metal Ions and Biology and Medicine*; Collery, P., Poirier, L. A., Manfait, M. and Etienne, J. C., Ed.; John Libbey Eurotext: Paris, 1990; Vol. 1, pp 437-442.

- 12) Köpf-Maier, P.; Köpf, H. Organometallic Titanium, Vanadium, Niobium, Molybdenum and Rhenium Complexes- Early Transition Metal Antitumour Drugs, In *Metal Compounds in Cancer Therapy*; Fricker, S. P., Ed.; Chapman and Hall: London, 1994, pp 109-146.
- 13) Keppler, B. K. *New J. Chem.* **1990**, *14*, 389-403.
- 14) Korfel, A.; Scheulen, M. E.; Schmoll, H. J.; Gründel, O.; Harstrick, A.; Knoche, M.; Fels, L. M.; Skorzec, M.; Bach, F.; Baumgart, J.; Sab, G.; Seeber, S.; Thiel, E.; Berdel, W. E. *Clin. Cancer Res.* **1998**, *4*, 2701-2708.
- 15) Berdel, W. E.; Schmoll, H. J.; Scheulen, M. E.; Korfel, A.; Knoche, M. F.; Harstrick, A.; Bach, F.; Baumgart, J.; Sass, G. *J. Cancer Res. Clin. Oncol.* **1994**, *120*[Suppl], R172.
- 16) Christodoulou, C. V.; Ferry, D. R.; Fyfe, D. W.; Young, A.; Doran, J.; Sheehan, T. M. T.; Eliopoulos, A.; Hale, K.; Baumgart, J.; Sass, G.; Kerr, D. J. *J. Clin. Oncol.* **1998**, *16*, 2761-2769.
- 17) Köpf-Maier, P.; Köpf, H. *Struct. Bonding* **1988**, *70*, 103-185.
- 18) Köpf-Maier, P.; Köpf, H. *Drugs of the Future* **1986**, *11*, 297-320.
- 19) Köpf-Maier, P. Antitumour Bis(cyclopentadienyl)metal Complexes, In *Metal Complexes In Cancer Chemotherapy*; Keppler, B. K., Ed.; VCH Verlagsgesellschaft: Weinheim, 1993, pp 259-296.
- 20) Lümmen, G.; Sperling, H.; Luboldt, H.; Otto, T.; Rübber, H. *Cancer Chemother. Pharmacol.* **1998**, *42*, 415-417.
- 21) Köpf-Maier, P.; Köpf, H.; Wagner, W. *Naturwissenschaften* **1981**, *68*, 272-273.
- 22) Köpf-Maier, P.; Köpf, H. *Naturwissenschaften* **1980**, *67*, 415-416.
- 23) Köpf-Maier, P.; Krahl, D. *Chem. Biol. Interact.* **1983**, *44*, 317-328.
- 24) Köpf-Maier, P.; Krahl, D. *Naturwissenschaften* **1981**, *68*, 273-274.
- 25) Kelland, L. R. Platinum Anticancer Drugs, In *Metal Compounds in Cancer Therapy*; Fricker, S. P., Ed.; Chapman and Hall: London, 1994, pp 32-45.
- 26) Clearfield, A.; Warner, D. K.; Saldarriaga-Molina, C. H.; Ropal, R.; Bernal, I. *Can. J. Chem.* **1975**, *53*, 1622-1629.

- 
- 27) Bochmann, M. *Organometallics* 2. *Complexes with Transition Metal-Carbon p-Bonds*; Oxford: New York, 1994; Vol. 13.
- 28) Köpf-Maier, P.; Klapötke, T.; Köpf, H.; Preiss, F.; Marx, T. *Anticancer Res.* **1986**, *6*, 33-37.
- 29) Köpf-Maier, P.; Köpf, H.; Wagner, W.; Hesse, B. *Eur. J. Cancer* **1981**, *17*, 665-669.
- 30) Köpf-Maier, P.; Klapötke, T. *Arzneim-Forsch.* **1987**, *37*, 532-534.
- 31) Köpf-Maier, P.; Hesse, B.; Köpf, H. *J. Cancer Res. Clin. Oncol.* **1980**, *96*, 43-51.
- 32) Köpf-Maier, P. *Cancer Chemother. Pharmacol.* **1989**, *23*, 225-230.
- 33) Friedrich, M.; Villena-Heinsen, C.; Farnhammer, C.; Schmidt, W. *Eur. J. Gynecol. Oncol.* **1998**, *19*, 333-337.
- 34) Villena-Heinsen, C.; Friedrich, M.; Ertan, A. K.; Farnhammer, C.; Schmidt, W. *Anti-Cancer Drugs* **1998**, *9*, 557-563.
- 35) Harstrick, A.; Schmoll, H.-J.; Sass, G.; Poliwoda, H.; Rustum, Y. *Eur. J. Cancer* **1993**, *29A*, 1000-1002.
- 36) Mueller, B.; Lucks, S.; Mueller, R.; Mohr, W. Water-Soluble Pharmaceutical Composition Containing Metallocene Complex. Eur. Pat. Appl. EP Patent 407804, 1991.
- 37) Christodoulou, C. V.; Eliopoulos, A. G.; Young, L. S.; Hodgkins, L.; Ferry, D. R.; Kerr, D. J. *Brit. J. Cancer* **1998**, *77*, 2088-2097.
- 38) Köpf-Maier, P.; Köpf, H. *Angew. Chem. Int. Ed.* **1979**, *18*, 477-478.
- 39) Köpf-Maier, P.; Köpf, H.; Wagner, W. *Cancer Chemother. Pharmacol.* **1981**, *5*, 237-241.
- 40) Köpf-Maier, P.; Köpf, H. *Z. Naturforscher* **1979**, *34b*, 805-807.
- 41) Köpf-Maier, P.; Köpf, H. *ACS Symp. Ser.* **1983**, *209*, 315-333.
- 42) Köpf-Maier, P.; Leitner, M.; Voigtländer, R.; Köpf, H. *Z. Naturforscher* **1979**, *34c*, 1174-1176.
- 43) Köpf-Maier, P.; Leitner, M.; Köpf, H. *J. Inorg. Nucl. Chem.* **1980**, *42*, 1789-1791.

- 44) Köpf-Maier, P.; Klapötke, T. *J. Cancer Res. Clin. Oncol.* **1992**, *118*, 216-221.
- 45) Köpf-Maier, P.; Klapötke, T. *Cancer Chemother. Pharmacol.* **1992**, *29*, 361-366.
- 46) Köpf-Maier, P.; Hesse, B.; Voigtländer, R.; Köpf, H. *J. Cancer Res. Clin. Oncol.* **1980**, *97*, 31-39.
- 47) Köpf-Maier, P.; Grabowski, S.; Liegener, J.; Köpf, H. *Inorg. Chim. Acta* **1985**, *108*, 99-103.
- 48) Köpf-Maier, P.; Klapötke, T.; Köpf, H. *Inorg. Chim. Acta* **1988**, *153*, 119-122.
- 49) Köpf-Maier, P.; Tornieporth-Oetting, I. C. *Biometals* **1996**, *9*, 267-271.
- 50) Klapötke, T. M.; Köpf, H.; Tornieporth-Oetting, I. C.; S., W. P. *Organomet.* **1994**, *13*, 3628-3633.
- 51) Klapötke, T. M.; Köpf, H.; Tornieporth-Oetting, I. C.; S., W. P. *Angew. Chem. Int. Ed.* **1994**, *33*, 1518.
- 52) Köpf-Maier, P.; Klapötke, T. *Arzneim-Forsch.* **1989**, *39*, 488-490.
- 53) Köpf-Maier, P.; Grabowski, S.; Köpf, H. *Eur. J. Med. Chem.* **1984**, *19*, 347-352.
- 54) Köpf-Maier, P.; Kahl, W.; Klouras, N.; Hermann, G.; Köpf, H. *Eur. J. Med. Chem.* **1981**, *16*, 275-281.
- 55) Köpf-Maier, P.; Janiak, C.; Schumann, H., unpublished results.
- 56) Yasuda, H.; Yasuhara, T.; Yamamoto, H.; Takei, K.; Nakamura, A. *Chem. Express* **1988**, *3*, 375-378.
- 57) Kuo, L. Y.; Liu, A. H.; Marks, T. J. Metalloocene Interactions with DNA and DNA-Processing Enzymes, In *Metal Ions in Biological Systems*; Sigel, A. and Sigel, H., Ed.; Marcel Dekker, Inc., 1996; Vol. V33, pp 53-85.
- 58) Toney, J. H.; Marks, T. J. *J. Am. Chem. Soc.* **1985**, *107*, 947-953.
- 59) Kuo, L. Y.; Mercuri, G.; Kanatzides, M. S.; Marks, T. J. *J. Am. Chem. Soc.* **1987**, *109*, 7207-7209.
- 60) Kuo, L. Y.; Kanatzidis, M. G.; Sabat, M.; Tipton, L.; Marks, T. J. *J. Am. Chem. Soc.* **1991**, *113*, 9027-9045.

*References*

- 61) Toney, J. H.; Brock, C. P.; Marks, T. J. *J. Am. Chem. Soc.* **1986**, *108*, 7263-7274.
- 62) Döppert, K. *Makromol. Chem. Rapid Commun.* **1980**, *1*, 519-522.
- 63) Döppert, K. *J. Organomet. Chem.* **1987**, *319*, 351-354.
- 64) Döppert, K. *J. Organomet. Chem.* **1979**, *178*, C3-C4.
- 65) Harding, M. M.; Prodigalidad, M.; Lynch, M. J. *J. Med. Chem.* **1996**, *39*, 5012-5016.
- 66) Murray, J. H.; Harding, M. M. *J. Med. Chem.* **1994**, *37*, 1936-1941.
- 67) Witttrisch, H.; Schröer, H. P.; Vogt, J.; Vogt, C. *Electrophoresis* **1998**, *19*, 3012-3017.
- 68) Köpf-Maier, P. *J. Struct. Biol.* **1990**, *105*, 35-45.
- 69) Yang, P.; Guo, M. *Coord. Chem. Rev.* **1999**, *185-186*, 189-211.
- 70) Harding, M. M.; Harden, G. J.; Field, L. D. *FEBS Lett.* **1993**, *322*, 291-294.
- 71) McLaughlin, M. L.; Cronan, J. M. J.; Schaller, T. R.; Sneller, R. D. *J. Am. Chem. Soc.* **1990**, *112*, 8949-8952.
- 72) Yang, P.; Guo, M. L.; Yang, B. S. *Chin. Sci. Bull.* **1994**, *39*, 997-1002.
- 73) Zhang, Z. G.; Jin, L. *Chin. J. Chem.* **1997**, *15*, 225-233.
- 74) Rius, C.; Zorrilla, A. R.; Cabañas, C.; Mata, F.; Bernabeu, C.; Aller, P. *Mol. Pharmacol.* **1991**, *39*, 442-448.
- 75) Kratz, F. Interactions of Antitumour Metal Complexes with Serum Proteins. Perspectives for Anticancer Drug Development, In *Metal Complexes in Cancer Chemotherapy*; Keppler, B. K., Ed.; VCH Verlagsgesellschaft: Weinheim, 1993, pp 391-429.
- 76) Sun, H.; Li, H.; Weir, R. A.; Sadler, P. J. *Angew. Chem. Int. Ed.* **1998**, *37*, 1577-1579.
- 77) Messori, L.; Orioli, P.; Banholzer, V.; Pais, I.; Zatta, P. *FEBS Lett.* **1999**, *442*, 157-161.
- 78) Guo, M.; Sun, H.; Sadler, P. J. *J. Inorg. Biochem.* **1999**, *74*, 150.
- 79) Sun, H.; Li, H.; Sadler, P. J. *Chem. Rev.* **1999**, *99*, 2817-2842.
- 80) Guo, M.; Sadler, P. J. *J. Chem. Soc., Dalton Trans.* **2000** 7-9.

*References*

---

- 81) Ishiwata, K.; Ido, T.; Monma, M.; Murakami, M.; Fukuda, H.; Kameyama, M.; Yamada, K.; Endo, S.; Yoshioka, S.; Sato, T.; Matsuzawa, T. *Appl. Radiat. Isot.* **1991**, *42*, 707-712.
- 82) Douglas, W. E.; Green, M. L. H. *J. Chem. Soc. Dalton Trans.* **1972** 1796-1800.
- 83) Prout, K.; Daran, J. C. *Acta Cryst.* **1978**, *B34*, 3586-3591.
- 84) Gilje, J. W.; Roesky, H. W. *Chem. Rev.* **1994**, *94*, 895-910.
- 85) Harding, M. M.; Mokdsi, G.; Mackay, J. P.; Prodigalidad, M.; Lucas, S. W. *Inorg. Chem.* **1998**, *37*, 2432-2437.
- 86) Kuo, L. Y.; Kuhn, S.; Ly, D. *Inorg. Chem.* **1995**, *34*, 5341-5345.
- 87) Kröger, N.; Kleeberg, U. R.; Mross, K.; Edler, L.; Saß, G.; Hossfeld, D. K. *Onkologie* **2000**, *23*, 60-62.
- 88) Gassman, P. G.; Macomber, D. W.; Hershberger, J. W. *Organomet.* **1983**, *2*, 1470-1472.
- 89) Robbins, J. L.; Edelstein, N.; Spencer, B.; Smart, J. C. *J. Am. Chem. Soc.* **1982**, *104*, 1882-1893.
- 90) Reynolds, L. T.; Wilkinson, G. J. *Inorg. Nucl. Chem.* **1959**, *9*, 86-92.
- 91) Pacheco, D.; Hernandez, M. I.; Lubinkowski, J. J.; Calderón, J. L. *Inorg. Chim. Acta* **1976**, *18*, L25-L27.
- 92) March, J. *Advanced Organic Chemistry*; 4th ed.; John Wiley & Sons: New York, 1992.
- 93) Möhring, P. C.; Vlachakis, N.; Grimmer, N. E.; Coville, N. J. *J. Organomet. Chem.* **1994**, *483*, 159-166.
- 94) Qian, Y.; Huang, J.; Huang, T.; Chen, S. *Transition Met. Chem.* **1996**, *21*, 393-397.
- 95) Kucht, A.; Kucht, H.; Song, W.; Rausch, M. D.; Chien, J. C. *Applied Organomet. Chem.* **1994**, *8*, 437-443.
- 96) Gassman, P. G.; Winter, C. H. *J. Am. Chem. Soc.* **1986**, *108*, 4228-4229.
- 97) Conway, B. G.; Rausch, M. D. *Organomet.* **1985**, *4*, 688-693.

- 
- 98) Rausch, M. D.; Lewison, J. F.; Hart, W. P. *J. Organomet. Chem.* **1988**, 358, 161-168.
- 99) Hart, W. P.; Macomber, D. W.; Rausch, M. D. *J. Am. Chem. Soc.* **1980**, 102, 1196-1198.
- 100) Macomber, D. W.; Hart, W. P.; Rausch, M. D. *Adv. Organomet. Chem.* **1982**, 21, 1-55.
- 101) Thiele, J. *Chem. Ber.* **1901**, 34, 68.
- 102) Peters, D. *J. Chem. Soc.* **1960** 1832-1837.
- 103) Enders, M.; Köhler, K.; Frosch, W.; Pritzkow, H.; Lang, H. *J. Organomet. Chem.* **1997**, 538, 163-170.
- 104) Jutzi, P.; Kleimeier, J. *J. Organomet. Chem.* **1995**, 486, 287-289.
- 105) Hughes, A. K.; Marsh, S. M. B.; Howard, J. A. K.; Ford, P. S. *J. Organomet. Chem.* **1997**, 528, 195-198.
- 106) Stahl, K. P.; Boche, G.; Massa, W. *J. Organomet. Chem.* **1984**, 277, 113-125.
- 107) Jutzi, P.; Redeker, T.; Neumann, B.; Stammer, H. G. *Organomet.* **1996**, 15, 4153-4161.
- 108) Wang, T.-F.; Lee, T.-Y.; Chou, J.-W.; Ong, C.-W. *J. Organomet. Chem.* **1992**, 423, 31-38.
- 109) McGowan, P. C.; Hart, C. E.; Donnadiou, B.; Poilblanc, R. *J. Organomet. Chem.* **1997**, 528, 191-194.
- 110) Bradley, S.; McGowan, P. C.; Oughton, K. A.; Thornton-Pett, M.; Walsh, M. E. *Chem. Commun.* **1999** 77-78.
- 111) Herberich, G. E.; Gaffke, A.; Eckenrath, H. *J. Organomet.* **1998**, 17, 5931-5932.
- 112) Bertuleit, A.; Fritze, C.; Erker, G.; Fröhlich, R. *Organomet.* **1997**, 16, 2891-2899.
- 113) Bernheim, M.; Boche, G. *Angew. Chem. Int. Ed.* **1980**, 19, 1010-1011.
- 114) Guo, M.; Sun, H.; Bihari, S.; Parkinson, J. A.; Gould, R. O.; Parsons, S.; Sadler, P. J. *Inorg. Chem.* **2000**, 39, 206-215.

*References*

---

- 115) Guo, M.; Sun, H.; McArdle, H. J.; Gambling, L.; Sadler, P. J. *Biochem.* **2000**, *39*, 10023-10033.
- 116) Köpf-Maier, P.; Köpf, H. *J. Organomet. Chem.* **1988**, *342*, 167-176.
- 117) Vashisht Gopal, Y. N.; Jayaraju, D.; Kondapi, A. K. *Arch. Biochem. Biophys.* **2000**, *376*, 229-235.
- 118) Jayaraju, D.; Vashisht Gopal, Y. N.; Kondapi, A. K. *Arch. Biochem. Biophys.* **1999**, *369*, 68-77.
- 119) Vashisht Gopal, Y. N.; Jayaraju, D.; Kondapi, A. K. *Biochem.* **1999**, *38*, 4382-4388.
- 120) Wang, J. C. *Annu. Rev. Biochem.* **1996**, *65*, 635-692.
- 121) Austin, C. A.; Marsh, K. L. *BioEssays* **1998**, *20*, 215-226.
- 122) Insaf, S. S.; Danks, M. K.; Witiak, D. T. *Curr. Med. Chem.* **1996**, *3*, 437-466.
- 123) Fossé, P.; René, B.; Charra, M.; Paoletti, C.; Saucier, J. M. *Mol. Pharmacol.* **1992**, *42*, 590-595.
- 124) Gatto, B.; Capranico, G.; Palumbo, M. *Curr. Pharm. Design* **1999**, *5*, 195-215.
- 125) René, B.; Fossé, P.; Khelifa, T.; Jacquemin-Sablon, J.; Bailly, C. *Mol. Pharmacol.* **1996**, *49*, 343-350.
- 126) Marini, J. C.; Miller, K. G.; Englund, P. T. *J. Biol. Chem.* **1980**, *255*, 4976-4979.
- 127) Takano, H.; Kohno, K.; Ono, M.; Uchida, Y.; Kuwano, M. *Cancer Res.* **1991**, *51*, 3951-3957.
- 128) Christodoulou, J.; Kashani, M.; Keohane, B. M.; Sadler, P. J. *J. Anal. At. Spectrom.* **1996**, *11*, 1031-1035.
- 129) Bal, W.; Christodoulou, J.; Sadler, P. J.; Tucker, A. *J. Inorg. Biochem.* **1998**, *70*, 33-39.
- 130) Richon, V. M.; Schulte, N.; Eastman, A. *Cancer Res.* **1987**, *47*, 2056-2061.
- 131) Micetich, K.; Zwelling, L. A.; Kohn, K. W. *Cancer Res.* **1983**, *43*, 3609-3613.

*References*

- 132) Hromas, R. A.; Andrews, P. A.; Murphy, M. P.; Burns, C. P. *Cancer Lett.* **1987**, *34*, 9-13.
- 133) Böhm, S.; Oriana, S.; Spatti, G. B.; Tognella, S.; Tedeschi, M.; Zunino, F.; Di Re, F. In *Platinum and Other Metal Coordination Compounds in Cancer Chemotherapy*; Nicolini, M., Ed.; Martinus Nijhoff Publishing: Boston, 1988, pp 456-459.
- 134) Zhang, Z.; Yang, P. *Chem. J. Chin. Univ.-Chin.* **1999**, *20*, 1682-1684.
- 135) Aramini, J. M.; Saponja, J. A.; Vogel, H. J. *Coord. Chem. Rev.* **1996**, *149*, 193-229.
- 136) Moore, G. L. *Introduction to Inductively Coupled Plasma Atomic Emission Spectrometry*; Elsevier: Amsterdam, 1989; Vol. 3.
- 137) Marshall, J.; Evans, E. H.; Fisher, A.; Chenery, S. *J. Anal. At. Spectrom.* **1997**, *1997*, 263R-290R.
- 138) Komaromy-Hiller, G. *Anal. Chem.* **1999**, *71*, 338R-342R.
- 139) Salvin, W. *Anal. Chem.* **1986**, *58*, 589A-597A.
- 140) Kunze, J.; Wimmer, M. A.; Koelling, S.; Schneider, E. *Fresenius J. Anal. Chem.* **1998**, *361*, 496-499.
- 141) Tohno, Y.; Tohno, S.; Utsumi, M.; Minami, T.; Ichii, M.; Okazaki, Y.; Nishiwaki, F.; Moriwake, Y. *Biol. Trace Elem. Res.* **1998**, *59*, 167-175.
- 142) Codell, M. *Analytical Chemistry of Titanium Metals and Compounds*; Interscience: New York, 1959; Vol. 9.
- 143) Labouriau, A.; Earl, W. L. *Chem. Phys. Lett.* **1997**, *270*, 278-284.
- 144) Dormond, A.; Fauconet, M.; Leblanc, J. C.; Moise, C. *Polyhedron* **1984**, *3*, 897-900.
- 145) Moore, E. A.; Healy, A. *J. Chem. Soc. Faraday Trans.* **1995**, *91*, 1735-1739.
- 146) Gassman, P. G.; Campbell, W. H.; Macomber, D. W. *Organomet.* **1984**, *3*, 385-387.
- 147) Mason, J. *Chem. Rev.* **1987**, *87*, 1299-1312.
- 148) Berners-Price, S. J.; Kuchel, P. W. *J. Inorg. Biochem.* **1990**, *38*, 305-326.
- 149) Berners-Price, S. J.; Kuchel, P. W. *J. Inorg. Biochem.* **1990**, *38*, 327-345.

- 150) Glasoe, P. K.; Long, F. A. *J. Phys. Chem.* **1960**, *64*, 188-190.
- 151) Evaluating and Isolating Synthetic Oligonucleotides. A complete guide distributed by Applied Biosystems Inc. 1992.
- 152) Arthurs, M.; Bickerton, J. C.; Kirkley, M.; Palin, J.; Piper, C. J. *Organomet. Chem.* **1992**, *429*, 245-256.
- 153) Kratz, F.; Hartman, M.; Keppler, B.; Messori, L. *J. Biol. Chem.* **1994**, *269*, 2581-2588.
- 154) Kratz, F.; Keppler, B. K.; Hartmann, M.; Messori, L.; Berger, M. R. *Metal-Based Drugs* **1996**, *3*, 15-23.
- 155) Keppler, B. K.; Friesen, C.; Vongerichten, H.; Vogel, E. Budotitane, a New Tumor-Inhibiting Titanium Compound: Preclinical and Clinical Development, In *Metal Complexes in Cancer Chemotherapy*; Keppler, B. K., Ed.; VCH Verlagsgesellschaft: Weinheim, 1993, pp 297-323.
- 156) Keller, H. J.; Keppler, B. K.; Schmähl, D. *Arzneim.-Forsch.* **1982**, *32*, 806-807.
- 157) Keppler, B. K.; Schmähl, D. *Arzneim.-Forsch.* **1986**, *36*, 1822-1828.